PROCEEDINGS OF INTERNATIONAL SYMPOSIUM ON A NEW ERA IN FOOD SCIENCE AND TECHNOLOGY 2019

-PART 1-

INTERNATIONAL SYMPOSIUM ON A NEW ERA IN FOOD SCIENCE AND TECHNOLOGY 2019

ORGANIZER:

THE UNITED GRADUATE SCHOOL OF AGRICULTURAL SCIENCE, GIFU UNIVERSITY

-PART 2-

UGSAS-GU & BWEL JOINT POSTER SESSION ON AGRICULTURAL AND BASIN WATER ENVIRONMENTAL SCIENCES 2019

ORGANIZERS:

THE UNITED GRADUATE SCHOOL OF AGRICULTURAL SCIENCE, GIFU UNIVERSITY

GIFU UNIVERSITY REARING PROGRAM FOR BASIN WATER ENVIRONMENTAL LEADERS

DATE: OCTOBER 9-10, 2019

VENUE: GIFU UNIVERSITY, JAPAN

PROGRAM
–PART 1-

DAY ONE: Wednesday, October 9
Time: 9:00-16:45

Time Table

Venue: 6F in UGSAS Building, Gifu University

9:00-9:30 **Registration**

9:30-9:35 **Opening Remarks**
Prof. Masateru Senge (Dean of UGSAS-GU)

Kyenote Speeches

Venue: 6F in UGSAS Building, Gifu University
Session Chair: ***Prof. Tomio Yabe (Gifu University)***

9:35-10:05 **Keynote Speech 01**
Assoc. Prof. Nozomu Sakurai (National Institute of Genetics)

10:05-10:35 **Keynote Speech 02**
Dr. Shirley C. Agrupis (President of Mariano Marcos State University)

10:35-10:55 **Coffee Break**

10:55-11:25 **Keynote Speech 03**
Prof. Utpal Bora (Indian Institute of Technology Guwahati)

11:25-11:55 **Keynote Speech 04**
Assoc. Prof. Mohamad Yusof Maskat (Universiti Kebansaan Malaysia)

11:55-12:10 **Photo Shoot**

Venue: 6F in UGSAS Building, Gifu University

12:10-13:00 **Lunch Break**

Special Lecture

Venue: Room 100, Engineering Building, Gifu University

13:00-14:00 **Special Lecture**
Prof. Gary D. Christian (University of Washington)

14:00-14:30 **Break**

Scientific Sessions

Venue: 6F in UGSAS Building, Gifu University

Session 1 —Bioactives and Health / Prebiotics and Probiotics—
Session Chair: ***Prof. Tomoyuki Nakagawa (Gifu University)***

14:30-14:45 **01.** ***Prof. Das Shonkor Kumar (Bangladesh Agricultural University)***

14:45-15:00 **02.** ***Prof. Chen-jian Liu (Kunming University of Science and Technology)***

15:00-15:15 **03.** ***Prof. Xiaoxiong Zeng (Nanjing Agricultural University)***

15:15-15:45 **Coffee Break**

Session 2 —Physical Properties of Food—
Session Chair: ***Assis. Prof. Teppei Imaizumi (Gifu University)***

15:45-16:00 **01.** ***Assoc. Prof. Md. Sultan Mahomud***
(Hajee Mohammad Danesh Science and Technology University)

16:00-16:15 **02.** ***Assoc. Prof. Pongphen Jitareerat***
(King Mongkut's University of Technology Thonburi)

16:15-16:30 **03.** ***Dr. Maharani Pertiwi Koentjoro***
(Nahdlatul Ulama University of Surabaya)

16:30-16:45 **04.** ***Dr. Achmad Ridwan Ariyantoro*** **(*Sebelas Maret University*)**

DAY TWO: Thursday, October 10

Time: 9:00-15:00

Time Table

9:00-9:30 **Registration**

Scientific Sessions

Venue: 6F in UGSAS Building, Gifu University

Session 3 —Comprehensive Food Science and Others—

Session Chair: ***Prof. Takahisa Nishizu (Gifu University)***

9:30-9:45 **01.** ***Assoc. Prof. Nancy Dewi Yuliana (Bogor Agricultural University)***

9:45-10:00 **02.** ***Prof. Irmanida Batubara (Bogor Agricultural University)***

10:00-10:15 **03.** ***Prof. A.H.M. Nurun Nabi (University of Dhaka)***

10:15-10:30 **04.** ***Dr. Komariah (Sebelas Maret University)***

10:30-10:45 **05.** ***Assis. Prof. Gang Ma (Shizuoka University)***

10:45-11:00 **Coffee Break**

Session 4 —Quality Control of Food—

Session Chair: ***Prof. Kohei Nakano (Gifu University)***

11:00-11:15 **01.** ***Prof. Sanjib Kumar Panda (Central University of Rajasthan)***

11:15-11:30 **02.** ***Assoc. Prof. Khandra Fahmy (Andalas University)***

11:30-11:45 **03.** ***Assoc. Prof. Md. Harun Ar Rashid (Bangladesh Agricultural University)***

11:45-12:00 **04.** ***Dr. Abdullah Iqbal (Food Research Institute, NARO)***

12:00-12:15 **05.** ***Assis. Prof. Teppei Imaizumi (Gifu University)***

12:15-12:20 **Closing Remarks**
Dr. Fumiaki Suzuki
(Vice President / Director of International Affairs & Public Relations)

Venue: 2F Conference Room, UGSAS Building, Gifu University

12:20-13:00 **Lunch Break**

13:00-15:00 **-PART 2-** *Please refer to the next page for details.

Venue: 6F in UGSAS Building, Gifu University

UGSAS-GU & BWEL Joint Poster Session on Agricultural and Basin Water Environmental Sciences 2019

UGSAS-GU & BWEL Joint Poster Session on Agricultural and Basin Water Environmental Sciences 2019

Organized by The United Graduate School of Agricultural Science, Gifu University (UGSAS-GU)
Gifu University Rearing Program for Basin Water Environmental Leaders (BWEL)

PROGRAM
–PART 2-

DAY TWO: Thursday, October 10
Time: 13:00-15:00
Venue: 6F in UGSAS Building, Gifu University

Time Table

13:00-14:40 **Poster Presentation**

14:40-14:55 **Best Presentation Award ceremony**

14:55-15:00 **Closing Remarks**
Prof. Fusheng Li (Head of the Promotion Office of Gifu University Rearing Program for Basin Water Environmental Leaders)

Presenters

P01: ***Nayla Majeda Alfarafisa (UGSAS-GU)***
P02: ***Putri Wulandari Zainal (UGSAS-GU)***
P03: ***Eko Andrianto (UGSAS-GU)***
P04: ***Fakfan Luangapai (Graduate School of Natural Science and Technology, Gifu University)***
P05: ***Yolani Syaputri (UGSAS-GU)***
P06: ***Raj Kishan Agrahari (UGSAS-GU)***
P07*: Panyapon Pumkaeo (UGSAS-GU)*
P08*: Hiroto Yamshita (UGSAS-GU)*
P09*: Annisyia Zarina Putri (UGSAS-GU)*
P10*: Arif Delviawan (UGSAS-GU)*
P11*: Maihemuti Mijiti (UGSAS-GU)*
P12*: Rachmad Adi Riyanto (UGSAS-GU)*
P13*: Vany Fadhilah*
(Graduate School of Integrated Science and Technology, Shizuoka University)
P14*: Devendra Kumar Maravi (Indian Institute of Technology Guwahati)*
P15*: Tabli Ghosh (Indian Institute of Technology Guwahati)*
P16*: Purabi Bhagabati (Indian Institute of Technology Guwahati)*
P17*: Neha Mulchandani (Indian Institute of Technology Guwahati)*
P18*: Kona Mondal (Indian Institute of Technology Guwahati)*
P19*: Le Anh Tuan (UGSAS-GU; BWEL)*
P20*: Ruoming Cao (UGSAS-GU; BWEL)*
P21*: Cahyo Wisnu Rubiyanto (UGSAS-GU; BWEL)*
P22*: Islam Md Rashidul*
(Graduate School of Natural Science and Technology, Gifu University; BWEL)
P23*: Tahmidul Ashik*
(Graduate School of Natural Science and Technology, Gifu University; BWEL)

P24*: Ryota Matsuura*
(Graduate School of Natural Science and Technology, Gifu University; BWEL)
P25*: Akihiro Hayano*
(Graduate School of Natural Science and Technology, Gifu University; BWEL)
P26*: Masaya Toyoda (Graduate School of Engineering, Gifu University; BWEL)*
P27*: Takanori Ishii*
(Graduate School of Natural Science and Technology, Gifu University; BWEL)
P28*: Faisal Arsyad*
(Graduate School of Natural Science and Technology, Gifu University; BWEL)
P29*: Daichi Iijima*
(Graduate School of Natural Science and Technology, Gifu University; BWEL)
P30*: Hiroki Maruyama*
(Graduate School of Natural Science and Technology, Gifu University; BWEL)
P31*: Naoki Akiyama*
(Graduate School of Natural Science and Technology, Gifu University; BWEL)
P32*: Wenjiao Li (Graduate School of Engineering, Gifu University; BWEL)*
P33*: Shiamita Kusuma Dewi*
(Graduate School of Natural Science and Technology, Gifu University; BWEL)

CONTENTS

— PART 1 —

KEYNOTE SPEECHES

SPECIAL LECTURE

SCIENTIFIC SESSION

— PART 2 —

UGSAS-GU & BWEL Joint Poster Session on Agricultural and Basin Water Environmental Sciences 2019

-PART 1-

INTERNATIONAL SYMPOSIUM ON A NEW ERA

IN FOOD SCIENCE AND TECHNOLOGY

2019

KEYNOTE SPEECHES

Wednesday, 9th October 2019
9:35 am - 11:55 am

6th Floor, UGSAS Building, Gifu University

ORGANIZER:

THE UNITED GRADUATE SCHOOL OF AGRICULTURAL SCIENCE, GIFU UNIVERSITY

Construction of a Metabolome Database for Uncovering the Chemical World in Foods

Nozomu SAKURAI[1 *]

[1] Bioinformation and DDBJ Center, National Institute of Genetics, 1111 Yata, Mishima, Shizuoka 411-8540, Japan

* Corresponding Author: sakurai@nig.ac.jp

SUMMARY

Food analysis is required for safety assessments, quality controls, traceability, evaluations of nutrition and functions of foods. Metabolomics–a technology for comprehensive detection of small molecules in the samples–is prospective for food analysis. However, a long-standing unsolved issue, namely, a lot of unidentified metabolite peaks remain in the data obtained by mass spectrometry (MS)-based untargeted metabolome analyses, makes it difficult to understand the results. A lot of computational tools for the prediction of chemical structure by MS data have been reported, and the prediction accuracy has been improved rapidly. However, the substantial issue of the poor annotation of the compound peaks is, a lack of information for prioritizing the candidate peaks for further detailed investigation, rather than the accuracy of the prediction tools. We constructed a database, Food Metabolome Repository (http://metabolites.in/foods), by which a sample specificity of the queried peak can be obtained, and this information should be a key for the prioritization. Untargeted metabolome data obtained from 222 foods using liquid chromatography (LC)-high resolution MS are available at the repository. The repository can also be a good resource for annotation of unknown peaks detected in human biofluid. By assuming the modified molecules such as glucuronidates and sulfur conjugates, the mass value of the original molecule without the attached moiety (in this case, glucuronic acid and sulfate) can be calculated, and the existence of the original molecule in foods can be searched. These molecules in human biofluid might be used as biomarkers for intake of a specific food. A wide diversity of chemicals is expected in the food criteria because a wide range of organisms and various compound modification processes such as cooking and fermentation are involved there. Therefore, Food Metabolome Repository should be useful not only for the food science but also for the general metabolome analyses. In DNA Data Bank of Japan (DDBJ), we are now constructing a new public repository for the metabolome data, named “MetaboBank”, for primarily Japanese and Asian researchers. Enhancement of a variety of foods and analytical methods for food metabolome data should contribute to elucidate the chemical world in foods and further use of the chemical information for food science and human health.

Keyword: food metabolomics, LC-MS, database, compound identification

Philippine Black Garlic (PhBG): Its Physico-Chemical Properties and Potential for Food and Pharmaceutical Application

Shirley C. AGRUPIS[1*], Milen Fileza M. INOCENCIO[1], Aira Cassandra S. Castro[1], Dionisio S. BUCAO[2*]

[1] Mariano Marcos State University, Brgy. 16 Quiling Sur, City of Batac 2906

[2] University Innovation and Technology Services Office, Research Directorate, RL Building, MMSU, City of Batac 2906, Ilocos Norte, Philippines

* Corresponding Author: mmsuop@yahoo.com

SUMMARY

Garlic is the flagship commodity crop in the entire province of Ilocos Norte. The province is considered a champion garlic supplier in the Philippines (Ilocosnorte.gov.ph, 2016) for contributing 67 to 70 percent of the total garlic production of the country annually. According to the records of the office of the Provincial Agriculturist of Ilocos Norte as reported by Lazaro of balita.ph, the whole province produced at least 6,855 metric tons of garlic during the harvest season in the first quarter of 2014. It contributes to forty percent (40%) of the province's gross domestic product and an effective tool for poverty alleviation of the farmers. Garlic is known for its many health benefits. Garlic is widely used for several conditions linked to the blood system and heart, including atherosclerosis (hardening of the arteries), high cholesterol, heart attack, coronary heart disease and hypertension. It is also used today by some people for the prevention of lung cancer, prostate cancer, breast cancer, stomach cancer, rectal cancer, and colon cancer (Nordqvist, 2015). What makes raw garlic such a healthful and potent vegetable is the compound allicin, which accounts for its pungent odor. However, according to Mercola (2014), allicin is a very unstable compound which is decomposed into simpler molecules in less than an hour when garlic is cooked, crushed, aged or processed.

Recently, a processed garlic called black garlic is becoming popular for its unique appearance, taste and most specially, its health benefits. Black garlic is produced by processing ordinary garlic under constant high temperature and humidity up to 30 days. During processing, the garlic changes its color from white to dark brown. This is due to Maillard Reaction, a non-enzymatic browning reaction that also causes the change in flavor, texture, smell and nutrient content (Bae, et al., 2014). Studies have also shown that the compound s-allyl cysteine is higher in concentration in black garlic than raw garlic. This compound, compared to allicin is absorbed more easily by the body (Hobson, 2012). Other articles have claimed that antioxidants of black garlic increased (Choi, et al., 2014 and Sato, et al., 2006) which may also increase the medicinal benefits of black garlic which include anticancer.

In partnership with Takara Inc. in Takko-machi, Aomori, Japan, black garlic was produced at MMSU, using low cost available processing. At present, MMSU-Takara Inc. is currently implementing joint R&D project under the Japan International Cooperation Agency (JICA). The PhBG produced was subjected to initial characterization and test to evaluate the physico-chemical properties and their potential medical application specifically in cancer treatment. To evaluate these, two in vitro assays were performed- DPPH or antioxidant assay and the MTT cytotoxicity assay. The PhBG was found as effective as Fluorouracil in destroying A549 cancer cell lines and better than raw garlic. On the other hand, PhBG, raw garlic and Fluorouracil showed the same level of potency against HCT116 colon cancer cells. Chemically, PhBG mineral contents' such as sodium calcium, iron, potassium and zinc increased. It contains phytochemicals such as alkaloids, flavonoids, phenol, tannins, steroids and terpenoids. Furthermore, PhBG also has higher phenolic and flavonoid content than raw garlic. The results of this study would provide information on the potential of Philippine black garlic as a food product and open possibilities in a cost-effective and non-invasive treatment for cancer.

Keywords: Black garlic, physico-chemical characteristics, phytochemicals, Ilocos Garlic, cytotoxicity, colon cancer, lung cancer

Sustainable Food Security: Importance of Policy and Technology

Utpal Bora*

Department of Biosciences and Bioengineering, Indian Institute of Technology Guwahati, Kamrup 781039, Assam, India

* Corresponding Author: ubora@iitg.ac.in

SUMMARY

Today the world is less undernourished then two decades ago. Although the proportion of undernourished people declined from 15 per cent in 2000-2002 to 11 per cent in 2014-2016, more than 790 million people still lack regular access to adequate food. Goal 2 of SDG focus on "Zero Hunger" by 2030 and aims at ensuring the global population with "enough good-quality food to lead a healthy life". It seeks sustainable solutions to end hunger in all its forms and achieving food security.

Sustainable solutions lie at the level of production, processing, consumption of food and reduction of loss at every step. Availability of land and water as well as technology and markets, increased investments through international cooperation to bolster the agricultural productivity and food processing would be critical given the pressure due to urbanization and climate change. In my lecture I would be discussing about the interdependencies of various SDG goals that could ensure us food security and how technology, policy and knowledge discovery both traditional and modern would play critical roles in achieving Zero hunger.

Keyword: Sustainable Development Goals, Food security, Zero Hunger, Climate change

Deodourization of Noni Extract: A Food Processing Approach

Mohamad Yusof Maskat, Haslaniza Hashim, Nur Hafiza Zairuh*

Faculty of Science and Technology, Universiti Kebangsaan Malaysia, 43600 Bangi, Selangor, Malaysia
* Corresponding Author: yusofm@ukm.edu.my

SUMMARY

Noni (*Morinda citrifolia*) is a tropical fruit that has been traditionally used for various therapies. The use of noni is not localized only to Malaysia but also in several other countries such as Indonesia, Polynesia, other Pacific Islands and other places. Traditionally, noni has been used for medicinal purposes by the Polynesians since 2000 years ago. Many researchers have also studied the beneficial properties of noni which include antimicrobial properties, anti cancer properties, antioxidant properties, anti inflammatory properties and others.

Although noni contained several beneficial properties, its usage has been limited due to its undesirable odour. When noni fruits ripen, it emits an undesirable odour which has been described as butyric acid-like rancid smell. Fifty one volatile compoundshas been determined in noni fruit which include organic acids, alcohol (3-methyl-3-butane-1-ol), esther (methyl octanoate, methyl decanoate), ketone (2-heptanone), dan lactone. Organic acid content of noni was high especially octanoic, hexanoic and decanoic acid which can reach 50-70%. From the volatile compounds that was identified, the main volatile compound was octanoic acid (72%) and hexanoic acid (8%) which consisted of medium chain fatty acids of 6 and 8 carbons, respectively. Olfactory gas chromatography data also supported the finding that the undesirable odour of noni was contributed mainly by octanoic acid.

Traditional production of noni extract involves fermenting the noni fruits. It has been reported that fermented noni extract has less undesirable odour compared to fresh extract. It has been reported that Saccharomyces cerevisiae has an acyl-coA synthetase that is able to degrade octanoic acid. Results showed that inoculum size of S. cerevisiae has negative effect on octanoic acid content and undesirable odour intensity among trained panellists. Fermented noni extract also showed reduced octanoic acid content and undesirable odour intensity compared with unfermented samples. To further increase the capacity of octanoic acid degradation by S. cerevisiae, glucose at a concentration of 0-30 g/L was added during fermentation. Addition of 6 g/L of glucose produced the lowest octanoic acid content and lowest intensity of undesirable odour after 48 hours of fermentation. Thus, it can be concluded that the addition of glucose at limited amount facilitated the metabolism of octanoic acid by S. cerevisiae in noni extract.

Due to octanoic acid being the contributing compound to the undesirable odour of noni extract, deacidification using ion exchange resin was studied. Three types of weak base anion exchange resins (Amberlite IRA 67, Duolite A7 and Amberlite IRA 96) of different resin weight (0, 5, 10%, w/v) were used. Deacidification of *M. citrifolia* juice using the resins significantly decreased the octanoic acid content compared to fresh juice where Amberlite IRA 67 gave the highest reduction of octanoic acid followed by Duolite A7 and Amberlite IRA 96. The results indicated that deacidification of the juice using 10% of resin weight (w/v) gave higher percentage of antioxidant activity and TPC. Results also showed a similar trend when different weight of resin was used where Amberlite IRA 67 > Duolite A7 > Amberlite IRA 96 for DPPH, FRAP, TPC and antioxidant compounds.

Keyword: noni, Morinda citrifolia, deodourization, fermentation, ion exchange resin

-PART 1-

INTERNATIONAL SYMPOSIUM ON A NEW ERA

IN FOOD SCIENCE AND TECHNOLOGY

2019

SPECIAL LECTURE

Wednesday, 9th October 2019
13:00 pm - 14:00 pm

Room 100, Engineering Building, Gifu University

ORGANIZER:

THE UNITED GRADUATE SCHOOL OF AGRICULTURAL SCIENCE, GIFU UNIVERSITY

The Ethics of Scientific Writing: How to Write and How Not to Write a Paper

Gary D. Christian

Department of Chemistry, University of Washington, Box 351700, Seattle, WA 98195-1700
christian@chem.washington.edu

SUMMARY

Scientific writing for peer-reviewed journals is how scientists communicate their work to the world. It is important to tell a clear and compelling story, beginning with justification for the work, placing it in the context of prior work, and its significance in advancing the field, i.e., what problem is being addressed? Manuscripts are submitted to peer-review by experts, selected by the editor. Only a select number will be published, depending on novelty, significance to the field, demonstrated applicability, appropriateness for the journal, and so forth. Peer-review is for the benefit of the author as well as for the editor, and helps improve the quality and impact of the paper. Ethics in publication is of paramount importance, and has become more of an issue for editors in recent years, particularly with the advent of the electronic age.

I will relay my experiences as an Editor-in-Chief for *Talanta* over thirty years, providing guidance on how to structure and present a paper so editors, reviewers and readers will have a good understanding of your accomplishments, and pitfalls to avoid. Real-world examples of manuscripts that do not follow established and ethical guidelines will be given, along with cases of outright scientific fraud in the chemical literature. And hints will be given of how authors can use peer review to their advantage.

-PART 1-

INTERNATIONAL SYMPOSIUM ON A NEW ERA

IN FOOD SCIENCE AND TECHNOLOGY

2019

SCIENTIFIC SESSION

Wednesday, 9th October 2019
14:30 pm - 16:45 pm

Thursday, 10th October 2019
9:30 am - 12:15 pm

6th Floor, UGSAS Building, Gifu University

ORGANIZER:

THE UNITED GRADUATE SCHOOL OF AGRICULTURAL SCIENCE, GIFU UNIVERSITY

Green Tea Departs Baleful Effects on Health in Swiss Albino Mice

Das SHONKOR KUMAR*, Kundu SWARUP KUMAR

Bioresearch laboratory (Cancer and Herbal Research Center), Department of Anatomy and Histology, Faculty of Veterinary Science, Bangladesh Agricultural University, Mymensingh-2202. Bangladesh

* Corresponding Author: skdas76@yahoo.com

SUMMARY

A myriad of health claims are being made in favor of the consumption of green tea due to its easy availability and greater popularity in spite of its certain health risk have started to emerge. This study was aimed to determine the baleful effects on health due to excessive green tea intake in model mice. Total ten (10) experimental Swiss albino mice (age of 5 weeks and avg. weight 18-20gm) were taken and divided into two (2) groups such as Control (C) and Treated (T) groups, each having 5 mice. The control group (1 male+4 female) was fed with the normal mice pellet and water but the treated group (1 male + 4 female) was given green tea instead of water (3ml/mice two times per day) and mice pellet for 21 days. After the experimental tenure, the mice (both the control and treated groups) were sacrificed ethically and the samples (Blood, liver, kidney, lungs, brain and testes) were collected for investigation. The results of the study revealed that the treated group became motionless than the control group. Grossly, the liver surface of the treated mice became dark red in color with considerable hepatomegaly found; hemorrhage found in lungs whether the brain, testes and kidney were found normal although kidney glomerulus has a minor change. Histologically, mild central vein dilation with severe congestion, sinusoidal dilation and severe venous congestion were found in the portal vein of the liver of treated mice. Hematologically, it was found that hemoglobin level of the treated female mice became lower than that of the control group mice. On the other hand, within this experimental period female mice of both groups gave births (18 pups) which were devoid of any abnormality. Therefore, it can be concluded that excess green tea intake in a day might have baleful effects on health and people need to be conscious about this. It also needs further in-depth investigation to understand the pathway of causing such baleful effects on health both at gross and cellular level.

Keywords: green tea, baleful effects, Swiss albino mice, health impacts

Introduction

Tea is one of the most popular beverages, which are most commonly used in China and Japan (Nawab and Farooq, 2015). Green tea is an evergreen shrub derived from the plant *Camellia sinensis* (Theaceae). The principal active ingredients of green tea include polyphenolic compounds such as epicatechin (EC), epicatechin-3-gallate (ECG), epigallocatechin (EGC) and epigallocatechin-3-gallate (EGCG) along with the other polyphenols in green tea include flavanols and their glycosides and depsides such as cholorogenic acid, quinic acids, carotenoids, trigalloylglucose, lignin, protein, chlorophyll, minerals, caffeine and a small amount of methylxanthines (Liu *et al.,* 2008).

Green tea offers many attractive & beneficial effects. It possesses antioxidant, anti-angiogenesis, antiproliferative, antitumor and anti-carcinogenic properties (Cooper *et al.,* 2005). Green tea is also used as protective agent in exercise enhancement, diabetes, inflammatory bowel disease, skin disorders, hair loss, weight loss and iron overload (Sinija and Mishra, 2008).

High doses of green tea consumption (*i.e*. 5–6 liters per day) may cause nausea, vomiting, abdominal bloating/pain, dyspepsia, flatulence and diarrhea (Laurie *et al.,* 2005) as well as excessive consumption of caffeine from green tea may also cause central nervous system stimulation such as dizziness, insomnia, tremors, restlessness, confusion, diuresis, heart rate irregularities and psychomotor agitation (Tomasulo, 2004). Regular consumption of green tea is thought to reduce the risk of cardiovascular disease (CVD) but has also been associated with liver toxicity (Frank *et al.,* 2008).

Materials and Methods

Total ten (10) experimental Swiss albino mice (at the age of 5 weeks and avg. weight 18-20gm) were purchased from the Department of Pharmacy, Jahangirnagar University, Dhaka, Bangladesh. The mice were adapted at Animal Care Room, for the period of 7 days before being used for the experiment. Then the mice were divided into two groups such as Control (C) and Treated (T) groups, each having 5 mice. The control group (1 male+4 female) was fed with the normal mice pellet and water whether the treated group (1 male + 4 female) was given green tea instead of water (3ml/mice two times per day) and mice pellet for 21 days. After the experimental tenure, the mice (both the control and treated groups) were sacrificed ethically and the samples (Blood, liver, kidney, lungs, brain and testes) were collected in order to investigate the gross, histological and hematological changes. Finally Haematoxylin & Eosin staining was done for histological study

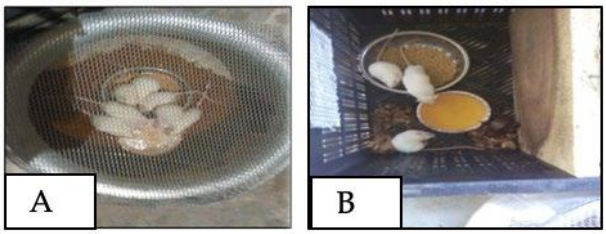

Fig. 1 Feeding mice pellet & water (A-control group), mice pellet & green tea (B-treated group).

Results and Discussion

The results of the study revealed that the treated group mice became motionless than the control group mice. On the other hand, within this experimental period female mice of both groups gave births (18 pups) which were devoid of any abnormality.

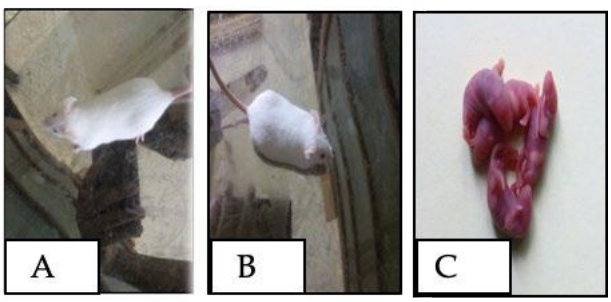

Fig 2 Active & alert mice (A-control group), motionless mice (B-treated group), normal mouse pups (C-treated group).

From the gross study, we found that liver surface became dark red in color with considerable hepatomegaly in the treated group of mice. Hemorrhage found in lungs whether the brain, testes and kidney were found normal.

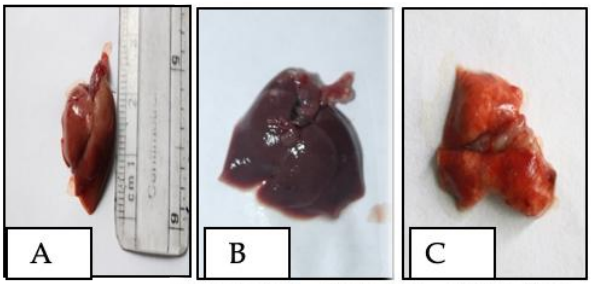

Fig 3 Gross morphological observation of the liver. Normal morphological appearance (Reddish, smooth, and shiny) of liver was found in the (A) control group. Liver became dark red in color with considerable hepatomegaly in the (B) and hemorrhage (black arrow) also found in the lung (C) due to excessive green tea intake.

From the histological study, we found that, mild central vein dilation with severe congestion, sinusoidal dilation and severe venous congestion in the portal vein of the liver of treated group of mice.

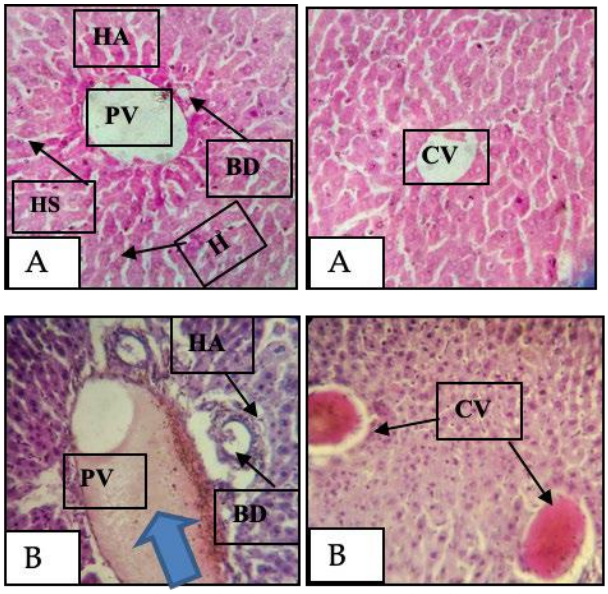

Fig 4 Histological observation of the liver showing normal (control group) liver architecture in the (A) control group of mice. Liver showing severe venous congestion (blue arrow) in the portal vein (PV) and mild central vein dilation (black arrow) with severe congestion in the (B-treated group) due to excessive green tea intake. CV= Central vein, PV=Portal vein, BD= Bile duct, HA=Hepatic artery, HS=Hepatic sinusoids, H= Hepatocytes. Images were photographed with a 40x objective (H and E stain).

From the hematological study, it was found that hemoglobin level of the treated female mice significantly *(** $p<0.01$)* reduced than the control group mice.

[Results are as Mean ± SE (standard error) of 5 mice in each group. One-way ANOVA was performed as the test

of significance. There was a significant variation in the hemoglobin level. The difference was considered to be significant when ** $p<0.01$, * $p<0.05$ compared to normal control group].

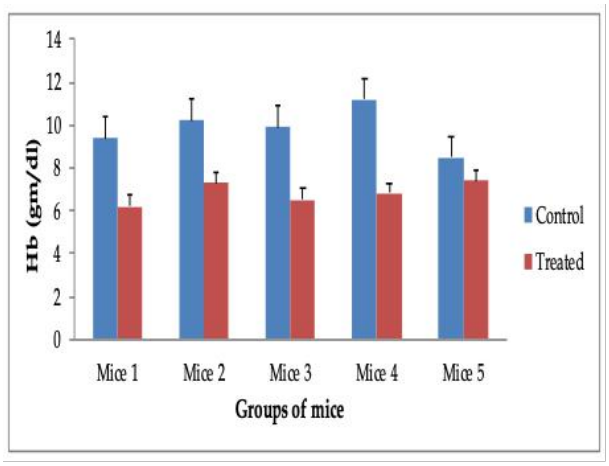

Fig. 5 Reduction of hemoglobin level due to excessive green tea intake.

Green tea is a natural antioxidant that has been used in the most enduring of food cultures-Chinese and Japanese tea. The aim of this research was achieved in Swiss albino mice in where liver became dark red in color with considerable hepatomegaly as well as severe venous congestion in the portal vein (PV) and mild central vein dilation with severe congestion found due to excessive green tea intake. Similar finding was found by El Daly, (2011). Mazzanti *et al.,* (2009) stated that hepatotoxicity is probably occurs due to epigallocatechin gallate or its metabolites. From our research we found, the principal active ingredients of green tea is polyphenolic compounds such as epicatechin (EC), epicatechin-3-gallate (ECG), epigallocatechin (EGC) and epigallocatechin-3-gallate (EGCG). So green tea may cause hepatotoxicity. According to Fan, (2016) iron deficiency anemia occurs due to excessive green tea drinking. In our study we found, hemoglobin level of the treated female mice significantly (*$p<0.01$) reduced than the control group mice. Green tea is safe to drink in moderate amounts during pregnancy and epigallocatechin is an active ingredient and a powerful antioxidant in green tea which is important during pregnancy stated by Navarro-Perán, (2005). In our study, we found that mice of both (control and treated) groups gave births (18 pups) which were devoid of any abnormality.

Conclusion

Although green tea is found to be popular recently among the health conscious people but the exact baleful effects rendered by it on health is unclear until today. The present study indicates that green tea has detrimental effects on health specially hepatomegaly, decreasing hemoglobin concentration and massive congestion in both central and portal vein. For future it needs further indeed investigation to understand the pathway of causing such baleful effect on the body both in gross and cellular level.

Acknowledgements

Sincere thanks to the Department of Anatomy and Histology, Faculty of Veterinary Science, Bangladesh Agricultural University, Mymensingh-2202 for technical help in histological slide preparation. A special acknowledgement to MoST, Bangladesh for providing the NST fellowship as a financial support to conduct the research smoothly.

References

Cooper, R., Morré, D. J., & Morré, D. M. (2005). Medicinal benefits of green tea: Part I. Review of noncancer health benefits. *Journal of Alternative & Complementary Medicine*, *11*(3), 521-528.

El Daly, A. A. (2011). Effect of Green Tea Extract on the Rat Liver; Histo-architectural, Histochemical and Ultrastructural Studies. *Journal of American Science*, 7(5), 65-73.

Fan, F. S. (2016). Iron deficiency anemia due to excessive green tea drinking. *Clinical case reports*, 4(11), 1053.

Frank, J., George, T. W., Lodge, J. K., Rodriguez-Mateos, A. M., Spencer, J. P., Minihane, A. M., & Rimbach, G. (2008). Daily consumption of an aqueous green tea extract supplement does not impair liver function or alter cardiovascular disease risk biomarkers in healthy men. *The Journal of Nutrition*, 139(1), 58-62.

Laurie, S. A., Miller, V. A., Grant, S. C., Kris, M. G., & Ng, K. K. (2005). Phase I study of green tea extract in patients with advanced lung cancer. *Cancer chemotherapy and pharmacology*, 55(1), 33-38.

Liu, J., Xing, J., & Fei, Y. (2008). Green tea (Camellia sinensis) and cancer prevention: a systematic review of randomized trials and epidemiological studies. *Chinese medicine*, *3*(1), 12.

Mazzanti, G., Menniti-Ippolito, F., Moro, P. A., Cassetti, F., Raschetti, R., Santuccio, C., & Mastrangelo, S. (2009). Hepatotoxicity from green tea: a review of the

literature and two unpublished cases. *European journal of clinical pharmacology*, 65(4), 331-341.

Navarro-Perán, E., Cabezas-Herrera, J., García-Cánovas, F., Durrant, M. C., Thorneley, R. N., & Rodríguez-López, J. N. (2005). The antifolate activity of tea catechins. *Cancer research*, 65(6), 2059-2064.

Nawab, A., & Farooq, N. (2015). Review on green tea constituents and its negative effects. *J Pharm Innov*, *4*(1), 21-24.

Sinija, V. R., & Mishra, H. N. (2008). Green tea: Health benefits. *Journal of Nutritional & Environmental Medicine*, 17(4), 232-242.

Tomasulo, P. (2004). Natural Medicines Database http://www. naturaldatabase. com. *Journal of consumer health on the internet*, 8(2), 75-85.

Gut Microbiota Alterations from Different *Lactobacillus* Probiotic-Fermented Yoghurt Treatments in Slow-transit Constipation

Chen-Jian Liu[1], Xiao-Ran Li[1*], Xiao-Dan Tang[2], Jie Yu[3], Hai-Yan Zhang[1]

[1] Faculty of Life Science and Technology, Kunming University of Science and Technology, Chenggong, Kunming 650500, Yunnan, China

[2] Department of Gastroenterology, First People Hospital of Yunnan Province, Kunming 650032, Yunnan, China

[3] Yunnan University of Traditional Chinese Medicine, Kunming 650500, Yunnan, China

[*] Corresponding author: starkeyran@163.com

SUMMARY

Constipation is a frequent complaint, and probiotics could have a potentially synergistic effect on intestinal transit. In the present study, yoghurt intake improved the symptoms of slow-transit constipation, which was confirmed in 144 mice (nine groups, n=16) with loperamide-induced constipation. Yoghurt fermented with different probiotics was administered orally. Loperamide treatment caused a marked increase in first defecation time and a decrease in the charcoal transit ratio ($P<0.05$), while loperamide treatment after intake of a new formulation of yoghurt could significantly improve defecation time and intestinal health. Significant ($P < 0.001$) decreases in butanoic acid content were observed in groups given three different strains of yoghurt. Yoghurt intake could also change the intestinal bacterial community composition, which was supported by operational taxonomic unit-related analysis as well as principal coordinates analysis. Our results showed conclusive evidence indicating that yogurt is an excellent functional food that improves the symptoms of slow-transit constipation.

Introduction

Constipation can be divided into three broad categories: normal-transit constipation, slow-transit constipation, and disorders of defecatory or rectal evacuation (obstructive defecation) (Lembo and Camilleri 2003). There is a clear relationship between increased colonic transit time (CTT) and increased symptom severity in patients with chronic constipation (Park et al. 2015).

Probiotics are nonpathogenic microorganisms that, when ingested in adequate amounts, exert health benefits on the host. There has been growing evidence suggesting that probiotics may have a beneficial role in alleviating constipation symptoms, at least with certain probiotic strains (Turan et al. 2014). Functional foods such as yoghurt could be promising in alleviating motility problems of the gastrointestinal tract that relate to constipation. Yoghurt fermented by probiotic is considered a probiotic source with anti-bacterial, anti-mycotic, anti-neoplastic, and immunomodulatory properties. Yoghurt-derived probiotics have been raised as alternative therapeutics for various digestive disorders, and they also show favourable effects on constipation with fewer toxic effects (Choi et al. 2014).

To evaluate the effects of different probiotic strains of fermented yoghurt on changes in faecal parameters, the present study examined the intestinal charcoal transit ratio, short-chain fatty acid content, bacterial community composition in the faeces, and intestinal contents after dissection in loperamide-induced constipated mice after administration of yoghurt. Two formulations of strains were used: *Lactobacillus bulgaricus* and *Streptococcus thermophiles* (Fig. 1).

Materials and Methods

1. *Yoghurt product preparation*

The commercial formulation used in this study consists of two species: *Lactobacillus bulgaricus* and *Streptococcus thermophilus*. The novel formulation used in this study consisted of three species: *Lactococcus lactis*, *Lactobacillus plantarum* and *Lactobacillus casei*. Bacterial concentrations in the yogurt were 10^6 colonies forming units (CFU) per millilitre.

2. *Experimental design*

A total of 144 male Kunming mice (eight weeks old upon receipt; Dashuo, China) were used following acclimatization for 7 days in this study (Fig. 1). Samples collected before the experiment were identified as being collected on day 0. The mice were randomly assigned to nine groups (n=16 in each group, eight mice per cage) in a room with controlled temperature (25±2°C) and humidity (50–70%). The mice were kept under a 12 h: 12 h light: dark cycle. Eight groups were: control mice (C), constipated mice without yoghurt (Y0), constipated mice receiving two probiotic strains of fermented yoghurt with different doses per day (4 mL, Y2H; 2 mL Y2M; 1 mL, Y2L), and constipated mice receiving three probiotic strains of fermented yoghurt with different doses per day (4 mL, Y3H; 2 mL Y3M; 1 mL, Y3L). The positive control group (PC) was given Live Combined *Bifidobacterium* and *Lactobacillus* tablets at 650 mg/kg (Jinshuangqi, China) (Fig. 1). Constipation was induced in the animals by oral administration of 6 mg/kg loperamide hydrochloride (Sigma, MO, USA) in a volume of 6 mg/kg (dissolved in ddH_2O), whereas the control mice (C group) were administered normal water only. Half an hour after taking loperamide or water, all mice were given ink gastric perfusion (10% activated carbon powder and 10% gum arabic). All animals were treated in accordance with the Guidelines for Care and Use of Laboratory Animals of Kunming University of Science and Technology, Kunming, Yunnan, China.

Eight mice randomly selected from each group were euthanized by cervical dislocation 25 min later. Mesentery was isolated from the intestinal cavity and intestinal samples were collected at the upper end of the clipping from the pylorus, bottom to the ileocecal bowel. The length of the total small intestine and the pylorus to the forefront of ink were measured. The intestinal charcoal transit ratio was calculated as follows: charcoal transit ratio (%) = ((total small intestinal length − charcoal meal transit distance)/total small intestinal length) × 100.

3. *Determination of SCFAs*

The standards of acetic acid (A116165), propionic acid (D110443), butanoic acid (B110439) and hexanoic acid (H103630) were chromatographically pure. Hexanoic acid was used as an internal standard. Oxalic acid dehydrate, sodium azide and ultrapure water were also used in this study. The content of short chain fatty acid was calculated according to the standard curve. The analysis of short chain fatty acid was conducted with a gas chromatography system (GC7890, Agilent, USA) coupled to a flame ionization detector (FID).

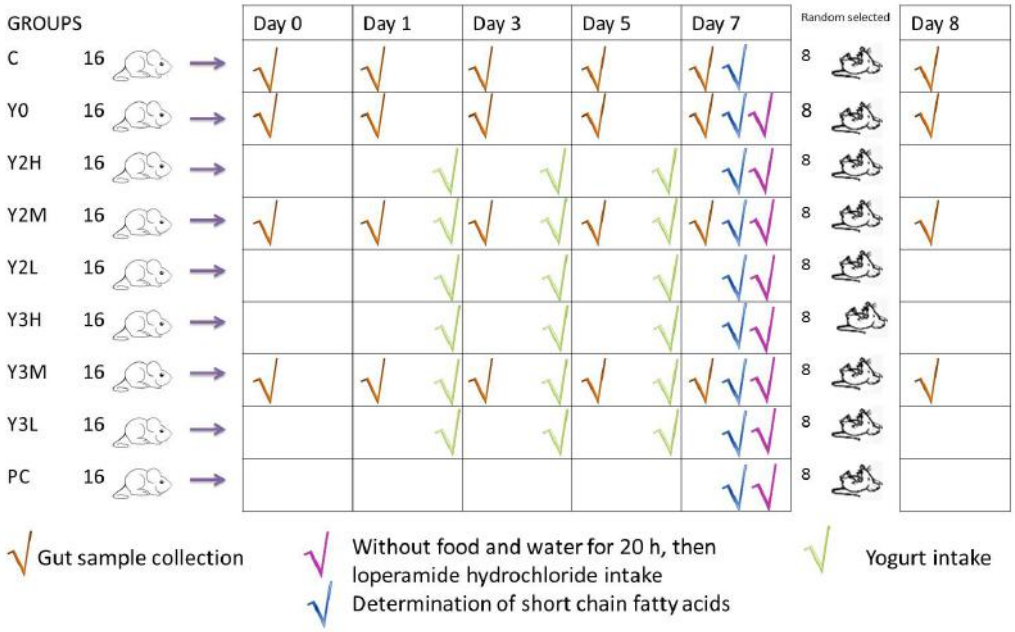

Fig. 1 Experimental design. Nine groups of mice were used as recipients of different treatments: (C) controls; (Y0) constipated mice without yoghurt; constipated mice receiving yoghurt fermented with two probiotic strains at a different dose per day (4 mL, Y2H; 2 mL Y2M; and 1 mL, Y2L); constipated mice receiving fermented yoghurt with three probiotic strains at a different dose per day (4 mL, Y3H; 2 mL Y3M; and 1 mL, Y3L); (PC) positive control.

4. *Bacterial analysis procedure and statistics analysis*

The following four groups were selected for analysis of gut bacterial community: C, Y0, Y2M and Y3M groups. Faecal and small intestine content samples were stored at -20°C prior to DNA extraction. The bacterial 16S rRNA gene was amplified with the following barcoded primers: 343F and 798R. Purified PCR product was mixed for sequencing using the Illumina MiSeq^{TM} system (Illumina, USA). Sequence processing was performed by combining features of Mothur v1.35.1 (Schloss et al. 2009). In addition, sequences were assigned to operational taxonomic units with 97% sequence homology.

All results are presented as the mean±s.d. Differences between groups were investigated using two-way analysis of variance (ANOVA). Differences were considered as significant at $P < 0.05$. Differences in bacterial taxa and host phenotypes among treatments were determined by one-way analysis. RDAs of the C, Y0, Y2M, and Y3M group based on faecal parameters, intestinal charcoal transit ratio and levels of SCFAs were performed using Canoco 5 software.

5. *Nucleotide sequences*

The sequences were deposited in the Short Read Archive under the accession number SRP093954.

Results and Discussion

Mice were observed daily during the experimental period, and no meaningful changes in body weight gain were detected in the mice in all groups during the whole experiment. Favourable effects on first defecation time were detected with all three concentrations of the three yoghurt strains, compared with the control group and non-yoghurt group. The highest intestinal charcoal transit ratio was detected in the groups receiving the yoghurt with three bacterial strains. A significant (P <0.05) increase in the intestinal charcoal transit ratio was detected in the group receiving a high dose of the three-strain yoghurt compared to the control group and non-yoghurt group. More favourable increases in intestinal charcoal transit were detected in all three-strain yoghurt concentration groups compared to the control group and non-yoghurt group (Table 1). A normal intestinal charcoal transit ratio is an obvious sign of improvement in clinical symptoms and an increase in intestinal charcoal transit ratio in yoghurt intake groups was in agreement with other studies (Park, Chae et al. 2015). Chronic constipation is a common clinical condition, which is associated with marked decreases in the quality of life. A marked increase in colonic transit time as well as a decrease in intestinal charcoal transit ratio, the basic symptoms of slow-transit constipation, are significantly improved after yoghurt intake especially with the three-strain yoghurt.

Table 1 also summarizes the results of major SCFA concentrations in intestinal content samples from each group of mice. Among the three major SCFAs, the content of acetic acid was significantly lower only in the Y2L group. Significant ($P < 0.001$) decreases in butanoic acid content were observed in three Y3 groups. SCFAs in PC group didn't show significant difference to the control group and non-yoghurt group. SCFAs producing gut bacteria may affect constipation (Kang et al. 2015). In previous studies, SCFAs being administered into the gut

Table 1 Mice fecal parameters, intestinal charcoal transit ratio and Contents (%) of short-chain fatty acids (SCFAs) comparing nine groups

Groups	First defecation time (min)	Dry weights (g)	Intestinal charcoal transit ratio (%)	Acetic acid (%)	Propionic acid (%)	Butanoic acid (%)
C	163±79	0.20±0.32	0.54±0.11	0.85±0.06	0.20±0.01$^{\#}$	0.32±0.01
Y0	228±129	0.08±0.03	0.50±0.13	0.79±0.05	0.16±0.01*	0.31±0.01
Y2H	153±82	0.06±0.03	0.56±0.16	0.89±0.15	0.21±0.03$^{\#\#}$	0.34±0.03
Y2M	98±48$^{\#}$	0.07±0.01	0.54±0.14	0.77±0.11	0.18±0.02	0.30±0.02
Y2L	166±38	0.08±0.03	0.50±0.06	0.66±0.04$^{*,\#}$	0.16±0.01*	0.21±0.00$^{***,\#\#\#}$
Y3H	118±52$^{\#}$	0.07±0.03	0.73±0.10$^{**,\#\#}$	0.95±0.16	0.19±0.02$^{\#}$	0.24±0.01$^{***,\#\#\#}$
Y3M	52±24$^{**,\#\#}$	0.07±0.04	0.67±0.06$^{*,\#}$	0.74±0.14	0.19±0.03	0.21±0.02$^{***,\#\#\#}$
Y3L	71±21$^{**,\#\#}$	0.06±0.03	0.61±0.1	0.85±0.14	0.17±0.02	0.29±0.03
PC	247±9**	0.09±0.03	0.64±0.08$^{\#}$	0.87±0.11	0.16±0.02*	0.33±0.03

Values are expressed as mean ± SD of 8 mice.
* P<0.05 and ** p<0.001 compared with C group.
# P<0.05 and ## p<0.001 compared with Y0 group.

demonstrated conflicting findings; some studies showed accelerated colonic transit (Mitsui et al. 2005), while others slowed colonic transit (Dass et al. 2007). The reason may be that SCFAs enhance colonic fluid and sodium absorption and thus may aggravate the symptoms of constipation (Binder and Mehta 1989).

The Silva database v123 was used to assign taxonomy to sequences from phylum to genus level. At the phylum level, a total of 28 different bacterial phyla and Candidatus phyla were identified in each sample. The whole bacterial community was similar in each of the four groups. The majority of sequences belonged to *Bacteroidetes* (55.5±3.4%), *Firmicutes* (26.5±2.7%) and *Proteobacteria* (16.9±1.3%), which encompassed more than 98% of all sequences. The two groups receiving yoghurt showed a higher percentage of the phylum *Bacteroidetes* but lower percentage of the phylum *Firmicutes*. The sequences could be definitively assigned into 170 different genera, with an average of 56.2% of sequences being unclassified at the genus level. The nine bacterial genera *Parasporobacterium*, *Desulfobaculum*, *Natronoflexus*, *Pseudoflavonifractor*, *Isobaculum*, *Alkalitalea*, *Sporotomaculum*, and *Cosenzaea*.

A total of more than 3000 OTUs were observed in this study. The top 100 abundant OTUs were defined as core OTUs which represented 79.1% of the total sequences (Fig. 2). The names of OTU were based on the number of sequences. The most abundant OTU0001 showed 100% identity to the uncultured bacterium clone HFDE2698FD10 from dietary-fat-induced taurocholic acid promoting pathobiont expansion and colitis in Il10(-/-) mice (Devkota et al. 2012). This OTU could be aligned with *Bacteroidales*, which was caused by saturated (milk-derived) fat diets. OTU0002 was similar to uncultured *Bilophila* sp. Clone GS16, which was also isolated from the mouse gut (Berry et al. 2015). This bacterium belonged to the family *Desulfovibrionaceae*, which might be related to protein digestion. Both OTU0001 and OTU0002 did not show any difference between samples of the four groups on day 8.

Comparing the sequence percentages of day 8 samples between Y3M and C groups, OTU0003, OTU0008, OTU0012, OTU0019, OTU0029, OTU0032, OTU0037, OTU0046, OTU0047, OTU0049, OTU0069, OTU0093 and OTU0094 showed significant differences ($P<0.05$). The percentage of OTU0003 was higher in Y3M than in the C group. However, the percentage of OTU0003

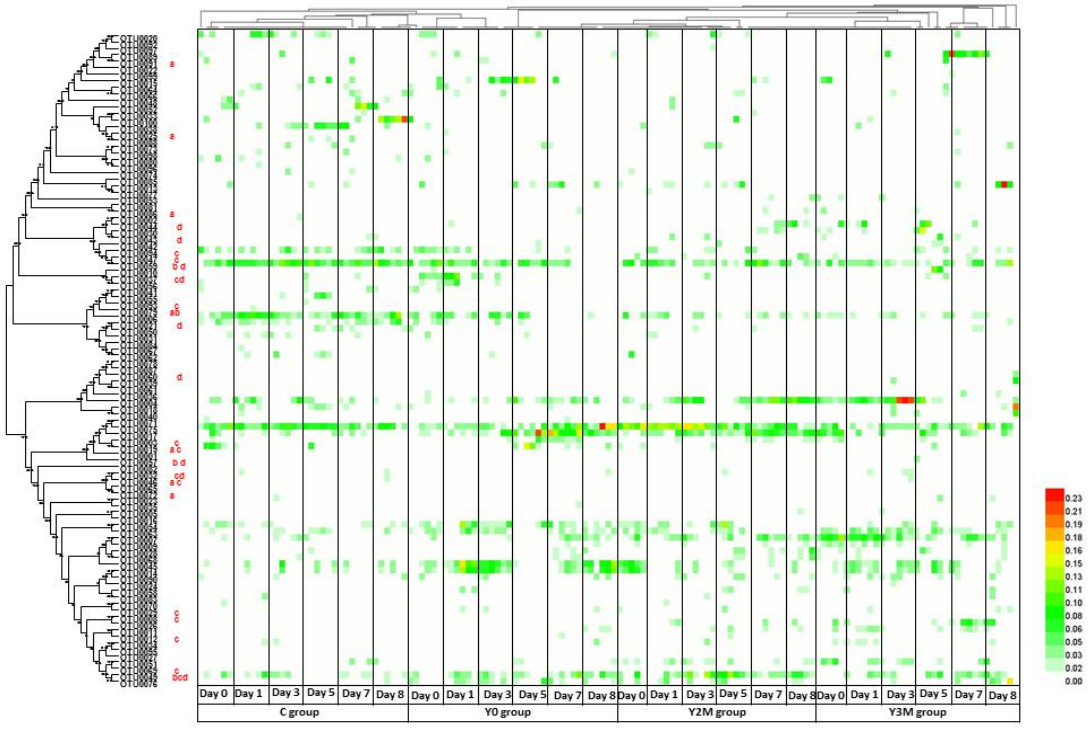

Fig. 2 The abundance of the top 100 OTUs in four groups during the eight-day experimental procedure depending on OTUs identified with a 3% cut-off. The red letters after OTU names indicate OTU percentages of the day 8 samples that are significantly different between different groups: a, C compared to the Y2M group; b, Y0 compared to the Y2M group, c, C compared to the Y3M group; and d, Y0 compared to the Y3M group.

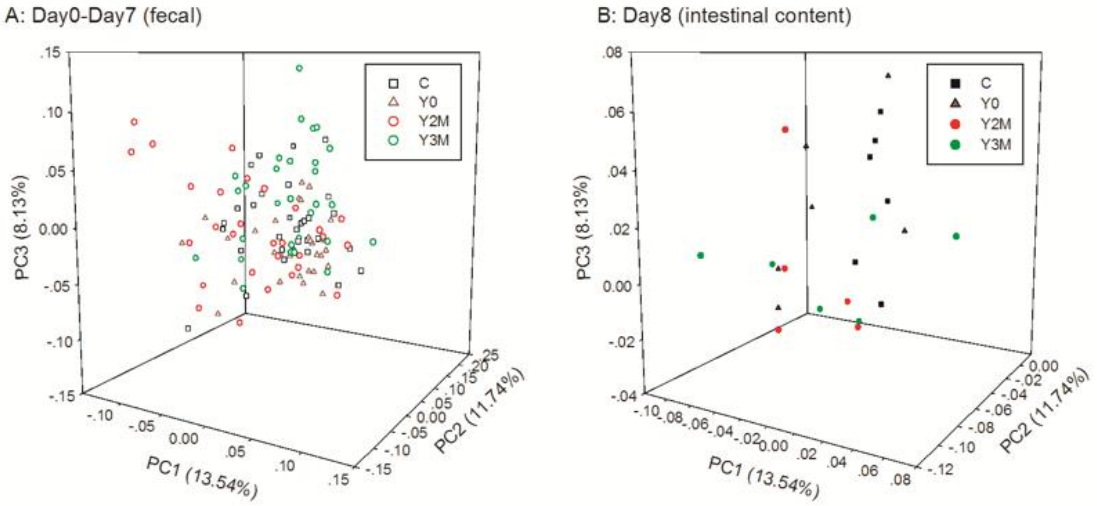

Fig. 3 PCA analysis of the unweighted Unifrac dissimilarities comparing gut microbiota of C, Y0 Y2M and Y3M groups. Each point corresponds to a sample coloured by: black square, C group; dark red triangle: Y0 group; red circle: Y2M group; and green circle: Y3M group; A (hallow): faecal samples on day 0 to day 7; B (solid): intestinal content samples on day 8. The percentage of variation explained by the plotted principal coordinates is indicated on the axes.

was much higher in the Y0 group The OTU0003 was similar to the OTU0019 mentioned above, and both OTUs showed a similar trend, especially low abundance, in the Y3M group. OTU0008, OTU0012, OTU0029 and OTU0069 showed less than 90% similarity to any known bacterium but were 100% similar to uncultured bacterium clones isolated from mouse guts (Devkota, Wang et al. 2012; Lawley et al. 2012).

Previous studies have found that mammalian gut microbial composition can be associated with probiotic intake (Quigley 2007). An exploratory principal coordinates analysis (PCA) on weighted UniFrac dissimilarities was performed to evaluate variation of different groups in bacterial composition. Overall, 33.3% of the total variation was explained by the first three principal coordinates (PC1 = 13.5%, PC2 = 11.7%, PC3 = 8.1%) (Fig. 3). In faecal and intestinal content samples, Y3M and Y2M groups were slightly different from other groups, and were not exactly similar to each other. Hence, yoghurt intake seems to play dominant roles in determining variation in gut microbial composition. Further, samples from the same group were not exactly clustered, which meant even the same diet could result in different intestinal microbes.

The correlations between mouse physiological properties and day 8 samples of the four groups were analysed using Redundancy Analysis (RDA) (Fig. 4). The results of RDA did not show exactly similar relationships

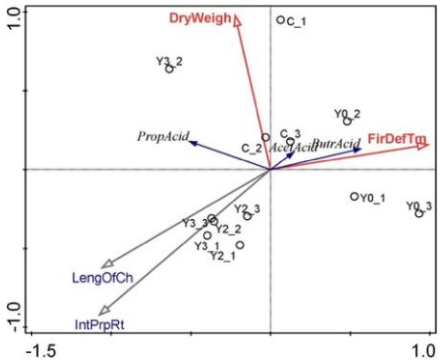

Fig. 4 Redundancy Analysis (RDA) of the C, Y0, Y2M, and Y3M groups based on faecal parameters, intestinal charcoal transit ratio and levels of SCFAs. The lengths of vectors indicate the strength of the correlation between the variables and the ordination scores. DryWeigh: dry weights of faeces; FirDefTm: first defecation time (red word); LengOfCh: length of charcoal meal transferred; IntPrepRt: intestinal charcoal transit ratio; AcetAcid: acetic acid; PropAcid: Propionic acid; and ButrAcid: butanoic acid.

as those determined by one-way analysis. Y2M and Y3M groups were significantly related to length of charcoal meal transferred and intestinal charcoal transit ratio indicating yoghurt intake indeed changed the intestinal microbial community structure, and these changes can significantly decrease intestinal charcoal transit ratio. The Y0 group has a great influence on the first defecation time, which was confirmed by first defecation time results (Table 1). C and

Y0 groups showed a relationship with acetic acid and butanoic acid content, which was not similar with one-way analysis.

Conclusion

Constipation is a common problem and probiotics may contribute to ameliorating the symptoms of functional constipation. This study suggested that the use of yoghurt decreased the defecation time and led to a significant improvement in stool consistency. Yoghurt, especially the three-strain yoghurt used in this study, was also associated with improvements in SCFA concentrations in faeces and increased the intestinal charcoal transit ratio. Further, no significant changes in mouse body weight after yoghurt intake were found, indicating that neither two-strain or three-strain yoghurt will affect mouse health. Although yogurt intake as a functional food could not significantly increase probiotic numbers, intestinal microbial community structures were changed after yoghurt intake, which was confirmed by PCA and RDA analyses. In the top 100 abundant OTUs, a total of 18 OTUs showed significant differences between yoghurt intake and C groups, and 10 OTUs showed significant differences between yoghurt intake and Y0 groups. These OTUs were most often detected in studies of intestinal inflammation, indicating that these OTUs might be correlated with an unhealthy gut. Our results suggest that yoghurt improved gut health, making the development of new yoghurts fermented by different strains necessary.

Acknowledgements

This work was supported by the Discipline Direction Team foundation of Kunming University of Science and Technology (grant number 14078326).

References

Berry, D., E. Mader, et al. (2015). Tracking heavy water (D_2O) incorporation for identifying and sorting active microbial cells. *Proc Natl Acad Sci U S A* 112(2): E194-E203.

Binder, H. J. and P. Mehta (1989). Short-chain fatty acids stimulate active sodium and chloride absorption in vitro in the rat distal colon. *Gastroenterology* 96(4): 989-996.

Choi, J.-S., J. W. Kim, et al. (2014). Synergistic effect of fermented rice extracts on the probiotic and laxative properties of yoghurt in rats with loperamide-induced constipation. Evid Based Complement Alternat Med 2014: 878503-878503.

Dass, N. B., A. K. John, et al. (2007). The relationship between the effects of short-chain fatty acids on intestinal motility in vitro and GPR43 receptor activation. *Neurogastroenterology and Motility* 19(1): 66-74.

Devkota, S., Y. W. Wang, et al. (2012). Dietary-fat-induced taurocholic acid promotes pathobiont expansion and colitis in Il10(-/-) mice. *Nature* 487(7405): 104-108.

Kang, D.-W., J. K. DiBaise, et al. (2015). Gut microbial and short-chain fatty acid profiles in adults with chronic constipation before and after treatment with lubiprostone. *Anaerobe* 33: 33-41.

Lawley, T. D., S. Clare, et al. (2012). Targeted restoration of the intestinal microbiota with a simple, defined bacteriotherapy resolves relapsing clostridium difficile disease in mice. *PLoS Pathog* 8(10): e1002995.

Lembo, A. and M. Camilleri (2003). Current concepts: Chronic constipation. *N Engl J Med* 349(14): 1360-1368.

Mitsui, R., S. Ono, et al. (2005). Neural and non-neural mediation of propionate-induced contractile responses in the rat distal colon. *Neurogastroenterology and Motility* 17(4): 585-594.

Park, H. J., M. H. Chae, et al. (2015). Colon transit time may predict inadequate bowel preparation in patients with chronic constipation. *Intest Res* 13(4): 339-345.

Quigley, E. M. M. (2007). Bacteria: A new player in gastrointestinal motility disorders-infections, bacterial overgrowth, and Probiotics. *Gastroenterol Clin North Am* 36(3): 735-748.

Schloss, P. D., S. L. Westcott, et al. (2009). Introducing mothur: open-source, platform-independent, community-supported software for describing and comparing microbial communities. *Appl Environ Microbiol* 75(23): 7537-7541.

Turan, I., O. Dedeli, et al. (2014). Effects of a kefir supplement on symptoms, colonic transit, and bowel satisfaction score in patients with chronic constipation: A pilot study. *Turkish Journal of Gastroenterology* 25(6): 650-656.

Effects of Food Polysaccharides on Host's Health Associated with the Modulation of Gut Microbiota

Dan Chen, Guijie Chen, Yu Ding, Hong Ye, Xiaoxiong Zeng*

College of Food Science and Technology, Nanjing Agricultural University, Nanjing, Jiangsu, 210095, People's Republic of China

* Corresponding Author: zengxx@njau.edu.cn

SUMMARY

Natural polysaccharides show a variety of effects on host's health. In our recent works, polysaccharides from Fuzhuan brick tea (FBTPS), flower of tea plant (*Camellia sinensis*) (TFPS), fruits of *Lycium barbarum* (LBPS), bee pollen of Chinese wolfberry (WBPPS), *Gracilaria rubra* (GRPS), leaves of mulberry (*Morus alba*) (MALPS), *Brassica rapa* (BRPS), mycelium of *Pholiota dinghuensis* Bi (PDPS), *Paecilomyces hepiali* (PHPS) and *Stachys floridana* (SFPS) were prepared for the evaluation of their bioactivities including antioxidation, hypoglycemic, hypolipidemic and immunomodulating effects. FBTPS, TFPS, LBPS, GRPS, MALPS, BRPS and SFPS were typical acidic heteropolysaccharides. FBTPS was mainly composed of Man, Rha, GalA, Glc, Gal and Ara with little molar contents of Rib and GlcA, TFPS composed of GalA, Gal, and Rha, GRPS consisted of Gal and Fuc, and LBPS consisted of GlcA, GalA, Glc, Gal and Ara. All of the polysaccharides exhibited antioxidative capacity *in vitro* or *in vivo*. FBTPS could significantly impair obesity induced by high-fat diet. TFPS, LBPS, MALPS, BRPS, PDPS, PHPS and SFPS intervention remarkably alleviated the immunocompromise in cyclophosphamide-induced mice. It was revealed that the polysaccharides mentioned above could reach the large intestine safely and were broken down and gradually utilized by human gut microbiota, so the distal gut is the key location where the polysaccharides played its role in. On the contrary, the polysaccharides could significantly modulate the composition and abundance of gut microbiota, and regulate their metabolites, such as short-chain fatty acids (SCFAs) to affect host's health. It was found that the effects of FBTPS on impairing high-fat-induced obesity and TFPS and LBPS on alleviating cyclophosphamide-induced immunocompromise were related to their modulation of gut microbiota.

Introduction

Polysaccharides are a class of structurally diverse macromolecules that are linked together by monosaccharide residues *via* glycosidic bonds. It is worth noting that polysaccharides have the greatest structural variability compared with other natural biopolymers such as proteins and nucleic acids and therefore have the highest capacity to carry biological information. The nucleotides in the nucleic acid and the amino acids in the protein can only be linked to each other in a manner, and the monosaccharide units in the polysaccharide can be connected to each other at a plurality of points to form a plurality of branches or linear structures (Shi, 2016).

The sources of polysaccharides are very diverse. The polysaccharides may be derived from higher photosynthetic plants, fungi, algae, bacteria, etc. At the cellular level, polysaccharides represent both reserve compounds in the cytoplasm (such as starch) and structural components of the biofilm or cell wall of organisms (such as cellulose). The separation, purification and utilization of polysaccharides are essentially dependent on their structural characteristics. The main structures of natural polysaccharides are extremely complex and diverse, but the basic structure of the main chain is often dextran, xylan, fructan, mannan, etc., or a polymer of two or more monosaccharides (such as galactomannan and pectin). Their branched structures are diverse and show great diversity (Chen & Seviour, 2007; Shi, 2016; Shi, Dong, & Ding, 2014; Shi, Fu, & Chen, 2007; Thombare, Jha, Mishra, & Siddiqui, 2016).

Emerging studies have shown that polysaccharides have complex biological activities and multiple functions, especially influence on the immune function of the host. Most of the biological activities and functions of polysaccharides, as it were, related to the immune system

(Wang, Petrella, Nicosia, Bellomi, & Rizzo, 2016). Although the research of polysaccharides started later than the other three types of life macromolecules (proteins, nucleic acids and lipids), due to its important physiological functions and extensive applications are being continuously advanced in the life process, causing increasing people's interests. For now, polysaccharides have become a crucial part of the development of natural medicines and healthcare products. On the basis of incomplete statistics, at least 30 kinds of polysaccharides in the world are currently undergoing standard clinical trials in anti-tumor, anti-viral, and diabetes treatments, respectively (Villares, Mateo-Vivaracho, & Guillamón, 2012). In 2002, global sales of carbohydrate drugs and healthcare products surpassed $19.3 billion (Shi & Wang, 2011). Obviously, the sleeping carbohydrate giant is waking up. Allegedly, studies of the structure and function of polysaccharides have become the third landmark in the exploration of the mysteries of life after the research of proteins and nucleic acids. At present, many countries attempt to use advanced biochemical tools and biotechnology to find more productive polysaccharides and their derivatives from traditional medicine, microbes and marine organisms to overcome diseases such as tumors. Besides, the structure-activity relationship and mechanism of action of polysaccharides were studied. So far, pectin from some plants, β-glucans from higher fungi especially mushrooms, and some sulfate polysaccharides from algae have been intensively studied, among polysaccharides from natural products.

Complex carbohydrates are an important part of the human diet and are ingested in the form of soluble starch and non-starch polysaccharides. Analysis of the human genome revealed that the lack of genes was founded in encoding non-starch polysaccharide degrading enzymes, recognizing that the composition of the human gut microbiota is of considerable worth to human nutrition (Kaoutari, Armougom, Gordon, Raoult, & Henrissat, 2013; Tasse et al., 2010). In recent years, with the discovery of lytic polysaccharide monooxygenases (LPMOs) and polysaccharide utilization loci (PULs), the classical view of microbial polysaccharide degradation has been further developed. Usually the number of enzymes contained in an enzymatic system of a microorganism is directly related to the complexity of the polysaccharide target (Hemsworth, Déjean, Davies, & Brumer, 2016). A growing amount of evidence suggests that the gut microbiota may serve as an important modulator of the crosstalk between dietary polysaccharides and host health. Thus, a number of potential strategies or candidates based on modulation of gut microbiota by dietary polysaccharides, have been presented and evaluated for prevention of diseases and improvement of our health. In recent years, we have been specialized in systematic study on the preparation and valuation of health-promoting functions of dietary polysaccharides. So far, a series of polysaccharides from more than 10 kinds of food source materials with great potential for exploitation were investigated. Recently and more strikingly, our recent works showed that dietary polysaccharides can generally pass through digestive system untouched by human enzymes and transporters, and survive to encounter gut microbiota in large intestine, which act as an important source of energy for gut microbiota thereby shape the composition and physiology of gut microbiota. Thus, we report here the research progress of dietary polysaccharides in our team.

Materials and Methods

1. *Materials*

The polysaccharides in our team were mainly from Fuzhuan brick tea, flower of tea plant (*Camellia sinensis*, Longjing 43), the fruits and bee pollens of *L. barbarum* L., seaweed *G. rubra*, mulberry leaves, *Brassica rapa* L., *Pholiota dinghuensis* Bi, *Paecilomyces hepiali* HN1 and *Stachys floridana* Schuttl. ex Benth, respectively.

2. *Preparation of polysaccharides*

Generally, the polysaccharides were extracted by hot water at about 90 ℃ for several times. Each infusion was filtered and centrifuged at 4000 rpm for 20 min, and the resulting supernatants were collected, mixed with four times volume of ethanol and kept overnight. After centrifuged again, the precipitation was collected, dissolved with water, deproteinized using Sevag method, dialyzed against water and lyophilized, affording crude polysaccharides. The crude products were purified by column chromatography of DEAE cellulose, Sephadex G-50/100, affording purified fractions of polysaccharides for structural and biological evaluation.

3. *Structural characterization*

The structure of polysaccharides was investigated by high-performance liquid chromatography (HPLC), Fourier transform-infrared spectroscopy (FTIR), methylation analysis, gas chromatography-mass (GC-MS), and nuclear

magnetic resonance (NMR) spectroscopy.

4. *Assays of bioactivities and digestibility*

The antioxidant activities *in vitro* of polysaccharides were evaluated by chemical methods, such as Fe^{2+} chelating power and scavenging activities on 2,2-azinobis-(3-ethyl-benzothiazolin-6-sulfonic acid) (ABTS), 1,1-diphenyl-2-picrylhydrazyl (DPPH) free radicals and hydroxyl superoxide, and cell methods such as H_2O_2-induced oxidative injury in PC12 cell. The hepatoprotective activity of polysaccharides was studied using carbon tetrachloride-induced liver injury mice. A RAW 264.3 cell model was used to investigate the immunomodulation capacity *in vitro* (Di et al., 2017), the cyclophosphamide-induced mice were used to investigate the *in vivo* antioxidative and immunomodulation effects (Chen et al., 2019; Di et al., 2017; Ding etal., 2019). The hypolipidemic activities were evaluated by high-fat diet induced mice (Chen et al., 2018). The digestibility of polysaccharides *in vitro* was investigated by simulate digestive system (saliva, simulated gastric and small intestinal conditions). The fermentation *in vitro* by gut microbiota was carried out to investigate the effect of polysaccharides on the gut microbiota.

Results and Discussion

10 kinds of representative polysaccharides from various natural materials were obtained and the monosaccharide compositions are shown in Table 1. Overall, all of these polysaccharides were typical heteropolysaccharides. FBTPS was mainly composed of Man, Rha, GalA, Glc, Gal and Ara with little molar contents of Rib and GlcA, TFPS composed of foremost GalA, Gal and Rha, GRPS consisted of Gal and Fuc, and LBPS consisted of GlcA, GalA, Glc, Gal and Ara. WBPPS was mainly made up of Ara, Gal and GalA. MALPS consisted of Man, Rha, GlcA, Glc, Gal, and Ara. BRPS was mainly composed of GlaA, Ara and Gal, PDPS was mainly made up of Glc. PHPS was mainly composed of Man, Glc, Gal with little molar contents of Rha, Rib, Ara, Xyl, GalA, and GlcA. SFPS consisted of Rha, GlcA, GlaA, Glc, Gal and Ara.

Structure of polysaccharide is very complicated, so it is quite difficult to obtain homogeneous polysaccharide fractions. This is one of the main factors to impede polysaccharide research development. It was found that PHP-1, PHP-2 and PHP-3 were consisted of the backbone of mannan with the units of →2,6)-α-D-Man*p*-(1→ and side chain →6)-α-D-Man*p*-(1→*O*-2 including →2)-α-D-Man*p*-(1→ and non-reducing end α-D-Man*p*, β-D-Gal*p*. The main chain of MALPS-3a was composed of α-(1→3)-Ara and β-(1→4)-D-Gal, and the side chain of 1,3,5-Ara, 1,3,6-Glc, 1,2-Rha, 1,4-GalA and the side chain ends were Glc and Ara (Wu, 2014). The main chain of MALPS-3b was composed of a smooth region formed by repeated ligation of α-1,4-GalA and a hair region formed by the alternate connection of α-1,4-GalA (methylation and acetylation of a partial carboxyl group of GalA) and α-1,2-Rha (Rha has a branch at the 4-position with the side chain includes β-1,4-Gal, α-1,5-Ara, and α-1,3-Ara) (Yuan, 2016).

As abundant evidences have demonstrated that oxidative stress is related to a wide range of disease. Thereinto, antioxidant enzymes in liver, which contribute to the major defense against reactive oxygen species (ROS), play an important role in controlling lipid peroxidation. Our results showed that all of these polysaccharides exhibited antioxidative capacity *in vitro* in cell or *in vivo* in mice (Chen et al., 2018; Di et al., 2017; Yuan et al., 2015). For example, GRPS exhibited strong scavenging activities against ABTS and superoxide radicals and lipid peroxidation inhibition. At a cellular level, GRPS-3-2 showed the strongest protective effect on H_2O_2-induced oxidative injury in PC12 cells. FBTPS showed significant amelioration of high-fat diet-induced oxidative injury in mice (Chen et al., 2018). LBPS could reverse the cyclophosphamide (Cy)-induced liver injury in mice, by significantly decreasing the levels of ALT and MDA, and increasing the levels of GSH, SOD and CAT. TFPS, LBPS, MALPS, BRPS, PDPS, PHPS and SFPS intervention remarkably alleviated the immunocompromise in Cy-induced mice (Chen et al., 2019; Ding, Yan, Chen, et al., 2019).

Digestion is the necessary way for food to play a nutritional function, so it is necessary to evaluate the digestibility of dietary polysaccharides. We have found that the molecular weights of these polysaccharides were not changed under the human saliva and simulated gastrointestinal conditions, indicating that these polysaccharides were not degraded in the alimentary tract. However, the molecular weights of FBTPS, TFPS, LBPS, WBPPS and GRPS were reduced after 24 h of fecal microbiota fermentation *in vitro*, revealing a decomposition capacity of microbiota on these

Table 1 The monosaccharide compositions of 10 kinds of polysaccharides (or their purifications) (mol %).

	Man	Rib	Rha	GlcA	GlaA	Glc	Gal	Xyl	Ara
FBTPS	3.4-4.7	1.5-2.7	9.6-13.4	1.2-1.9	24.3-34.1	11.5-22.0	19.2-24.6		11.8-19.0
TFPS	1.61	3.09	3.26	0.42	50.09	4.88	16.15	5.18	15.33
LBPS				0.31	0.75	0.13	2.40		2.46
WBPPS	0.38	0.09	0.17		0.64	0.22	0.67	0.08	1.03
GRPS-1*							1.79		
GRPS-2*							2.76		
MALPS	0.51		5.13	2.23	3.02	2.13	2.95		2.55
BRPS	0.58		1.14		54.92	1.65	12.39		23.72
PDPS	0.92					92.54	1.82	1.48	2.18
PHPS-1#	53.62	3.20	3.51			13.10	14.17		2.24
PHPS-2#	55.26	3.05	2.85	0.73	0.58	14.08	15.52		4.47
PHPS-3#	25.60	3.78	7.30	6.75	4.43	13.76	30.05	1.35	7.84
SFPS			7.75	1.65	14.92	1.87	33.17		40.64

* The fractions purified from GRPS with DEAE cellulose column and Sephadex G-50 column.
# The fractions purified from PHPS with DEAE cellulose column and Sephadex G-100 column.

polysaccharides. Thus, it was considered that distal gut was the most important place for these polysaccharides to exert their bioactivities.

Trillions of bacteria colonized in the gut forming a mutually beneficial symbiotic relationship with the host during long-term co-evolution. Gut microbes and their metabolites play an important role in maintaining host health (Nicholson et al., 2012). It was found that FBTPS, TFPS, LBPS, WBPPS and GRPS had the significant effect on regulating gut microbiota and promoting the SCFAs production (Chen et al., 2017; Chen et al., 2017; Di et al., 2018; Ding, Yan, Peng, et al., 2019; Zhou et al., 2018). Specifically, either FBTPS TFPS, LBPS or GRPS could significantly reduce the ratio of Firmicutes to Bacteroidetes in phylum level, which was associated with energy metabolism and the risk of obesity (Ley, Turnbaugh, Klein, & Gordon, 2006). Besides, FBTPS significantly increased the levels of *Prevotella* and *Bacteroides*, TFPS enriched *Prevotella*. The relative abundances of genera *Bacteroides*, *Bifidobacterium*, *Phascolarctobacterium*, *Clostridium XlVb*, *Prevotella* and *Collinsella* were enhanced after LBPS fermentation. WBPPS could significantly increase the relative abundances of genera *Prevotella, Dialister, Megamonas, Faecalibacterium*, and *Alloprevotella* and decrease the numbers of genera *Bacteroides, Clostridium XlVa, Parabacteroides, Parasutterella, Escherichia/Shigella*, *Phascolarctobacterium, Clostridium sensu stricto* and *Fusobacterium*.

Thus, a potentially viable concept, modulating the gut microbiota by dietary polysaccharides as new therapeutic target for the prevention of diseases and improvement of health, has been presented. Recently, we have revealed that the immunomodulate effects and the protection of liver against oxidative damage of TFPS and LBPS was associated with the modulation of gut microbiota and their metabolites such as SCFAs (Chen et al., 2019; Ding, Yan, Chen, et al., 2019). Additionally, FBTPS-induced modulation in the gut microbiota was highly associated with metabolic syndrome in obese mice, and these changes might be an important mechanism for FBTPS mediating its beneficial metabolic effects. Therefore, the possible mechanism of metabolic syndrome prevention by FBTPS is that indigestible FBTPS reach the large intestine and then modulate the gut microbiota (Chen et al., 2018).

To normal mice, polysaccharides also exhibited positive effects on maintain host's health. The abundance of *Lactobacillus* in the gut of mice that were administrated with TFPS or LBPS at the dosage of 200 mg/kg/d for 3 months was significantly increased, while the abundance of *Akkermansia* was significantly reduced. Besides, the content of short-chain fatty acids in the gut after ingestion of TFPS and LBPS was significantly higher than that in the normal diet group. TFPS and LBPS intervention showed no significant effect on intestinal morphology, but the expression of claudin1 and claudin5 was increased. These results indicated that TFPS and LBPS had a positive effect on improving intestinal homeostasis (unpublished data). Overall, a summary of our recent work is shown in Fig. 1.

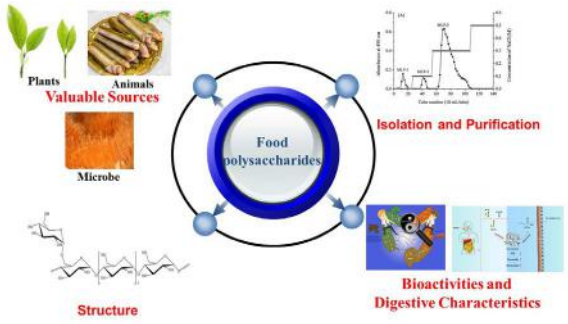

Fig. 1 Summary of our works.

Conclusion

In recent years, a series of polysaccharide were obtained from more than 10 kinds of food source materials, and their structures were preliminarily investigated in our lab. All the polysaccharides were typical heteropolysaccharides, completely made up two or more monosaccharides, and exhibited significantly antioxidant capacities *in vitro* or *in vivo*. Besides, FBTPS could significantly alleviate high-fat diet obesity. The intervention with TFPS, LBPS, MALPS, BRPS, PDPS, PHPS or SFPS remarkably improved Cy-induced immunocompromise in mice. The dietary polysaccharides could escape the digestive system without digestion. The indigestible polysaccharides then safely reached the distal gut where they could be broken down and utilized by the gut microbiota. In turn, the polysaccharides could significantly regulate he composition and abundance of the gut microbiota and their metabolites, such as SCFAs, to affect the health of the host. Furthermore, our work showed that the reduction of high-fat-induced obesity and the reduction of Cy-induced immunodeficiency by dietary polysaccharides were related to their regulation of the gut microbiota, suggested that the gut microbiota may serve as an important modulator of the crosstalk between dietary polysaccharides and our health.

Acknowledgements

The studies were supported by the National Key Research and Development Program of China (2017YFD0400200, 2017YFD0400800 and 2018YFC1604404), Postgraduate Research & Practice Innovation Program of Jiangsu Province (KYCX18_0725 and KYCX17_0632), National Natural Science Foundation of China (31201454 and 31972025) and a project funded by the Priority Academic Program Development of Jiangsu Higher Education Institutions.

References

Chen, D., Chen, G. J., Ding, Y., Wan, P., Peng, Y. J., Chen, C. X., ... Ran, L. W. (2019) Polysaccharides from the flowers of tea (*Camellia sinensis* L.) modulate gut health and ameliorate cyclophosphamide-induced immunosuppression. *Journal of Functional Foods*, 61, 103470.

Chen, D., Chen, G. J., Wan, P., Hu, B., Chen, L. G., Ou, S. Y., ... Ye, H. (2017) Digestion under saliva, simulated gastric and small intestinal conditions and fermentation *in vitro* of polysaccharides from the flowers of *Camellia sinensis* induced by human gut microbiota. *Food & Function* 8(12), 4619-4629.

Chen, G. J., Wang, M. J., Xie, M. H., Wan, P., Chen, D., Hu, B., ... Liu, Z. H. (2018) Evaluation of chemical property, cytotoxicity and antioxidant activity *in vitro* and *in vivo* of polysaccharides from Fuzhuan brick teas. International J*ournal of Biological Macromolecules* 116, 120-127.

Chen, G. J., Xie, M. H., Wan, P., Chen, D., Dai, Z. Q., Ye, H., ... Liu, Z. H. (2018) Fuzhuan Brick Tea Polysaccharides Attenuate Metabolic Syndrome in High-Fat Diet Induced Mice in Association with Modulation in the Gut Microbiota. *Journal of Agricultural and Food Chemistry* 66(11), 2783-2795

Chen, G. J., Xie, M. H., Wan, P., Chen, D., Ye, H., Chen, L. G., ... Liu, Z. H. (2017). Digestion under saliva, simulated gastric and small intestinal conditions and fermentation *in vitro* by human intestinal microbiota of polysaccharides from Fuzhuan brick tea. *Food Chemistry* 244, 331-339.

Chen, J., & Seviour, R. (2007). Medicinal importance of fungal β-(1→3), (1→6)-glucans. *Mycological Research* 111(6), 635-652.

Di, T., Chen, G., Sun, Y., Ou, S., Zeng, X., Ye, H. (2018) *In vitro* digestion by saliva, simulated gastric and small intestinal juices and fermentation by human fecal microbiota of sulfated polysaccharides from *Gracilaria rubra*. *Journal of Functional Foods* 40, 18-27.

Di, T., Chen, G. J., Sun, Y., Ou, S. Y., Zeng, X. X., Ye, H. (2017) Antioxidant and immunostimulating activities *in vitro* of sulfated polysaccharides isolated from *Gracilaria rubra*. *Journal of Functional Foods* 28, 64-75.

Ding, Y., Yan, Y. M., Chen, D., Ran, L. W., Mi, J., Lu, L., ...

Cao, Y. L. (2019) Modulating effects of polysaccharides from the fruits of *Lycium barbarum* on the immune response and gut microbiota in cyclophosphamide-treated mice. *Food & Function* 10(6), 3671-3683.

Ding, Y., Yan, Y. M., Peng, Y. J., Chen, D., Mi, J., Lu, L., ... Cao, Y. L. (2019) *In vitro* digestion under simulated saliva, gastric and small intestinal conditions and fermentation by human gut microbiota of polysaccharides from the fruits of *Lycium barbarum*. *International Journal of Biological Macromolecules* 125, 751-760.

Hemsworth, Glyn R., Déjean, G., Davies, Gideon J., Brumer, H. (2016) Learning from microbial strategies for polysaccharide degradation. *Biochemical Society Transactions* 44(1), 94-108.

Kaoutari, A. E., Armougom, F., Gordon, J. I., Raoult, D., & Henrissat, B. (2013) The abundance and variety of carbohydrate-active enzymes in the human gut microbiota. *Nature Reviews Microbiology* 11(7), 497-504.

Ley, R. E., Turnbaugh, P. J., Klein, S., & Gordon, J. I. (2006). Microbial ecology: human gut microbes associated with obesity. *Nature* 444(7122), 1022-1023.

Ma, L. P. (2012) Extraction, purification, antitumor and emmunoregulation activity of polysaccharide from *Stachys floridana* Schuttl. ex Benth, Nanjing Agricultural University. (Doctoral dissertation).

Nicholson, J. K., Holmes, E., Kinross, J., Burcelin, R., Gibson, G., Jia, W., & Pettersson, S. (2012) Host-gut microbiota metabolic interactions. *Science* 336(6086), 1262-1267.

Shi, L. (2016) Bioactivities, isolation and purification methods of polysaccharides from natural products: A review. *International Journal of Biological Macromolecules* 92, 37-48.

Shi, L., Dong, Q., Ding, K. (2014) Structure elucidation and immunomodulatory activity in vitro of a xylan from roots of *Cudrania tricuspidata*. *Food Chemistry* 152, 291-296.

Shi, L., Fu, Y. L., Chen, K. S. (2007) A novel water-soluble α-(1→4)-glucan from the root of *Cudrania tricuspidata*. *Fitoterapia*, 78(4), 298-301.

Shi, S. S., & Wang, S. C. (2011) Bioactivities of polysaccharides. *China Bulletin Life Science* 23, 662-670

Tasse, L., Bercovici, J., Pizzut-Serin, S., Robe, P., Tap, J., Klopp, C., ... Potocki-Veronese, G. (2010) Functional metagenomics to mine the human gut microbiome for dietary fiber catabolic enzymes. *Genome Research* 20(11), 1605-1612.

Thombare, N., Jha, U., Mishra, S., Siddiqui, M. Z. (2016) Guar gum as a promising starting material for diverse applications: A review. *International Journal of Biological Macromolecules* 88, 361-372.

Villares, A., Mateo-Vivaracho, L., Guillamón, E. (2012) Structural Features and Healthy Properties of polysaccharides occurring in mushrooms. *Agriculture* 2012(2), 452-471.

Wang, P., Petrella, F., Nicosia, L., Bellomi, M., Rizzo, S. (2016) Molecular imaging of stem cell transplantation for liver diseases: Monitoring, clinical translation, and theranostics. *Stem Cells International* 2016, 8.

Wu, Z. W. (2014) Optimization fermentation, purification, stuctureal elucidation and bioactivity of exopolysaccharides from *Paecilomyces hepiali*, Nanjing Agricultural University. (Doctoral dissertation).

Xu, R. J., Ye, H., Sun, Y., Tu, Y. Y., Zeng, X. X., (2012) Preparation, preliminary characterization, antioxidant, hepatoprotective and antitumor activities of polysaccharides from the flower of tea plant (*Camellia sinensis*), *Food and Chemical Toxicology* 50(7), 2473-2480.

Yuan, Q. X., Xie, Y. F., Wang, W., Yan, Y. H., Ye, H., Jabbar, S., Zeng, X. X. (2015) Extraction optimization, characterization and antioxidant activity *in vitro* of polysaccharides from mulberry (*Morus alba* L.) leaves. *Carbohydrate Polymers* 128, 52-62.

Yuan, Q. X. (2016) Isolation, purification, structure and bioactivity of polysaccharides from mulberry (*Morus alba* l.) leaves, Nanjing Agricultural University. (Doctoral dissertation).

Effect of Micellar κ-Casein Dissociation on the Formation of Soluble Protein Complexes and Acid Gel Properties

Md. Sultan MUHOMUD[1,2], Nakako KATSUNO[1], Takahisa NISHIZU[1*]

[1] Department of Applied Life Science, Gifu University, Yanagido1-1, Gifu 501-1193, Japan

[2] Department of Food Engineering and Technology, Hajee Mohammad Danesh Science and Technology University, Dinajpur-5200, Bangladesh.

[*] Corresponding author: nishizu@gifu-u.ac.jp

SUMMARY

This study investigated the role of the dissociation of micellar κ-casein by using cross-linking agent (glutaraldehyde) on the formation of soluble protein complexes and texture of resulting gels. Reconstituted skim milk with different levels of added glutaraldehyde (SM-GTA) and skim milk without glutaraldehyde (SM) were processed with or without heating followed by study of structural properties of prepared acid gel. Acid gels made from heated SM (without GTA) had higher firmness, water holding capacity, storage modulus and dense microstructure than that from heated SM-GTA. The electrophoretic analysis demonstrated that the levels of κ-casein in the serum phase was decreased with increasing GTA concentration in SM attributed to the GTA depreciated the dissociation of micellar κ-casein and subsequent decline in the formation of the soluble protein complexes. Such reduction of soluble protein complexes in SM-GTA resulted in weaker acid gels in comparison to the gel made from SM without GTA.

Keywords: casein micelles, κ-casein, glutaraldehyde, soluble protein complexes, acid gel

Introduction

Textural characteristic of acid milk gel is one of the most important attribute which play a crucial role in sensory evaluation and in consumer acceptability. Heat treatment of milk causes the denaturation of whey proteins, which can in turn interact with the κ-casein via thiol-disulphide exchanges reactions to form whey protein/κ-casein aggregates (Vasbinder et al., 2003; Ozcan et al., 2015). Theses aggregates strengthen the firmness of acid gels. Moreover, it is demonstrated in our previous study (Mahomud et al., 2017) that the formation of the soluble protein complexes as a new significant complex in the heated milk as well as whey proteins enriched milk may increase the network connectivity and promote the number and strength of contact points which cause the firmer gels.

However, formation of such soluble protein complexes is dependent on dissociation of κ-casein followed by interaction with denatured β-lactoglobulin which can be increased continuously with increasing the temperature (Anema et al., 2008). Another approach to alter casein micellar structure is to add cross-linking agent, such as glutaraldehyde (GTA) or genipin into milk resulting in severely inhibited dissociation of micellar κ-casein as well as the formation of soluble protein complexes.

Therefore, the aim of this study was to investigate the effect of the dissociation of micellar κ-casein by using cross-linking agent (GTA) on the formation soluble protein complexes and on the properties of acid gels. By adding the small amount of GTA to SM, it is possible to protect casein micelles from dissociation of micellar κ-casein and reduced the formation of soluble protein complexes.

Materials and Methods

1. *Preparation of milk samples*

Skim milk (SM) was prepared by adding 12 g skim milk powder (Difco™ Skim milk, Wako, Osaka, Japan) with 100 g deionized water to give a milk solution of 10.7% total solids (w/w).

2. *Addition of a cross-linking agent to milk samples*

The cross-linking agent GTA (25% in water, Nacalai Tesque, Kyoto, Japan) was added to unheated SM to give GTA concentrations of 0.1, 0.3, and 0.5mM, respectively.

3. *Heat treatment and centrifugation of milk samples*

The treated milk samples were subjected to heat treatment at 85 °C for 30 min. After heating, the milk samples were rapidly cooled in an ice bath and put 1.5 mL plastic tubes for centrifugation at 20,100 × g and 25 °C for 60 min.

4. *Polyacrylamide gel electrophoresis*

Sodium dodecyl sulfate polyacrylamide gel electrophoresis (SDS-PAGE) was performed using a Bio-Rad mini-gel slab electrophoresis system.

5. *Measurement of casein micelle size*

The size of the casein micelles in heated and unheated milk samples were analyzed by dynamic light scattering (DLS) at 20 °C using a Malvern Zetasizer Nano-ZS (Malvern Instruments Ltd., Malvern, UK).

6. *Preparation of acid gels*

The milk samples were acidified using GDL at a concentration of 2.0% (w/w) at a temperature of 30 °C until the pH of the milk reached 4.6.

7. *Water holding capacity of the acid gels*

A sample of about 25 g of acid gels (AG) was centrifuged (KN-70, Kubota, Tokyo, Japan) at 1250 × g for 25 min. The whey expelled (WE) was carefully separated and weighed. WHC was calculated as follows:

$$\text{WHC } (\%) = \frac{\text{A } - \text{WE}}{\text{A}} \times 100$$

8. *Firmness of the acid gels*

The firmness of the acid gels was determined by a texture analyzer (Sun Rheometer CR-200D, Sun Scientific Co., Tokyo, Japan) using a single-compression cycle test.

9. *Rheological measurement of the acid gels*

The rheological properties of the acid gels during and after acidification were measured using a controlled stress rheometer (AR2000, G2KG, TA Instruments, Newcastle, DE, USA) with a cup and bob geometry consisting of two coaxial cylinders (diameters 37.03 and 35.01 mm).

10. *Confocal laser scanning microscopy*

The microstructure of the acid gels was monitored using confocal laser scanning microscopy (LSM710, Carl Zeiss microscopy GmbH, Jena, Germany).

11. *Statistical analysis*

Any significant difference between sample means was determined with Tukey's honest significant difference test at a significance level of $P < 0.05$.

Results and Discussion

1. *Effect of adding glutaraldehyde to skim milk on the protein interactions and distribution*

Reducing and non-reducing SDS-PAGE of milk samples were carried out to observe the covalent aggregation of denatured whey proteins with micellar κ-casein (Fig. 1A & B). The dissociating micellar κ-casein was involved with denatured β-lactoglobulin in the formation of the heat-induced aggregation in the serum phases of heated samples which was treated as soluble protein complexes (Singh & Creamer, 1991).

It has been shown that high intense band of κ-casein was observed in the heated SM (Fig. 1 B, lane 2) compared to the heated SM-GTA (Fig. 1 B, lane 4, 6, 8). As the concentration of added GTA to SM was increased, the level of dissociating κ-casein was decreased in serum phases. The dissociation of micellar κ-casein from casein micelles was affected adversely by the addition of GTA in SM.

The reason behind the formation of soluble protein complexes is due to the dissociation of micellar κ-casein from the casein micelles to the serum phase in heated SM (Guyomarc'h et al., 2009). The heat induced aggregation

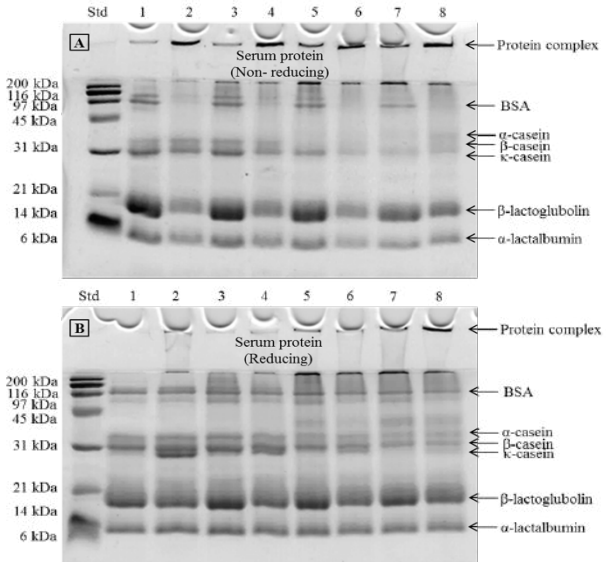

Fig. 1 SDS-PAGE of Gels A (non-reducing) and gels B (reducing) where Lanes 1, 3, 5 and 7 are unheated dispersions and lanes 2, 4, 6 and 8 are heated dispersion of SM and SM-GTA, respectively.

between β-lactoglobulin and κ-casein was remarkable higher in serum of SM compared to SM-GTA. This is due to the preferential heat-induced aggregation of the β-lactoglobulin and dissociating κ-casein in the serum phases which was also reported by Rodriguez and Dalgleish (2006).

2. *Effect of adding glutaraldehyde to skim milk on the particle size of the casein micelles*

The particle size of the casein micelles of milk samples before and after heat treatment is presented in the Table 1. For the heated milk samples, the particle size of the SM-GTA was lower than that of the SM samples. Casanova et al. (2017) demonstrated that the decrease in the casein micelle size could take place when casein micelles were treated with cross-linking agents. The decrease in particle size of SM-GTA with increasing the concentration of GTA could be explained by the smoothing surface of the casein micelles.

Table 1 Z-average particle diameter of unheated and heated milk samples treated with 0, 0.1, 0.3, 0.5 mM glutaradehyde (GTA), respectively.

Sample	Z-average particle diameter in milk samples (nm)	
	Unheated	Heated
SM	205.33 ± 1.94^{a}	192.78 ± 3.27^{a}
SM+0.1 mM GTA	199.80 ± 4.38^{ab}	188.14 ± 2.33^{ab}
SM+0.3 mM GTA	196.41 ± 1.64^{ab}	187.68 ± 1.57^{ab}
SM+0.5 mM GTA	192.85 ± 4.86^{b}	185.81 ± 2.23^{b}

Results are expressed as means of three trials. [a, b] Different lowercase superscripts in the same column are significantly different ($P < 0.05$).

3. *Water holding capacity and firmness of acid gels prepared from skim milk with added glutaraldehyde*

The water holding capacity (WHC) of acid gels made from SM and SM-GTA is shown in Fig. 2A. A significant ($P < 0.05$) increase in WHC was observed in the acid gels prepared from heated SM compared with those prepared from heated SM-GTA. Increased the WHC of acid gels made from heated milk samples was indicated that heat treatment had a great impact on the WHC of acid gels due to the denaturation of whey proteins and their interaction with micellar κ-casein. According to Lee and Lucey (2003), the denaturation of whey proteins and formation of soluble protein complexes creating a homogeneous porous structure, into which free water was immobilized and entrapped.

The effect of addition of GTA to SM on the firmness of set acid gels is presented in Fig. 2B. The acid gel made from heated SM was showed significantly ($P < 0.05$) higher firmness compared with those made from heated SM-GTA. Addition of GTA to SM caused a significant lower firmness in set acid gels compared with no addition of GTA to SM. This result is in agreement with that of Donato et al. (2007) who reported that soluble protein complexes may be important to increase stiffness of the acid gels.

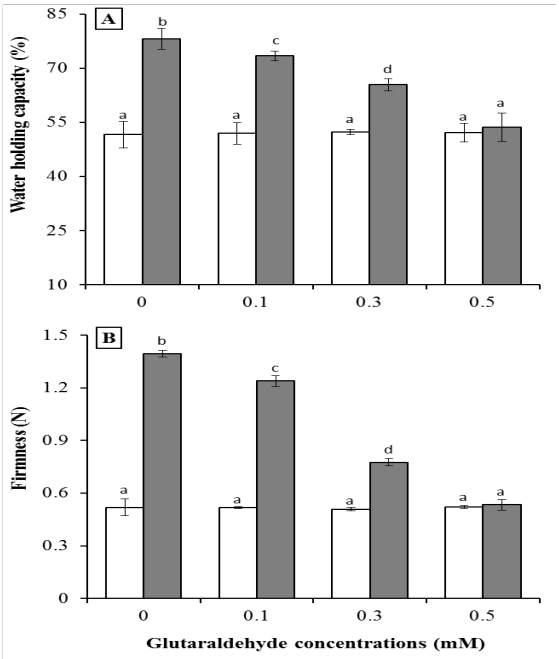

Fig. 2 Water holding capacity (A) and firmness (B) of acid gels made from unheated dispersions (□) and heated dispersions (■) of SM and SM-GTA.

4. *Rheological properties of acid gels prepared from skim milk with added glutaraldehyde*

The changes in storage modulus (G′) of the SM and SM-GTA samples as the reduction of pH from 6.7 to 4.6 using GDL are presented in Fig. 3A. The effect of the addition of small concentration GTA to SM on the rheological properties of acid gels was monitored to determine G′ every 3 min during acidification. Acid gels prepared from heated SM without addition of GTA showed higher final G′ values than those made heated SM with addition of GTA (Fig. 3A). Heating milk at a higher temperature accelerates the denaturation of β-lactoglubolin which forms complex with κ-casein either in the serum phase or in casein micelles (Singh & Creamer, 1991). The active participation of denatured whey proteins in the gel

network by the formation of heat-induced aggregation of β-lactoglubolin with κ-casein stimulates to build the number and strength of bonds between protein complexes, resulting in the increase of storage modulus of acid gels (Lucey et al., 1998).

Other studies (Guyomarc'h et al., 2009) reported that the increased level of soluble protein complexes in the heated SM enhanced to increase the G′ values of the acid gels. Therefore, it may be concluded that dissociation of micellar κ-casein stimulates to form a soluble protein complexes which is responsible for increasing the storage modulus (G′) of acid gels.

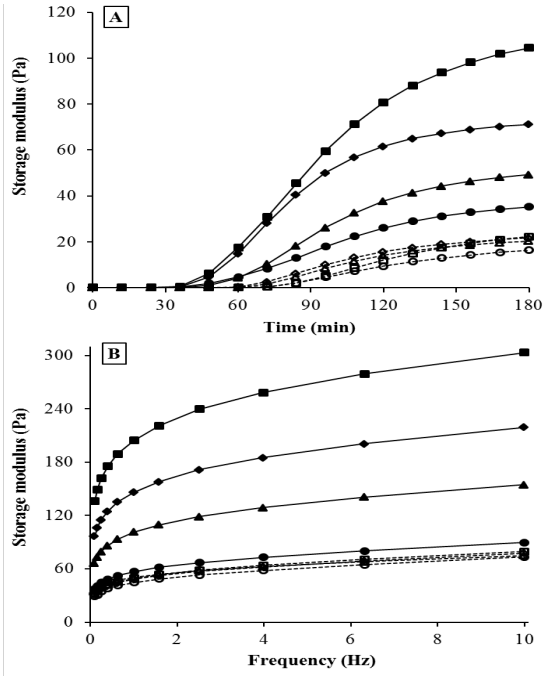

Fig. 3 Storage modulus (G′; A) of gel and storage modulus (G′; B) as a function of frequency sweep made from unheated milk (dotted line) of SM (□), SM+0.1mM GTA (◇), SM+0.3mM GTA (△), and SM+0.5mM GTA (○), respectively and heated milk (solid line) of SM (■), SM+0.1mM GTA (◆), SM+0.3mM GTA (▲), and SM+0.5mM GTA (●), respectively.

5. *Microstructure of acid gels prepared from skim milk with added glutaraldehyde*

The effect of the addition of cross-linking reagents to SM on the microstructure of acid gels analyzed by CLSM is shown in Fig. 4. Acid gels prepared from unheated SM with or without added GTA appeared to have a coarse network with little interconnectivity and more open networks with larger porous space (Fig. 4 A, B, C & D). On the other hand, acid gels prepared from heated SM with or without added GTA had a more branched and compact protein network with less porous space (Fig. 4 E, F, G & H). However, there was more compact microstructure observed in the acid gels made from heated SM compared with those of heated SM with the addition of different concentration of GTA. The possible reasons for increasing compact networks is the presence of more aggregating protein complexes between denatured β-lactoglubolin and κ-caseins in the serum phase (Schorsch et al., 2001). In heated SM without GTA, as a high number of denatured β-lactoglubolin was aggregated with dissociating κ-casein to form soluble protein complexes and some of them was aggregated with micellar κ-casein to form micelle-bond complexes (Lucey et al., 1998). Consequently, the total number of bonds and amount of protein involvement in the protein networks would be higher in acid gel made from heated SM than those made from SM-GTA.

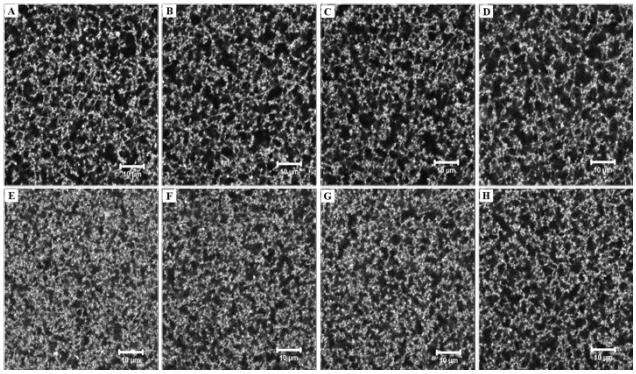

Fig. 4 Confocal laser scanning microscopy images of acid gels made from unheated dispersions of SM (A), SM+0.1mM GTA (B), SM+0.3mM GTA (C), and SM+0.5mM GTA (D), respectively and heated dispersions of SM (E), SM+0.1mM GTA (F), SM+0.3mM GTA (G), and SM+0.5mM GTA (H), respectively.

Conclusion

The dissociation of micellar κ-casein from casein micelles after heat treatment is reduced remarkably with increasing the concentration of GTA in SM. Formation of soluble protein complexes are hence a result of dissociation of micellar κ-casein, which is limited after addition of GTA to SM. The gelation properties of the resultant acid gels are influenced by the application of the small concentration of GTA to SM. The acid gels made from heated SM were showed a high WHC, high firmness, and dense microstructure compared those of made from heated SM-

GTA.

Acknowledgements

The authors are grateful to the Japanese Government for granting the fund through the MEXT scholarship to the PhD scholar.

References

Anema, S. G. (2008). On heating milk, the dissociation of kappa-casein from the casein micelles can precede interactions with the denatured whey proteins. *Journal of Dairy Research*, *75*(4): 415–421.

Casanova, F., Silva, N. F. N., Gaucheron, F., Nogueira, M. H., Teixeira, A. V. N. C., Perrone, I. T., Alves, M. P., Fidelis, P. C., and Carvalho, A. F. D. (2017) Stability of casein micelles crosslinked with genipin: a physicochemical study as a function of pH, *International Dairy Journal.* doi: 10.1016/j.idairyj.2016.12.006

Donato, L., Alexander, M., and Dalgleish, D. G. (2007). Acid gelation in heated and unheated milks: interactions between serum protein complexes and the surfaces of casein micelles. *Journal of Agricultural and Food Chemistry*. *55*: 4160–4168.

Guyomarc'h, F., Jemin, M., Le Tilly, V., Madec, M. N., and Famelart, M. H. (2009). Role of the heat-induced whey protein/κ-casein complexes in the formation of acid milk gels: a kinetic study using rheology and confocal microscopy. *Journal of Agricultural and Food Chemistry. 57*: 5910–5917.

Lee, W. J., and Lucey, J. A. (2003). Rheological properties, whey separation, and microstructure in set-style yogurt: effects of heating temperature and incubation temperature. *Journal of Texture Studies. 34*(5-6): 515-536.

Lucey, J. A., Tamehana, M., Singh, H., and Munro, P. A. (1998). Effect of interactions between denatured whey proteins and casein micelles on the formation and rheological properties of acid skim milk gels. *Journal of Dairy Research. 65*: 555–567.

Mahomud, M. S., Katsuno, N., Zhang, L., and Nishizu, T. (2017). Physical, rheological and microstructural properties of whey protein enriched yogurt influenced by the heating milk at different pH values. *Journal of Food Processing and Preservation.* doi: 10.1111/jfpp.13236.

Ozcan, T., Horne, D. S., and Lucey, J. A. (2015). Yogurt made from milk heated at different pH values. *Journal of Dairy Science*. *98*: 1–10.

Rodriguez, C., and Dalgleish, D. G. (2006). Structures and some properties of soluble protein complexes formed by the heating of reconstituted skim milk powder. *Food Research International. 39*: 472–479.

Schorsch, C., Wilkins, D. K., Jonest, M. G., and Norton, I. T. (2001). Gelation of casein-whey mixtures: effects of heating whey proteins alone or in the presence of casein micelles. *Journal of Dairy Research*. *68*(3): 471–481.

Singh. H., and Creamer, L. K. (1991). Aggregation and dissociation of milk protein complexes in heated reconstituted concentrated skim milk. *Journal of Food Science*. *56*: 238–246.

Vasbinder, A. J., Alting, A. C., Visschers, R. W. and de Kruif, C. G. (2003). Texture of acid milk gels: formation of disulfide cross-links during acidification. *International Dairy Journal. 13*: 29–38.

Impacts of Anti-browning Agents and Blanching Against Browning and Fungal Growth in Trimmed Aromatic Coconut Fruit

Kittiya PAYUHAMAYATAKUL[1], Apiradee UTHAIRATANAKIJ[1,2], Varit SRILAONG[1,2], Panida RENUMARN[3], Kanlaya SRIPONG, Pongphen JITAREERAT[1,2*]

[1] Postharvest Technology Program, School of Bioresources and Technology, King Mongkut's University of Technology Thonburi, Bangkok 10150, Thailand

[2] Postharvest Technology Innovation Center, Commission on Higher Education, Bangkok 10400, Thailand

[3] Department of Innovation and Product Development Technology, Faculty of Agro-Industry, King Mongkut's University of Technology North Bangkok, Prachinburi Campus, Prachinburi province, Thailand.

[*] Corresponding Author: pongphen.jit@kmutt.ac.th

SUMMARY

Major problem of exporting trimmed aromatic coconuts are fungal infection and browning of coconut mesocarp. Thus, the effectiveness of sodium chlorite)SC(and acidified sodium chlorite)ASC(for controlling browning and fungal infection on trimmed coconut fruit were studied in compared with filtrated water and 3% sodium metabisulfite)SMS; commercial treatment(. Dipping pieces of coconut mesocarp in 250 mg/l SC and ASC for 5 min showed the great inhibition of browning but did not inhibit fungal growth. Comparative effectiveness of SC and ASC was investigated by dipping trimmed fruit in filtrated water, 3% SMS and 250 mg/l of SC and ASC for 5 min, then kept at 4 °C for 20 days. The SC treated fruit showed lower browning, brown pigment, and the activity of polyphenol oxidase)PPO, key browning enzyme(in compared with filtrated water and ASC treated fruit. However, the effectiveness of SC to inhibit browning and fungal growth still was lower than SMS treatment. Effectiveness of SC was enhanced when incorporated with blanching and PCV film wrapping. Effects of blanching with hot vapor)HV(and PVC film on browning and fungal contamination of trimmed fruit were studied. The fruit were treated with filtrated water, SMS and HV for 90 sec followed by 250 mg/l SC (HV + SC). After that, each treated fruit were separated into two groups to wrap with PVC film and un-wrapped before kept at 4°C for 25 days. Fruit treated with HV+SC+PVC showed lower color changes (ΔE) of mesocarp, brown pigment and *o*-quinone than filtrated water)both wrapped and unwrapped) and HV + SC)un-wrapped) treatments. Application of HV+SC+PVC also inhibited PPO and peroxidase activities, but did not affect on TA, TSS, percentage of transmittance and thiobarbituric acid)TBA) value of coconut juice. Moreover, overall acceptance of coconut had the highest score compared with other treatments, except SMS treatment. This result suggested that HV + SC + PVC could suppress browning and control fungal contamination without any negative effects on the quality of coconut fruit, even though its effectiveness was not equal with SMS treatment.

Keywords: aromatic coconut, blanching, browning, hot vapor, sodium chlorite

Introduction

Thailand is a great source of agricultural production that serve to the world population. Thailand produces many tropical fruits that are used for consuming in the country and exporting to aboard. Aromatic coconut (*Cocos nucifera* L.) is an important economical fruit that has been promoted as the sport drink by The Food and Agriculture Organization of the United Nations (FAO, 2000). Because coconut water contains a lot of health benefit components such as glucose, fructose, sucrose, potassium, sodium, vitamins and antioxidants (Kailaku et al., 2015). For the coconut trading, the green shell of coconut fruit is peeled and trimmed for being the convenience to consumers and reducing the transportation costs (Paull and Ketsa, 2015). Peeling and trimming the coconut is a cause of rapid browning and easy to infect by various fungi on coconut mesocarp leading to short storage life. It has been known that browning of fruit or vegetables happens after wounding. The browning is a result of the formation of

brown compounds from the oxidation of phenolic compounds by polyphenol oxidase (PPO) (He and Luo, 2007). Sodium metabisulfite (SMS) at 3% is commercially used to prevent browning and fungal infection of trimmed coconut but it can be a cause of asthma for consumers (Lu et al., 2006). Thus, this research was looking for the alternative methods that be safe to the consumer and environment.

Sodium chlorite (SC, $NaClO_2$) and acidified sodium chlorite (ASC) are strong oxidizing agents, which have been accepted by the FDA for use in foods. SC and ASC have dual effects as a anti-microbial agent and anti-browning inhibitor (Lu et al., 2006; He et al., 2008). Recommended concentration of SC to use for fresh produce ranges 500-1200 mg/l (Rao, 2007). In case of ASC, it is produced by the addition of citric acid to SC solution and adjust the pH to be 2.3-2.9. The USDA Food Safety and Inspection Service (FSIS) allows to use 500-1,200 mg/l ASC dip or spray in fruit and vegetables (Rao, 2007).

Heat treatments have been commercially used to maintain the quality to harvested products by minimizing disease infection and insect infestation during storage. Moreover, heat treatment can inhibit the enzyme activities of microorganisms and plant tissue (Corcure et al., 2004). Luckanatinvong et al. (2011) reported that hot steaming the aromatic coconut fruit at 60, 80 and 100 ˚C for 90, 180 and 270 sec followed by dipped in 0.9% SMS for 3-5 min, after that wrapped up with polyvinyl chloride (PVC) film reduced mesocarp browning and decay during cold storage (2±1°C). Especially coconut steamed with hot vapor at 100˚C for 90 sec showed the best quality in term of aromatic and sweet water.

Thus, this research was to study the combined effects of SC, ASC, blanching with hot vapor and PVC film on browning, fungal growth and quality of trimmed aromatic coconut.

Materials and Methods

1. *Effects of SC and ASC at different concentrations on browning and fungal growth of coconut mesocarp pieces*

Aromatic coconut fruit 6 months after anthesis were peeled the green shell. Pieces of coconut mesocarp were obtained by vertical shearing and cutting them into small pieces, approximately 4 x 4.5 x 0.7 cm in size, and immediately dipped in filtrated water)control(, 3% SMS, 250-1000 mg/l SC or ASC for 5 min. All samples were drained and placed into plastic baskets, then covered with a polyethylene plastic)PE(bag and kept at 4 °C for 10 days. Each treatment had four replicates. The inhibition of browning and fungal growth on mesocarp pieces were evaluated every 2 days.

2. *Effects of SC and ASC on browning and fungal growth of trimmed coconut fruit*

Green shelled coconut fruit were peeled and immediately dipped in filtrated water)control(, 3% SMS, 250 mg/l SC or ASC, each for 5 min. All fruit samples were packed as described above and kept at 4 ºC for 20 days. Each treatment had four replicates (fruit). Fungal growth inhibition, browning pigment and PPO activity of coconut mesocarp were investigated 5 days interval.

3. *Combined effects of SC, hot vapor and PVC film on browning and quality of trimmed coconut fruit*

Green shelled coconut fruit were peeled and immediately dipped in filtrated water)control(, 3% SMS, hot vapor for 90 sec followed by 250 mg/l SC (HV + SC). After that, each set of treated fruit were separated into two groups for wrapping with PVC film and un-wrapping with PVC film. All fruit were kept at 4°C for 25 days. Each treatment had four replicates (fruit). Fungal growth inhibition, color difference (ΔE), browning pigment, the activity of PPO and POD of coconut mesocarp were investigated 5 days interval. Titratable acid (TA), total soluble solids (TSS) content, percentage of transmittance and thiobarbituric acid)TBA) value of coconut juice were also determined 5 days intervals.

4. *Quality and biochemical analysis*

Color changes of coconut mesocarp were determined using a Minolta DP-301 colorimeter)Konica Minolta; Tokyo, Japan(. L^*, a^* and b^* values were recorded for calculating the difference color of mesocarp)ΔE(and percentage of browning inhibition as described by Maskan)2001(and Sapers and Douglas)2007(respectively. The total soluble solid content, titratable acid and percent of transmittance of the coconut water was determined using hand refractometer)ATAGO PAL-1(, the method of A.O.A.C. (1990) and Campos et al.)1996(respectively. O-quinone content, polyphenol oxidase)PPO(and peroxidase activity in mesocarp were measured according to the method of Degl' Innocenti et al. (2007), Duan et al.)2007(and Zhang and Shao (2005), respectively.

5. *Microbiological analysis*

Coconut mesocarp were cut into the small pieces (1.0

x 1.0 cm). Five pieces randomly selected and placed on potato dextrose agar)PDA(contained antibiotic to inhibit bacterial growth. PDA plates were incubated at 27±2 °C for 3 days. Numbers of coconut pieces showed the fungal mycelium were counted and calculated as the percent of fungal growth.

6. *Statistical analysis*

Data were analyzed using the ANOVA procedure in the general linear models procedure of SAS 9.0)SAS Institute; Cary, NC, USA(for completely randomized design experiments. Data were presented as mean ± SE. Each treatment contained four replicates. Significance was tested at $p \leq 0.05$ using Duncans multiple range test.

Results and Discussion

Browning and fungal infection are the major problem for trimmed aromatic coconut trade. The present work showed the effectiveness of SC and ASC on browning and fungal infection of the pieces of coconut mesocarp. Result found that dipping pieces of coconut mesocarp in 250-1,000 mg/l SC or ASC for 5 min showed the great inhibition of browning in compared with the control (filtrated water) but there were not effects to inhibit fungal growth (data not shown). Effect of SC and ASC on fungal growth in this experiment differed from the previous research. Microbial contamination on fresh cut pear and fresh cut potato was reduced by treating with 300 mg/l SC (Xiao et al., 2011) and 500 mg/g ASC (Sun et al., 2012).

250 mg/l SC and ASC were selected to compare their effectiveness on browning inhibition of trimmed coconut fruit. Trimmed fruit were dipped in filtrated water, 3% SMS and 250 mg/l of SC and ASC for 5 min before storage. The SC treated fruit showed lower brown pigment and PPO activity in compared with filtrated water and ASC treated fruit (Fig. 1). This result implied that SC is a greater strong oxidizing agent than ASC although the effectiveness of SC and ASC to inhibit browning still was lower than SMS treatment. Several researches demonstrated that application of SC could reduce browning by inactivating the browning enzyme such as PPO activity in fresh-cut apple (Luo et al., 2011) and rose apple (Mola et al., 2016). He et al. (2008) stated that SC might oxidize the co-factor (Cu^{2+}) of PPO resulting to change the enzyme structure to be inactivate form.

Enhancing the effectiveness of SC solution on the inhibition of browning and fungal growth was found when

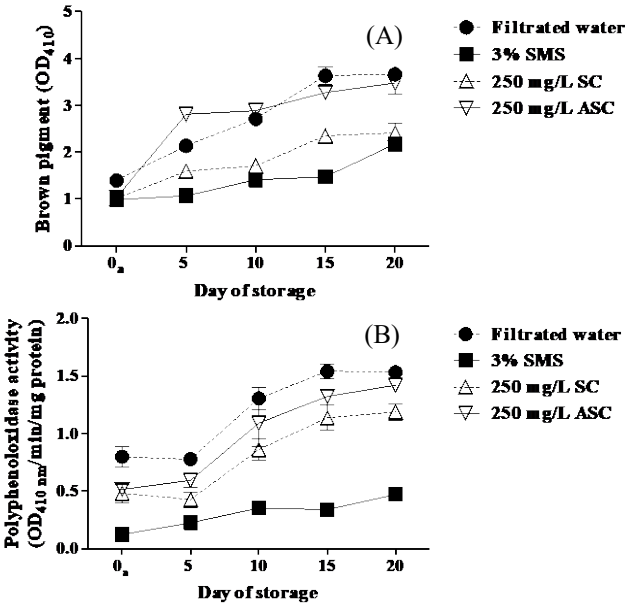

Fig. 1 Browning pigment (A) and polyphenol oxidase activity (B) of the mesocarp of trimmed coconut treated with filtered water (control), 3 % SMS and 250 mg/l

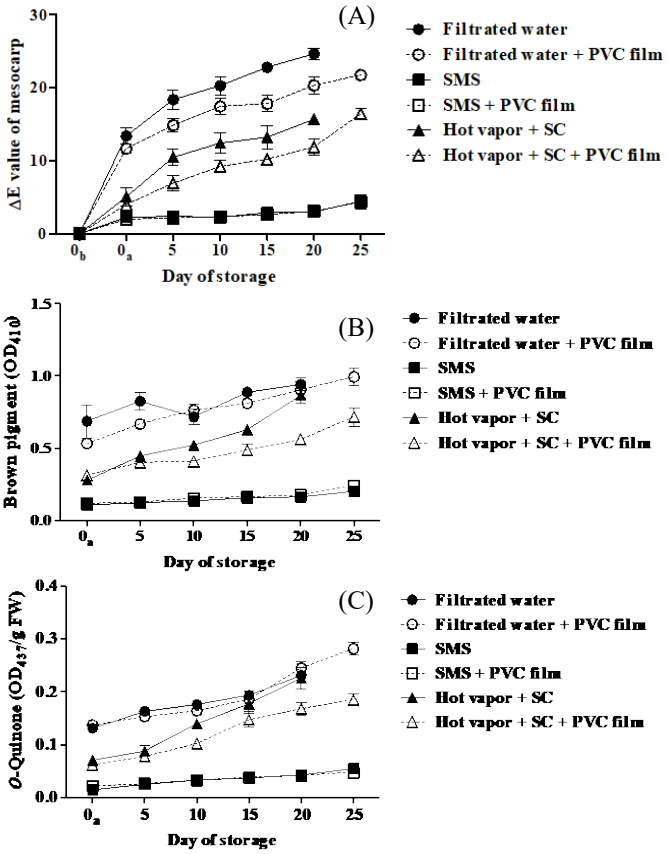

Fig. 2 Color difference (ΔE, A), browning pigment (B) and *O*-quinone content (C) of the mesocarp of trimmed coconut treated with hot vapor for 90 sec, then dipping in 250 mg/l SC for 5 min followed by wrapping or unwrapping with PVC film .Coconut treated with filtered water or 3% MS with and without PVC film were used as the controls. All samples were stored at 4 °C for 25 days.

incorporated with HV for 90 sec with PCV film. Trimmed coconut fruit treated with HV+SC with and without PVC wrapping showed greatest effects to inhibit browning as indicated by lower values of color difference (ΔE), brown pigment and *o*-quinone content (Fig. 2). Treatment of HV+SC+PVC also inhibited PPO and peroxidase activities (Fig. 3), but was not effects on TA, TSS, percentage of transmittance and thiobarbituric acid)TBA) value of coconut juice (data not shown). Moreover, it was found that HV+SC+PVC treatments could suppress the fungal growth when compared with the filtrated water treatment (Fig. 4) These results could explain that the reduction of microbial growth and browning might be caused by heat treatment inactivated the enzyme activities of microbial and plant tissue (Corcure et al., 2004) such as browning enzymes (PPO and POD) (Klein and Lurie, 1992; Luo et al., 2015). Oday Husham Kamil et al. (2011) stated that heat treatment affected on the chemical reactions of fungal cells. Fungal growth become slow down if the temperature is higher than the optimal temperature due to less efficiently chemical reaction. However, if the temperature is over than the critical point, the fungal growth will stop, the lipid and protein structure of fungi are changed, and cell components begin to be damaged resulting to fungal d eath. The other reason of fungal death may be involved with antimicrobial property of SC. SC is a strong oxidizing agent that can provide active chlorine dioxide)ClO_2(. ClO_2 can interfere the microbial protein synthesis resulted to limit microbial growth)Trinetta et al., 2012(. However, this result showed that trimmed coconut fruit treated with HV+SC with PVC wrapping showed the better result to control browning than HV+SC without PVC wrapping. This can be explained that PVC wrapping prevented oxygen transmission from the outside through inside of the film. Therefore, under the low level of oxygen condition, PPO activity will be slow down due to low oxidation in coconut mesocarp (He and Luo, 2007).

Therefore, this result suggested that HV+SC+PVC could reduce the fungal infection and browning of coconut without negative effect on the coconut quality even through its effectiveness was not equal with SMS treatment.

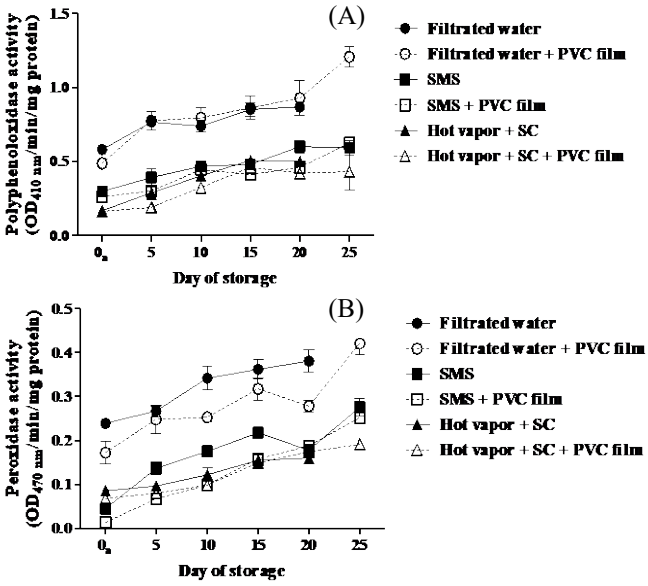

Fig. 3 Polyphenol oxidase (A) and peroxidase (B) of the mesocarp of trimmed coconut treated with hot vapor for 90 sec, then dipping in 250 mg/l SC for 5 min followed by wrapping or unwrapping with PVC film .Coconut treated with filtered water or 3% SMS with and without PVC film were used as the controls. All samples were stored at 4 °C for 25 days.

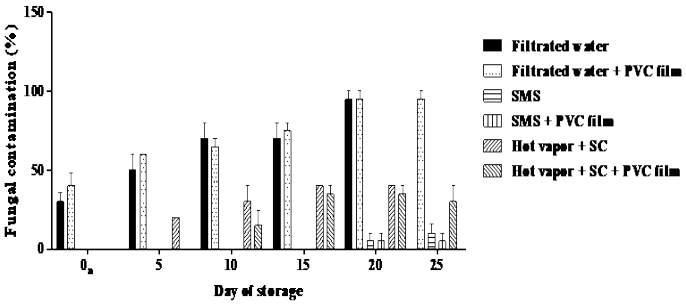

Fig. 4 Fungal growth on the mesocarp of trimmed coconut treated with hot vapor for 90 sec, then dipping in 250 mg/l SC for 5 min followed by wrapping or unwrapping with PVC film .Coconut treated with filtered water or 3 %SMS with and without PVC film were used as the controls. All samples were stored at 4 °C for 25 days.

Conclusion

Sodium chlorite (SC) at 250 mg/l showed the greater anti-browning effect than acidified sodium chlorite (ASC) at 250 mg/l but at this concentration were less effect to control fungal growth on trimmed coconut. The efficiency of SC against browning and fungal infection of trimmed coconut was enhanced when cooperated with hot vapor for

90 sec followed by wrapping with PVC film although their effectiveness was not equal with SMS treatment. Furthermore, HV + SC + PVC treatment did not have any negative effects on the quality of trimmed coconut fruit such as TA, TSS, percentage of transmittance and thiobarbituric acid (TBA) value of coconut juice.

Acknowledgements

This research was supported by The National Research Council of Thailand)NRCT(of the fiscal year 2017. The authors thank to The United Graduate School of Agricultural Science (UGSAS), Gifu University, Japan for supporting some equipment in this study.

References

A.O.A.C. (1990). Official methods of analysis of The Association of official analytic chemists.

Campos, C.F., Souza, P.E.A., Coelho, J.V., and Gloria, M.B.A. (1996). Chemical composition, enzyme activity and effect of enzyme inactivation of flavor quality of green coconut water. *Journal of Food Processing and Preservation* 20, 487–500.

Corcuera, J.I.R.D., Cavalieri, R.P. and Powers, J.R. (2004). Blanching of foods [Online], Available: https://pdfs.semanticscholar.org/8a19/726d0c7d7cf60b5ce8bef8cf3863542aa8ed.pdf [9 August 2019].

Degl'Innocenti, E., Pardossi, A., Tognoni, F. and Guidi, L. (2007). Physiological basis of sensitivity to enzymatic browning in "lettuce", "escarole" and "rocket salad" when stored as fresh-cut products. *Food Chemistry*, 104(1), 209–215.

Duan, X., Su, X., You, Y., Qu, H., Li, Y. and Jiang, Y. (2007). Effect of nitric oxide on pericarp browning of harvest longan fruit in relation to phenolic metabolism. *Food Chemistry* 104, 571–576.

FAO (2000). Coconut water as energy drink for joggers and athletes-First patent granted to un-food agency. Press Release 00/51.

He, Q. and Luo, Y. (2007). Enzymatic browning and its control in fresh-cut produce. *Stewart Postharvest* 6, 1–7

He, Q., Luo, Y.G. and Chen, P. (2008). Elucidation of the mechanism of enzymatic browning inhibition by sodium chlorite. *Food Chemistry* 110, 847–851.

Kailaku, S.I., Syah, A.N.A., Risfaheri, Setiawan, B. and Sulaeman, A. (2015). Carbohydrate-electrolyte characteristics of coconut water from different varieties and its potential as natural isotonic drink. *International Journal on Advanced Science Engineering Information Technology* 5(3), 174–177.

Klein, J.D. and Lurie, S. (1992) Reviews: Heat treatments for improved postharvest quality of horticultural crops. *Hort Technology* 2(3), 316–320.

Lu, S., Luo, Y. and Feng, H. (2006). Inhibition of apple polyphenol oxidase activity by sodium chlorite. *Journal of Agricultural and Food Chemistry* 54, 3693–3696.

Luckanatinvong, V., Somkeaw, P. and Siriphanich, J. (2011). Quality of blanched aromatic coconut for export. *Agricultural Science Journal* (Thailand) 42 (3), 181–184.

Luo, Y., Lu, S., Zhou, B. and Feng, H. (2011). Dual effectiveness of sodium chlorite for enzymatic browning inhibition and microbial inactivation on fresh-cut apples. *LWT- Food Science and Technology* 44(7), 1621–1625.

Luo, Z., Ki, D., Xie, J., Feng, S. and Wang, Y. (2015). Effect of heat treatment on quality and browning of fresh-cut sugarcane. *Journal of Food Processing and Preservation* 39, 688–696.

Maskan, M. (2001). Kinetics of colour change of kiwifruits during hot air and microwave drying. *J. Food Eng* 48. 169–175.

Mola, S., Uthairatanakij, A., Srilaong, V., Aiamla-or, S., and Jitareerat, P. (2016). Impacts of sodium chlorite combined with calcium chloride, and calcium ascorbate on microbial population, browning, and quality of fresh-cut rose apple. *Agriculture and Natural Resources* 50, 331–337.

Oday Husham Kamil, Dumitru Lupuliasa, Doina Draganescu, and Lavinia Vlaia. 2011. Interrelations of drying heat and survival of different fungal spores within the tablets formulation. Studia Unversitatis 'Vsile Goldis', Seria Stiintele Vietii, 21(2), 339–342.

Paull, R.E. and Ketsa, S. (2015). Coconut: postharvest quality-maintenance guidelines [Online], Available: www.ctahr.hawaii.edu/oc/freepubs/pdf/F_N-45.pdf [4 February 2016]

Rao, M.V. (2007). www.fao.org/fileadmin/templates/agns/pdf/jecfa/cta/68/Acidified_Sodium_Chlorite.pdf

Saper, G.M. and Douglas, F.W. (1987). Measurement of enzymatic browning at cut surface and in juice of raw apple and pear fruits. *Journal of Food Science* 5, 1258–1262.

Sun, S.H., Kim, S.J., Kwak, S.J. and Yoon, K.S. (2012). Efficacy of sodium hypochlorite and acidified sodium chlorite in preventing browning and microbial growth on fresh-cut produce. *Preventive Nutrition and Food Science* 17, 210–216.

Trinetta, V., Morgan, M. and Linton, R. (2012). Chlorine dioxide for microbial decontamination of food. Microbial Decontamination in the Food Industry, pp.533–562.

Xiao, Z., Luo, Y., Luo, Y., and Wang, Q. (2011). Combined effects of sodium chlorite dip treatment and chitosan coatings on the quality of fresh-cut d'Anjou pears. *Postharvest Biology and Technology* 62, 319–326.

Zhang, X. and Shao, X. (2005). Characterization of polyphenol oxidase and peroxidase and the role in browning of loquat fruit. Czech *Journal Food Science* 33, 109–117.

Effect of Edible Laccase on Chinese Bread Texture

Maharani Pertiwi KOENTJORO[1*], Desy Lailatul RACHMAH[2],
Endry NUGROHO PRASETYO[2]

[12]Department of Medical Laboratory Technology, Faculty of Health, Nahdlatul Ulama University of Surabaya, Jl. Jemursari 51–57, Surabaya, 60237, Indonesia
[2] Department of Biology, Faculty of Science, Institut Teknologi Sepuluh Nopember, Gedung H Kampus ITS Keputih Sukolilo, Surabaya, 60111, Indonesia
[*] Corresponding Author: maharani@unusa.ac.id

SUMMARY

Laccase application in the food industry is an alternative and innovative solution for natural ingredients since it is able to improve the food quality especially for baking industry. Laccase is a natural catalyst which could improve the structure of gluten in dough by increasing phenol oxidation resulting a better bread texture, taste, volume, and freshness. The aim of this study was to evaluate *Trametes versicolor* laccase oxidation on physicochemical quality of Chinese bread. Laccase were pasteurized to obtain edible laccase with the final activity as 774.7 U/ml. Laccase treatment managed to reduce bread hardness until 9.55 N. The softening phenomenon was related to the laccase–mediated depolymerization of the cross–linked network. Chemical parameters of laccase treatment were 0.065 ppm lower than control. The functional group in the polymer pretreatment mixture of edible laccase observed by Fourier Transform Infrared Spectrometer (FTIR) showed the formation of disulfide group at a wavelength of 450–500 cm^{-1}. The Scanning Electron Microscope analysis revealed formation of gluten protein which has smaller and uniform pores compared to the control group. Based on the results obtained in the present study, laccase from *Trametes versicolor* can be considered a promising application to improve quality of Chinese bread at industrial level.

Keywords: laccase, *Trametes versicolor*, physicochemical quality, Chinese bread

Introduction

Laccase (EC 1.10.3.2) is a type of enzyme containing polyphenol oxidase, which can oxidize polyphenols, methoxy–substituted phenols, and diamine (Minnusi et al. 2002). Among plants, fungi, and bacteria, white–rot fungi are the major laccase producer. Laccase by *Trametes versicolor* has been produced using lignin containing materials (Shraddha et al. 2011; Imran et al. 2012; Offia–Olua, 2014).

Laccase in the food industry has been implemented in a dough as bread quality improver to increase volume or crumb structure and softness in the baked products (Minnusi et al. 2002; Imran et al. 2012; Osma et al. 2010). Laccase from *T. versicolor* have been evaluated to their ability to increase the strength of the gluten structure prior oxidizing lignocellulose in flour (Kaur et al. 2014; Minnusi et al. 2002). The elastic properties of low–protein flour used in making Chinese bread has a weak gluten index therefore it needs to be improved using laccase (Gulia and Khatkar, 2015).

Generally, the baking industry uses artificial food additives such as baking soda (sodium bicarbonate) to increase volume and delighting texture. Long–term of chemicals consumption could result negative impact of human health thereby reducing serum iron and calcium levels in the body which lead to specific doses toxicity (Fakhri et al. 2016). It is well known that the addition of certain enzymes to the dough have unwanted side effects. Since the enzyme are denaturated and inactivated by heat during cooking process (Gallagher et al. 2009). Therefore, the application of laccase as an enhancer of the texture of the bread is less health risks.

The objective of this study was to determine the effects of edible laccase from *T. versicolor* on the texture of Chinese bread by measuring phenol content, functional groups, and micro visual characters.

Materials and Methods

1. *Laccase production*

1.1 *Organism and cultivation conditions*

The *T. versicolor* fungi are a culture collection of Microbiology and Biotechnology Laboratory, Department of Biology, Institut Teknologi Sepuluh Nopember (ITS) Surabaya, Indonesia. The fungi cultures were maintained on Potato Dextrose Agar (PDA) medium and incubated at 28°C, for 6 days before using as seeding. The procedures of maintaining fungi culture is briefly explained as follows. Sporulated PDA medium were dislodged and washed with PBS sterile. As much as 10 mL of 10^8 CFU fungi spores' suspension were inoculated into 100 mL of Potato Dextrose Broth (PDB) (pH 6.0) and incubated for 6 days at room temperature (25°C) with a rotary shaker at 130 rpm (Jo et al. 2010; Qin et al. 2017).

1.2 *Partially edible laccase production*

All experiments were carried out in 300–mL Erlenmeyer flasks containing 100 mL culture medium. The medium contained 4.5 g/L rice husk, 1.5 g/L yeast extract, 1 g/L $C_6H_{12}O_6$, 0.5 g/L NH_4Cl and 100 mL of salt solution. The salt solution contained 2 g/L KH_2PO_4, 0.5 g/L $MgSO_4.7H_2O$, 0.1 g/L $CaCl_2.2H_2O$ and 0.5 g/L KCl and maintained pH 5.0, (Koentjoro et al. 2016). $CuSO_4$ was added by dissolving 100 mg in 1 L of dH_2O as laccase inducer. The medium was autoclaved at 121°C for 15 min. Each flask was inoculated using an agar piece 1 cm^2 cut from an actively growing fungal culture. The flasks were incubated at 30°C on a rotary shaker (130 rpm). The culture broth was filtered, clarified by centrifugation at 10,000 rpm for 15 min, frozen, defrosted and then filtered to remove the precipitated polysaccharides. The resulting clear filtrate was used for the further experiment. Partially edible laccase was sterilized by pasteurizing (or High Temperature Short Time) (HTST) is as follows, a total of 50 mL of laccase solution was placed in a water bath heated at 72°C for 25 seconds (Ranieri et al. 2009).

2. *Characterization of laccase*

2.1 *Laccase activity*

Laccase activity was determined as the increase in absorbance at 468 nm due to the oxidation of 2,2 –azino–bis (3 ethylbenzothiazoline–6–sulfonate) (ABTS) at 30°C (Koentjoro et al, 2016). The reaction mixture contained 200 µL 10 mM ABTS, 300 µL enzyme solution in 500 µL 100 mM citrate buffer, pH 4.5.

Oxidation of ABTS was observed spectrophotometrically at 436 nm for 5 minutes. The laccase activity is calculated based on the ABTS standard curve. One unit (U) of laccase activity was defined as the amount of enzyme required to oxidize 1 µmol ABTS per minute and considered equivalent to 1 unit of enzyme activity ($\varepsilon 420 = 36000\ M^{-1}\ cm^{-1}$ and path length l = 1 cm) (Wolfenden and Wilson, 1982).

2.2 *Isoelectric point (pI)*

To investigate the isoelectric point of supernatant, as much as one mL of laccase was incubated in each tube containing a phosphate buffer with variable pH level (3.0, 4.0, 5.0, 6.0, 7.0 and 8.0) at room temperature for overnight. The occurring of precipitation was monitored and justified as the isoelectric point of laccase in particular pH level.

2.3 *Total Protein determination in enzyme solution*

Total Protein concentration in supernatant was determined by Bradford method using Bovine Serum Albumin (BSA) as standard. Reaction was started by addition of 0.1 mL of supernatant and 5 mL of Bradford reagent (10 mg of Coomassie Brilliant Blue G–250 in 5 mL of 95% ethanol, 10 mL of 85% phosphoric acid, and 85 mL of dH_2O). The changes in absorbance due to laccase content in supernatant were recorded by spectrophotometer in absorbance at 595 nm.

3. *Preparation of laccase modified Chinese bread*

Dough was made manually by mixing flour with enzymes, yeast, water and sugar. The experimental formulations set are shown in Table 1. The average of duplicate data was used in analysis. The dough in each experimental formulation was divided into 6 similar weight. The dough was placed in a bowl covered with a

Table 1 Composition of bread with different levels of edible laccase

Sample	Sample 1	Sample 2	Sample 3	Sample 4
Treatment	Negative control	Non–Edible Laccase	Edible Laccase	Baking soda
Flour wheat low protein (gr)	100	100	100	100
Non–Edible Laccase	0	1.5	0	0
Edible Laccase	0	0	1.5	0
Baking soda (gr)	0	0	0	400
Yeast (gr)	2.2	2.2	2.2	2.2
Water (mL)	50	50	50	50
Sugar (gr)	20	20	20	20

plastic foil and allowed to stand at room temperature (28°C) for 45 minutes. The dough was then steamed for 7 minutes (Laohaprasit and Sricharoenpong, 2018).

4. *Laccase modified Chinese bread analysis*

4.1 *Total phenol content*

Total phenolic content was determined according to Folin–Ciocalteu method with slightly modified. Every extraction solution of bread (10 mL) was mixed with 10 mL of 96% ethanol and 5 mL of 0.1% HCl for 10 min. The reaction mixtures were allowed shaking in a rotary shaker for 30 minutes at room temperature. The mixtures were then centrifuged for 10 minutes at 4,000 rpm and the supernatant was collected. Every extraction of supernatant (1 mL) was mixed with 100 µL of Folin–Ciocalteu reagent and 1 mL of sodium carbonate 15% (w/v). After incubation for 1 hour at room temperature, the absorbance was measured at 710 nm using a spectrophotometer. Total phenol was calculated from the calibration curve of tannic acid and expressed as milligram of tannic acid equivalent per gram of dough (mg TAE/g).

4.2 *Texture profile analysis*

Evaluation of dough properties (hardness) was carried out by texture profile analysis. The test consists of compressing a bite–piece of bread two times in a reciprocating motion that imitates the action of the jaw and extracting from the resulting force–time curve a hardness parameters. The test was applied on bread by using following procedures. Each sample was placed on the Texture Analyzer (SMS) mod.TA.HDi 500 (Stable Micro Systems, Surrey, UK) preparation table followed by applying a pressure using a piston diameter of 75 mm (Ayala–Soto et al. 2017).

4.3 *Scanning Electron Microscope (SEM)*

The micro structural of starch granules in bread with different formulation were studied using Scanning Electron Microscope. Samples were prepared by knife cutting then placed on a carbon tip followed by gold and palladium coating. The SEM images of each samples were taken at magnification of 3,000 (Wojciechowicz–Budzisz et al. 2015).

4.4 *Fourier Transform Infrared Spectroscopy (FTIR) Analysis*

The FTIR analysis in this study has been carried out in order to identify functional groups shifting in every treatment at a wavelength between 800–3600 cm^{-1} (Amir et al. 2013).

5. *Statistical analysis*

The data obtained were then analyzed using of one–way variance (ANOVA) Duncan test using Minitab 14.0 (Minitab 14 Statistical software, 2014). Meanwhile, a qualitative descriptive design was conducted for texture and functional group analysis.

Results and Discussion

1. *Production and characterization of edible laccase*

The activity of laccase before and after pasteurization were calculated as 799.4 and 774.7 U/mL, respectively (Table 2). These results demonstrated the pasteurization processes has no effect on laccase activity.

Table 2 Activity and quantitative estimation of laccase production

Laccase	Activity (U/mL)	Protein Contain (mg/mL)
Before pasteurization	799.4	0.02
After pasteurization	774.7	0.11

The pI of the non–and edible laccase was determined on pH 3.0. This information is helpful to developing purification scheme as a crucial factor in enzyme purification, the precipitation occurs is avoided (Xia, 2007). This result is consistent with the study of Afreen et al (2017) which stated that generally, laccase has an isoelectric point between at pH 3.0–3.1.

The pasteurization did not change the total protein in laccase solution as shown in Table 2. It is indicated that laccase can be pasteurized using heating with a certain temperature and time that serves to kill pathogenic microorganisms while maintaining physical properties (Verhoeckx et al. 2015).

2. *Texture Analysis (Test Hardness)*

Bread treated with edible laccase was demonstrated in deformation in cavity characters (Fig. 1). The pretreatment–control had a greater cavity compared to non–and edible laccase pretreatment. Moreover, between non–and edible laccase Chinese bread has a small and uniform cavity. The result confirms the findings of Salinheimo et al (2007) and Tsegaye et al. 2018.that the bread treated with laccase has a small and uniform cavity. The small and uniform cavities, due to the ability of the laccase to form crosslinking in arabinoxilan through ferulic acid side groups allowing strengthen of gluten and more ability to retain gas (Meybodi et al. 2015). Therefore, the

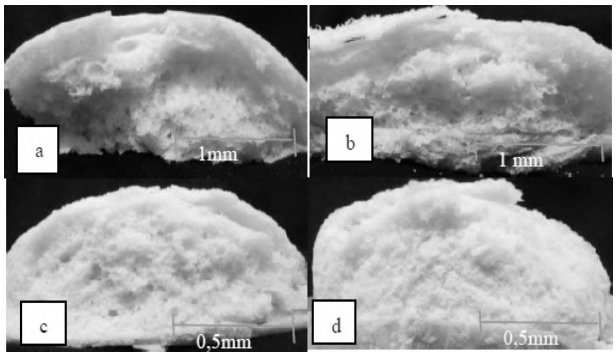

Fig. 1 Cross Section of Chinese Bread with a Variety of Pretreatment a) Control b) baking soda c) non–edible laccase d) edible laccase.

pasteurization does not affect the protein component of laccase.

3. *Total Phenol Analysis*

Analysis of total phenols in various treatments for dough are reported in Table 3. The non–pretreatment and edible laccase experimental group both of them have a lower total phenol concentration of 0.096 and 0.065 ppm respectively compared to a control of 0.168 ppm. This is because of ability of laccase to oxidize phenolic compounds such as ferulic acid that act as laccase mediator in a laccase–mediator system (LMS) reaction mode (Imran et al. 2012; Everette et al. 2014). The higher amount of oxidized phenol, it will increase the formation of disulfide groups (Linares–García et al. 2019). The ferulic acid is oxidized and formed radicals and continues to oxidize the sulfidryl (SH) groups. The oxidation can affect the natural disulfide formation (S–S) in gluten polymers and increase the rate of protein depolymerization lead to increase gluten networks (Linares–García et al. 2019).

Texture analysis on various treatments are shown in Table 4. Pretreatment of edible laccase and controls had a significantly different hardness value of 9.55 and 21.9 N respectively. These results indicated that the addition of laccase to the dough was able to reduce the hardness of the Chinese bread. This is consistent with the statement (Osma et al. 2010; Brijwani et al. 2010) that the laccase shows an oxidizing effect to improve the structure of gluten in the dough and can reduce stiffness, increase volume, improve crumb structure, and increase the softness of bread. Indeed, one good parameter of bread quality is a soft texture and low hardness (Borla et al. 2014). In addition, in Table 4 the non–and edible laccase pretreatment showed non–significantly different of hardness level which shows that pasteurization has no effect on the laccase protein component due to glycosylation. The edible laccase has a greater hardness value (9.55N) compared to non–edible one (9.15 N), this is most probably because of the different laccase activity shown in Table 2.

Table 4 A comparison of the physicochemical characteristics of bread

Pretreatment	Hardness (N)
Control	21.9 ± 0.269^{b}
Baking soda	17.97 ± 3.514^{b}
Non–Edible Laccase	9.15 ± 0.869^{a}
Edible Laccase	9.55 ± 0.262^{a}

Notes: Values with different superscript letters within a column are significantly different ($p \leq 0.05$. Data are expresses as means values of two samples ± standard deviation

4. *Scanning Electron Microscope (SEM) Analysis*

SEM analysis was taken to investigate the effect of laccase on microstructure of whole bread. This technique allowed a qualitative description of the structural cell and their distribution.

As shown in Fig. 2, that the microstructure of gluten bread was more uniform and more number of pores after adding of laccase due to higher volume of gas was released during dough fermentation.

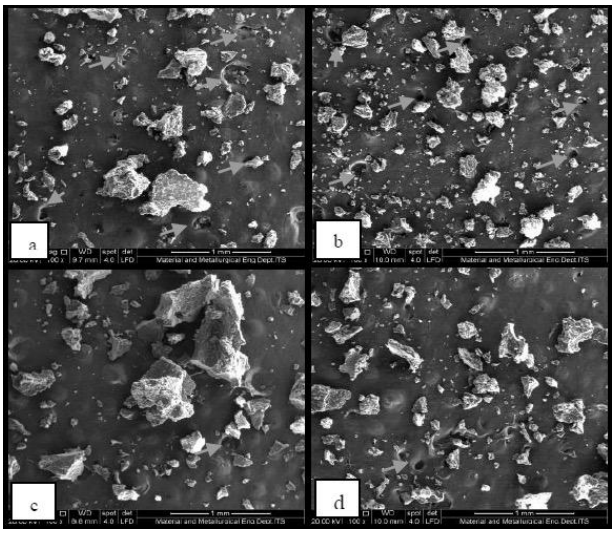

Fig. 2 SEM of a) control; b) baking soda; c) non–edible laccase; d) edible laccase at 1000X magnification Arrows show pores on gluten tissue.

The pore structure can be caused by the presence of an elastic gluten protein matrix which is able to withstand the development of gas while the cell walls was not easily broken (Ortolan and Steel, 2017).

5. *FTIR analysis*

FTIR spectroscopy of bread functional groups at various pretreatments was done in the range of 400–4000 cm^{-1} (Fig. 4). Characters of spectral bands were similar for control and laccase containing bread. Major peaks were indicated absorption of OH groups at a wavelength range of 3000–3,700 cm^{-1}.

In the range of 450–500cm^{-1} there is a change in the peak (peak) spectra at the pretreatment of non–edible laccase and edible laccase. At this wavelength range is the absorption of disulfide groups (S–S) (Amir et al. 2013). Disulfide groups are formed due to the oxidation process in sulfidryl groups which can affect the natural disulfide formation (S–S) (Linares–García et al. 2019).

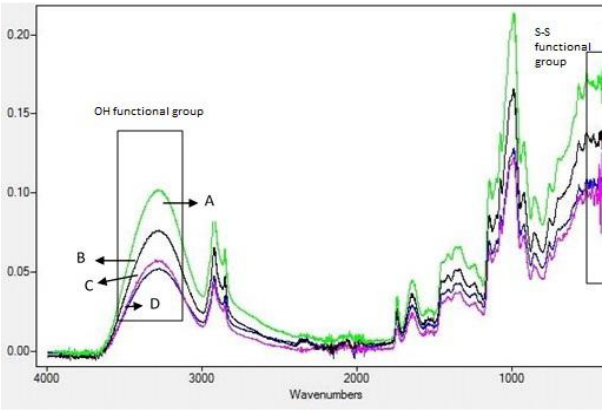

Fig. 3 FTIR spectra of bread in variety treatment

Conclusion

Laccase can be pasteurized excellently without decrease their activity. Pretreatment of edible laccase was able to reduce the value of bread hardness up to 9.55 N. The functional group in the polymer pretreatment mixture edible laccase formed a disulfide group formation at a wavelength of 450–500cm^{-1}. The structure of gluten was formed in uniform pores compared to controls. Therefore, applying laccase as natural food additives is able to improve bread texture quality.

Acknowledgements

The authors would like to thank the anonymous reviewers for their insightful suggestions.

References

Afreen S, Shamsi TN, Baig MA, Ahmad N, Fatima S, Qureshi MI, Hassan MI, Fatma T. 2017. A novel multicopper oxidase (laccase) from cyanobacteria: Purification, characterization with potential in the decolorization of anthraquinonic dye. *PLOS ONE*, https://doi.org/10.1371/journal. pone.0175144.

Amir, R. M, Anjum, F. M., Khan, M. I., Khan, M. R., Pasha, I., Nadeem, M. (2011) Application of Fourier transform infrared (FTIR) spectroscopy for the identification of wheat varieties. *Journal Food Science and Technology* 50, 1018–1023.

Ayala–Soto, F. E., Serna–Saldívar, S. O., Welti–Chanes, J. (2017) Effect of arabinoxylans and laccase on batter rheology and quality of yeast–leavened gluten–free breads. *Journal of Cereal Science* 73, 10–17.

Bertrand B, Martínez–Morales F, and Trejo–Hernándes MR. 2013. Fungal laccases: Induction and production. *Revista Mexicana de Ingeniería Química*, 12 (3): 473–488.

Borla OP, Motta EL, Saiz AI, Fritz R. 2004. Quality parameters and baking perfoemance of commercial gluten flours. *Swiss Society of Food Science and Technology*, 37: 723–729.

Brijwani, K., Rigdon, A., Vadlani, P. V. (2010) Fungal laccase: prduction, function and application in food processing. *Enzyme Research* 2010, 1–11.

Everette, D. Jace., Q. M. Bryant., A. M. Green., Y. A. Abbey., G. W. Wangila., R. B. Walker. A Thorough Study of Reactivity of Various Compound Classes Toward the Folin–Ciocalteu Reagent. *J Agric Food Chem* 58(14) (2014) 8139–8144.

Fakhri, Y., Amanidaz. N., Zandsalimi, Y., Dadar. M., Moradi. A., Moradi, B., Amirhajeloo, L. R., Keramati, H., Rafieepour, A. (2016) Association between sodium bicarbonate consumption and human health: A systematic review. *International Journal of Medical Research and Health Sciences* 5, 22–29.

Koentjoro, M. P, Fitriana, M., Isdiantoni, Prasetyo, E. N. (2016) Enzymatic modification of cotton fiber for promising smart medical based material. *Proceedings – 2018 1st International Conference on Bioinformatics, Biotechnology, and Biomedical Engineering*, BioMIC 2018, DOI: 10.1109/BIOMIC.2018.8610599.

Gulia N. and Khatkar B.S. 2015. Quantitative and Qualitative Assessment of Wheat Gluten Proteins and their Contribution to Instant Noodle Quality. *International Journal of Food Properties*, 18 (8): 1648–1663.

Hughes, A., Brown, A., Valento, M. (2016) Hemorrhagic encephalopathy from acute baking soda ingestion. *Western Journal of Emergency Medicine* 17, 619–622.

Imran, M., Asad, M. J., Hadri, S. H., Mehmood. S. 2012.

Production and Industrial Applications of Laccase Enzyme. *Journal of Cell and Molecular Biology* 10, 1–11.

Jo W–S, kang M–J, Choi S–Y, Yoo Y–B, Seok S–J, Jung H–Y. 2010. Culture Conditions for Mycelial Growth of Coriolus versicolor. *Mycobiology*, 38 (3): 195–202.

Kaur, S., Nigam V. (2014) Production and application of laccase enzyme in pulp and paper industry. *International Journal of Research in Applied, Natural and Social Sciences* 2, 153–158.

Laohaprasit N and Sricharoenpong K. 2018. Development of Chinese steamed bread with Jerusalem artichoke (*Helianthus tuberosus* L.) tubers. *Food Research*, 2 (3): 263–269.

Linares–García L, Repo–Carrasco–Valencia R, Paulet PG, Schoenlechner R. 2019. Development of gluten–free and egg–free pasta based on quinoa (Chenopdium quinoa Willd) with addition of lupine flour, vegetable proteins and the oxidizing enzyme Pox. *European Food Research and Technology*: https://doi.org/10.1007/s00217–019–03320–1.

Meybodi, N. M., Mohammadifar, M. A., Feizollahi, E. (2015) Gluten–free bread quality: A Review of the improving factors. *Journal of Food Quality and Hazards Control* 2, 81–85.

Minnusi, R. C., Pastore, G. M. Duran, N. (2002) Potential applications of laccase in the food industry. *Trends in Food Sciences and Technology* 13, 205–216.

Offia–Olua, B. I. (2014) Chemical, functional and pasting properties of wheat (Triticum spp)–walnut (Juglansregia) flour. *Food and Nutrition Sciences* 5, 1591–1604.

Ortolan F and Steel CJ. 2017. Protein characteristics that affect the quality of vital wheat gluten to be used in baking: A review. *Comprehensive Reviews in Food Science and Food Safety*, 16 (3): https://doi.org/10.1111/1541–4337.12259.

Osma, J. F., Herrera–Toca, J. L. Rodrı́guez–Couto, S. (2010) Uses of laccases in the food industry. *Enzyme Research* 2010, 1–8.

Gallagher, E. (2009) Improving gluten–free bread quality through the application of enzymes. *Agrofood Industry hi–tech* 20, 34–37.

Qin, Z., Yue, Q., Borras–Hidalgo, O., Liu, X. (2017) Laccase enzyme from Trametes versicolor with a high decolorizing ability on malachite green. *EC Microbiology* 10, 127–133.

Ranieri, M. L., Huck, J. R. Sonnen, M. Barbano, D. M., Boor. K. J. (2009) High temperature, short time pasteurization temperatures inversely affect bacterial numbers during refrigerated storage of pasteurized fluid milk. *Journal of Dairy Science* 92, 4823–4823.

Selinheimo E, Autio K, Kruus K, Buchert J. 2007. Elucidating the mechanisms of laccase and tyrosinase in wheat bread making. *Journal of Agriculture and Food Chemistry*, 55: 6357–6365.

Shraddha, Shekher, R. Sehgal, S., Kamthania, M., Kumar, A. (2011) Laccase: Microbial sources, production, purification, and potential biotechnological applications. *Enzyme Research* 2011, doi:10.4061/2011/217861.

Tsegaye Z, Tefera G, Gizaw B, Abatenh E. 2018. Characterization of Yeast Species Isolated from Local Fruits used for Bakery Industrial Application. *Journal of Applied*, 1 (1): 2581–7566.

Verhoeckx KCM, Vissers YM, Baumert JL, Faludi R, Feys M, Flanagan S, Herouet–Guicheney C, Holzhauser T, Shimojo R, Bolt NCV, Wichers H, Kimber I. 2015. Food processing and allergenicity. *Food and Chemical Toxicology*, 80: 223–240.

Wojciechowicz–Budzisz, A., Gil, Z., Spychaj, R., Czaja, A., Pejcz, E., Czubaszek, A., Zmijewski, M. (2015) Effect of Acetylated Retrograded Starch (Resistant Starch RS4) On the Nutritional Value and Microstructure of the Crumb (SEM) of Wheat Bread. *Journal of Food Processing and Technology* 6, DOI: 10.4172/2157–7110.1000450.

Wolfenden B. S. and Willson R. L. 1982. “Radical–cations as reference chromogens in kinetic studies of one–electron transfer reactions,” *Journal Chemical Society Perkin Transactions*, vol. 2, pp. 805–812, 1982.

Physical, Chemical and Sensory Properties of the White Bread from Acetylated Jack Bean Flour

Achmad Ridwan ARIYANTORO[1*], Bambang Sigit AMANTO[1], Rizki NOVITASARI[2]

[1] Department of Food Science and Technology, Faculty of Agriculture, Sebelas Maret University, Jalan Ir. Sutami 36 A, Kentingan, Surakarta, 577, Indonesia

[2] Alumni of Department of Food Science and Technology, Faculty of Agriculture, Sebelas Maret University, Jalan Ir. Sutami 36 A, Kentingan, Surakarta, 577, Indonesia

[*] Corresponding Author: ridwan030586@gmail.com

SUMMARY

White bread is the preferred type of bread and it can be consumed by a variety of ages. Production of white bread in Indonesia is increasing every year. The main ingredients of white bread are wheat flour. Unfortunately, wheat could not grow very well in Indonesia. It will affect the increment of the number of imports in wheat flour. Therefore, it is necessary to substitute wheat flour with the others. The alternative is jack bean flour, which has been made from local commodities and it has high carbohydrate and protein content. Native jack bean flours still have weaknesses such as unstable viscosity on high temperature and shear stress, high retrogradation and syneresis. The modification can overcome these problems, one of the methods is acetylation process.

The aim of this research was to determine the selected formula of white bread, which has good sensory properties. Physical properties (baking expansion) and chemical properties (moisture, ash, fat, protein, carbohydrates and salt content) of white bread using acetylated jack bean flour (AJBF) also were investigated. The results show white bread with good sensory is F2. It has baking expansion (126.35 %), moisture (37.86 %wb), ash (1.93 %db), fat (2.70 %db), protein (5.68 %db), carbohydrate (52.26 %db) and salt content (1.88 %db). The results suggest that 10% of AJBF can be used in bread making and it has higher protein content than wheat bread (control).

Introduction

The production of white bread in Indonesia is increasing every year. According to Setyawan (2006), the production of white bread increased from 2000 to 2003 reached 25.106.495 kg. The main material of white bread is wheat flour. Unfortunately, wheat cannot be cultivated in Indonesia, so Indonesia have imported from abroad. Wheat flour imports in 2014 reached 756,241 tons. Therefore, it needs a substitute flour with other flour in making bread to reduce wheat imports One of flour which it is can be used as substitute is jack bean flour.

Jack bean has high potency because it has high nutrition such as protein, carbohydrates, amino acid non-essentials and mineral. The carbohydrates content on jack bean is very high (50-60%) (Olalekan, and Bosede, 2010). It has also contained protein content approximately 29-32% (Doss, 2011). Also, it has high starch content, so it can be changed to flour. The native jack bean flour has some weaknesses, such as low ability to swell and the unpleasant and taste. Therefore, it need to improve the functional properties with modification.

Starch modification is a method for improving the functional properties of native starch. There are many modification methods have been used to increase starch properties, which can be divided into physical, chemical, and enzymatic treatment (Zavarese and Dias, 2011). One of chemical modification method is acetylation. Starch acetate is widely used in the food industry because it increased viscosity, solubility compared with native starch. The objective of the research is to investigate the effect of acetylated jack bean flour on the properties of the white bread.

Materials and Methods

1. *Material*

The main material in this research is jack bean flour, which is obtained from the local market. The other material for the bread making and the chemical material for the

analysis.

2. *Acetylated Jack Bean Flour (AJBF)*

Jack bean seeds were soaked in 1% baking soda solution for 8 hours, and it was boiled for 5 minutes. It was removed the skin to obtain jack bean seed without skin. It was soaked again in 1% baking soda solution for 16 hours (with water changes every 8 hours). It was cut and it was dried in a cabinet dryer at 60ºC for 7 hours. Then, it was grounded and sieved to obtain jack bean flour.

Jack bean flour was soaked with ratio of 1: 3 with solution acetic acid (0.15% acetic acid in 450 ml of distilled water). It was heated in a water bath at a temperature of 45ºC for 90 minutes. The water was separated from the solution. Wet flour was dried using a cabinet dryer at 60ºC for 7 hours. It was grounded and sieved to obtain AJBF.

3. *Bread making*

All ingredients (wheat flour (WF), AJBF, milk powder, yeast, bread improver, water, sugar and salt) was mixed with mixer. The formula of breads are F1:100%WF;F2:90%WF:10%AJBF;F3:80%WF:20%AJBF;and F4:70%WF:30%AJBF). It was kneaded until smooth, fermented and baked at 180ºC for 20 minutes.

4. *Sensory test*

The sensory test was done using scoring method with panellist. Panellists give score on white bread parameter: colour, aroma, taste, texture and overall. They give score with range 1 to 5, which is 1 is disliked a lot and 5 is liked a lot.

5. Baking expansion test

The baking expansion of white bread was calculated by measuring the volume before and after baking process. The volume of white bread was performed by measuring the surface area of the sliced bread.

6. *Statistical analysis*

Data were analyzed statistically using the SPSS Software (Version 12, IBM, USA). Analysis of variance and DMRT tests with a significance threshold of $p < 0.05$ were used to compare the differences among samples.

Results and Discussion

1. *Sensory properties*

Sensory analysis was carried out in colour, texture, aroma, taste and overall. The sensory properties of white bread were shown in Table 1. The results show that the more AJBF lead to decrease in sensory properties (colour, aroma, taste, texture and overall). The AJBF has darker colour than wheat flour, so the use more AJBF cause the colour of white bread darker compare with white bread from wheat flour. The dark color of AJBF of white bread make the panellist give low score (2.93) compare with control (4.20).

The AJBF has unpleasant odour compare with wheat flour. The increment of more AJBF in bread making leads to decrease the aroma score by panellist. The aroma score of F1, F2, and F3 were 3.13, 2.63 and 2.50, respectively. The other sensory property in this research is taste. The AJBF has special taste with beany taste. White bread using more the AJBF could decrease panellist score.

Table 1 The effects of AJBF on sensory properties of white bread

Sample	Colour	Aroma	Taste	Texture	Overall
F0	4.20^{a}	3.93^{a}	4.23^{a}	3.90^{a}	4.23^{a}
F1	3.83^{ab}	3.13^{b}	3.20^{b}	3.70^{b}	3.37^{b}
F2	3.47^{b}	2.63^{c}	3.00^{b}	3.27^{bc}	3.20^{bc}
F3	2.93^{c}	2.50^{c}	2.77^{b}	3.00^{c}	2.90^{c}

Values represent the mean of triplicate measurements ± SD (Standard Deviation). Means within columns with different letters are significant.
Score : 1 = disliked a lot, 2 = disliked, 3 = neutral, 4 = liked, 5 = liked a lot.
Sample :
F0 : 100% wheat flour (WF)
F1 : 90% WF : 10 % AJBF
F2 : 80% WF : 20 % AJBF
F3 : 70% WF : 30 % AJBF

The texture of white bread from AJBF has harder than white bread. The AJBF has not gluten content compare with white bread. It cannot hold the gas from fermentation stage in the bread making. Therefore, the texture of the AJBF white bread has denser and harder compare with wheat flour. Affandi (2016) reported that brownies with modified jack bean flour lead to decrease the texture. The decrease in texture due to wheat flour has high water absorption capacity. In other hand, another flour has low water absorption capacity, so in the baking process resulted in more water evaporation lead to denser texture (Dahlia, 2014).

The panellist score in overall parameters shows the

same trend with the other parameter of sensory properties. The more AJBF lead to decrease overall score compare with white bread. But, the F2 has better sensory properties compare with F2 and F3 based on the results of sensory properties.

2. *Physical Properties*

Baking expansion test was used in this research for physical properties. The baking expansion of white bread was calculated by measuring the volume before and after baking process. The baking expansion of white bread was presented in Table 2.

The baking expansion is closely related to the ability of the dough to form and hold the gas produced during fermentation. The most important component of wheat flour is gluten, which affects the elasticity of the dough and support viscoelastic properties. The substitution of AJBF has significantly different effect on the baking expansion of white bread.

Table 2 The effects of AJBF on baking expansion of white bread

Sample	Baking expansion (%)
F0	157,78[a]
F1	126,35[b]
F2	112,41[b]
F3	91,50[c]

Values represent the mean of triplicate measurements ± SD (Standard Deviation). Means within columns with different letters are significant.

Sample :

F0 : 100% wheat flour (WF)

F1 : 90% WF : 10 % AJBF

F2 : 80% WF : 20 % AJBF

F3 : 70% WF : 30 % AJBF

It can be seen that the greater of AJBF, the baking expansion of white bread will be decreased from 157.78% to 126.35%. This is caused by a decrease in the gluten content in the white bread dough. If the gluten content in the dough was reduced, the development of the dough is also getting smaller. Gluten was only obtained from wheat flour because the AJBF does not have gluten. Gluten functions to keep the dough steady and can hold CO_2 gas during the fermentation process lead to the dough can expand. that the reaction of gliadin and glutenin with water (hydration) will form an elastic mass called gluten which is a gas-binding (Bennion and Hughes 1970). Gluten is a part of wheat protein which when hydrated cannot be dissolved in water. In addition, gluten is a wheat protein which is very important role in the final results of the dough.

3. *Chemical properties*

From the sensory and physical properties, F2 has chosen for chemical analysis. The result of chemical properties of white bread was presented in Table 3. The moisture, ash, fat, protein, carbohydrate and NaCl content were investigated. The results suggest that moisture, ash, fat and NaCl were not significantly differenced with F1.

Table 3 The effects of AJBF on chemical properties of white bread

Sample	Moist.	Ash	Fat	Protein	Carbo.	NaCl
F0	32.29a	2,32a	3,57a	4,55a	57,10a	2,03a
F1	37,86[a]	1,93a	2,70a	5,68b	52,26b	1,88a

Values represent the mean of triplicate measurements ± SD (Standard Deviation). Means within columns with different letters are significant.

Sample :

F0 : 100% wheat flour (WF)

F1 : 90% WF : 10 % AJBF

F2 : 80% WF : 20 % AJBF

F3 : 70% WF : 30 % AJBF

F2 has significantly different in protein content (5.68%) higher than F1 (4.55 because the AJBF has higher protein compared with wheat flour. The result in agreement with Ariyantoro (2014), the protein content of modified jack bean flour has higher than wheat flour. If the AJBF was used in the white bread-making, so white bread has higher protein content compare with wheat bread.

Conclusion

The making of white bread using AJBF were investigated. More concentration of AJBF in the bread-making lead to decrease sensory and baking expansion properties. 10% AJBF of white bread has not significantly different with wheat bread in moisture, ash, fat and NaCl. However, the use 10% AJBF in the white bread making has successfully increased protein content compare with wheat bread.

References

Affandi, D.R., Ariyantoro, A. R., Khairini, R. S. (2016) The Effects Of Adding Modified Jack Bean Flour (Canavalia Ensiformis) As Wheat Flour Substitution On The Chemical, Physical, And Sensory Charactreristics of Baked Brownies. *Jurnal Teknosains Pangan*, 5.

Ariyantoro, A. R., Rachmawanti, D., Imroah, I. (2016) Physicochemical characteristics of modified jack bean flour (Canavalia ensiformis) with various lactic acid concentration and soaking time. *Agritech*, 36, 1–6.

Bennion, M., Hughes, O. (1970). Introductory Foods, 6th edition. Collier Macmillan Publisher. London.

Dahlia, Lies. 2014. Hidup Sehat Tanpa Gluten. *Alex Media Komputindo*. Jakarta.

Doss, A., Pugalenthi, M., Vadivel, V. (2011) Nutritional evaluation of wild jack bean (Canavalia ensiformis DC) seeds in Different locations of south India. *World Apllied Sciences Journal* 13, 1606–1612.

Olalekan, A. J., Bosede, B. F., (2010) Comparative Study on Chemical Composition and Functional Properties of Three Nigerian Legumes (Jack Beans, Pigeon Pea and Cowpea). *Journal of Emerging Trends in Engineering and Applied Sciences (JETEAS)* 1, 89–95.

Setyawan, H. (2006) Analisis Sikap dan Preferensi Konsumen dalam Pembelian Produk Bakery Tradisional Kartika Sari Bandung. Bachelor Thesis. Bogor Agricultural Institute.

Zavareze, E.D.R., Dias, A.R.G. (2011) Impact of heat-moisture treatment and annealing in starches: *A review. Carbohydr. Polym. 2011*, 83, 317–328.

Metabolomics and Bioactivity Profiles of Torbangun (*Plectranthus amboinicus)* Grown in Japan and in Indonesia

Nancy Dewi YULIANA[1*], Muhammad Anwari SUGIHARTO[1], Hanifah Nuryani LIOE[1], Masao GOTO[2], Yuko Takano ISHIKAWA[2]

[1] Department of Food Science and Technology, Bogor Agricultural University, IPB Dramaga Campus, Jalan Raya Dramaga, PO BOX 220, Bogor, Indonesia

[2] Functionality Evaluation Unit, Food Function Division, Food Research Institute, NARO, 305-8642 Kannondai 2-1-12, Tsukuba Ibaraki Japan

[*] Corresponding Author: nancy_dewi@ipb.ac.id; juliana.luthfia@gmail.com

SUMMARY

The leaves of torbangun (*Plectranthus amboinicus*, PA) are commonly consumed as vegetable in North Sumatra. It is traditionally used to stimulate breastmilk in breastfeeding women. Recent study showed that PA have antidiabetic and antioxidant activities. NMR-metabolomics was used in this study to show phytochemicals variation between *PA* grown in Japan and in Indonesia since environmental factors might influence the plant's secondary metabolite profile and their health beneficial properties. The results showed that flavonoids and triterpenes were among discriminating factors of the variation between the two groups. Targeted comparative analysis of PA specific flavonoids concentration using a validated HPLC-MWD method showed that Japanese samples contained higher concentration of total flavonoids than that of Indonesian samples. The Japanese samples contained higher amount of luteolin and apigenin than Indonesian samples. Eriodyctiol was detected only in Indonesian samples. On the contrary, more intensive DPPH reduction and α-glucosidase inhibition activities were found in the Indonesian samples. Thus, the flavonoids might not the only group of compounds related to the bioactivity, but it should be confirmed by further research targeting other groups of compounds such as triterpenes.

Introduction

Plant metabolites has provided as an incomparable source for bioactive compounds. *Plectranthus amboinicus* Lour., or being famous with its local name, Torbangun, is one of *Plectranthus* species commonly used as vegetable and condiment in North Sumatra Indonesia. In this region, it is also traditionally used to stimulate breastmilk production of breastfeeding women (Damanik, 2006). This species was also reported to show) anti-inflammatory and antitumor activities (Gurgel et al. 2009). However, different climate in the place where the plants are grown might affect the active compounds responsible for the abovementioned Torbangun functional properties.

In this research, NMR metabolome profile of Torbangun grown in Japanese and Indonesia were compared. Their antioxidant and α-glucosidase inhibition activities were also measured to see whether the different in the metabolome lead to activities variations.

Materials and Methods

1. *Single solvent plant extraction method*

All plant are freeze dried, powdered and stored in freezer prior analysis. About 100 g of each are sonicated using 80% MeOH for 30 minutes, filtered and put in rotavapor to remove the solvent. This step will be conducted in Indonesia.

2. *α-glucosidase-inhibition assay in-vitro*

α-glucosidase inhibition assay is conducted according to method described by Sancheti et al. (2009) using 96 wells plate and Elisa Reader.

3. *Total flavonoids content as described by Ahn et al. (2007)*

To 0.5 ml of sample extract was added 0.5 ml of 2% $AlCl_3$–ethanol solution. After 1 h at room temperature, the absorbance was measured at 420 nm. EEP samples were evaluated at a final concentration of 20 lg/ml. Total

flavonoid contents were calculated as milligrams per gram quercetin equivalents (mg/g QE) from a calibration curve. Analysis was performed in 5 replicates, each in duplo.

4. *Comprehensive extraction for metabolomics study*

Extraction was performed in a stainless-steel column (5.0 cm length, 2.0 cm diameter) according to a method described by Yuliana et al. (2011). The mixture of 1.0 g of dried powdered sample and 5 g of methanol washed 20-35 mesh sea sand were packed into the column. Sea sand was then again added until it reached the top of the column. The column was closed at the lower end with cotton and connected to Jasco PU-980 Gulliver HPLC pump (Jasco, Tokyo, Japan). The combination of solvents used for the extraction was n-hexane, acetone, and milliQ-water. The solvents were delivered by gradient started from n-hexane, acetone, then water. Extraction was performed for 75 min with solvent flow rate of 3 ml/min. The fractions were collected in 10 ml tubes every 5 min with an automatic fraction collector. A total of 15 fractions were obtained at the end of the extraction. Three replicates were made with each extraction. Every fraction was then dried using vaporizer (Eyela Centrifugal Vaporizer CVE-200D, Tokyo Rikakikai Co., Ltd., Japan).

5. *NMR measurement*

Dried methanolic extracts of each plants, are dissolved in methanol-*d6* subjected to 1H NMR measurement. NMR spectra were recorded according to method described previously by Kim et al. (2010) which is suitable for metabolomics-based experiment. The ^{1}H NMR spectra were automatically reduced to ASCII files. Bucketing was performed by AMIX software (Bruker, Karlsruhe, Germany). Spectral intensities were scaled to total intensity and reduced to integrated regions of equal width (0.04) corresponding to the region of δ -0.5 – 10.0 ppm. Chemical shift of NMR solvent and water are excluded. The data was analyzed with OPLS-DA (Orthogonal projection to the least square-discriminant analysis) using SIMCA ver. 13 (Umetrics, Umea Sweden).

Results and Discussion

The results of this study showed that Indonesian Torbangun had better antioxidant and anti-diabetic properties than its Japanese counterpart. IC_{50} value for both samples is presented in Table 1. The difference could be attributed to the differences of phytochemicals due to the different in the climate where the plants grown. The OPLS-DA analysis of NMR data showed that Japanese and Indonesian samples are well separated (Fig. 1), which means that their metabolome profiles indeed significantly different.

Flavonoids profiling for these two samples were then conducted using validated HPLC – MWD method and the results were presented in Table 2. The table shows that Indonesian Torbangun had lower total flavonoids content that Japanese Torbangun. The result of specific flavonoids measurement indicated that Indonesian Torbangun had lower luteolin but higher eriodictyol than Japanese Torbangun, while the amount of apigenin of both samples was almost similar.

From these results (Table 1 and Table 2), we might assume that the compounds responsible for antioxidant and α-glucosidase inhibition activity could be specific flavonoids which is only present in Indonesian sample, such as eriodictyol, or probably non-flavonoids compound, which should be confirmed further in the next experiment.

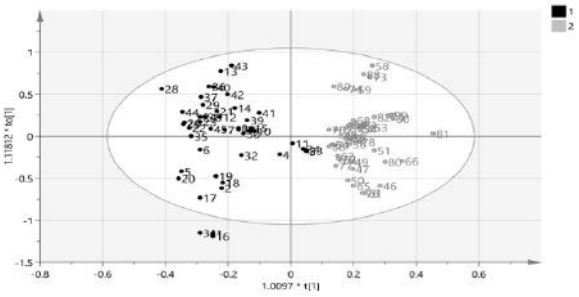

Fig. 1 OPLS-DA Score plot of 1H NMR profile of Torbangon grown in Japan (1) and Indonesia (2)

Table 1 Comparison of antioxidant and α -glucosidase inhibition activity of Indonesian and Japanese Torbangun

Sample	IC_{50} (µg/mL)	
	DPPH	AGI*
Indonesia	14.4 ± 1.2^{b}	1181.9 ± 113.5^{b}
Japan	24.0 ± 0.3^{a}	4451.4 ± 290.0^{a}
Vitamin C	1.6 ± 0.3^{c}	-
Acarbose	-	0.02 ± 0.001^{c}

*AGI = α -glucosidase inhibition activity All value are means from 3 replications. Different letter in same row shows significant differences (p = 0.05)

Table 2 Flavonoid profile of Indonesian and Japanese Torbangun (Api=apigenin, Lut = luteolin, Er = eriodictyol, TF = total flavonoid)

Sample	Flavonoid Concentration (µg/g)			
	Api	Lut	Er	TF*
Indonesia	571[a]	584[b]	4547	4146[b]
Japan	532[b]	1100.6[a]	nd	7934 [a]

* in µg quercetin/g. All value are means from 3 replications. Different letter in same row shows significant differences (p = 0.05)

Conclusion

NMR based metabolomics and targeted HPLC analysis revealed that bioactive compounds content of Torbangun leaves grown in Japan and Indonesia are significantly different, at least for several flavonoids measured in this study. The differences lead to different level of DPPH antioxidant and α -glucosidase inhibition activity. Further research on the detail profiling of compounds other than flavonoids would be interested to conduct.

Acknowledgements

The authors would like to thank the Ministry of Research Technology and Higher Education of the Republic of Indonesia for funding this research under International Collaboration Competitive Grant No. 1572/IT3.11/PN/2018. We would also like to acknowledge the UNU-KIRIN Fellowship Follow-up Grant for 2016-2018 for partial financial contribution to this study.

References

Ahn, MR. Kumazawa S, Usui Y, Nakamura J, Matsuka M, Zhu F, Nakayama T. (2007) Antioxidant activity and constituents of propolis collected in various areas of China. *Food Chemistry* 101 1383–1392.

Gurgel APAD., da Silva, JG., Grangeiro, ARS., Oliveira, DC., Lima, CMP., da Silva, ACP., Oliveira, RAG., Souza, IA. (2009) In vivo study of the antiinflammatory and antitumor activities of the leaves from *Plectranthus amboinicus* (Lour) Spreng (Lamiaceae). *Journal of Ethnopharmacology* 125: 361-363.

Sancheti, S., Seo, SY. (2009) *Chaenomeles sinensis*: a potent α- and β-glukosidase inhibitor. *American Journal of Pharmacology and Toxicology* 4(1):8-11.

Yuliana, ND., Khatib, A., Verpoorte, R., Choi, YH (2011) Comprehensive extraction method integrated with NMR metabolomics. A new bioactivity screening method for plants: Adenosine A1 receptor binding compounds in orthosiphon stamineus benth. *Analitycal Chemistry* 83(17), 6902-6906.

Evolving Potential Functional Foods to Meet Modern Needs in Commercial Product

Irmanida BATUBARA[1, 2*], Susi INDARIANI[1], C. Hanny WIJAYA[1,3], Katrin ROOSITA[1,4]

[1] Tropical Biopharmaca Research Center, Bogor Agricultural University, Bogor, Indonesia
[2] Faculty of Mathematics and Natural Sciences, Bogor Agricultural University, Bogor, Indonesia
[3] Faculty of Agricultural Technology, Bogor Agricultural University, Bogor, Indonesia
[4] Faculty of Human Ecology, Bogor Agricultural University, Bogor, Indonesia
[*] Corresponding Author: ime@apps.ipb.ac.id

SUMMARY

Over the last decade, demand for "healthy" foods and beverages has increased in many parts of the world. This phenomenon shows that consumers nowadays have the tendency to go back to nature, including the use of functional foods for disease prevention and treatment. Indonesia is known for its local wisdom with functional food potential, such as ethnobotanically valuable plants, traditional foods and traditional drinks or 'jamu'. Functional foods believed to promote general health and reduce the risk of diseases are becoming increasingly popular. The development of these products is a key research priority for functional foods development and a challenge for both industry and science sectors. The paper will highlight the findings obtained during the product development starting from the idea, invention and into the ready to market product. Several studies were carried out in the scientific investigation contexts of functional food development, including Java Tea based functional drinks, cajuputs candy, galohgor cookies and powder drinks, and red fruit.

Introduction

Over the last decade, demand for "healthy" foods and beverages has increased in many parts of the world (Ozen et al., 2012) and the diffusion of functional foods throughout the market has blurred the distinction between pharma and nutrition (Eussen et al., 2011). This phenomenon shows that consumers nowadays have the tendency to go back to nature, including the use of functional foods for disease prevention and treatment.

Indonesia is known for its local wisdom with functional food potential, such as ethnobotanically valuable plants, traditional foods and traditional drinks or 'jamu'. These foods have health benefits, beyond the basic nutritional functions. In general, functional food is food that not only provides essential nutrients to the body, but also promote general health, provides a protective effect on the body (or even healing) for some diseases and reduce the risk of diseases. The Indonesia National Agency of Drug and Food Control define functional foods is processed foods containing one or more functional components which based on scientific studies have certain physiological functions, proven to be harmless and beneficial to health (BPOM, 2005). The development of these products is a key research priority for functional foods development and a challenge for both industry and science sectors. The paper will highlight the findings obtained during the product development starting from the idea, invention and into the ready to market product. Several studies were carried out in the scientific investigation contexts of functional food development, including Java Tea based functional drinks, cajuputs candy, galohgor cookies and powder drinks, and red fruit.

Java Tea Based Functional Drinks

Many of various traditional drinks, we called herbal drinks or 'jamu', are produced from traditional medicinal ingredients such as Java tea. Research on Java tea-based functional drinks has shown promising health benefits such as antioxidant (Wijaya et al., 2007). A Java tea-based functional drink prepared using fresh ingredients was reported to possess 532.307–726.818 ppm ascorbic acid equivalent antioxidant capacity (AEAC) (Wijaya et al.,

2007). Furthermore, this drink has antihyperglycemic activity (Wijaya et al., 2011; Indariani et al., 2014). This functional drink was able to restrain the increase of blood glucose level in diabetic mice, while it didn't cause a decrease of blood glucose level in the normal mice. Beverage formulas with the addition of ginger extract had a steadier hyperglycemic ability because it was able to lower the blood glucose level for 20 days during the study period. The beverage provision to diabetic mice was able to restrain further damage on islet of Langerhans. Langerhans in diabetic mice, which were given beverage with or without the addition of ginger extract or insulin, has a larger amount and larger size of Langerhans when compared to positive control mice (diabetic), although the amount is still less than the amount of Langerhans from normal mice group. In the diabetic mice group treated with insulin, an improvement of the Langerhans were observed (Indariani et al., 2014). Wijaya (2010), also reported that ginger extract can increase the glucose uptake by isolate hemidiaphragm cells. It is postulated that gingerol from ginger extract could increase the insulin sensitivity upon glucose, and improve the hyperglycemia condition (Sekiya et al., 2004).

Java Tea-based beverage in ready-to-drink (RTD) type has a limitation in distribution. Converting the ready-to-drink beverage into effervescent, which is simple and easy carrying, using nanoencapsulation technology also improve the shelf life (Chusen et al., 2012). Encapsulation protects bioactive compounds from degradation by hindering their direct exposure to adverse environments, such as the light, oxygen, chemicals, etc. A study has proved that encapsulation can increase bioavailability of bioactive compounds (Fathi et al., 2014). Another study has proved that encapsulation of active ingredients within polysaccharide is a powerful means of protecting them from degradation and for enhancing their bioactivity (Putheti, 2015). Chitosan is one of the polysaccharides that is used in nanoparticles-based playing a vital role in sustained and targeted drug delivery, nowadays.

Effervescent Java Tea-based functional beverage using nanoencapsulation technology has been reported by Wijaya et al. (2013). It showed that nanoencapsulation could reduce the size of particle (223.4±23.8 nm), with the polydispersity index (0.747), and suppressed the bitter taste intensity (2.74) of the Java tea-based beverage. It had preferred taste than that the non-nano encapsulated one. Rekasih et al. (2018) has been reported nano encapsulated beverage was more effective than the ready-to-drink and microencapsulated beverages in suppressing the reduction of feed intake and body weight, decreasing blood glucose level (7.98 %). Nano encapsulated beverage was better in protecting the viability of Langerhans (49.09 %) and β cell (32.50 %) than microencapsulated and ready-to-drink beverages. This encapsulated Java tea-based beverages can intervention attenuated the formation of malondialdehyde in diabetic rats from 36.63% to 51.95%. In addition, micro- and nano-encapsulated drink suppressed the fluctuation of blood glucose level and body weight. In vitro assessment showed that micro- and nano-encapsulated drink suppressed the formation of MDA at 5.25% and 72.16%, respectively (Naibaho et al., 2019).

However, utilization of fresh ingredients is often limited by availability and short shelf-life. To produce this tea on an industrial scale, extracts of Java tea, sappan wood, ginger, and curcuma were modified using simplicia instead of fresh ingredients. Modification of extraction processes and ingredients may impact the functional efficacy of the product as well as its sensory properties. Formula optimization has been done by Wijaya et al. (2018) for the modified Java tea-based functional drink in terms of both maximum antioxidant properties (efficacy) and sensory properties (color, taste, and aroma). Formula optimization was performed by response surface methodology (RSM) using *Design Expert*® 7 software. Java tea-based functional drink was successfully formulated from simplicia extracts with optimum sensory and antioxidant properties. The antioxidant activity of the optimum formula was 335.69 ± 48.30 ppm ascorbic acid equivalent *antioxidant* capacity and the sensory acceptance scores (on a scale of 1–7) were 5.6 for color, 5.8 for taste, 5.2 for aroma, and 5.2 for overall attributes (corresponding to 'like slightly' to 'like moderately'). Simplicia extracts in appropriate combinations can be used instead of fresh ingredients for the large-scale production of a Java tea-based functional drink while maintaining efficacy and palatability (Wijaya et al., 2018).

Cajuputs Candy

Cajuputs candy includes medicated sweets in the form of "hard candy" with mixed flavor formulations which consist of primary flavor (cajuput oil) and secondary flavor (crystalline menthol, cinnamon oil and peppermint oil). Hard candy is the name for candy that is processed at a temperature of 140-150 °C, hard textured and has a clear appearance or like a crystal. Cajuputs candy can relieve the

throat and maintain homeostasis of the mouth flora. The main composition and process of making candy original cajuputs refers to patent that was granted in 2000 (ID 0 000 385 S) with slight modifications, where the composition consisting of sucrose (granulated sugar), glucose (DE 42) and water, additional flavor of pure cajuput oil, peppermint, menthol, and maltol (Wijaya et al., 2000).

The formula candy has a balance between the superiority of taste (sensory reception) and active physiological ability with its ability to inhibit *S. mutans* biofilm formation which can cause dental caries and suppresses viability of *C. albicans* which can infect wounds in the oral cavity (Wijaya et al., 2012). The provision of flavor components of cajuput and peppermint oil could produce synergistic effects compared to single flavor component. The addition of cajuput oil at 0.6% has been able to inhibit the viability of *C. albicans*. The activities of the cajuput oil showed positive correlation with its concentration (Wijaya et al., 2014).

While cajuputs candy non sucrose with the main composition is isomaltose, acesulfame-K, water, cajuput oil, peppermint and honeydew flavor (Wijaya et al., 2014). Because it uses the main ingredients isomaltose and water, then in addition to low-calorie cajuputs candy non sucrose also contains ingredients that do not cause dental caries, so that it is potentially used as an oral health care product. Currently the two variants of Cajuputs Candy are being investigated for their ability to maintain balance (homeostasis) of the mouth flora.

Cookies Galohgor and Powder Drinks

Galohgor is one of the traditional herbal medicine in West Java, Indonesia. The traditional herb was prepared from 56 kinds of material consist of 38 medicinal plants, 5 herbs and spices, 7 nuts and 6 rhizomes in composition. This traditional herb commonly consumed by postpartum mothers in the Sundanese tribe in West Java. Roosita et al. (2003) reported that galohgor has efficacious for increase milk breast production and health maintain. It contains various important minerals, such as Fe, Zn, Cu, and Mn. In addition, it also contains many other functional compounds such as antioxidants, alkaloids, triterpenoids and glycosides as well as steroids, flavonoids, and saponins (Roosita et al. 2014).

Besides, it was also reported that galohgor have long been studied as therapeutic agents in DM management (Ghorbani 2014; Roosita et al. 2006). Administration of 0.37 g/kg body weight of rats that consumed Galohgor decreases the lower levels of T3 and T4 and increases the body antioxidant levels (Roosita 2003; Leatemia 2010). It can also lower blood glucose levels, increases serum adiponectin and reserves the liver glycogen level in the streptozotocin-induced mice (Firdaus 2016). This effect is thought to be caused by the activity of various bioactive substances contained in the galohgor.

The galohgor is traditionally made by roasting and pounding method to produce a coarse powder consumed directly (Roosita & Wientarsih 2013). The crude herbal mixtures are generally difficult to consume in the long term because not everyone is accustomed to consume herbs and to accept the taste in its original form (Goel & Kaur 2013). Therefore, the galohgor cookies and powder drinks are made to improve the acceptance and flavor of the product so that it can serve as an alternative choice for functional food products. Cookie form is chosen because it is one of the most popular snacks in Indonesia. While powder drink has a longer shelf life than any other drink. Setyaningsih et al. (2017), reported that galohgor products in the form of cookies and powdered drinks significantly decreased oxidative stress in type 2 diabetes mellitus. This research showed that adjusted mean changes of antioxidant activity with DPPH method for intervention group compared with control group were +4,07% and +1,78 % ($p>0,05$), and MDA were -0,56 nmol/ml and +7,05 nmol/ml($p<0,05$).

Damayati et al., (2018) also reported that the administration of cookies and galohgor powder drinks tends to lower total cholesterol, triglyceride levels, LDL levels, and maintain HDL levels better than the control group. However, the differences were not statistically significant between the groups. Thus, intervention package containing cookies and galohgor cookies and powder drinks as much as 2 g of Galohgor extract per day for 38 days is suggested for type 2 DM patients because it has health benefits specially to decrease VAT to help prevent DM complications.

Red Fruit (*Pandanus conoideus* Lamk)

Buah Merah or red fruit (*Pandanus conoideus* Lamk) is an indigenous plant from Papua Island that belongs to genus Pandanus. This plant spread in Papua, New Guinea, and began planted in some areas in Indonesia (Hadad et al., 2006). Papuan people usually utilize red fruits as food and consume directly, as sauce or use the oil for so much purpose. Red fruit oils used as natural products

for medicine (Arumsari et al., 2013; Wijaya and Pohan, 2009).

Local people in Papua extracted the oil from the fruits by heating method and use for some purpose like food and medicine (Hening et al., 2008). Red fruit oils has high level of monounsaturated fatty acid (oleic acid), β-carotene, β-cryptoxanthin, α-tocopherol, phenolic compound and flavonoid that potentially become functional food and medicine. Red fruit oils empirically used by local people as natural medicine for many diseases such as cancer, rheumatoid arthritis and stroke, HIV Aids (Kie et al., 2009; Rohman et al., 2012; Mun'im et al., 2006).

The potential plant as natural products has to be followed by the data of safety level of the product. The substance and chemical compound of plant products may result in chronic toxicity or acute toxicity. Therefore, the information about the toxicity of red fruit oils is very important. Wismandanu et al. (2016), reported that red fruit oils can be categorized as Category 5 GHS (Globally Harmonized System for Chemical Classification Substances and Mixtures) as practically non-toxic materials, based on the 2001 OECD acute toxicity. No animals showed toxic symptoms in 300 and 2000 mg/kg dosing group. One animal in 5000 mg/kg BW dosing group had diarrhea one hour after administration. No animal dead in this experiment after 14 days observation. AST and ALT mean value for rats on 300 mg/kg BW, 2000 mg/kg BW, and 5000 mg/kg BW dosing groups are 22.70±1:05 IU/L, 24.15±8.89 IU/L and 24.54 ± 6.26 IU/L and 18.04±0.77 IU/L, 19.69±3.08 IU/L, 16.78±1.60 IU/L, respectively. No statistically significant difference of the value of AST and ALT levels in each treatment group ($p>0.05$). Therefore, in this research, red fruit oils no cause liver injury.

Conclusion

There is a lot of potential natural resources and local wisdom that are potential as functional food. The development of ethnobotanically valuable plants and traditional products is a key research priority for functional foods development. It's a challenge for both industry and science sectors to study it scientifically, from the idea, invention and into the ready to market product.

References

Arumsari, NI, Riyanto, S, Rohman, A. (2013) Some Physico-chemical Properties of Red Fruit oil (*Pandanus conoideus* Lamk) from Hexane and Chloroform fraction. J. Food Pharm. Sci 1, 30-34.

BPOM. The Indonesia National Agency of Drug and Food Control. 2005. PerKa BPOM No. HK 00.0s.52.06 Tahun 2014 Tentang Ketentuan Pokok Pengawasan Pangan Fungsional (Main Provisions for Functional Food Monitoring). Jakarta, Indonesia: BPOM.

Cushen, M, Kerry, J, Morris, M, Cruz-Romero, M, Cummins, E. (2012) Nanotechnologies in the food industry: Recent developments, risks and regulation. Trends in Food Sci & Tech 24, 30-46.

Damayati, RP, Roosita, K, Sulaeman, A. (2018) Effect of Galohgor Cookies and Powder Drinks on Visceral Adipose Tissue and Lipid Profile in Patients with Type 2 Diabetes Mellitus. J. Gizi Pangan 13(3), 137-144.

Eussen, SR, Verhagen, H, Klungel, OH, Garssen, J, van Loveren, H, van Kranen, HJ, Rompelberg, CJ. (2011) Functional foods and dietary supplements: products at the interface between pharma and nutrition. Eur J Pharmacol 668, S2–9.

Fathi, M, Mart, AI, McClements, DJ. (2014) Review Nanoencapsulation of food ingredients using carbohydrate based delivery systems. Trends in Food Sci & Tech 39, 18-39.

Firdaus. (2016) Peran ekstrak nutrasetika galohgor untuk mengatasi resistensi insulin pada tikus diabetes yang diinduksi *Streptozotocin* (STZ) [tesis]. Bogor: Institut Pertanian Bogor.

Ghorbani, A. (2014) Clinical and experimental studies on polyherbal formulations for diabetes: Current status and future prospective. J Integr Med 12(4), 336-345.

Goel, S, Kaur, T. (2013) Impact of hypoglycemic herbal mixture based biscuits intervention on blood glucose level and lipid profile of type 2 diabetic subjects. IJFANS 2(2), 84-90.

Hadad, Atekan, M., Malik, A., Wamaer, D. (2006) Karakteristik dan potensial tanaman buah merah (*Pandanus conoideus* Lamk.) di Papua, Prosiding Seminar Nasional BPTP Papua, Jayapura 24-25 Juli 2006. Balai Besar Pengkajiandan Pengembangan Teknologi Pertanian, Bogor, 243-255.

Hening, P, Puspita, EW, Ria, K. (2008) Efek Pemberian Minyak Buah Merah (*Pandanus conoideus* Lamk) Terhadap Pertumbuhan In Vivo Tumor Kelenjar Susu Mencit C3H : Tinjauan Khusus Aktivitas Proliferasi Dan Apoptosis. Jurnal Bahan Alam Indonesia.

Indariani, S, Wijaya, CH, Rahminiwati, M, Winarno, MW. (2014) Antihyperglycemic activity of functional drinks

based on Java tea (*Orthosiphon aristatus*) in streptozotosin induced diabetic mice. Int Food Research J 21, 349-355.

Khie, K, Andhika, OA, Chakravitha, M. (2009) Inhibition of NF-κB Pathway as the Therapeutic Potential of Red Fruit (*Pandanus conoideus* Lamk) in the Treatment of Inflammatory Bowel Disease. JKM 9(1), 69-75.

Leatemia, RR. (2010) Aktivitas antioksidan jamu galohgor pada tikus putih (*Rattus sp.*) [tesis]. Bogor: Program Pasca Sarjana, Institut Pertanian Bogor.

Naibaho, J, Safithri, M, Wijaya, CH. (2019) Anti-hyperglycemic activity of encapsulated Java tea-based drink on malondialdehyde formation. J Appl Pharm Sci 9(04), 088–095.

Mun'im, A, Andrajati, R, Susilowati, H. (2006) Tumorigenesis inhibition of water extract of red fruit (*Pandanus conoideus* Lamk) on Sprague-Dawley rat female induced by 7,12- dimetilbenz(a)antrasen (DMBA). Indonesia Journal of Pharmaceutical Science 3, 153- 161.

Rekasih, M, Muhandri, T, Safithri, M, Wijaya, CH. (2018) Antihyperglycemic Activity of Java Tea-Based Functional Drink-Loaded Chitosan Nanoparticle in Streptozotocin-Induced Diabetic Rats. BMC Complementary and Alternative Medicine (Review Process).

Rohman, A, Sugeng, R, Che Man. (2012) Characterizaton of red fruit (*Pandanus conoideus* Lamk) oil. International Food Research Journal 19(2), 563-567.

Roosita, K. (2003) Efek Jamu pospartum pada involusi uterus dan produksi susu tikus (*Rattus sp*.) (produk jamu tradisional desa Sukajadi, kecamatan Tamansari, kabupaten Bogor) [tesis]. Bogor: Institut Pertanian Bogor.

Roosita, K, Kusharto, CM, Sekiyama, M, Ohtsuka, R. (2006) Penggunaan tanaman obat oleh pengobat tradisional di desa Sukajadi wilayah hutan wisata Curug Nangka Bogor. Media Gizi dan Keluarga 30(1), 77-87.

Roosita, K, Wientarsih, I. (2013) Pengembangan sediaan madu-galohgor sebagai nutraceutical berbasis lokal untuk kecukupan gizi ibu menyusui. Penelitian Perguruan Tinggi. Lembaga Penelitian dan Pengabdian Kepada Masyarakat. Bogor: Institut Pertanian Bogor.

Roosita, K, Sa'diah, S, Rohadi, Wientarsih, I. 2014. Optimasi proses ekstraksi nutraseutikal galohgor. Simposium Penelitian Bahan Obat Alami PERHIPBA XVI. Solo.

Sekiya, K, Atsuko, O, Shuichi, K. (2004) Enhancement of insulin sensitivity in adipocytes by ginger. Biofactors 22 (1-4), 153-156.

Setyaningsih, S, Roosita, K, Damayanthi, E. (2017) Effect Galohgor's Product nAntioxidant Activity and Decreased Oxidative Stress in Type 2 Diabetic Patients. Jurnal Media Kesehatan Masyarakat Indonesia 13(4), 310-318.

Ozen, AE, Pons, A, Tur, JA. (2012) Worldwide consumption of functional foods: a systematic review. Nutr Rev 70, 472–81.

Putheti, S. (2015) Application of nanotechnology in food, nutraceuticals and pharmaceuticals. e-Journal of Sci & Tech.

Wijaya, CH, Halimah, Taqi, FM. (2000) Cajuputs candy composition for throat lozenges. Patent of Indonesia ID 0 000 385 S.

Wijaya, CH, Achmadi, SS, Herold, Indariani, S. (2007) Formulation and The Processing of Java Tea based functional drink (*Orthosiphon aristatus*). Patent of Indonesia IDP000033791.

Wijaya, CH, Rahminiwati, M, Chen, H, Kordial, N, Lo, D. (2010) In Vitro and Ex Vivo Anti-hyperglycemic Activities of Java Tea (*Orthosiphon aristatus* BI. Miq) – based Functional Drink. Proceeding of 15th World Conggress of Food Science and Technology. Cape Town: Afrika Selatan

Wijaya, CH, Rahminiwati, M, Indariani, S, Herold, Kordial, N, Afandi, A, Lo, D. (2011) Formulation of Java Tea based functional drink to Overcome and Prevention of Hyperglycemic. Patent of Indonesia IDP000041053.

Wijaya, CH. (2012) Cajuputs Candy Composition that Can Inhibit Microbial Growth Causes of Dental Caries. Patent of Indonesia IDP000040695.

Wijaya, CH, Nurtama, B, Afandi, FA. (2013) Effect of nanoencapsulation on the sensory, physico-chemical, and functional quality of Java Tea base functional drink (*Orthosiphon aristatus* B1. Miq). Oktrooi Roosseno and Indonesia Herb Council, Manado, Indonesia.

Wijaya, CH, Rachmatillah, AF, Bachtiar, BM. (2014) Inhibition of Cajuputs Candy Toward the Viability of *Candida albicans* by using In Vitro Assay. J. Teknol. dan Industri Pangan 25(2), 158-167.

Wijaya, CH, Bachtiar, BM, Indariani, S, Christie, Ratna, B, Iftari, W, Tan, E. (2014) Composition and Processing

of Non Sukrosa Cajuputs as A Mouth Health Care. Patent of Indonesia P00201406482.

Wijaya, CH, Sutisna, N, Nurtama, B, Muhandri, T, Indariani, S. (2018) Development of Java Tea based Functional Drink: Scale-up Formula Optimization based on the Sensory and Antioxidant Properties. J App Pharm Sci 8(09), 055-060.

Wijaya H, Pohan, HG. (2009) Kajian Teknis Standar Minyak Buah Merah (*Pandanus conoideus* Lamk) (Eng: technical study of red fruit standard). Prosiding PPI Standardisasi, 1-12.

Wismandanu, O, Maulidya, I, Indariani, S, Batubara, I. (2016) Acute toxicity of red fruits (*Pandanus conoideus* Lamk) oil and the hepatic enzyme level in rat. The Journal of Phytopharmacology 5(5), 176-178.

Evaluation of Whole Mitochondrial DNA Sequence in Healthy and Type 2 Diabetic Individuals with Reference to Bangladeshi Population

Sajoy Kanti Saha, Md Hasib, Ashish Das, Nafiul Huda, Tahirah Yasmin, Md Ismail Hosen, A.H.M. Nurun Nabi*

Laboratory of Population Genetics, Department of Biochemistry and Molecular Biology, University of Dhaka, Dhaka-1000, Bangladesh.

* Correspondence to nabi@du.ac.bd

SUMMARY

Type 2 diabetes (T2D) is one of the global health burden and food is one of the modifiable risk factors of T2D. The genes of the mitochondria are important to the energy production, both to ATP production and heat generation. Mitochondrial DNA (mtDNA) variation is likely to contribute to an imbalance in cellular energy homeostasis, insulin secretion and beta cell functions which in turn is linked to the risk of developing diabetes. We aim to explore the whole mtDNA sequence in Bangladeshi healthy individuals and thus, compare mtDNA variation with that of diabetic patients. A total of 26 pairs of primers were designed. mtDNA was extracted from a total of 29 unrelated Bangladeshi (thirteen healthy and sixteen type 2 diabetic patients) individuals and sequences were obtained by Sanger sequencing platform. Contigs were assembled and analyzed using Geneious software by comparing with the revised Cambridge reference sequence of mtDNA (NC_012920.1). Haplogrep2 and Phylotree17 tools were employed for determining haplogroups. MITOMASTER facilitates determination of total variants of each participant. Total 25 diverse haplogroups were identified. Haplogroup M and its subgroups were the most frequent (65.5%) followed by haplogroup R (24.2%), U (6.9%) and C (3.4%). It was found that healthy individuals had a total of 879 variants (varied from 43-183). Of them, 11 were predicted to be the most pathogenic while 18 were possibly pathogenic. On the other hand, out of 1139 variants (varied from 45-117) found in diabetic patients, 3 were the most pathogenic and 9 were possibly pathogenic. We found 47 variants unique to healthy individuals while 74 were unique to diabetic patients. Among these, frequencies of 8 unique variants (30%-54%) and 6 unique variants (31%-50%) were found to be the highest respectively in healthy individuals and diabetic patients. We believe that our baseline data of whole mtDNA sequence of our population would facilitate further research to validate frequencies of new variations unique to diabetes in diagnosing and investigating genetic linkages of non-communicable diseases in Bangladesh.

Introduction

According to International Diabetes Federation (IDF), 425 million people world-wide are suffering from diabetes and among them, 82 million people resides in South East Asian region. By the year 2045, the prevalence will be 151 million. Bangladesh is also one of the worst affected region where in 2017, 6.9% of the Bangladeshi adults were suffering from diabetes [1]. It influences functions of different organs that either reduces life expectancy or leads to death [2.3]. Diabetes is a polygenic diseases and it is a phenotypes of >150 genotypes, which are characterized by impaired glucose tolerance and impaired control of intermediary metabolism [4]. The functions of different organs are influenced by the disease, which either reduces life quality or leads to death in some cases. Mitochondrion is involved in energy metabolism through glucose metabolism and insulin secretion. Electron-transport chain within mitochondria synthesizes ATP that mediates insulin secretion from pancreatic β-cells [5]. Beta cell destruction and disturbances in insulin secretion are critical in the pathogenesis of T2D [6].

Many strains of mice and rats were used to study diabetes at genetic levels. For example, BHE/Cdb rat mimics the human phenotype with a mutation in mitochondrial DNA. Studies of twins have shown that if one twin develops type 1 diabetes, the other twin has a 60% chance of developing the disease. In contrast, with type 2 diabetes, if one twin develops diabetes, the other has a

100% chance of developing the disease [7,8]. A decrease in mitochondrial function or mitochondrial DNA (mtDNA) copy number has been correlated with insulin resistance and dysregulated lipid metabolism [9-11]. Alterations of mitochondrial DNA has been found to be associated with the risk of developing type 2 diabetes in different populations with incompatible findings. A mutation, 3243A→G, within mtDNA has been found to be associated with maternally linked diabetes [12]. mtDNA G10398A variant in ND3 gene has shown association with type 2 diabetes [13,14] either independently or through interacting with other candidate genes [15,16]. A weak association of T2D with mtDNA variants in Tunisian population was reported but such association was missing when values were adjusted with age, gender and BMI. Also, association of certain mtDNA genetic backgrounds (haplotypes, haplogroups) with T2D was reported in Asians [17], but not in Caucasians [18,19]. Studies showed that mitochondrial C5178A contributes to human longevity [20], has protective effects against oxidative damage [21], anti-atherosclerotic effects in diabetic patients [22], and decreases the possibility of lung cancer [23]. It has also been reported that mtDNA polymorphisms are related to interindividual functional variability in human cognition [24], personality [25], athletic performance [26], and longevity [27]. Mutations in mitochondrial DNA are also associated with mitochondrial myopathy, encephalopathy, lactic acidosis, and stroke-like episodes (MELAS) [28,29], variety of malignancies, including breast, colorectal, ovarian, gastric, hepatocellular, kidney, pancreatic, thyroid, and prostate cancer [30]. Using complete mitochondrial genome sequencing, US Caucasian, Hispanic, and African Americans were differentiated [31]. Thus, mtDNA has enormous contribution in forensic purposes. Considering the variation among different ethnic groups, the understanding of genetic diversity for specific populations is mandatory, not only for research but for practical applications such as human identification [32]. However, information related to whole mtDNA sequence and variants are completely missing for Bangladeshi population.

Thus, this study aims to i) identify all mtDNA variants and probable potential mutations, ii) identify major haplogroups in Bangladeshi healthy individuals and T2D diabetic patients, iii) compare mtDNA variants from type 2 Bangladeshi diabetic individuals with that of Asian populations. In this report, we provide the results of mtDNA analysis of 29 Bangladeshi individuals.

Materials and Methods

A total of 29 unrelated Bangladeshi individuals were enrolled. Among them, 13 were healthy individuals and 16 were individuals with type 2 diabetes. This study was approved by the ethical review committee of the Faculty of Biological Sciences, University of Dhaka, Bangladesh. Using the levels of plasma fasting glucose (≥7.0 mmol/L) and levels of HbA1c (≥6.5%) set by the World Health Organization, patients with type 2 diabetic patients were selected. Each individual was informed about the study and after getting their consent, 5 mL of venous blood was taken in EDTA containing vacutainer tubes. Anthropometric and demographic data were obtained from the data available in the structured questionnaire obtained during interview. Mitochondrial DNA was extracted from each sample according to the method described by Sajoy et al (2019) [33]. Using Primer3 (v 0.4.0) web based tool (http://bioinfo.ut.ee/primer3-0.4.0/), 26 pairs of primers were designed by deploying Revised Cambridge Reference Sequence (rCRS) of the Human Mitochondrial DNA (NC_012920.1). For each pair of primer, reaction conditions were set and amplicons (sizes ranges from 542bp-891bp) were validated in 1.5% agarose gel electrophoresis. PCR products were cleaned directly or from gel using the Wizard® SV Gel and PCR Clean-Up System (Promega, USA) where necessary followed by single pass Sanger Sequencing. Chromatograms were analyzed using DNA Baser (v 4.36.0.2) and Geneious software (v R11). MEGA (v 10.0.4) was used for aligning. Haplogrep2 and Phylotree17 tools were employed for determining haplogroups. MITOMASTER available at https://www.mitomap.org/foswiki/bin/view/MITOMASTER/WebHome facilitates determination of total variants of each participant. Human mtDNA Genome Polymorphism Database was used for the comparative analyses of the variants present in ancestral haplogroups and Asian population.

Results

1. *Haplogroup analyses*

One major M haplogroups and three sub-haplogroups R, U, C were respectively identified in 46.14%, 30.76%, 15.38%, 7.69% of the total healthy participants (Table 1). More analyses revealed that healthy individuals belonged to the M64, M53b, M30c, M18, M5b, M2a and C7b subgroups were originated from M haplogroup while rest

of them fit in R5a2b, R6a2, R6b, U2c'd and U2b2 subgroups originated from major N haplogroup. On the other hand, 78.57% and 21.43% of diabetic individuals belonged to M haplogroup and R sub-haplogroup. Of them subgroups M3a, M5a, M18, M34a, M35a, M38, M42, M45, M49c, M65 were from M haplogroup and subgroups R0, R5a1, R6a were from R haplogroup.

2. *Comparison of SNPs between Asian and Bangladeshi diabetic population with respect to rRNAs*

A total of 41 single nucleotide polymorphisms were found within the mtDNA sequences that encode for rRNAs in T2D Asian population. For comparison, SNPs reported more than >10% in the database were considered. A total of 22 and 19 SNPs within mtDNA sequence encoding respectively 12s rRNA and 16s rRNA are reported among Asians. While our sequence data revealed 40 SNPs in Bangladeshi population with T2D. According to database (www.http://mtsnp.tmig.or.jp), highest frequency of variations were observed at positions 2706 (transition, A/G), 3106 (Deletion, C/-), 3010 (transition, G/A) within 16s rRNA and 1438 (transition, A/G), 709 (transition, G/A) within 12s rRNA. In our population, all frequencies matched with that of the SNPs reported in the database except the deletion mutation found at position 3106. The data have been presented in Table 2.

3. *Comparison of SNPs between Asian and Bangladeshi diabetic population with respect to non-coding sequences*

A total of 127 single nucleotide polymorphisms were reported in the database while in Bangladeshi population 67 SNPs have been identified (Table 3). For the comparative analysis, we considered the most prevalent SNPs reported in the database from 47%-100%. Highest frequency of variations were observed at positions 73, 263, 489, 16223, 16362, 16519 and all of them were transition mutations.

4. *Comparison of SNPs between Asian and Bangladeshi diabetic population with respect to protein coding sequences*

According to database, Asian individuals with type 2 diabetes had total of 351 SNPs within the protein coding regions of mitochondrial DNA. For the comparative analysis, we considered the most prevalent SNPs reported in the database from 35%-100%. SNPs at positions 4769, 7028, 11719, 14766, 15326 within the protein coding regions of ND2, COI, CytT71, CytbT194A and ND5, respectively were found in 100% Asian people with T2D that completely matched with the variants identified in Bangladeshi population with T2D. While SNP at position 6680 within NADH-dehydrogenase subunit 4 (ND4) was 100% prevalent in Asian diabetic individuals, in Bangladeshi individuals with T2D, this SNP was missing. Other SNPs were identified at varying frequencies. However, though prevalence of SNPs at positions 4883, 5178, 8414, and 14668 in Asian diabetic population varied from 35%-40%, such variants in Bangladeshi population were not identified. Table 4 demonstrated the variants between the two groups.

5. *Comparison of SNPs between Asian and Bangladeshi diabetic population with respect to tRNAs*

According to database, 29 variants were found in type 2 diabetic Asian individuals within the mtDNA sequences that encode 16 tRNAs at varying frequencies. In our population, 22 variants were identified within the mtDNA sequences that encode tRNAs for Thr, Arg, Met, Trp and Glu as shown in Table 5. Among them, the most variants were observed within the sequence that encode Arg in Bangladeshi individuals with T2D compare to Asian counterparts.

Discussion

Though exact causative gene responsible for developing or commencing diabetes is not identified yet but multiple genes associated directly or indirectly with the development or with the risk of diabetes have been recognized. Mitochondria, the power house of a cell and one of the central organs in energy metabolism in human body [34], became part of the cell through endosymbiosis, contains 16569 nucleotides containing circular DNA that encodes for 13 proteins, 22 transfer RNAs (tRNAs) and 2 ribosomal RNAs [35] , which is inherited maternally [36]. Thus, any mutation within mtDNA sequence related to disease only follow maternal lineage not paternal [37]. Sanger sequencing is one of the most comprehensive, cost effective and relatively faster methods of determining variants/mutations within a DNA sequence [38,39] . Capillary based Sanger sequence technique for determining whole mitochondrial DNA sequence in Bangladeshi individuals. Identification of disease associated single nucleotide polymorphisms or variants indeed play pivotal role in understanding the pathogenesis of diabetes. In this regard, nuclear DNA has attained

more attention than mtDNA. However, due to lack of intronic sequences and protection of histones, mtDNA has got possibility of 6-17 fold higher rate of mutation than nuclear DNA [40] that may put mtDNA more vulnerable towards its association with diseases. Thus, analyses of mtDNA to find out disease association should get similar priorities as it was achieved by nuclear DNA. We, for the first time, are comparing the whole mtDNA sequence of individuals with T2D and healthy controls with reference to Bangladeshi population using capillary based Sanger sequencing platform. We deployed primer walking approach by designing 24 pairs of primers that generated overlapping regions between each of the amplicon. The primers were designed in such a way that each amplicon overlapped at least 60 bases. As a result, contigs were assembled with high confidence by removing first 15-40 nucleotides with poor quality.

mtDNA sequence analysis revealed varying frequencies of variants within the regions that encode rRNA, tRNA, coding sequence, non-coding sequence both in healthy individuals and patients with T2D. A total of 4 and 2 different haplogroups were identified respectively in healthy and diabetic individuals. It was found that individuals with M haplogroup and its associated subhaplogroups are more prevalent in diabetic individuals. Han Chinese population haplogroup M9 while for Japanese, Korean, and Finnish haplogroups F, D5 and J, respectively conferred susceptibility to T2D [17,18,41]. Linkages between the occurrence of type 2 diabetes and mitochondrial genetic variations like point mutation, and duplication have been implicated in different ethnic groups [42,43]. Our recent study did not find any association of G10398A polymorphism with the risk of T2D when total participants were considered. However, G10398A polymorphism played a protective role against development of T2D in male, not in female, individuals. Further, significant association of mtDNA C5178A polymorphism with the risk of T2D was evident in study participants. Mutation m.3243A>G affects oxidative phosphorylation and ATP production [44]. T3394C (causes changes from tyrosine to histidine) and G4491A (causes changes from valine to isoleucine) mutations are hypothesized as the functional polymorphism to be associated with the risk of T2D [45]. Our study revealed single nucleotide polymorphisms in mtDNA sequence that reside in regions for rRNA, non-coding regions, regions for tRNA and coding regions with varying proportions. Sequence analysis revealed absence of deletion mutation (C/-) at position 3106 within mtDNA sequence that encodes 16s rRNA, transition mutations (A/G, C/T, C/A, C/T, C/T) respectively at positions 8860, 4883, 5178, 14668, 8414 within non-coding regions of mtDNA sequence are absent in Bangladeshi population with T2D which were reported in Asian diabetic population. According to database, SNPs have been identified in 16 out of 22 regions within mtDNA that encode tRNAs for 20 amino acids while in our population SNPs were identified in regions that encode 5 tRNAs.

This study attempted to analyze whole mitochondrial DNA sequence in Bangladeshi population using Sanger sequencing platform. Further studies with high throughput sequencing technologies may reveal more variants with lower frequency.

Acknowledgement

This study was supported by the research grant provided by the Ministry of Education, Government of the Peoples Republic of Banglade sh. Sajoy Kanti Saha is a PhD student and recipient of PhD fellowship from the Ministry of Science and Technology, Government of the Peoples Republic of Bangladesh.

References

1. Whiting DR, Guariguata L, Weil C, Shaw J. (2011) IDF diabetes atlas: global estimates of the prevalence of diabetes for 2011 and 2030. Diabetes Res Clin Pract. 94(3):311-21.
2. Soumya D, Srilatha B. (2011) Late stage complications of diabetes and insulin resistance. J. Diabetes Metab. *2*, 2.
3. Habib SL, Rojna M. (2013) Diabetes and risk of cancer. ISRN Oncol. 2013:583786.
4. Kim JH, Stewart TP, Soltani-Bejnood M, Wang L, Fortuna JM, Mostafa OA, Moustaid-Moussa N, Shoieb AM, McEntee MF, Wang Y, Bechtel L, Naggert JK. (2006) Phenotypic characterization of polygenic type 2 diabetes in TALLYHO/JngJ mice. J Endocrinol. 191(2):437-46.
5. Cheng Z, Tseng Y, White MF. (2010) Insulin signaling meets mitochondria in metabolism. Trends Endocrinol Metab. 21(10):589-98.
6. Cerf M. E. (2013) Beta cell dysfunction and insulin resistance. Frontiers in endocrinology. *4*, 37.
7. Prasad RB, Groop L. (2015) Genetics of type 2 diabetes-

pitfalls and possibilities. Genes. *6*(1), 87–123.

8. E. Nilsson, P. A. Jansson, A. Perfilyev, P. Volkov, M. Pedersen, M. K. Svensson, P. Poulsen, R. Ribel-Madsen, N. L. Pedersen, P. Almgren, J. Fadista, T. Ronn, B. Klarlund Pedersen, C. Scheele, A. Vaag, C. Ling. (2014) Altered DNA Methylation and Differential Expression of Genes Influencing Metabolism and Inflammation in Adipose Tissue From Subjects With Type 2 Diabetes. Diabetes. 63(9): 2962.
9. Lowell BB, Shulman GI. (2005) Mitochondrial dysfunction and type 2 diabetes. Science. 307(5708):384-7.
10. Gianotti TF, Sookoian S, Dieuzeide G, García SI, Gemma C, González CD, Pirola CJ. (2008) A decreased mitochondrial DNA content is related to insulin resistance in adolescents. Obesity (Silver Spring). 16(7):1591-5.
11. Sookoian S, Rosselli MS, Gemma C, Burgueño AL, Fernández Gianotti T, Castaño GO, Pirola CJ. (2010) Epigenetic regulation of insulin resistance in nonalcoholic fatty liver disease: impact of liver methylation of the peroxisome proliferator-activated receptor γ coactivator 1α promoter. Hepatology. 52(6):1992-2000.
12. Chinnery PF, Elliott HR, Patel S, Lambert C, Keers SM, Durham SE, McCarthy MI, Hitman GA, Hattersley AT, Walker M. (2005) Role of the mitochondrial DNA 16184-16193 poly-C tract in type 2 diabetes. Lancet. 366(9497):1650-1651.
13. A. Bhat, A. Koul, S. Sharma, E. Rai, S.I. Bukhari, M.K. Dhar, R.N. Bamezai. (2007) The possible role of 10398A and 16189C mtDNA variants in providing susceptibility to T2DM in two North Indian populations: a replicative study. Hum. Genet. 120, pp. 821–826.
14. K. Darvishi, S. Sharma, A.K. Bhat, E. Rai, R.N. Bamezai. (2007) Mitochondrial DNA G10398A polymorphism imparts maternal Haplogroup N a risk for breast and esophageal cancer. Cancer Lett. 249, pp. 249–255.
15. Rai, *et al*. (2007) Interaction between the UCP2-866G/A, mtDNA 10398G/A and PGC1alpha p.Thr394Thr and p.Gly482Ser polymorphisms in type 2 diabetes susceptibility in North Indian population. Hum. Genet. 122, pp. 535–540.
16. Rai, *et al*. (2012) The interactive effect of SIRT1 promoter region polymorphism on type 2 diabetes susceptibility in the North Indian population. PLoS One. 7, pp. e48621.
17. Fuku N, Park KS, Yamada Y, Cho YM, Matsuo H, Segawa T, Watanabe S, Kato K, Yokoi K, Nozawa Y, *et al*. (2007) Mitochondrial Haplogroup N9a Confers Resistance against Type 2 Diabetes in Asians. Am J Hum Genet. 80(3): 407-415.
18. Mohlke KL, Jackson AU, Scott LJ, Peck EC, Suh YD, Chines PS, Watanabe RM, Buchanan TA, Conneely KN, Erdos MR, *et al*. (2005) Mitochondrial polymorphisms and susceptibility to type 2 diabetes-related traits in Finns. Hum Genet, 118(2):1-10.
19. Saxena R, de Bakker PI, Singer K, Mootha V, Burtt N, Hirschhorn JN, Gaudet D, Isomaa B, Daly MJ, Groop L, *et al*. (2006) Comprehensive association testing of common mitochondrial DNA variation in metabolic disease. *Am J* Hum Genet. 79(1):54-61.
20. Takagi K, Yamada Y, Gong JS, Sone T, Yokota M. (2004) Association of a 5178C→A (Leu237Met) polymorphism in the mitochondrial DNA with a low prevalence of myocardial infarction in Japanese individuals. Atherosclerosis. 175(2): 281–28.
21. Moreno-Loshuertos R, Acín-Pérez R, Fernández-Silva P, Movilla N, Pérez-Martos A, et al. (2006) Differences in reactive oxygen species production explain the phenotypes associated with common mouse mitochondrial DNA variants. Nat Genet. 38(11): 1261–1268.
22. Wallace DC. (2005) A mitochondrial paradigm of metabolic and degenerative diseases, aging, and cancer: a dawn for evolutionary medicine. Annu Rev Genet. 39: 359–4.
23. Zheng S, Qian P, Li F, Qian G, Wang C, Wu G, et al. (2012) Association of Mitochondrial DNA Variations with Lung Cancer Risk in a Han Chinese Population from Southwestern China. PLoS ONE. 7(2): e31322.
24. Skuder P, Plomin R, McClearn GE, Smith DL, Vignetti S, et al. (1995) A polymorphism in mitochondrial DNA associated with IQ? Intelligence. 21:1–11.
25. Kato C, Umekage T, Tochigi M, Otowa T, Hibino H, et al. (2004) Mitochondrial DNA polymorphisms and extraversion. Am J Med Genet. 128B:76–79.
26. Tanaka M, Takeyasu T, Fuku N, Li-Jun G, Kurata M. (2004) Mitochondrial genome single nucleotide polymorphisms and their phenotypes in the Japanese. Ann N Y Acad Sci. 1011:7–20.
27. Tanaka M, Gong J, Zhang J, Yamada Y, Borgeld HJ, et al. (2000) Mitochondrial genotype associated with longevity and its inhibitory effect on

mutagenesis. Mech Ageing Dev.116:65–76.

28. Goto Y, Nonaka I, Horai S. (1990) A mutation in the tRNA(Leu)(UUR) gene associated with the MELAS subgroup of mitochondrial encephalomyopathies. Nature. 348:651–653.
29. Kobayashi Y, Momoi MY, Tominaga K, Momoi T, Nihei K, et al. (1990) A point mutation in the mitochondrial tRNA(Leu)(UUR) gene in MELAS (mitochondrial myopathy, encephalopathy, lactic acidosis and stroke-like episodes). Biochem Biophys Res Commun. 173:816–822.
30. Chatterjee, A., Mambo, E. and Sidransky, D. (2006) Mitochondrial DNA mutations in human cancer. Oncogene. 25, 4663–4674.
31. King JL, LaRue BL, Novroski NM, Stoljarova M, Seo SB, Zeng X, Warshauer DH, Davis CP, Parson W, Sajantila A, Budowle B. (2014) High-quality and high-throughput massively parallel sequencing of the human mitochondrial genome using the Illumina MiSeq. Forensic Sci Int Genet. 12:128-35.
32. Holland MM, Parsons TJ. (1999) Mitochondrial DNA Sequence Analysis - Validation and Use for Forensic Casework. Forensic Sci Rev. 11(1):21-50.
33. Saha SK, Akther J, Huda N, Yasmin T, Alam MS, Hosen MI, Hasan AKMM, Nabi AHMN (2019) Genetic association study of C5178A and G10398A mitochondrial DNA variants with type 2 diabetes in Bangladeshi population. Meta Gene. 19: 23-31.
34. Wallace DC. (2007) Why do we still have a maternally inherited mitochondrial DNA? Insights from evolutionary medicine. Annu Rev Biochem. 76: 781–821.
35. Anderson S,Bankier AT,Barrell BG,de Bruijn MH,Coulson AR, et al. (1981) Sequence and organization of the human mitochondrial genome. Nature. 290: 457–465.
36. Giles RE,Blanc H,Cann HM,Wallace DC. (1980) Maternal inheritance of human mitochondrial DNA. Proc Natl Acad Sci U S A. 77: 6715–6719.
37. Cree LM,Samuels DC,Chinnery PF. (2009) The inheritance of pathogenic mitochondrial DNA mutations. Biochim Biophys Acta. 1792: 1097–1102.
38. Sanger F,Nicklen S,Coulson AR. (1977) DNA sequencing with chain-terminating inhibitors. Proc Natl Acad Sci U S A.74: 5463–5467.
39. Schrijver I,Pique LM,Traynis I,Scharfe C,Sehnert AJ. (2009) Mitochondrial DNA analysis by multiplex denaturing high-performance liquid chromatography and selective sequencing in pediatric patients with cardiomyopathy. Genet Med. 11: 118–126.
40. Naue J, Horer S, Sanger T, Strobl C, Hatzer-Grubwieser P, Parson W, Lutz-Bonengel S. (2015) Evidence for frequent and tissue-specific sequence heteroplasmy in human mitochondrial DNA. Mitochondrion. 20:82–94.
41. Liao WQ et al. (2008) Novel mutations of mitochondrial DNA associated with type 2 diabetes in Chinese Han population. Tohoku J Exp Med. 215, 377–384.
42. Tawata M, Hayashi JI, Isobe K, Ohkuno E, Ohtaka M, Chen J, Aida K, Onaya T. (2000) A new mitochondrial DNA mutation at 14577 T/C is probably a major pathogenic mutation for maternally inherited type 2 diabetes. Diabetes. 49(7):1269–1272.
43. Liou CW, Huang CC, Wei YH. (2001) Molecular analysis of diabetes mellitus-associated A3243G mitochondrial DNA mutation in Taiwanese cases. Diab Res Clin Pract. 54(Suppl 2):S39.
44. Maassen JA, Janssen GM, T Hart LM. (2005) Molecular mechanisms of mitochondrial diabetes (MIDD). Ann Med. 37: 213–221.
45. Wen-Qiang Liao, Yan Pang, Chang-An Yu, Jian-Yan Wen, Yi-Guan Zhang, Xiao-Hui Li. (2008) Novel Mutations of Mitochondrial DNA Associated with Type 2 Diabetes in Chinese Han Population. The Tohoku Journal of Experimental Medicine. 215 (4):377-384.

Rice Quality Under Ratooning Farming System

KOMARIAH[1*], Rahajeng Putu Widiani PRISWITA[2]

[1] Faculty of Agriculture, Sebelas Maret University, Jl. Ir. Sutami No. 36A, Kentingan, Surakarta, 57126, Indonesia

[2] Master Program of Environmental Science, Graduate School, Sebelas Maret University, Jl. Ir. Sutami No. 36A, Kentingan, Surakarta, 57126, Indonesia

[*] Corresponding Author: komariah@staff.uns.ac.id

SUMMARY

The increasing rice demand to meet the growing population need should pay attention to the natural resources availability. Producing rice with ratooning farming system could save time, water, seeds and labor resources, therefore this system must be introduced and implemented worldwide with improved practices according to local condition. Very few studies reported that the quality of rice produced from ratooning system was not lower than the main crop. However, more related studies is urgent to support the policy decision on rice ratooning farming system.

Introduction

Rice is the staple food for most of the Asian people, hence the rice production must be improved in the term of quality and quantity. The world rice production in 2018 was approx. 728 million tones, where 63% (approx. 459 million tones) were produced in Eastern and Southeastern Asia (IRRI (International Rice Research Institute), 2019). The rice (paddy) production during 3 decades at each continent (except Australia) and the world is presented in Table 1, showing the rice production increased year by year. This is in contrast with the land conversion issues which lead to the shrinking farm land areas. Green revolution, rice breeding technology and the genetic engineering to create high yielding potential rice seeds seemed to meet the challenges on rice demand (Khush, 2005).

However, rice demand increase should be able to meet the less land, less water, and less chemical or other inputs due to competition with the growing population. Less water availability and water scarcity has been the critical issue of crop production under the climate change condition across the world. Rice ratooning offers the high efficiency of water, seeds and chemical inputs hence lower the production cost (Negalur, Yadahalli, Chittapur, Guruprasad, & Narappa, 2017).

Ratoon is the practice of farming to obtain a second or more crop from tillers originating from the stubble of the harvested crop (Chauhan, Vergara, & Lopez, 1985), with the shorter vegetative period after the first harvested

Table 1 Rice (paddy production) over 3 decades at some continents and the world in tones

Region	1996	2006	2016
Africa	15.944.498	21.989.568	32.497.773
Americas	27.219.877	33.684.603	36.029.484
Asia	521.318.379	580.605.576	667.932.238
Europe	3.204.652	3.406.389	4.219.382
World	568.659.290	640.705.682	740.961.445

Source: (IRRI, 2019)

(Busyra, Adri, 2014). Ratooning is also defined as the bassal sucker for the propagation, such as in banana, sugarcane, pineapple, sorghum, cotton, pearl millet and rice. The first harvest crop is called as main crop and each succeeding harvest after is determined as first ratoon, second ratoon, and so on (Santos, Fageria, & Prabhu, 2003). Rice ratooning farming system had been practiced at limited areas in some countries, including Philippines, Indonesia, India, Thailand, United States, Brazil, Japan, Ethiopia (Bahar & De Datta, 1977). Twice harvesting can be performed in southwestern Japan and warmer regions (Nakano & Morita, 2007). Ratooning could save time (nursery and field preparation, transplanting, etc.), resources (labour, seeds, etc.) and gave higher productivity (Munda, Das, & Patel, 2009).

Crop Productivity Under Ratooning

Ratoon is a very special local-wisdom farming

system, which can be performed up to more than 3 regenerations on sorghum (House, 1995). The rice yield of the first ratoon was found to be approximately 50% lower than the main crop (Calendacion, Garrity, & Ingram, 1992; Pasaribu, Triadiati, & Anas, 2018). In the contrary, (Itabiyi, Adebowale, Shittu, Adigbo, & Sanni, 2016) reported that the ratoon agronomic properties of the NERICA rice variety were higher than the main crop. However, proper land management practices such as proper fertilizer application, earlier planting season and optimal variety selection (Dou, Tarpley, Chen, Wright, & Mohammed, 2016).

Ratoon grain yield of Bellemont and Lemont rice cultivars were not influenced by row spacing or seeding rate, while the filled grain number accounted for over 85% than the main crop (Jones & Snyder, 1987). The yield of ratoon season mainly depended on more ratoon spikes, 35%-40% of dry matter accumulation in ratoon spikes derived from the transportation of main crop stubble and 60%-65% from the photosynthetic production of the leaves of ratoon rice itself (ShangShou, ChuanYing, WeiZhao, YiZhen, & CongHua, 2003). Improved practices of rice ratooning using IR-64 cultivar gave 202% higher productivity over the local practices (Munda et al., 2009).

Rice Quality

The capacity of rice plants to produce a ratoon crop used to be noticeably influenced by means of their carbohydrate content and the phytohormones that continue to be in the intercalary meristem tissues of stubble after harvest. (Alizadeh & Habibi, 2016) reported that the amylase content in the ratoon crop were higher than the main crop (22.93 and 21.97%, respectively), and the alkali spreading also showed similar results (5.5 and 4.27, respectively (Table 2). Proximates, Amino acids, fatty acids, minerals and vitamins were not significantly different between the main crop and ratoon crop, except the fiber and Vitamin B2 were higher under the main crop (Nam et al., 2013).

The total carbohydrate concentration was positively correlated with growth duration, while higher nitrogen concentration was found in the shorter growth duration period, 117 and 137 days (Garcia, Mabbayad, & Vergara, 1980). The sugar and starch concentrations in the main crop promoted the grain yield of the ratoon crop (Manjappa & Prabhakar, 2003), while the carbohydrate in the stubble and the root of the main crop determined the ratoonability (Samson & Zandstra, 1980). Although starch was translocated from the stem to the panicle in the second crop when the first crop was cut at a height of 15 cm, insufficient starch was translocated to the panicle when the first crop was cut at 5 and 0 cm because of the low temperatures after heading, hence it is effective to cut stubble lower to reduce the overall loss of nutrition from a crop (Nakano et al., 2010).

Not many information found regarding the rice quality produced from the ratooning system, but it was found that the genetic characteristics positively and strongly correlated with the sucrose concentration of sugarcane's ratoon (Milligan, Gravois, & Martin, 1996). On the other hand, the main crop of sorghum contained much higher mean concentrations of the cyanogenic glycoside, and dhurrin, than the ratoon (Vinutha, Anil Kumar, Blümmel, & Srinivasa Rao, 2017). So far, the article reported by (Alizadeh & Habibi, 2016) is found to be the only information on rice quality regarding with ratooning farming system. In general, rice ratoon resulting in bigger grain width and thickness, and higher Amylose Content and Alkali Spreading Value (APV) Value, but lower grain length and whiteness degree (Table 2).

Conclusion

Rice ratoon is a promising efficient farming technology that supports environment and meet the global challenge. In general, the quality of rice resulted from ratooning was, somehow, not lower than the main crop. Therefore, more studies regarding rice quality under ratooning farming system is urgent to support the policy for rice ratooning implementation.

Acknowledgements

The authors acknowledge The United Graduate School of Agriculture Science, Gifu University , japan for provide funding to present this study in the International Symposium of a New Era in Food Science and Technology in Gifu University 9-10 October 2019.

Table 2. Rice Quality under Ratooning Farming System (Alizadeh & Habibi, 2016)

Crop type-Cultivar*	Lenght of grain† (mm)	Width of grain† (mm)	Grain thicknss† (mm)	Slenderness ratio	Whiteness degree (%)	Amylose content (%)*	Alkali Spreading Value (ASV)*	Grain length elongation (%)*	Grain chalkiness (%)*
Hashemi									
- Main Crop	7.64^{a}	1.93^{b}	1.69^{c}	3.96^{a}	46.70^{a}	22.10^{b}	4.36^{b}	1.68^{ab}	10.67^{b}
- Ratoon	7.52^{b}	1.95^{b}	1.71^{c}	3.85^{b}	39.26^{b}	23.80^{a}	5.80^{a}	1.72^{a}	11.60^{ab}
Alkazemi									
- Main Crop	7.43^{c}	2.02^{a}	1.78^{b}	3.68^{bc}	45.54^{a}	21.90^{b}	4.18^{b}	1.67^{ab}	13.74^{a}
- Ratoon	7.28^{d}	2.05^{a}	1.82^{a}	3.55^{c}	40.37^{b}	22.40^{b}	5.42^{a}	1.71^{a}	10.46^{b}
Tarom									
- Main Crop	7.27^{d}	1.86^{c}	1.58^{d}	3.91^{b}	47.12^{a}	21.70^{b}	4.26^{b}	1.63^{b}	11.26^{ab}
- Ratoon	7.09^{e}	1.84^{c}	1.61^{d}	3.85^{b}	40.81^{b}	22.60^{b}	5.28^{a}	1.66^{ab}	9.74^{b}
Mean All									
- Main Crop					46.45^{a}	21.97^{b}	4.27^{b}	1.67^{a}	11.89^{a}
- Ratoon					40.14^{b}	22.93^{a}	5.50^{a}	1.70^{a}	10.60^{a}

* The means that have at least one common letter in each column, do not have significant difference (P>0.05).
†Each data is the mean of 50 measurements.

References

Alizadeh, M. R., & Habibi, F. (2016). A Comparative Study on the Quality of the Main and Ratoon Rice Crops. *Journal of Food Quality*. https://doi.org/10.1111/jfq.12250

Bahar, F. A., & De Datta, S. K. (1977). Prospects of Increasing Tropical Rice Production through Ratooning1. *Agronomy Journal*. https://doi.org/10.2134/agronj1977.00021962006900040003x

Busyra, Adri, and E. (2014). No Title. In *Seminar Nasional Lahan Suboptimal 2014* (pp. 578–584). Palembang.

Calendacion, A. N., Garrity, D. P., & Ingram, K. T. (1992). Lock lodging: a new technology for ratoon rice cropping. *Philippine Journal of Crop Science*.

Chauhan, J. S., Vergara, B. S., & Lopez, F. S. S. (1985). Rice ratooning. *IRRI Research Paper Series*.

Dou, F., Tarpley, L., Chen, K., Wright, A. L., & Mohammed, A. R. (2016). Planting Date and Variety Effects on Rice Main and Ratoon Crop Production in South Texas. *Communications in Soil Science and Plant Analysis*. https://doi.org/10.1080/00103624.2016.1243705

Garcia, R. N., Mabbayad, B. B., & Vergara, B. S. (1980). Effects of growth duration and different levels of light intensity on the ratooning ability of rice. *Philippine Journal of Crop Science*.

House, L. R. (1995). Sorghum and Millets : History, Taxonomy, and Distribution. In *Sorghum and Millets: Chemistry and Technology*.

IRRI (International Rice Research Institute). (2019). No Title. Retrieved August 25, 2019, from http://ricestat.irri.org:8080/wrsv3/entrypoint.htm.

Itabiyi, O. V. I., Adebowale, A. A., Shittu, T. A., Adigbo, S. O., & Sanni, L. O. (2016). Effect of ratooning process on the engineering properties of NERICA rice varieties. *Quality Assurance and Safety of Crops and Foods*. https://doi.org/10.3920/QAS2014.0449

Jones, D. B., & Snyder, G. H. (1987). Seeding Rate and Row Spacing Effects on Yield and Yield Components of Ratoon Rice1. *Agronomy Journal*. https://doi.org/10.2134/agronj1987.00021962007900040008x

Khush, G. S. (2005). What it will take to Feed 5.0 Billion Rice consumers in 2030. *Plant Molecular Biology*, *59*(1), 1–6. https://doi.org/10.1007/s11103-005-2159-5

Manjappa, K., & Prabhakar, A. S. (2003). Relationship between main crop stem carbohydrate to ratoon crop yield. *Indian Journal of Agronomy*.

Milligan, S. B., Gravois, K. A., & Martin, F. A. (1996). Inheritance of sugarcane ratooning ability and the relationship of younger crop traits to older crop traits. *Crop Science*. https://doi.org/10.2135/cropsci1996.0011183X0036

00010008x

Munda, G. C., Das, A., & Patel, D. P. (2009). Evaluation of transplanted and ratoon crop for double cropping of rice (Oryza sativa L.) under organic input management in mid altitude sub-tropical Meghalaya. *Current Science*.

Nakano, H., Hattori, I., Sato, K., Morita, S., Kitagawa, H., & Takahashi, M. (2010). Effects of cutting height of the first crop on estimated total digestible nutrient concentration and yield in double-harvested rice. *Agronomy Journal*. https://doi.org/10.2134/agronj2009.0347

Nakano, H., & Morita, S. (2007). Effects of twice harvesting on total dry matter yield of rice. *Field Crops Research*. https://doi.org/10.1016/j.fcr.2006.12.001

Nam, K. H., Nam, K. J., An, J. H., Jeong, S. C., Park, K. W., Kim, H. B., & Kim, C. G. (2013). Comparative analysis of key nutrient composition between drought-tolerant transgenic rice and its non-transgenic counterpart. *Food Science and Biotechnology*. https://doi.org/10.1007/s10068-013-0222-6

Negalur, R. B., Yadahalli, G. S., Chittapur, B. M., Guruprasad, G. S., & Narappa, G. (2017). Ratoon Rice: A Climate and Resource Smart Technology. *International Journal of Current Microbiology and Applied Sciences*. https://doi.org/10.20546/ijcmas.2017.605.179

Pasaribu, P. O., Triadiati, & Anas, I. (2018). Rice ratooning using the salibu system and the system of rice intensification method influenced by physiological traits. *Pertanika Journal of Tropical Agricultural Science*.

Samson, B. T., & Zandstra, H. G. (1980). The effect of two temperature regimes on the ratoonability of some IRRI cultivars/experimental lines. *Philippine Journal of Crop Science*.

Santos, A. B., Fageria, N. K., & Prabhu, A. S. (2003). Rice ratooning management practices for higher yields. *Communications in Soil Science and Plant Analysis*. https://doi.org/10.1081/CSS-120018981

ShangShou, Z., ChuanYing, Z., WeiZhao, J., YiZhen, L., & CongHua, G. (2003). Yield formation of and cultivation techniques for super high-yielding ratooning rice. *Fujian Journal of Agricultural Sciences*.

Vinutha, K. S., Anil Kumar, G. S., Blümmel, M., & Srinivasa Rao, P. (2017). Evaluation of yield and forage quality in main and ratoon crops of different sorghum lines. *Tropical Grasslands-Forrajes Tropicales*. https://doi.org/10.17138/TGFT(5)40-49

Elucidating the Molecular Mechanism of β-Citraurin Accumulation in Citrus Fruit

Gang MA, Lancui ZHANG, Masaya KATO*

Department of Bioresource Sciences, Faculty of Agriculture, Shizuoka University, 836 Ohya, Suruga, Shizuoka 422-8529, Japan

* Corresponding Author: kato.masaya@shizuoka.ac.jp

SUMMARY

β-Citraurin, a C30 apocarotenoid, is a color-imparting pigment responsible for the reddish color of citrus fruits. In citrus fruits, the accumulation of β-citraurin is not a common event, it is only observed in the flavedos of some varieties during the fruit maturation. Although more than seventy years have passed since β-citraurin was first identified, the biosynthesis pathway is still unknown. In this study, to elucidate the molecular mechanism of β-citraurin accumulation, carotenoids contents and expression of genes related to carotenoid metabolism were investigated in two citrus varieties of Satsuma mandarin (*Citrus unshiu* Marc.), 'Yamashitabeni-wase', which accumulates β-citraurin predominantly, and 'Miyagawa-wase', which does not accumulate β-citraurin. The results suggest that *CitCCD4* was the key gene contributing to the biosynthesis of β-citraurin. In the flavedo of 'Yamashitabeni-wase', the expression of *CitCCD4* increased rapidly from October, which was consistent with the accumulation of β-citraurin. In the flavedo of 'Miyagawa-wase', the expression of *CitCCD4* remained at an extremely low level during the ripening process, which was consistent with the absence of β-citraurin. Functional analysis showed that the cleavage of β-cryptoxanthin and zeaxanthin at 7,8 or 7',8' position by CitCCD4 enzyme led to the formation of β-citraurin in citrus fruits. These results presented herein might contribute to elucidate the mechanism of β-citraurin accumulation in citrus fruits, which might facilitate the improvement in the citrus nutritional and commercial qualities.

Introduction

Carotenoids, a diverse group of pigments widely distributed in nature, fulfill a variety of important functions in plants and play a critical role in human nutrition and health (Krinsky et al., 2003; Ledford and Niyogi, 2005). As carotenoids contain a series of conjugated double bonds in the central chain, they can be oxidatively cleaved in a site-specific manner (Mein et al., 2011). The oxidative cleavage of carotenoids not only regulates their accumulation, but also produces a range of apocarotenoids (Walter et al., 2010). In higher plants, many different apocarotenoids derive from the cleavage of carotenoids, and have important metabolic functions, such as plant hormones, pigments, aroma and scent compounds, as well as signaling compounds (Fig.1).

Carotenoid cleavage dioxygenases (CCDs) are a group of enzymes that catalyze the oxidative cleavage of carotenoids (Ryle and Hausinger, 2002). CCDs are nonheme iron enzymes present in plants, bacteria and animals. In plants, CCDs belong to an ancient and highly heterogeneous family (CCD1, CCD4, CCD7, CCD8 and NCEDs). The similarity among the different members is very low apart from four strictly conserved histidine residues and a few glutamate residues (Kloer and Schulz, 2006; Walter et al., 2010). In Arabidopsis, the CCD family contains nine members (CCD1, NCED2, NCED3, CCD4, NCED5, NCED6, CCD7, CCD8 and NCED9), and orthologues in other plant species are typically named according to their homology with an Arabidopsis CCD (Huang et al., 2009). In plants, NCEDs locate in plastids and catalyze the cleavage of 9-*cis*-violaxanthin and 9'-*cis*-neoxanthin to form C_{25} epoxy-apocarotenal and xanthoxin, a precursor of ABA. This reaction is a rate-limiting step in ABA biosynthesis (Chernys and Zeevaart, 2000; Kato et al., 2006). CCD1 symmetrically cleaves the 9,10 and 9',10' double bonds of multiple carotenoid substrates to form C_{14} dialdehyde and two C_{13} products, which vary depending on the carotenoid substrate (Schwartz et al., 2001). When the substrate of CCD1 was β-carotene, the volatile apo-carotenoid β-ionone, which contributes to the fragrance of flowers and flavor of fruits, was generated (Kato et al.,

2006). CCD7 and CCD8 were identified from shoot branching mutants (Booker et al., 2004; Sorefan et al., 2003). Alder et al. (2012) reported that CCD7 and CCD8 together with D27 were involved in the biosynthesis of strigolactone, a shoot branching inhibitor hormone, using all-*trans*-β-carotene as a substrate. Compared with other CCDs, the function of CCD4 is poorly understood. In *Chrysanthemum morifolium*, CmCCD4a contributed to the white color formation by cleaving carotenoids into colorless compounds (Ohmiya et al., 2006). Recently, it has been reported that CsCCD4, CmCCD4a and MdCCD4 could cleave β-carotene to yield β-ionone (Rubio et al., 2008; Huang et al., 2009).

β-Citraurin, a C_{30} apocarotenoid, is a color-imparting pigment responsible for the reddish color of citrus fruits (Farin et al.,1983). In 1936, it was first discovered in Sicilian oranges (Cual, 1965). In citrus fruits, the accumulation of β-citraurin is not a common event, it is only observed in the flavedos of some varieties during the fruits maturation. The citrus varieties accumulating β-citraurin are considered more attractive because of their red-orange color (Ríos et al., 2010). Although more than seventy years have passed since β-citraurin was first identified, the pathway of its biosynthesis is still unknown. In the present study, we found that *CitCCD4* gene was involved in the synthesis of β-citraurin in citrus. To confirm the role of the *CitCCD4* gene further, functional analyses of the CitCCD4 enzyme were performed *in vitro*. The present study is the first to investigate the biosynthesis of β-citraurin in citrus fruits. The results might provide new strategies to enhance the nutritional and commercial qualities of citrus fruits.

Materials and Methods

1. *Plant Material*

Two varieties of Satsuma mandarin (*Citrus unshiu* Marc.), 'Yamashitabeni-wase' and 'Miyagawa-wase', cultivated at the Fujieda Farm of Shizuoka University (Shizuoka, Japan) were used as materials.

2. *Extraction and Determination of Carotenoids*

The identification and quantification of carotenoids were conducted according to the methods described by Kato et al. (2004). Total carotenoid is the sum of the content of various carotenoids detected in this study. The carotenoid concentration was estimated by the standard curves and expressed as micrograms per gram fresh weight.

3. *Isolation and Identification of β-Citraurin*

The carotenoids extracted from the flavedo of 'Yamashitabeni-wase' were loaded on a column of silica gel using a hexane:ethyl ether: isopropyl alcohol (7:3:1 [v/v]) solution as eluent. The red pigment was collected and evaporated to dryness. The collection was subjected to HPLC and identified by spectrophotometry and mass spectrometry. The UV-visible spectra were taken with a spectrophotometer. Fast atom bombardment mass spectrometry (FAB-MS) analysis was performed with the API 2000 triple stage quadrupole mass spectrometer.

4. *Total RNA Extraction and Real-time Quantitative RT-PCR*

Total RNA was extracted from the flavedos and juice sacs of 'Yamashitabeni-wase' and 'Miyagawa-wase' at different stages according to the method described by Ikoma et al. (1996). The cDNA was synthesized and the gene expression was confirmed by real-time PCR.

5. *Functional Analysis of CitCCD4 Enzyme in vitro*

The *CitCCD4* cDNA from 'Yamashitabeni-wase' was cloned into the pCold I vector. The recombinant plasmid was transformed into XL1-Blue cells. The transformants were plated in LB medium supplemented with carbenicillin (50 μg ml^{-1}), and incubated at 37 ˚C for 20 h. The colonies were incubated in 100 ml of 2×YT medium with carbenicillin (50 μg ml^{-1}) at 37 ˚C for 16 h. Then, 2 ml of culture solution was inoculated into 200 ml of 2×YT medium with carbenicillin (50 μg ml^{-1}). Cultures were grown at 37 ˚C until an OD_{600} of 0.7 was reached. The culture solution was quickly refrigerated at 15 ˚C and left to stand for 30 minutes. The expression of proteins was induced by the addition of IPTG, and the cultures were grown at 15 ˚C for an additional 24 h. The cells were harvested by centrifugation, frozen in liquid nitrogen, and then resuspended in 2.5 ml of extraction buffer (0.1 M Tris-HCl, pH 7.2, 30 mM Na-ascorbate, 5 mM dithiothreitol (DTT), 10% (v/v) glycerol, 0.05% (v/v) Triton X-100). After sonication and centrifugation, the complex was subjected to gel filtration using a PD-10 column.

The enzymatic activities of the recombinant CitCCD4 protein were assayed in a reaction mixture consisting of 0.1 M Tris-HCl, pH 7.2, 30 mM Na-ascorbate, 50 μM $FeSO_4$, 20 μg catalase, 0.05% (v/v) Triton X-100, 20% (v/v) glycerol, 1 mM carotenoid substrate (β-cryptoxanthin, zeaxanthin, all-*trans*-violaxanthin and 9-*cis*-violaxanthin) and 5 μg of the recombinant protein in a total volume of

200 µl at 27 ˚C for 3 h. After the incubation, 1 ml of water was added to the reaction mixture. The reaction products were partitioned three times into 1.2 ml of ethyl acetate, evaporated to dryness, and dissolved in methanol. An aliquot (20 µl) was analyzed by HPLC.

6. *Treatment with Ethylene and Red LED light*

Fruits of 'Yamashitabeni-wase' harvested in October were used as materials. For the ethylene treatment, fruits were treated with 50 µl L^{-1} ethylene for three days at 20 ˚C. For the red LED light treatment, fruits were irradiated with red LED lights (660 nm) at an intensity of 150 µmol $m^{-2}s^{-1}$ for three days at 20 ˚C. Fruits stored at 20 ˚C (RH 75%) in the dark were used as the control.

Results and Discussion

1. *Accumulation of β-Citraurin in the Flavedos of Citrus Fruits*

β-Citraurin, a C_{30} apocarotenoid, is a red pigment responsible for the attractively reddish peel color of citrus (Farin et al., 1983). However, the accumulation of β-citraurin is not a common event in citrus; it has been detected in only a few varieties (Xu et al., 2011). In the present study, we isolated β-citraurin from the flavedo of 'Yamashitabeni-wase' using a silica gel column and HPLC. The mass spectrum and absorption maximum of the β-citraurin were consistent with those reported by Farin and Agócs (Farin et al., 1983; Agócs et al., 2007; Fig. 1).

Additionally, changes in the content of β-citraurin were examined in the flavedos of two varieties of Satsuma mandarin, 'Yamashitabeni-wase' and 'Miyagawa-wase', during the fruit maturation process. The results showed that the content of β-citraurin increased significantly from October in 'Yamashitabeni-wase', while it was undetectable in 'Miyagawa-wase' throughout the ripening process (Fig. 2). This difference led to different peel colors between the two varieties. The accumulation of β-citraurin contributed to the reddish peel in 'Yamashitabeni-wase', while the complete absence of β-citraurin led to the yellowish peel in 'Miyagawa-wase'.

Although more than seventy years have passed since β-citraurin was first identified in citrus fruits, the pathway of β-citraurin biosynthesis has yet to be elucidated (Cual, 1965). In the present study, the contents of β-cryptoxanthin, zeaxanthin and β-citraurin rapidly increased from October in 'Yamashitabeni-wase'. The concomitant increase of β-cryptoxanthin, zeaxanthin and β-citraurin indicated that β-citraurin might be a breakdown product of β-cryptoxanthin

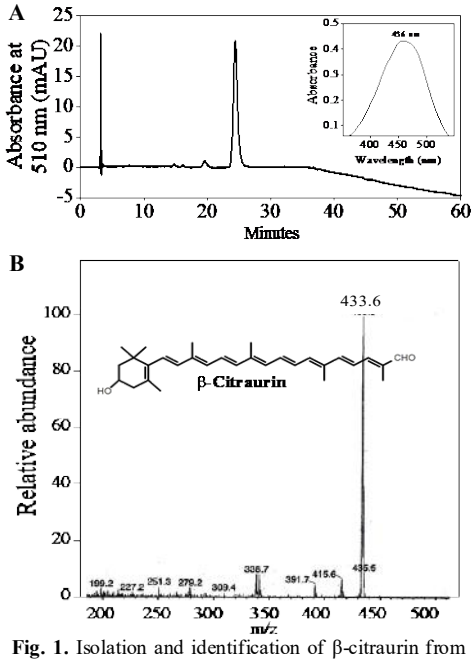

Fig. 1. Isolation and identification of β-citraurin from the flavedo of 'Yamashitabeni-wase'. (A) HPLC analysis and UV-visible light spectra of β-citraurin. (B) FAB-MS spectra of β-citraurin.

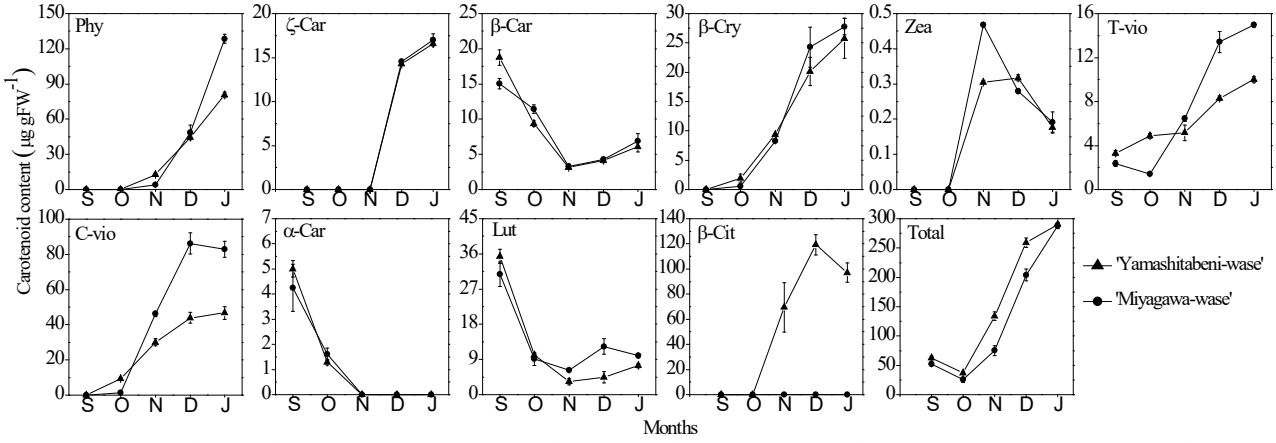

Fig. 2. Carotenoids accumulation in flavedos of 'Yamashitabeni-wase' and 'Miyagawa -wase' during the ripening process. S, September; O, October; N, November; D, December; J, January. Phy, phytoene; ζ-Car, ζ-carotene; β-Car, β-carotene; β-Cry, β-cryptoxanthin; Zea, zeaxanthin; T-vio, all-*trans*-violaxanthin; C-vio, 9-*cis*-violaxanthin; α-Car, α-carotene; Lut, lutein; β-Cit, β-citraurin; Total, total carotenoids.

and zeaxanthin. Additionally, in 'Miyagawa-wase', β-citraurin was not accumulated, zeaxanthin was further converted into all-*trans*-violaxanthin and 9-*cis*-violaxanthin, and as a result, the contents of all-*trans*-violaxanthin and 9-*cis*-violaxanthin were higher than those in 'Yamashitabeni-wase' (Fig. 2).

2. *Isolation and Sequence Analysis of CitCCD4*

To find the enzyme responsible for β-citraurin biosynthesis, we compared the expression of genes related to carotenoid metabolism between the two varieties of Satsuma mandarin, 'Yamashitabeni-wase' and 'Miyagawa-wase'. In the flavedo, a significant difference in the expression of *CitCCD4* was observed between the two varieties. In 'Yamashitabeni-wase', the expression of *CitCCD4* increased rapidly with a peak in December, which was consistent with the accumulation of β-citraurin (Fig. 3). In 'Miyagawa-wase', the expression of *CitCCD4* remained at a low level during the ripening process, which was consistent with the absence of β-citraurin in the flavedo (Fig. 3). Moreover, in the juice sacs, where β-citraurin was not accumulated, the expression of *CitCCD4* was extremely low in both 'Yamashitabeni-wase' and 'Miyagawa-wase' (data not shown). These results suggested that *CitCCD4* was a key factor for regulating β-citraurin biosynthesis.

3. *Functional Analyses of Recombinant CitCCD4 Enzyme*

Compared with other CCDs, the information about the functions of CCD4 is limited. In potato, down-regulation of CCD4 gene expression using RNAi resulted in increased violaxanthin content (Campbell et al., 2010).

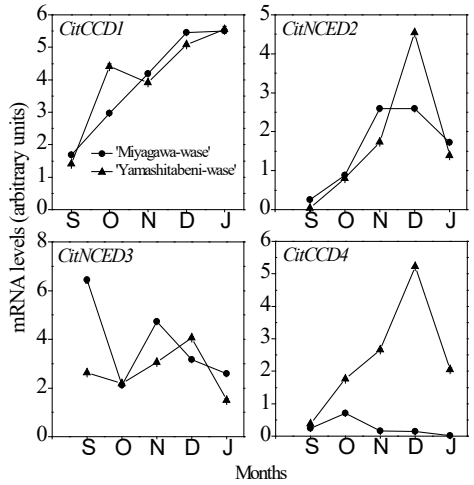

Fig. 3. Changes in the expression of genes related to carotenoid metabolism in flavedos of 'Yamashitabeni-wase' and 'Miyagawa-wase' during the ripening process.

In Chrysanthemum morifolium, CmCCD4a contributed to the white color formation by cleaving carotenoids into colorless compounds (Ohmiya et al., 2006). A common feature of CCD4 identified in several recent studies is a 9,10 or 9',10' cleavage activity to yield β-ionone (Huang et al., 2009; Rubio et al., 2008). However, the 7,8 or 7',8' cleavage activity of CCD4 remains to be confirmed. Bouvier *et al.* (2003) reported that CsZCD specifically catalyzed the cleavage of zeaxanthin at the 7,8 and 7',8' positions of the chromophore and initiated the formation of saffron secondary metabolites.

In the present study, we found that CitCCD4 enzyme exhibited substrate specificity. It cleaved β-cryptoxanthin and zeaxanthin at the 7,8 or 7',8' position (Fig. 4). But other carotenoids tested in the present study (lycopene, α-carotene, β-carotene, all-*trans*-violaxanthin and 9-*cis*-violaxanthin) were not cleaved by CitCCD4 enzyme. Moreover, the cleavage of β-cryptoxanthin and zeaxanthin by CitCCD4 enzyme led to the formation of β-citraurin. The specific cleavage reaction of CitCCD4 enzyme presented herein further confirmed the previous speculations that β-citraurin was a breakdown product of β-cryptoxanthin and zeaxanthin. In addition, when β-cryptoxanthin was used as the substrate for the cleavage reaction of the recombinant CitCCD4 enzyme, *trans*-β-apo-8'-carotenal, which eluted at 43 min, was also detected except for β-citraurin (Fig. 4). However, we have not been

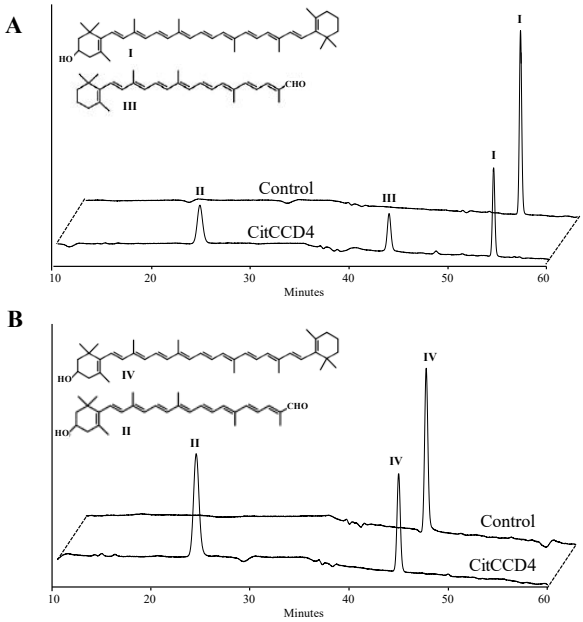

Fig. 4. Functional analysis of CitCCD4 enzyme *in vivo*. (A) HPLC analysis of the cleavage products from the incubation of β-cryptoxanthin with recombinant CitCCD4. (B) HPLC analysis of the cleavage products from the incubation of zeaxanthin with recombinant CitCCD4. Peak I, β-cryptoxanthin; Peak II, β-citraurin; Peak III, *trans*-β-apo-8'-carotenal; Peak IV, zeaxanthin.

able to detect *trans*-β-apo-8'-carotenal in the flavedos or

juice sacs of citrus fruits. It is possible that *trans*-β-apo-8'-carotenal might be further cleaved by other CCDs in the citrus fruits.

4. *Effects of Ethylene and Red LED Light on β-Citraurin Content and CitCCD4 Expression*

It has been reported that ethylene treatment increased the contents of carotenoids; as a result, the degreening process of citrus fruits was accelerated (Rodrigo and Zacarías, 2007). We previously found that red LED light was effective to enhance carotenoids contents, especially the content of β-cryptoxanthin, while blue LED light had no significant effect on the carotenoid content in the flavedo of Satsuma mandarin (Ma et al., 2012). In the present study, to investigate the regulatory effects of ethylene and red LED light on β-citraurin accumulation, fruits harvested in October were used as materials, as the changes in β-citraurin content were most significant at this stage. As shown in Fig. 5, the content of β-citraurin was increased by the ethylene and red LED light treatments. In the meanwhile, the accumulation of β-citraurin induced by ethylene and red light treatments was attributed to an increase in the expression of *CitCCD4*. The results presented herein provide more insights into the regulatory mechanism of β-citraurin metabolism in citrus fruits.

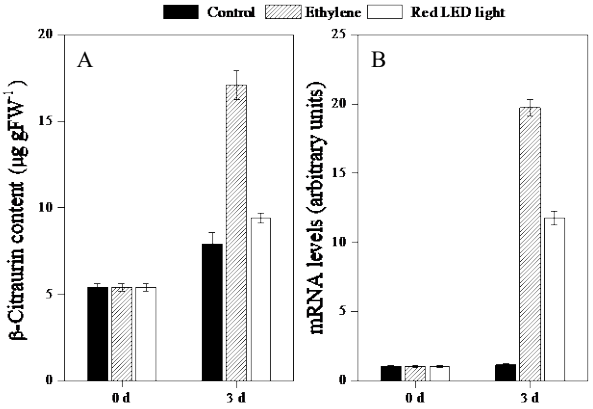

Fig. 5. Effect of ethylene and red LED light on β-citraurin content (A) and gene expression of *CitCCD4* (B) in flavedo of 'Yamashitabeni-wase'.

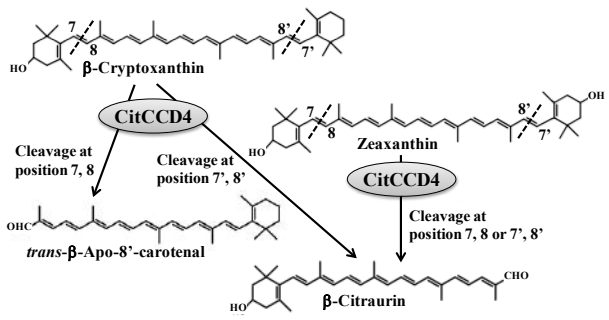

Fig. 6. β-Citraurin biosynthetic pathway in citrus fruits.

Conclusion

In the present study, the biosynthetic pathway of β-citraurin was investigated using two citrus varieties of Satsuma mandarin, 'Yamashitabeni-wase', which accumulates β-citraurin predominantly, and 'Miyagawa-wase', which does not accumulate β-citraurin. The results suggested that *CitCCD4* was a key gene regulating the biosynthesis of β-citraurin. The cleavage of β-cryptoxanthin and zeaxanthin by *CitCCD4* enzyme led to the formation of β-citraurin (Fig. 6). In addition, the ethylene and red light treatments were effective to enhance the content of β-citraurin by up-regulating the expression of *CitCCD4* in the flavedo of 'Yamashitabeni-wase'. These results presented herein might contribute to elucidate the mechanism of β-citraurin accumulation in citrus fruits, which might facilitate the improvement in the citrus nutritional and commercial qualities.

References

Agócs, A., Nagy, V., Szabó, Z., Márk, L., Ohmacht, R., Deli, J. (2007) Comparative study on the carotenoid composition of the peel and the pulp of different citrus species. *Innov Food Sci Emerg Technol* 8, 390-394.

AlderM, A., Jmil, M., Marzorati, M., Bruno, M., Vermathen, M., Bigler, P., Ghisla, S., Bouwmeester, H., Beyer, P., Al-Babili, S. (2012) The path from β-carotene to carlactone, a strigolactone-like plant hormone. *Science* 335, 1348-1351.

Booker, J., Auldridge, M., Wills, S., McCarty, D., Klee, H., Leyser, O. (2004) *MAX3*/CCD7 is a carotenoid cleavage dioxygenase required for the synthesis of a novel plant signalling molecule. *Curr Biol* 14, 1232-1238.

Bouvier, F., Suire, C., Mutterer, J., Camara, B. (2003) Oxidative remodeling of chromoplast carotenoids: identification of the carotenoid dioxygenase CsCCD and *CsZCD* genes involved in Crocus secondary metabolite biogenesis. *Plant Cell* 15, 47-62.

Campbell, R., Ducreux, L.J., Morris, W.L., Morris, J.A., Suttle, J.C., Ramsay, G., Bryan, G.J., Hedley, P.E., Taylor, M.A. (2010) The metabolic and developmental roles of carotenoid cleavage dioxygenase4 from potato. *Plant Physiol* 154, 656-664.

Chernys, J.T., Zeevaart, J.A.D. (2000) Characterization of the 9-*cis*-epoxycarotenoid dioxygenase gene family and the regulation of abscisic acid biosynthesis in

avocado. *Plant Physiol* 124, 343-353.

Cual, A.L. (1965) The occurrence of beta-citraurin and of beta-apo-8′-carotenal in the peels of california tangerines and oranges. *J Food Sci* 30, 13–18.

Farin, D., Ikan, R., Gross, J. (1983) The carotenoid pigments in the juice and flavedo of a mandarin hybrid (Citrus reticulata) vs Michal during ripening. *Phytochemistry* 22, 403-408.

Huang, F.C., Molnár, P., Schwab, W. (2009) Cloning and functional characterization of carotenoid cleavage dioxygenase 4 genes. *J Exp Bot* 60, 3011-3022.

Ikoma, Y., Yano, M., Ogawa, K., Yoshioka, T., Xu, Z.C., Hisada, S., Omura, M., Moriguchi, T. (1996) Isolation and evaluation of RNA from polysaccharide-rich tissues in fruit for quality by cDNA library construction and RT-PCR. *J Jpn Soc Hortic Sci* 64, 809-814.

Kato, M., Ikoma, Y., Matsumoto, H., Sugiura, M., Hyodo, H., Yano, M. (2004) Accumulation of Carotenoids and Expression of carotenoid Biosynthetic Genes during Maturation in Citrus Fruit. *Plant Physiol* 134, 824-837.

Kato, M., Matsumoto, H., Ikoma, Y., Okuda, H., Yano, M. (2006) The role of carotenoid cleavage dioxygenases in the regulation of carotenoid profiles during maturation in citrus fruit. *J Exp Bot* 57, 2153-2164.

Kloer, D.P., Schulz, G.E. (2006) Structural and biological aspects of carotenoid cleavage. *Cell Mol Life Sci* 63, 2291-2303.

Krinsky, N.I., Landrum, J.T., Bone, R.A. (2003) Biologic mechanisms of the protective role of lutein and zeaxanthin in the eye. *Annu Rev Nutr* 23, 171-201.

Ledford, H.K., Niyogi, K.K. (2005) Singlet oxygen and photo-oxidative stress management in plants and algae. *Plant Cell Environ* 28, 1037-1045.

Ma, G., Zhang, L., Kato, M., Yamawaki, K., Kiriiwa, Y., Yahata, M., Ikoma, Y., Matsumoto, H. (2012) Effect of blue and red LED light irradiation on β-cryptoxanthin accumulation in the flavedo of citrus fruits. *J Agric Food Chem* 60, 197-201.

Mein, J.R., Dolnikowski, G.G., Ernst, H., Russell, R.M., Wang, X.D. (2011) Enzymatic formation of apo-carotenoids from the xanthophyll carotenoids lutein, zeaxanthin and β-cryptoxanthin by ferret carotene-9',10'-monooxygenase. *Arch Biochem Biophys* 506, 109-121.

Ohmiya, A., Kishimoto, S., Aida, R., Yoshioka, S., Sumitomo, K. (2006) Carotenoid cleavage dioxygenase (CmCCD4a) contributes to white color formation in chrysanthemum petals. *Plant Physiol* 142, 1193-1201.

Ríos, G., Naranjo, M.A., Rodrigo, M.J., Alós, E., Zacarías, L., Cercós, M., Talón, M. (2010) Identification of a GCC transcription factor responding to fruit colour change events in citrus through the transcriptomic analyses of two mutants. *BMC Plant Biol* 10, 276.

Rubio, A., Rambla, J.L., Santaella, M., Gómez, M.D., Orzaez, D., Granell, A., Gómez-Gómez, L. (2008) Cytosolic and plastoglobule-targeted carotenoid dioxygenases from C*rocus sativus* are both involved in beta-ionone release. *J Biol Chem* 283, 24816-24825.

Ryle, M.J., Hausinger, R.P. (2002) Non-heme iron oxygenases. Curr Opin Chem Biol 6, 193-201.

Schwartz, S.H., Qin, X., Zeevaart, J.A.D. (2001) Characterization of a novel carotenoid cleavage dioxygenase from plants. *J Biol Chem* 276, 25208–25211.

Sorefan, K., Booker, J., Haurogne, K., Goussot, M., Bainbridge, K., Foo, E., Chatfield, S.P., Ward, S., Beveridge, C.A., Rameau, C. (2003) *MAX4* and *RMS1* are orthologous dioxygenase-like genes that regulate shoot branching in Arabidopsis and pea. *Genes Dev* 17, 1469-1474.

Walter, M.H., Floss, D.S., Strack, D. (2010) Apocarotenoids: hormones, mycorrhizal metabolites and aroma volatiles. *Planta* 232, 1-17.

Xu, J., Liu, B.Z., Liu, X., Gao, H.J., Deng, X.X. (2011) Carotenoids synthesized in citrus callus of different genotypes. *Acta Physiol Plant* 33, 745-753.

Metabolite Fingerprinting of Assam Tea (*Camellia sinensis* L.(O) Kuntze) Under Alumnium Stress

Sanjenbam Sanjibia Devi[1], Sanjib Kumar Panda[1,2*]

[1] Plant Molecular Biotechnology laboratory, Department of Life Science & Bioinformatics, Assam University Silchar

[2] Department of Biochemistry, School of Life Sciences, Central University of Rajasthan, Bandarsindri, 305817, Ajmer Rajastha

[*] Corresponding author: profskpanda73@gmail.com, sanjib.panda@curaj.ac.in

SUMMARY

Tea, *Camellia sinesis* (L.) *Kuntze* in the genus of *Camellia,* belongs to the family of Theaceae, is an economically important horticultural crop and most popular beverages and an important financial source for those tea producing countries in the world. Assam, a north eastern state of India is famous as the largest tea producing state, forming one of the major tea producing area globally. From the structural difference the tea catechins can be divided into dihydoxylated (ECG, EC and C) and trihydroxylated (EGCG, EGC and GC) with 5' position in the B ring . The presence of hydroxyl group at the 5' position in the B ring is shown by structure activity relationship and is the most potent scavenging antioxidant. Flavonoid 3'-hydroxylase (F3'H) and flavonoid 3',5'-hydroxylase (F3'5') are the soul enzymes which control the hydroxylation of narigenin and dihydrokaempferol at either 3' position or in both 3' and 5' position in B ring. With the flow of their downstream processing enzymes the intermediate resultant is to form dihydroxylated and trihydroxylated flavonoids. NMR is one of the popularly used multivariate method which offers a broad range of secondary metabolites evaluation to differentiate the quality of tea. Metabolomic study exemplifies the consolidation of the genetic background information that changes by the environmental stresses in plants. In our study, metabolite fingerprinting of tea leaves was performed to examine the response to alumnium stress in two tea varieties S3A3 and S3A1 (Assamica) by $_1$H NMR. Certain secondary metabolites were found from NMR peak of tea leaves. Among them carbohydrates were found less in stress conditions and in case of phenolic compounds (catechins) the number of peaks and intensity were slightly increased at stressed tea leaves. And other metabolites amino acids, caffeine, gallic acids, myo inositol and some organic acids were detected. Flavonoid 3'-hydroxylase (F3'H) and flavonoid 3',5'-hydroxylase (F3'5') are the enzymes affecting the ratio of dihydoxylated to trihydroxylated catechins in *Camellia sinensis.* Expression of these genes were analyzed by real time RT-PCR. Slight Changes were observed in ratio of dihydroxylated to trihydroxylated (RDTC) catechins under alumnium stress showing that alumnium stress affects the tea composition and could change the metabolic pathways.

Introduction

Tea, *Camellia sinesis* (L.) *Kuntze* in the genus of *Camellia,* belongs to the family of Theaceae, is an economically important horticultural crop and model system for studying self-incompatibility as well as an evergreen flowering plant. Tea is one of the most popular beverages and an important financial source for those tea producing countries in the world. Assam contributes around 50 percent of total tea produced in India. Barak valley and upper Assam has the maximum numbers of tea plantation. The climate of the state is such that it gives sweetness and an earthy flavor. Due to the extensive secondary metabolites in tea leaves yields many health benefits to human beings which includes polyphenols, theanine and volatile oils (Yamamoto et al. 1999, Rogers et al. 2008). India, beside being the second largest tea producer, is the highest consumer of tea. 82% of the total production is consumed inside and the remaining 18% is exported (Annual report 2016-17, Dept of Commerce, Govt. of India; www.commerce.gov.in). Assam, a north eastern state of India is famous as the largest tea producing state, forming one of the major tea producing area globally. The crops, growing in the soil of North East India is

inflicted with alumnium (Al) toxicity due to soil acidity in this region (Kumar et al. 2013). Excessive rainfall in culmination with deforestation is the main reason behind the flushing of essential cations from the soil rendering the soil acidic (Saha et al. 2012). However the tea plant (*Camellia sinensis*) being a typical alumnium (Al) hyper-accumulator grow relatively well on acidic soil polluted with high levels of soluble ionic Al. To understand the full mechanisms that are used by the Al; tolerant plant and species to fight with Al toxicity is important and to find out the specific genotype with most suitable and tolerant in acidic environment mainly to enhance the productivity, yield. One of fundamental economic solution for making the food production increased new cultivars development may be from the Al rich region is necessary (Silva 2012). The raw materials of tea making is one most important factor contributed to the quality of Northeast India Tea, this is mainly given by their constituents of polyphenol. The quality of black tea is contributed mainly by flavanol precisely catechins. Among the antioxidant catechins, epigallocatechin gallate (EGCG) is the most potent one and used as biochemical marker for NorthEast Indian tea (Gupta et al. 2002). The tea from Northeast India are mainly processed from *Camellia Assamica* leaf and it has the uniqueness due to the presence of wide range of catechins (Sabhapondit et al. 2012). The tea plant can be distinguished into three different verities according to their phenotypic characteristics, Assam, China and Cambod type. This classification of variation is followed only in Indian sun continent due to presence of huge population tea plant (Wight 1962). The constituents of tea leaves can easily differentiate between hybrids, an interrelationship between taxa can be set up with the presence and absence of different polyphenols (Roberts et al. 1958). NMR is one of the popularly used multivariate method which offers a broad range of secondary metabolites evaluation to differentiate the quality of tea. All these information al together with metabolomics has the possibility to furnish an authentic and conclusive envision or scenario of composition of tea related to their quality. $_1$H NMR metabolic profiling and fingerprinting are a treasure of information in wide range of secondary metabolites (Tarachiwin et al. 2007). For the tea quality evaluation NMR technique are preferred than the other analytical techniques due to giving more structural information. It helps to obtain the information about the molecular structure of tea constituents from NMR spectra.

The aim of this investigation is to evaluate the changes of chemical constituents after exposure to alumnium stress in tea leaves.

Materials and Methods

1. *Sample Preparation for NMR*

Two to three leaves of tea (soft and tender) were collected and were ground with the help of precooled mortar and pestle with liquid nitrogen. The ground samples were transferred into a plastic bag by a sterilized spatula. Allow it for free drying and then to deep freezer for further analysis. In the freeze dryer the samples were kept for 1-2 days and after this lyophilization process done weight the sample with Eppendorf tube for the analysis. Re-suspension of lyophilized samples in D_2O containing 0.3 mM TSP as a concentration standard and chemical shift reference (δ= 0 ppm). Centrifuge the sample at 14000g at 4^0C for 15 min to remove any particle. After the centrifugation, samples cannot be stored further and should go for NMR analysis immediately. Desired amount (0.7ml) of the sample is transferred into an NMR tube and take spectra (Bruker, H_1 NMR).

For the annotation of unknown compounds, the changes of chemical shift were taken from the previous reports through literature survey and name of the authors and their related details were summarized in the table form along with compounds which were found in our samples. With the help of MestReNova x64 software was used to identify the metabolites in tea leaf samples.

2. *Validation of gene expression by Quantitative RT-PCR analysis of F3'H and F3'5'H*

To validate the co relation of expression between the key genes F3'H and F3'5'H and the ratio dihydroxylated to trihydroxylated catechin (RDTC) in tea plant under alumnium stress according to the Wei et al. 2015. To see the impact of alumnium stress in their ratio this analysis was performed. *CsF3'5'H1* and *CsF3'H* (*CsF3'H1, CsF3'H2* and *CsF3'H3*) were picked for quantitative RT-PCR (qPCR) examination. The RNA was isolated as per method Muoki et al, 2011 from control and stressed (500µM) of leaf; whereas cDNA was prepared according to manufacturer's instructions (PrimeScript 1st Strand cDNA synthesis kit, Takara, Japan). The synthesized cDNA was normalized using GAPDH as housekeeping and the transcript analysis. Real time expression was calculated according to Wei et al. 2014.

Results

NMR is widely used for metabolic profiling in medicinal plants. It provides a fast detailed analysis. The effects of Al stress in tea leaf were studied for the metabolites study. Five different varieties were used in this study. 1H-NMR spectra was recorded at 23°C on Brucker. anomeric protons of carbohydrates were shown by the region of β- glucose, α-glucose, fructose and sucrose. We summarized the information based on the chemical shift from the previously reported and described authors. Shown the ^{1}H NMR spectral signal assignments of two different varieties of tea leaves and arranged in terms of PPM, intensity, width and area of the annotated compounds. The samples shown a characteristic changes between control and stress one as well as variety wise variation were clearly observed. The identification of compounds from tea plants control and stress of five varieties were performed and metabolites or compounds were assigned and comparison with published data (Yuan et al. 2014; Lee et al. 2010, 2011 a, b; Wahyuni et al. 2013; Tarachiwin et al. 2007; Le Gall et al. 2004; Kumar et al. 2016; Ohno et al. 2011; Kim et al. 2010). Enhancement of phenolic content and decrease of sucrose were mainly observed. Phenolic contents like ECGC, ECG, EGC, EC, C, some unknown catechins, theogallin, quinic acid, theaflavins, thearubigin 3,3'-digallate, theaflavin 3,3'-digallate hydroxycinnamic compound ; organic acids, γ-Amino- butyrate, citric acid, malic acid , fumaric acid, succunic acid, proline, theanine, tryptophan, glutamic acid, arginine, threonine, leucine, lysine, caffeine other fatty acids were detected. The presence of metabolites were signicantly different. The phenolic region was depicted at area. 5-8.5 ppm. Epicattechins derivatives and caffeine were detected in the tea leaves. For the identification of the compounds we took the help from the software MestReNova x64 and identified the compounds from tea leaf samples. The detected compounds or seconadry metatloites, chararcteristics of ^{1}H NMR signals were assigned with respected compound name chemical shift (ppm) and authors. In S3A1 variety the control and stressed there were a drastic different between control and stressed one, almost half of the number of peaks were lessly detected in stressed one. This variety shown that the alumnium stress in variety were highly impacts especially on carbohydrates, significantly decreased in stressed and slightly increased in phenolic compounds as well as the flavonoid components. Slightly increased in inositol compound but sudden dropping down

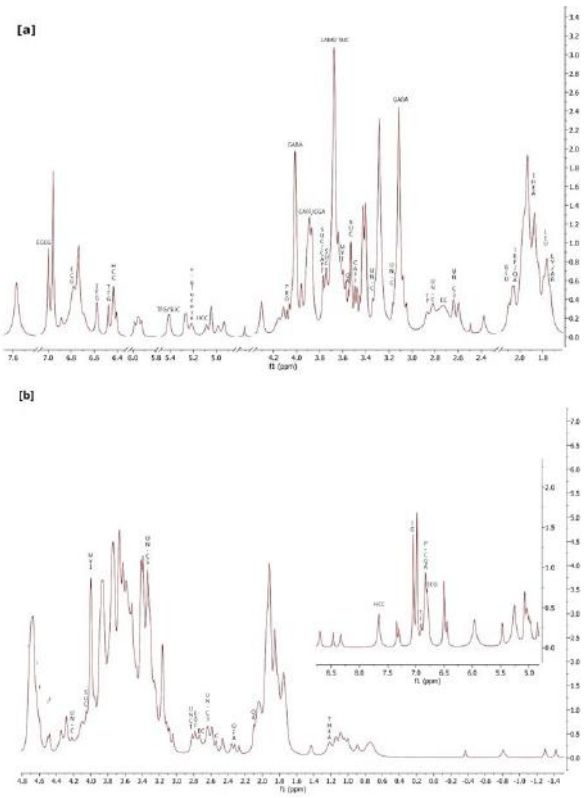

Fig.1 The Representative of ^{1}H-NMR spectra of tea leaf (a) spectrum of S3A1 control leaf; (b) spectrum of S3A1 stressed leaf.

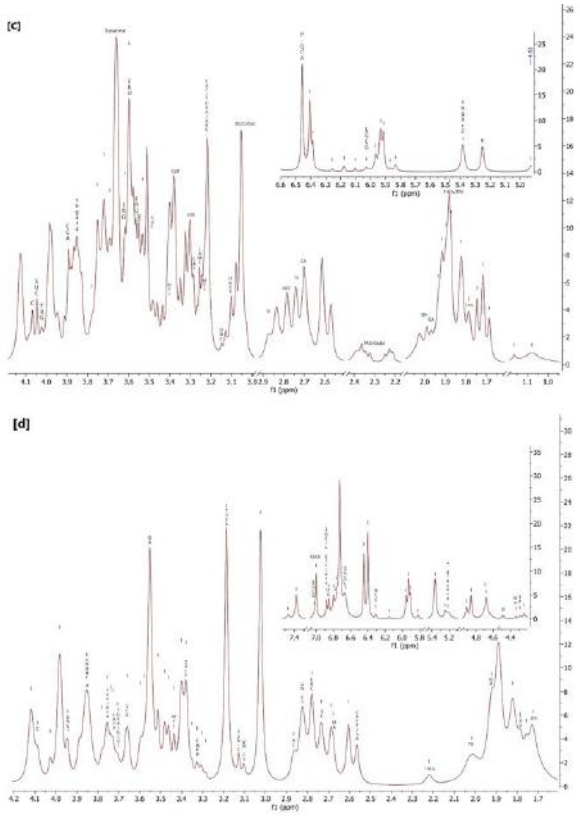

Fig. 2 The Representative of ^{1}H-NMR spectra of tea leaf (c) spectrum of S3A3 control leaf; (d) spectrum of S3A3 stressed leaf.

of sucrose level and could dected glucose at stressed one.

Four key genes F3'H (*CsF3'H1, CsF3'H2 CsF3'H3*) and F3'5'H (*CsF3'5'H1*) were selected and went for their real time RT-PCR expression analysis. These are responsible for the formation of dihydroxylated and trihydroxylated catechins. RNA were isolated according to the protocol (Mouki et al. 2012) from leaf only. The co relation and relationship between key genes and the ratio of dihydoxylated to trihydroxylated catechins (RDTC) were performed. (Fig; 3) . Only one concentration 500 µM were selected for the real time analysis. The ratios of their expressions of key genes (*CsF3'H1+ CsF3'H2 + CsF3'H3*) to *CsF3'5'H1* were calculated by the following protocol Wei et al. 2015. From the co relation analysis shown both two genes were highly co related each other in both stress and unstressed condition of tea plant by pointing towards the expression ratios F3'H to F3'5'H genes has the crucial role in determining the differentiation of RDTC under Al stress of tea plant. Different changes were observed in all the five varieties of tea plant and their relative expressions shown in Fig. 3, shows the *CsF3'H1*, *CsF3'H2* and *CsF3'H3*, the sum of *CsF3'H1+CsF3'H2+CsF3'H3* i.e F3'H showing the relative expression of *CsF3'5'H1* gene under aluminium stress and last were the ratio of dihydoxylated to trihydroxylated catechins (RDTC). We observed the highest ratio were found at S3A3 than S3A1. By our study revealed, aluminium treatment has the impact on the ratio of catechin composition on tea plant.

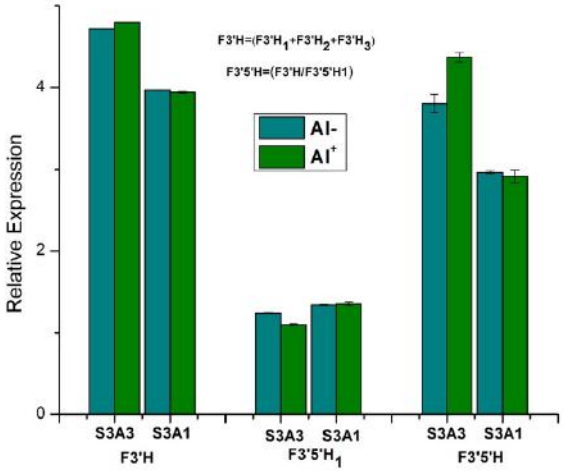

Fig.3 Co relation between F3'H and F3'5'H expression pattern ; Relative expression of F3'H1, F3'H2, F3'H3; relative expression of (F3'H1+F3H+,F3'H3); relative expression of F3'5;H1; ratio of F3'H and F3'5'H.

Discussion

Carbohydrates played an important role in stress tolerance mechanism and it is straightly connected with performance of photosynthesis. Plants utilized both starch and fructans as a source of energy during stress in placed of glucose. In our experiment the sucrose level in 1H MNR peak as well from total carbohydrate quantification were decreased from control to stress in all five varieties.

Sucrose is mainly decreased in stress condition and this compound may be trans-located to root tips to promote growth. The decrease of total sugar concentration were reported in tea plant (Chen et al. 2010; Mukhophadya et al, 2012) and in tobacco (Abdel –Basset et al. 2010). In our study also, carbohydrates content was decrease from control stress and significant increase were at 500 µM (Fig. 1&2). From investigation of total phenolic content, total flavonoid content, allocation of 1H MNR peaks of phenolic compounds, real time PCR of four genes *CsF3'H1+, CsF3'H2, CsF3'H3* and *CsF3'5'H1*. Similar reports were found by (Chen et al. 2011 and Hajiboland et al. 2013a) in tea plant. By the effect of certain enzymes phenolic compounds of tea plants occur in polymerization reaction with the variation of growth condition like temperature, location, drainage, light and weather can cause the variation in the types of polyphenols (Chen et al. 2013). In our investigation in hydroponic condition acidic medium, the changes in the catechins profile were found along with the phenolic related compounds under Al stress in tea plant. Tea plant content varieties of polyphenol compounds formed a complex along with Al. this makes to accelerate the absorption of Al without affecting other functions translocate into various parts of tea plants. The influence of catechins status in tea under aluminium stress were reported by Chen et al. 2011and found statistically significant co relation were found along with Al and ECG as well with total phenolic content. Presence of catechin complexes with Al in leaf were detected through Al NMR spectroscopy, there the chemical form of Al was complexed with catechin and uptake by the root cells, translocated to xylem cell and finally complex reached to leaf cells (Chen et al. 2011). Metabolomics study exemplifies the consolidation of the genetic background information changes by the environmental stresses in plants. And thus, can distinguish accurately the phenotype of plant species. To avoid the stress by the plant's responses certain stimuli of adverse effects is solely depend on particular stress tolerance. To do such things

plants make various alterations of their metabolism at certain conditions and mainly associated with modification of metabolism. The metabolites include sugars, amino acids, sugars alcohols, TCA intermediates. Although the alterations in the secondary metabolites are specific to each given species as well as highly specific to the type of stress.

Substantial enhancement of catechins in tea plant under Al stress might be the presence of potential binding site of Al *ortho-dihydroxyl* group of catechin. Inoue et al. 2002; Chen et al. 2006 (b) reported Al binds to catechin with help of C-3 and C-4 hydroxyl groups of ring B. The browning of catechin was significantly enhanced by Al ions was shown through visible absorption spectroscopy investigation (Chen et al. 2006, b). Not only the catechin profile alterations there were the changes in the nutritional mineral parameters also observed. From $_1$H NMR peak annotation of chemical shift in terms of PPM presence of trihydroxylated catechins were found in stress tea plants. Derivative of polyphenolics are synthesized through shikimate pathway leading to phenylalanine and phenylalanine ammonia lyase (PAL) an important enzyme in the biosynthesis of phenolic compound. Under the adverse and stressful conditions, the enzyme activity of PAL along with other enzymes which is responsible for phenylpropanoid pathway was increased (Wahid A et al. 2007). From the structural difference the tea catechins can be divided into dihydoxylated (ECG, EC and C) and trihydroxylated (EGCG, EGC and GC) with 5' position in the B ring (Wei et al. 2015). The presence of hydroxyl grouped at the 5' position in the B ring is shown by structure activity relationship and is the most potent scavenging antioxidant. Flavonoid 3'-hydroxylase (F3'H) and flavonoid 3',5'-hydroxylase (F3'5') are the only soul enzymes which controls the hydroxylation of narigenin and dihydrokaempferol at either at 3' position or in both 3' and 5' position in B ring (Toda et al. 2002). With the flow of their downstream processing enzymes the intermediate resultant is to form dihydroxylated and trihydroxylated flavonoids. By this way the dihydroxylated and trihydroxylated flavonoids that F3'Hs and F3'5'Hs have played an important role to affect the composition of these two. Calletarrin et al. 2006 studied the expression of both F3'H and F3'5'H genes and showed this affects directly to the accumulation of cyaniding (dihydroxylated)/ dephinidin- (trihydroxylated) in berry skin of grave vines based on anthocyanins that ascertains the variation of color among grape varieties, Callisterin et al. 2006.

Conclusion

In summary, our investigation furnishes an important information regarding the fingerprinting of metabolomics of tea plant. Our finding may help to insight the secondary metabolites accumulation of North East India (Assam) tea and selection of good quality based on biochemical constituents which confers the characteristics of the liquor. Not even this the existence of pure archetypes is become very doubtful due to extreme hybridization. This biochemical biomarkers could be provided as a tool in chemotoxonomic markers to differentiate various resources of tea. Therefore, an authentic clarification of varieties of Assam, Cambod and China could be built using catechin as a biomarker.

References

Abdel-Basset, R., Ozuka, S., Demiral, T., Furuichi, T., Sawatani, I., Baskin, T. I., ... & Yamamoto, Y. (2010). Aluminium reduces sugar uptake in tobacco cell cultures: a potential cause of inhibited elongation but not of toxicity. *Journal of experimental botany*, *61*(6), 1597-1610.

Annual report 2016-17, Dept of Commerce, Ministry of commerce and Industry, Govt. of India. www.commerce.gov.in.

Castellarin, S. D., Di Gaspero, G., Marconi, R., Nonis, A., Peterlunger, E., Paillard, S., ... & Testolin, R. (2006). Colour variation in red grapevines (Vitis vinifera L.): genomic organization, expression of flavonoid 3-hydroxylase, flavonoid 3, 5-hydroxylase genes and related metabolite profiling of red cyanidin-/blue delphinidin-based anthocyanins in berry skin. *Bmc Genomics*, *7*(1), 12.

Chen, L. S., Qi, Y. P., Jiang, H. X., Yang, L. T., & Yang, G. H. (2010). Photosynthesis and photoprotective systems of plants in response to alumnium toxicity. *African Journal of Biotechnology*, *9*(54), 9237-9247.

Chen, Q., Zhang, X. D., Wang, S. S., Wang, Q. F., Wang, G. Q., Nian, H. J., ... & Chen, L. M. (2011). Transcriptional and physiological changes of alfalfa in response to aluminium stress. *The Journal of Agricultural Science*, *149*(6), 737-751.

Chen, Q., Zhang, X. D., Wang, S. S., Wang, Q. F., Wang, G. Q., Nian, H. J., ... & Chen, L. M. (2011). Transcriptional and physiological changes of alfalfa in response to aluminium stress. *The Journal of*

Agricultural Science, *149*(6), 737-751.

Chen, S., Shen, X., Cheng, S., Li, P., Du, J., Chang, Y., & Meng, H. (2013). Evaluation of garlic cultivars for polyphenolic content and antioxidant properties. *PLoS One*, *8*(11), e79730.

Chen, Y. M., Wang, M. K., Zhuang, S. Y., & Chiang, P. N. (2006) (b). Chemical and physical properties of rhizosphere and bulk soils of three tea plants cultivated in Ultisols. *Geoderma*, *136*(1-2), 378-387.

Gupta, N., Gaurav, S. S., & Kumar, A. (2013). Molecular basis of alumnium toxicity in plants: a review. *American Journal of Plant Sciences*, *4*(12), 21.

Hajiboland, R., Bahrami-Rad, S., Bastani, S., Tolrà, R., & Poschenrieder, C. (2013) (a). Boron re-translocation in tea (Camellia sinensis (L.) O. Kuntze) plants. *Acta physiologiae plantarum*, *35*(8), 2373-2381.

Kim, H. K., Choi, Y. H., & Verpoorte, R. (2010). NMR-based metabolomic analysis of plants. *Nature protocols*, *5*(3), 536.

Kumar, A., Pandey, A., & Pattanayak, A. (2013). Evaluation of rice germplasm under jhum cultivation in North East India and breeding for alumnium tolerance. *Ind J Genet*, *73*(2), 153-161.

Kumar, D., Gulati, A., & Sharma, U. (2016). Determination of theanine and catechin in Camellia sinensis (Kangra Tea) leaves by HPTLC and NMR techniques. *Food analytical methods*, *9*(6), 1666- 1674.

Le Gall, G., Colquhoun, I. J., & Defernez, M. (2004). Metabolite profiling using 1H NMR spectroscopy for quality assessment of green tea, Camellia sinensis (L.). *Journal of Agricultural and Food Chemistry*, *52*(4), 692-700.

Lee, J. E., Lee, B. J., Chung, J. O., Hwang, J. A., Lee, S. J., Lee, C. H., & Hong, Y. S. (2010). Geographical and climatic dependencies of green tea (Camellia sinensis) metabolites: a 1H NMR-based metabolomics study. *Journal of agricultural and food chemistry*, *58*(19), 10582-10589.

Lee, J. E., Lee, B. J., Chung, J. O., Shin, H. J., Lee, S. J., Lee, C. H., & Hong, Y. S. (2011 b). 1H NMR-based metabolomic characterization during green tea (Camellia sinensis) fermentation. *Food Research International*, *44*(2), 597-604.

Lee, J. E., Lee, B. J., Hwang, J. A., Ko, K. S., Chung, J. O., Kim, E. H., ... & Hong, Y. S. (2011 a). Metabolic dependence of green tea on plucking positions revisited: A metabolomic study. *Journal of agricultural and food chemistry*, *59*(19), 10579-10585.

Mukhopadyay, M., Bantawa, P., Das, A., Sarkar, B., Bera, B., Ghosh, P., & Mondal, T. K. (2012). Changes of growth, photosynthesis and alteration of leaf antioxidative defence system of tea [Camellia sinensis (L.) O. Kuntze] seedlings under alumnium stress. *Biometals*, *25*(6), 1141-1154.

Muoki, R. C., Paul, A., Kumari, A., Singh, K., & Kumar, S. (2012). An improved protocol for the isolation of RNA from roots of tea (Camellia sinensis (L.) O. Kuntze). *Molecular biotechnology*, *52*(1), 82-88.

Ohno, A., Oka, K., Sakuma, C., Okuda, H., & Fukuhara, K. (2011). Characterization of tea cultivated at four different altitudes using 1H NMR analysis coupled with multivariate statistics. *Journal of agricultural and food chemistry*, *59*(10), 5181-5187.

Rogers, P. J., Smith, J. E., Heatherley, S. V., & Pleydell-Pearce, C. W. (2008). Time for tea: mood, blood pressure and cognitive performance effects of caffeine and theanine administered alone and together. *Psychopharmacology*, *195*(4), 569.

Saha, R., Chaudhary, R. S., & Somasundaram, J. (2012). Soil health management under hill agroecosystem of North East India. *Applied and Environmental Soil Science*, *2012*.

Tarachiwin, L., Ute, K., Kobayashi, A., & Fukusaki, E. (2007). 1H NMR based metabolic profiling in the evaluation of Japanese green tea quality. *Journal of agricultural and food chemistry*, *55*(23), 9330-9336.

Tarachiwin, L., Ute, K., Kobayashi, A., & Fukusaki, E. (2007). 1H NMR based metabolic profiling in the evaluation of Japanese green tea quality. *Journal of agricultural and food chemistry*, *55*(23), 9330-9336.

Toda, K., Yang, D., Yamanaka, N., Watanabe, S., Harada, K., & Takahashi, R. (2002). A single-base deletion in soybean flavonoid 3′-hydroxylase gene is associated with gray pubescence color. *Plant molecular biology*, *50*(2), 187-196.

Wahyuni, D. S. C., Kristanti, M. W., Putri, R. K., & Rinanto, Y. (2017, January). NMR Metabolic profiling of green tea (Camellia sinensis L.) leaves grown at Kemuning, Indonesia. In *Journal of Physics: Conference Series* (Vol. 795, No. 1, p. 012013). IOP Publishing.

Wei, K., Wang, L., Zhang, C., Wu, L., Li, H., Zhang, F., & Cheng, H. (2015). Transcriptome analysis reveals key flavonoid 3′-hydroxylase and flavonoid 3′, 5′-hydroxylase genes in affecting the ratio of dihydroxylated to trihydroxylated catechins in

Camellia sinensis. *PloS one*, *10*(9), e0137925.

Wei, K., Wang, L., Zhang, C., Wu, L., Li, H., Zhang, F., & Cheng, H. (2015). Transcriptome analysis reveals key flavonoid 3′-hydroxylase and flavonoid 3′, 5′-hydroxylase genes in affecting the ratio of dihydroxylated to trihydroxylated catechins in Camellia sinensis. *PloS one*, *10*(9), e0137925.

Yamamoto, N., Moon, J. H., Tsushida, T., Nagao, A., & Terao, J. (1999). Inhibitory effect of quercetin metabolites and their related derivatives on copper ion-induced lipid peroxidation in human low-density lipoprotein. *Archives of Biochemistry and Biophysics*, *372*(2), 347-354.

Yuan, Y., Song, Y., Jing, W., Wang, Y., Yang, X., & Liu, D. (2014). Simultaneous determination of caffeine, gallic acid, theanine,(−)-epigallocatechin and (−)-epigallocatechin-3-gallate in green tea using quantitative 1 H-NMR spectroscopy. *Analytical Methods*, *6*(3), 907-914.

Improving Postharvest Handling of 'Merah Delima' Papaya to Reduce Quality Loss During Transportation and Storage

Khandra FAHMY*

Faculty of Agricultural Technology, Andalas University, Kampus Unand Limau Manis, Padang, 25163, Indonesia

* Corresponding Author: khandrafahmy@ae.unand.ac.id

SUMMARY

This study aimed to determine the favorable condition for maintaining quality of 'Merah Delima' papaya during transportation and storage. Papaya was transported by using cardboard and cardboard with Modified Atmosphere Packaging (MAP) using Low Density Polyethylene (LDPE) under ambient temperature. After arrival in the market, fruit were stored at 10ºC and 25ºC for 21 days to check the shelf-life. The results showed that fruit packaged in cardboard with MAP reduced the mechanical injury of papaya after transportation. Combination with low-temperature storage at 10˚C maintained the quality and extended the shelf-life of papaya after transportation. Moreover, cardboard with MAP also alleviated chilling injury in papaya fruit during storage at 10˚C.

Introduction

'Merah Delima' papaya is a superior variety being developed in West Sumatra province, Indonesia. The characteristics of this papaya are orange-red flesh, sweet taste and chewy flesh. Usually, this papaya is distributed in local market and other provinces in Sumatra island. However, papaya is perishable commodity. Therefore, is needed the proper technology for maintaining quality particularly during transportation and storage.

In actual distribution chain, this papaya transported via land transportation using truck under ambient temperature. Fruits were put on the floor of the truck without any packaging. This condition is injury the fruit, resulting shorten the shelf-life and increases the amount of losses.

Low temperature storage is primary method for maintaining quality of perishable product. However, papaya is chilling-sensitive product (Kader, 2002), prolong storage at chilling-temperature increases susceptible to decay. MAP has been subjected in many studies for alleviating CI in chilling-sensitive product. Packaged persimmon in MAP prevent CI during transportation and storage at low temperature (Fahmy and Nakano, 2016). The ability of MAP to reduce CI is thought as reduction in O_2 and elevation of CO_2 inside the package. In previous study, the individual and combined effect of low O_2 and high CO_2 has been investigated to reduce CI (Fahmy and Nakano, 2014a).

In order to determine the favourable condition for preventing quality loss during transportation and extended the shelf-life after transportation, the effect packing style and temperature storage were investigated. In this experiment, a practical distribution of papaya chain from farm to table, papaya fruits were transported cardboard box and cardboard with MAP, and stored at 10ºC and 25ºC after transportation.

Materials and Methods

"Merah Delima" papaya (*Carica papaya* L.) at commercial maturity were harvested from the garden at Solok Regency, West Sumatra Province, Indonesia. Fruits were sorted and selected on the basis of uniform size and absence of visual defects. Fruits were packed in cardboard box (40.5 x 21 x 21.5 cm), and cardboard with MAP using LDPE. Both sides of cardboard were made four holes with a diameter 2 cm, respectively. After packaging, fruit were transported to the retailer market (Padang City) by using a mini-truck which is common vehicle using for transportation. During transportation, the vibration was recorded by using vibration recorder (data not shown). After arrival in the market, the mechanical injury was checked, and then stored at 10˚C and 25˚C in both of packaging for 21 days to check the shelf-life. Quality parameters such as weight loss, CI index, total soluble

solid (TSS) and malondialdehyde (MDA) content were investigated every 3 days. MDA content was measured as describe in Fahmy and Nakano (2014a), CI index was calculated according to Pesis et al. (2000), and TSS was measured by using refractometer (Atago, Japan).

The research was completely randomised with 3 replications (3 fruits per test). Statistical significance was determined by subjecting the mean values to analysis of variance and means were compared by Tukey's test at the 5% level of significance using R 3.5.1 (R Foundation).

Results and Discussion

Figure 1 showed that the percentage of mechanical injury after transportation from the farm to the market which observed by visual. The percentage of mechanical injury was higher on fruit packaged in cardboard than fruit packed in cardboard with MAP. It has been reported that application of MAP reduces the softening of persimmon fruit on the day of delivery and the day after delivery (Fahmy and Nakano, 2016). Packaged in MAP also maintains the quality during long term transportation of persimmon (Liamnimitr et al., 2018).

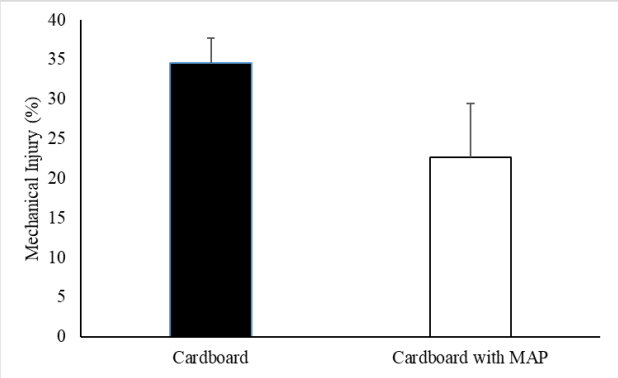

Fig. 1 Percentage of mechanical injury of 'Merah Delima' papaya after transportation. Fruits were packaged with cardboard and cardboard with MAP. Vertical bars represent standard error of the means (SE) for triplicate samples.

The weight loss of fruit increased significantly on the fruit packaged in cardboard without MAP, and rapid increased was shown on the fruit stored at 25˚C (Fig. 2). While, the increased of weight loss was suppressed on the fruit packaged in cardboard with MAP, and it was most suppressed stored at 10ºC. The result also shows that fruits stored at 25˚C had shelf-life 9 days and 12 days for cardboard and cardboard with MAP, respectively. Fruit stored at 10˚C could be kept until the end of storage.

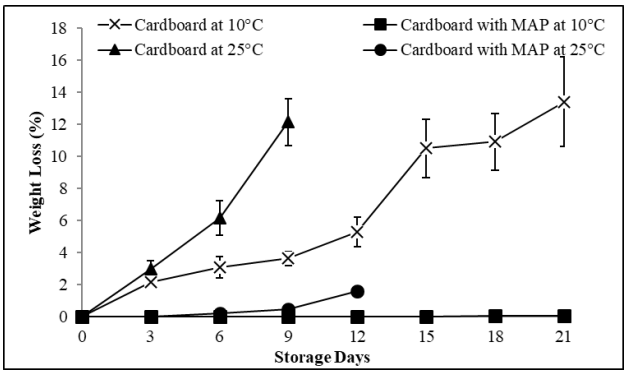

Fig. 2 Weight loss of 'Merah Delima' Papaya after transportation followed by 10˚C and 25˚C for 21 days. Fruits were packaged with cardboard and cardboard with MAP. Vertical bars represent standard error of the means (SE) for triplicate samples.

CI index of 'Merah Delima' papaya appeared on day 15 for both of packaging during storage at 10˚C (Fig. 3). However, the increase of CI index on the fruit packaged in cardboard with MAP was supressed until day 18, and then increased slightly until the end of storage. While, fruit packaged in cardboard without MAP, the index of CI increased rapidly, and on the end of storage was higher significantly compared with fruit packaged in cardboard with MAP. Pesis et al. (2000) also reported that MAP suppressed the development of CI symptoms in mango fruit.

TSS of papaya increased for both of packaging during storage at 10˚C and 25˚C, and then decreased after achieving the maximum value (Fig. 4). Fruit stored at 25˚C, the maximum values of TSS were occurred on day 3 and 6 for fruit packed in cardboard and cardboard with MAP, respectively. While, for fruit stored at 10˚C, showed

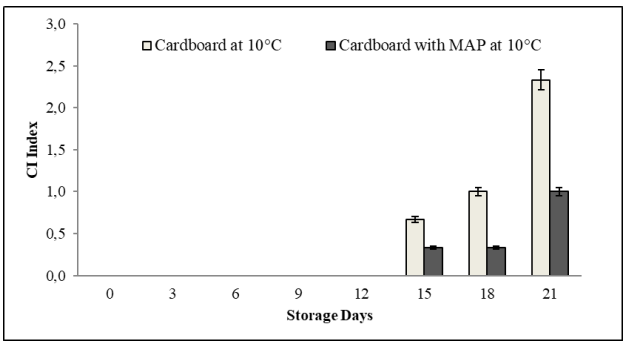

Fig. 3 CI index of 'Merah Delima' Papaya after transportation followed by 10˚C for 21 days. Fruits were packaged with cardboard and cardboard with MAP. Vertical bars represent standard error of the means (SE) for triplicate samples.

trend among both of packaging, which the maximum value of TSS occurred on day 15, and then decreased gradually until the end of storage.

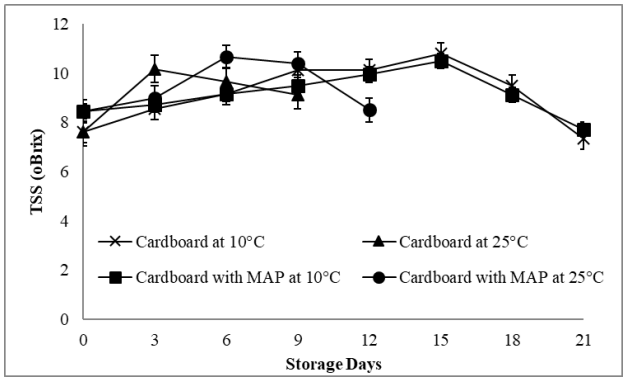

Fig. 4 TSS of 'Merah Delima' Papaya after transportation followed by 10˚C and 25ºC for 21 days. Fruits were packaged with cardboard and cardboard with MAP. Vertical bars represent standard error of the means (SE) for triplicate samples.

MDA content increased for both of packaging during storage at 10˚C and 25˚C (Fig. 5). Rapid increased in MDA content was showed on fruit packaged in cardboard at 25ºC, and it was suppressed on fruit packed in with MAP until day 3, and then increased quickly until the end of storage. While, for fruit stored at 10˚C, the MDA content showed similar trend until day 15 on both of packaging, and then it increased rapidly for fruit packaged in cardboard without MAP. Fahmy and Nakano (2014a) also found that the increases of MDA content of cucumber fruit were suppressed on the fruit stored under low O_2. MAP with LDPE film supressed the increases of MDA content

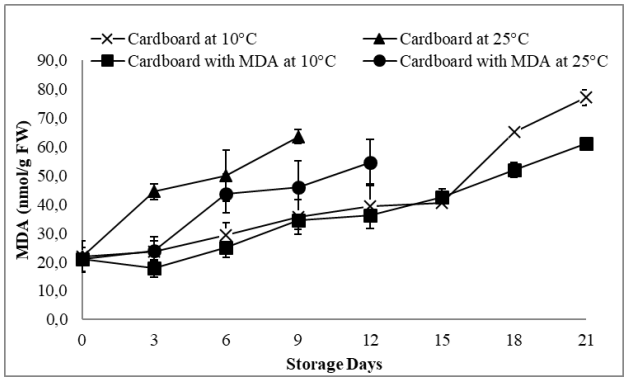

Fig. 5 MDA content of 'Merah Delima' Papaya after transportation followed by 10˚C and 25˚C for 21 days. Fruits were packaged with cardboard and cardboard with MAP. Vertical bars represent standard error of the means (SE) for triplicate samples.

(Fahmy and Nakano, 2014b). Stored of papaya fruit under high CO_2 suppressed the increases of MDA content (Fahmy et al., 2019)

Conclusion

Packaged of 'Merah Delima' papaya in cardboard with MAP reduced quality loss during transportation and storage. Combination treatment with low temperature storage showed best performance for maintaining quality and extending the shelf-life of papaya.

Acknowledgements

We would like to thank to Faculty of Agricultural Technology for financial support. We are grateful to The United Graduate School of Agricultural Science, Gifu University, Japan for supporting laboratory instrument at Lab Station in Postharvest Technology.

References

Fahmy, K., Nakano, K. (2014a) The individual and combined influences of low oxygen and high carbon dioxide on chilling-injury suppression in cucumber fruit Environ. Control Biol. 52 3 149–153.

Fahmy, K., Nakano, K. (2014b) Optimal design of modified atmosphere packaging for alleviating chilling injury in cucumber fruit Environ. Control Biol. 52(4), 233–240.

Fahmy, K., Nakano K., Violalita, F. (2015) Investigation on quantitative index of chilling injury in cucumber fruit based on the electrolyte leakage and malondialdehyde Int. J. Adv. Sci. Eng Inform. Technol. 5 71-74.

Fahmy, K., Nakano, K. (2016) Effective transport and storage condition for preserving the quality of Jiro persimmon in export market Agric. Agric. Sci. Procedia 9 279-290.

Fahmy, K., Violalita, F., Chatib, O.C., Yulia, R., Nakano, K. (2019). The individual influences of high CO_2 on chilling injury suppression of 'Merah Delima' papaya fruit. IOP Conferences Series: Earth and Environmental Science, 230 (1), 012016.

Kader, A. A. (2002). Postharvest biology and technology: An overview. In "Postharvest technology of horticultural crops" (ed. by Kader, A. A.), Ed. 3. Univ. California, Div. Agric. Nat. Resour., Oakland, CA, p 39–47.

Liamnimitr, N., Thammawong, M., Techavuthiporn, C., Fahmy, K., Suzuki, T., Nakano, K. (2018). Optimization of bulk modified atmosphere packaging for long-term storage of “Fuyu” persimmon frui. Potsharvest Biol. Technol., 135, 1-7.

Pesis, E., Aharoni, D., Aharon, Z., Ben-Arie, R., Aharoni, N., Fuchs, Y. (2000). Modified atmosphere and modified humidity packaging alleviates chilling injury symptoms in mango fruit. Postharvest Biol. Technol. 19: 93–101.

Effects of Maturity Stages and Organic Treatments to Control Postharvest Fungal Infection, Shelf life Extension and Quality Retention of Papaya for Nutritional Food Safety

Md. Harun Ar RASHID[1*], Md. Ahsan HABIB[1]

[1] Department of Horticulture, Bangladesh Agricultural University, Mymensingh 2202, Bangladesh
[*] Corresponding Author: harun_hort@bau.edu.bd

SUMMARY

An experiment was conducted to study the effects of maturity stages and organic treatments to control postharvest fungal infection, shelf life extension and quality retention of papaya at the Laboratories of the Departments of Horticulture and Agricultural Chemistry, Bangladesh Agricultural University, Mymensingh during the period from August to November 2018. The two-factor experiment consisted of two maturity stages viz. M_1: mature green colour and M_2: 0-10% yellowing on the fruit; and six organic postharvest treatments viz. control (T_0), hot water @ 50°C for 10 minutes (T_1), aloe vera extract @ 1% (T_2), garlic extract @ 1:1 (T_3), hot water + aloe vera (T_4), and hot water + garlic (T_5). The experiment was laid out in a completely randomized design with 3 replications. At the end of the storage period, it was found that combined application of maturity stages and organic treatments were significant on almost all the parameters studied except titratable acidity. Peel colour was light greenish yellow in hot water plus aloe vera and hot water plus garlic extract fruits, while yellow in rest of the treatment combinations under both maturity stages. The maximum weight loss (18.82%), TSS (14.68%), disease incidence (100%) and severity (80.67%) were recorded from control fruits, whereas the minimum values (18.82, 10.30, 58.33 and 15.17%, respectively) were found from hot water plus aloe vera followed by hot water plus garlic treated fruits under both maturity stages. However, the highest pulp to peel ratio (4.33), pulp pH (6.32), vitamin C (53.96 mg/100g) and shelf life (15.08 days) were obtained from the combined treatment of hot water plus aloe vera extract followed by hot water plus garlic extract, while the lowest values (3.10%, 5.02%, 39.77 mg/100g and 8.27 days, respectively) were observed in control under maturity stage 2 fruits. Therefore, it can be concluded that combined application of hot water plus aloe vera extract, followed by hot water plus garlic extract under both maturity stages found to be better in respect of reducing fungal infection, extension of shelf life and quality retention of papaya fruits without affecting the nutritive value.

Introduction

Papaya (*Carica papaya* L.) belonging to the family Caricaceae, is an evergreen herbaceous commercial fruit plant of tropical and subtropical region (Srinu et al. 2017). Papaya is consumed as fresh, as a vegetable or used for processed products such as drinks, jams, jellies, ice cream, pies and as dried and crystallized fruits world-wide (Jaime et al. 2007). Papaya is a nutritious table fruit of high digestive value and an excellent source of natural vitamins and minerals. Biochemically, papaya contains several proteins, alkaloids and proteolytic enzymes, which are successfully used in the pharmaceutical, medicinal and other industries such as preparation of chewing-gum, chill-proofing beer, tendering meats, preparation of fish protein concentrates, animal feed, developing roast beef-like flavors by partial hydrolysis of protein, production of dehydrated pulses and beans, and improvement of protein dispersibility index of soya flour (El Moussaoui et al. 2001).

Global papaya production in recent years is about 13.02 M tons (FAOSTAT, 2019), which is quite satisfactory, although approximately 40-70% of the produce is damaged due to postharvest fungal decay, pest disinfestations, physiological disorders, mechanical and chilling injuries (Rashid et al. 2015). After harvesting, the fruits start to live by using their own reserves and fruits mature progressively and during the storage, conditions are favourable to microorganisms, which cause fruit damage. Because of its naturally fragile and thin skin, papaya is damaged very easily by handling and infected by the main postharvest disease anthracnose (*Colletotrichum gloeosporioides*),

which is a major problem for papaya producers, traders and consumers in the tropics (Palhano et al. 2004). Sensitiveness to low temperature increases difficulties of papaya during. Harvesting at proper maturity stage is a very important determinant for storage-life and final fruit quality, while at improper maturity can lead to uneven ripening and over ripe fruits. Postharvest losses can be reduced by appropriate wrapping materials, heat treatment, low-dose gamma irradiation, chitosan and wax coating, plant extracts (aloe vera, onion, garlic, neem, etc.). Postharvest research related to fruit ripening and handling became more important during the last decade because of increasing consumer awareness, expansion in production and exports. The most important research issues are on keeping quality and postharvest storage life since extreme or fluctuating temperature treatments and mechanical damage combined with improper harvesting and handling can result in fruit with poor appearance, flavour and nutritional value (Proulx et al. 2005). However, a limited work has been done on the combined application of hot water and plant extracts under different maturity stages. Therefore, the present study was undertaken to investigate the effects of maturity stages and organic treatments to control postharvest fungal infection, shelf life extension and quality retention of papaya without affecting the nutritive value.

Materials and Methods

1. *Experimental location and material*

The experiment was conducted at the Laboratories of the Departments of Horticulture and Agricultural Chemistry, Bangladesh Agricultural University, Mymensingh during the period from August to November 2018. Papaya fruits (*Carica papaya* var. Shahi) of two maturity stages (mature green and beginning of yellow colour up to 10% of yellow surface) were collected from a farmer's field near the Bangladesh Fisheries Research Institute, Mymensingh in perfect quality conditions. On arrival at the laboratory, the fruits were washed with distilled water, cleaned properly and air-dried. The selected fruits were uniform in shape, size (20-25 cm in length) and weight (700-800 g). After grading, the fruits were individually wrapped in non-absorbent paper and then placed in a commercial packaging material under ambient temperature (25 ± 1°C) prior to further treatments. Fresh aloe vera leaves and garlic cloves were bought from the Supermarket in Mymensingh.

2. *Treatments and design of the experiment*

The two-factor experiment consisted of two maturity stages viz. M_1: mature green and M_2: 0-10% yellowing on the fruit; and six organic treatments viz. control (T_0), hot water @ 50°C for 10 minutes (T_1), aloe vera extract @ 1% (T_2), garlic extract @ 1:1 (T_3), hot water + aloe vera extract (T_4), and hot water + garlic extract (T_5). Trials were set up in a completely randomized design (CRD) with three replications and 5 different days of storage (0, 3, 6, 9, 12) for a total of 360 samples and each sample represented by one papaya.

3. *Application of postharvest treatments*

Postharvest treatments were sequentially applied to the fruits in order to study physico-chemical characteristics. For control treatment (T_0), ten fruits under each maturity stages were taken randomly from a papaya fruit lot. Hot water treatment (T_1) was done by individually dipping the fruits into the hot water at 50 °C for 10 minutes in an electric hot water bath. For aloe vera coating (T_2), the selected fruits were dipped in 1% aloe vera solution for 5 minutes. Aloe era gel was extracted from fresh aloe vera leaves and gel solution was prepared as described by Sharmin et al. (2015). For garlic treatment (T_3), initially stock garlic extract (1 kg garlic cloves and 1 L water) was prepared by crushing the fresh cloves in distilled water using a blender through straining and then cheesed. The stock extract was then used to prepare treatment of 1:1 concentration. To improve wettability of the solution 0.1 mL Tween 20 was added to the solution. The selected fruits under both maturity stages were dipped into the treatment solutions for 5 minutes. For combined treatment, hot water dipping was done first followed by aloe vera extract (T_4) and garlic extract coating (T_5), respectively. After application of all the treatments, fruits were air-dried, wrapped in non-absorbent paper and stored at 25 ± 1°C for normal ripening and data were monitored at 0, 3, 6, 9 and 12 days of storage.

4. *Parameters measured*

Changes in external colour of papaya fruits of two maturity stages were observed carefully, visually examined and recorded at four stages during storage through scoring using a colour chart. Weight loss of papaya was measured by weighing the individual fruits using a top pan electric balance (Rashid et al. 2019). Pulp to peel ratio was determined by separately weighing pulps and peels of fruits using electrical balance and measured by the ratio of

weight of fruit pulp to weight of peel. The pH of fruit juice was recorded using an electric pH meter, which was standardized with buffer solution as described by Ranganna (1994). The remaining juice from pH determination was used to measure TSS of fruit pulp and was determined by using a hand refractometer (Model N-1 α, Atago, Japan). Titratable acidity and ascorbic acid content of papaya fruit pulp was determined by Ranganna method (1994). For calculating disease incidence and severity, ten fruits were taken for each treatment and stored at ambient temperature (25 ± 1°C) for normal ripening. Fruits were critically examined every day for the appearance of the disease symptoms already published (Al Eryani-Raqeeb et al. 2009), and data were recorded every 3 days starting from the 3rd day of storage and used to calculate the percentage of visibly infected fruits in the entire population (Rashid et al. 2015). Disease severity was measured as described in terms of the proportion of the fruit surface occupied by lesions with <5% being acceptable for trading, 5–25% being viewed as tolerable for trade, 25–50% seen as having little possibility of commercial use and >50% as unusable (Azevedo, 1998). Shelf life was calculated from daily estimates of disease severity on the same 10 fruits from each replicate and considered as ended when the fruits had little or no commercial viability and eating quality (disease severity >25%).

5. *Data analysis*

The collected data were statistically analyzed using analysis of variance (ANOVA) where the significance of difference between pair of means was tested by least significant difference (LSD) at 1 and 5% levels of probability using MSTAT Computer programme.

Results and Discussion

1. *External colour*

The change in external colour was noticiable due to maturity stages and organic postharvest treatments (data not shown). The results showed that the external colour changes in fruits of control and single treatments were observed earlier than the combined treatments under both maturity stages. At the end of the storage period (12 DAS), peel colour was light greenish yellow in combined treatment of hot water plus aloe vera extract (M_1T_4) and hot water plus garlic extract (M_1T_5) fruits, while yellow in rest of the treatment combinations under both maturity stages. In the control, protoplast was changed into chromoplast normally, while in treated samples, this process was suppressed by the treatment effect (Rashid et al. 2019). The changes of these components affected the fruit colour from green into yellow in the skin. The results showed that combined treatment had better external appearance than the others of both maturity stages.

2. *Weight loss*

Combined application of maturity stages and organic treatments had significant influence on weight loss of papaya, which was gradually increased with the storage period (Table 1). At 12 DAS, the maximum weight loss was observed in M_2T_0 (18.82%) followed by M_1T_0 (17.85%), while the minimum weight loss was found from M_1T_4 (9.20) followed by M_2T_5 (9.78). This might be due to the coating effects of aloe vera and garlic extracts along with hot water, which could reduce transpiration and respiration by the papaya fruits.

3. *Pulp to peel ratio*

Pulp to peel ratio was significantly influenced by the combined effects of maturity stages and organic postharvest treatments (Table 2). It showed a decreasing trend from harvest to ripening. At 12 DAS, the maximum pulp to peel ratio was observed in M_1T_4 (4.33) followed by M_2T_4 (4.19), while the minimum pulp to peel ratio was recorded in M_2T_0 (3.10) followed by M_1T_0 (3.20). The decrease in pulp to peel ratio might be due to the change in sugar concentration in the peel compared to the pulp, which contributed to different change in osmotic pressure (Rashid, et al. 2019).

4. *Pulp pH*

Combined effects of maturity stages and organic postharvest treatments exhibited significant variation in pulp to peel ratio of papaya during storage (Table 2). Results revealed that pulp pH was increased with the storage period. At 12 DAS, the highest pulp pH was recorded from M_1T_4 (6.32) followed by M_2T_4 (6.19), while the lowest was observed in M_2T_0 (5.02) followed by M_1T_0 (5.05). This could be due to the increasing fashion of papaya pH during storage.

5. T*otal soluble solids (TSS) content*

The combined effect of maturity stages and organic postharvest treatments has significant influence on TSS of papaya (Table 2). Ghanta (1994) reported that TSS content

Table 1 Combined effects of maturity stages and organic treatments on the weight loss of papaya fruits at 12 days after storage (DAS)

Treatment combination	Weight loss (%)	Pulp to peel ratio	Pulp pH	TSS content (%brix)
M_1T_0	17.85	3.20	5.05	14.12
M_1T_1	14.68	3.77	5.47	13.77
M_1T_2	12.58	4.13	5.67	12.85
M_1T_3	13.56	4.09	5.55	13.00
M_1T_4	9.20	4.33	6.32	10.30
M_1T_5	10.53	4.15	6.10	10.67
M_2T_0	18.82	3.10	5.02	14.68
M_2T_1	15.20	3.69	5.43	14.12
M_2T_2	13.25	4.01	5.34	13.09
M_2T_3	13.66	3.82	5.88	12.72
M_2T_4	9.78	4.19	6.19	10.82
M_2T_5	10.95	4.09	6.04	11.30
$LSD_{0.01}$	0.324	0.075	0.092	0.266
Level of significance	**	**	**	**

**= Significant at 1% level of probability, M_1=Maturity stage 1 (Mature green colour), M_2=Maturity stage 2 (0-10% yellowing on the fruit surface), T_0=Control, T_1=Hot water@50°C for 10 minutes, T_2=Aloe vera extract@1%, T_3=Garlic extract@1:1, T_4=Hot water+aloe vera extract, T_5=Hot water+garlic extract.

Table 2 Combined effects of maturity stages and organic treatments on weight loss of papaya fruits at 12 days after storage (DAS)

Treatment combination	Titratable acidity (%)	Vitamin C (mg/ 100g)	Disease incidence (%)	Disease severity (%)
M_1T_0	2.40	39.77	100.0	73.33
M_1T_1	2.30	45.83	93.33	46.67
M_1T_2	1.67	48.02	81.67	31.67
M_1T_3	1.95	46.68	83.33	39.00
M_1T_4	1.05	53.96	58.33	15.17
M_1T_5	1.19	51.29	71.67	17.67
M_2T_0	2.55	41.40	100.0	80.67
M_2T_1	2.36	42.81	96.67	47.67
M_2T_2	1.74	47.11	86.67	33.33
M_2T_3	2.09	45.31	88.33	41.00
M_2T_4	1.29	49.63	61.67	16.50
M_2T_5	1.45	47.74	76.67	19.33
$LSD_{0.01}$	0.107	0.881	2.14	2.08
Level of significance	NS	**	**	**

**= Significant at 1% level of probability, NS=Not significant, M_1=Maturity stage 1 (Mature green colour), M_2=Maturity stage 2 (0-10% yellowing on the fruit surface), T_0=Control, T_1=Hot water@50°C for 10 minutes, T_2=Aloe vera extract@1%, T_3=Garlic extract@1:1, T_4=Hot water+aloe vera extract, T_5=Hot water+garlic extract.

in pulp gradually increased during the storage period irrespective of postharvest treatments. At 12 DAS, the highest TSS was observed in M_2T_0 (14.68%) followed by M_1T_0 (14.12%), while the lowest in M_1T_4 (10.30%) followed by M_1T_4 (10.67%). This might be due to the hydrolysis of starch into sugar (Pimentel and Walder, 2004). Sugar content is one of the main components of quality of papaya, so it is important that papaya should be harvested more mature and, if possible, in the maturation stage that elicits higher sugar concentration.

6. *Titratable acidity (TA)*

Combined effects of maturity stages and organic treatments exhibited no significant influence on TA content of papaya fruits (Table 2).

7. *Vitamin C content*

The combined treatment of maturity stages and organic treatments showed significant influence on vitamin C content of papaya (Table 2). The highest vitamin C (53.96 mg/100g) was observed in combined treatment of hot water plus aloe vera extract under maturity stage 1 fruits (M_1T_4) followed by 51.29 mg/100g in M_1T_5, while the lowest vitamin C was recorded in M_1T_0 (39.77 mg/100g) followed by M_2T_0 (41.40 mg/100g). Vitamin C levels rose immediately following each treatment and then declined in the expected way over the storage period.

8. *Disease incidence*

Three fungal diseases viz. anthracnose, stem end rot and Rhizopus rot were identified during storage by observing the typical symptoms caused by *Colletotrichum gloeosporioides*, *Botryodiplodia theobromae* and *Rhizopus stolonifer*, respectively (Fig. 1).

8.1 *Assesment of percent disease incidence*

Combined effect of maturity stages and organic treatments had significant influence on disease incidence of papaya (Table 2). Highest disease incidence (100%) was found in M_1T_0 and M_2T_0 at the end of the storage period and the

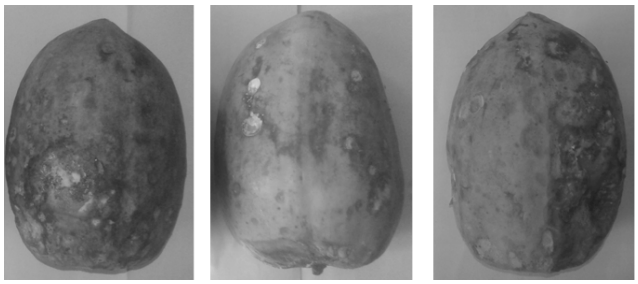

Fig.1 Photograph showing (a) Anthracnose (*Colletotrichum gloesporioides*), (b) Stem end rot (*Botryodiplodia theobromae*) and (c) Rhizopus fruit rot (*Rhizopus stolonifer*) of papaya in control treatment.

lowest was observed in M_1T_4 (15.17%) followed by M_1T5 (17.67%). Combined treatments such as heating and plant extracts may give synergistic effect and could give less detrimental effect to quality attributes of the papaya fruits. Miller and McDonald (1999) also reported that decay was manifested more in 1/3 yellow coloured fruits than mature green stage, probably because of the higher incidence of peel injuries during handling; decay organisms are known to enter into fruit at sites of injury. Hot water dipping for 10 min at 55 °C can be used to reduce postharvest fungal infection (Rashid et al. 2015). Though the hot water treatment reduce the incidence of anthracnose by reducing the available inoculum on the fruit surface, this treatment affects the polygalacturonase activity, ascorbic acid content and titratable acidity levels (Ferguson et al. 2000).

9. *Disease severity*

Combined effect of maturity stages and organic postharvest treatments had significant influence on disease severity of papaya (Table 2). The highest disease severity was found at M_2T_0 (80.67%) followed by M_1T_0 (73.33% and the lowest in M_1T_4 (12.36%) followed by M_2T_4 (16.50%). Recently, aloe vera gel has been used as an edible coating materials, which have various favourable effects on fruits and vegetables such as imparting a glossy appearance and better colour, retarding weight loss, or prolonging shelf-life by preventing microbial spoilage and biologically safe for different types of foods because of its film-forming properties, biodegradability and biochemical properties (Sharmin et al. 2015). It is composed mainly of polysaccharides and acts as a natural barrier to moisture and oxygen, which are the main agents of deterioration of fruits and vegetables (Misir et al. 2014). The ethanolic extract and fresh garlic cloves contain biologically natural fungicide substances (allicin), which are potentially used for control of many fungal diseases of fruits (Mondal et al. 2011; Nur Fatima et al. 2018).

10. *Shelf life*

Shelf life is the period from harvesting up to the last edible stage. This is the basic quality of fruits, which helps long marketing time, and it is the most important aspect in loss reduction technology of fruits. The extension of shelf life of fruit has been one of the prime concerns of marketing throughout the record of history. Statistically there was significant difference between the two maturity stages and organic postharvest treatments with respect to shelf life of papaya (Figure 2). Results revealed that the longest shelf life of papaya fruits was observed in M_1T_4 (15.08 day) followed by M_2T_4 (14.05 day), while the shortest shelf life (8.27 day) was recorded in $M2T_0$ followed by 8.48 day in (M_1T0). The delay in ripening on hot water and aloe vera coated fruits can occur due to the lower capacity of these fruits in producing ethylene, since this hormone has a stimulation role in the general metabolism, and seems to be implicated in the activation and regulation of some enzymes involved in ripening (Mondal et al. 2011). The increase in shelf life was probably due to the changes in the concentrations of various gases like the increase of O_2, the reduction of CO_2 and ethylene as well as the slowing down of the processes leading to delayed ripening and reducing decay by aloe vear and garlic extracts and hot water treatments.

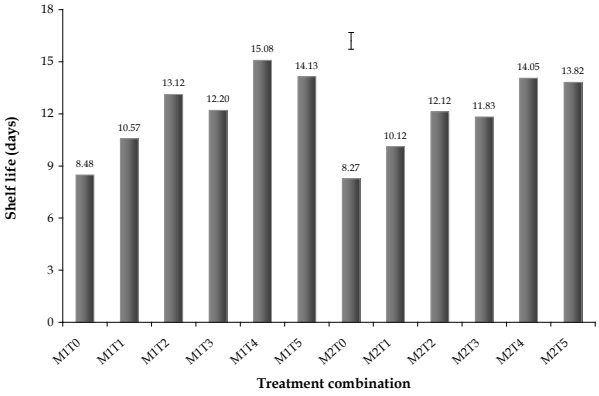

Fig. 2 Combined effect of maturity stages and organic treatments on shelf life of papaya fruits. The vertical bar represents LSD at 1% level of probability. (M_1=Maturity stage 1 (Mature green colour), M_2=Maturity stage 2 (0-10% yellowing), T_0=Control, T_1=Hot water@50°C for 10 minutes, T_2=Aloe vera extract@1%, T_3=Garlic extract@1:1, T_4=Hot water+aloe vera extract, T_5=Hot water+garlic extract.)

Conclusion

From the experimental results and discussion, it can be concluded that combined application of hot water plus aloe vera extract, followed by hot water plus garlic extract under both maturity stages found to be better in respect of reducing fungal infection, extension of shelf life and quality retention of papaya fruits without affecting the nutritive value.

Acknowledgements

The authors are pleased to thank the Bangladesh Agricultural University Research System (BAURES) for funding this work.

References

Al Eryani-Raqeeb, A., Mahmud, T. M. M., Syed Omar, S. R., Mohamed Zaki, A. R., Al Eryani, A. R. (2009) Effects of calcium and chitosan treatments on controlling anthracnose and postharvest quality of papaya (*Carica papaya* L.). International Journal of Agricultural Research 4, 53-68.

El Moussaoui, A., Nijs, M., Paul, C., Wintjens, R., Vincentelli, J., Azarkan, M., Looze, Y. (2001) Revisiting the enzyme stored in the laticifers of *Carica papaya* in the context of their possible participation in the plant defence mechanism. Cell and Molecular Life Sceinces 58, 556-570.

FAOSTAT. (2019) Crop production data. Food and Agriculture Organization of the United Nations, Rome(http://faostat3.fao.org/faostat-gateway/go/to/download/Q/*/E)

Ferguson, I. B, Ben-Yehoshua, S., Lurie, S., McDonald R. E, Mitcham E. J. (2000) Postharvest heat treatment introduction and workshop summary. *Postharvest Biology and Technology* 21, 1-6.

Jaime, A. Teixeira, D. S., Zinia, R., Duong T. N., Dharini, S., Abed G., Manoel, T. S. J., Paula, F. T. (2007) Papaya (*Carica papaya* L.) Biology and Biotechnology. Tree and Forestry Science and Biotechnology. Global Science Books.

Miller, W. R., McDonald, R. E. (1999) Irradiation, stage of maturity at harvest, and storage temperature during ripening affect papaya fruit quality. Hortscience 34, 1112–1115.

Misir, J., Brishti, H. F., Hoque, M. M. (2014) Aloe vera gel as a novel edible coating for fresh fruits: a review. American Journal of Food Science and Technology 2(3), 93-97.

Mondal, M. F., Islam, M. S. and Rashid, M. H. A. (2011) Effects of plant extracts on shelf life and postharvest diseases of papaya. Journal of the Bangladesh Society for Agricultural Science and Technology 8 (3&4), 93-96.

Nur Fatimma, A., Munirah, M. S., Sharifah Siti Maryam, S. A. R., Najihah, A., Nur Ain Izzati, M. Z. (2018) Efficacy of *Allium sativum* extract as post-harvest treatment of fruit rots of mango. Plant Pathology & Quarantine 8(2), 144–152.

Palhano, F. L., Vilches, T. T. B., Santos, R. B., Orlando, M. T. D., Ventura, J. A., Fernandes, P. M. B. 2004. Inactivation of *Colletotrichum gloeosporioides* spores by high hydrostatic pressure combined with citral or lemongrass essential oil. International Journal of Food Microbiology 95, 61-66.

Proulx, E., Cecilia, M., Nunes, M. C. N., Emond, J. P., Brecht, J. K. (2005) Quality attributes limiting papaya post harvest life at chilling and non-chilling temperatures. In: Proceedings of the Florida State Horticultural Society 118, 389- 395.

Ranganna, S. 1994. *Manual of Analysis of Fruit and Vegetable Products*. Tata McGraw-Hill Pub. Co. Ltd., New Delhi, p.634.

Rashid, M. H. A., Borman, B. C., Hasna, M. K., Begum, H. A. (2019) Effect of non-chemical treatments on postharvest diseases, shelf life and quality of papaya under two different maturity stages. *Journal of Bangladesh Agricultural University* 17(1), 14-25.

Rashid, M. H. A., Grout, B. W. W., Continella, A., Mahmud, T. M. M. (2015) Low-dose gamma irradiation following hot water immersion of papaya (*Carica papaya* Linn.) fruits provides additional control of postharvest fungal infection to extend shelf life. Radiation Physics and Chemistry 110, 77–81.

Sharmin, M. R., Islam, M. N., Alim, M.A. (2015) Shelf-life enhancement of papaya with aloe vera gel coating at ambient temperature. Journal of Bangladesh Agricultural University 13(1), 131-136.

Srinu, B., Manohar, R. A., Veena, J. K., Narender R. S., Harish, K. S. (2017) Effect of different post-harvest treatments on quality and shelf life of papaya. Journal of Pharmacognosy and Phytochemistry 6(5), 1788-1792.

Extraction of Chitosan from Shrimp and Crab Shell and Its Effect on the Quality of Pineapple Juice

Sharmin SULTANA[1], Md. Sajjad HOSSAIN[2], Abdullah IQBAL[1*]

[1] Department of Food Technology & Rural Industries, Bangladesh Agricultural University, Mymensingh-2202, Bangladesh

[2] Department of Chemical and Food Process Engineering, Rajshahi University of Engineering & Technology, Rajshahi-6204, Bangladesh

[*] Corresponding Author: iqbal21155@bau.edu.bd

SUMMARY

The present study was undertaken to extract chitosan from shrimp and crab shell by chemical method and to assess its effects on the qualities of pineapple juice. Chitosan was derived from shrimp and crab shell by the process of chemical treatment demineralization (2%HCl, 16hr), deproteinization (4% NaOH, 20hr) and deacetylation (60% NaOH, 650C, 20hr). Extracted chitosan's physicochemical and functional properties like fat binding capacity (FBC), water binding capacity (WBC), solubility, average molecular weight, ash content, moisture content and degree of deacetylation were studied. The degree of deacetylation and solubility of chitosan extracted from shells of shrimp and crab were found to be 76 and 65% and 91 and 70%, respectively. In a similar way, the WBC of shrimp and crab shell chitosan were found to be 445 and 260 % and the and FBC was found to be 360 and 210%, respectively. The average molecular weight of shrimp and crab chitosan was found 6273 and 6267 Dalton, respectively. Chitosan was added to pineapple juice at 0.2, 0.4 and 0.6 g/L concentration as a clarifying agent. The results showed that addition of the shrimp chitosan as a clarifying agent @ 0.6g/L at 25±2ºC for 90 min was more effective than the crab chitosan. Statistical analyses showed significant effect on sensory characteristics when added chitosan at 0.2-0.6 g/L in pineapple juice. This study showed that shrimp shell was better than crab shell for the preparation of chitosan and shrimp chitosan was more effective than crab chitosan as a preservative and clarifier on the quality of pineapple juice.

Introduction

Chitosan is deacetylated derivative of chitin, which is one of the most abundant polysaccharides occurring in nature next to cellulose (Ramasamy and Shanmugam, 1885) and found on the outer surface of the arthropod body, in the cell wall of mushrooms and in cell structures of algae and yeast (Kaya et al., 2015). Crustacean waste from crab shells is composed of chitin which forms a chitin-protein complex with proteins. Fish scales, shrimp and crab shells are composed of different components such as proteins (15–50%), minerals (30–50%) and chitin (15–30%) (Hajji et al., 2015, Hossain and Iqbal, 2014). The growing quantities of shell wastes from processing of crustaceans have become a major concern for seafood processing plants since their biodegradation is very slow. Global annual production of shell wastes from crustaceans is estimated at 1.41 million metric tons (Pérez Roda et al., 2019). These processing byproducts, however, may be used as an important source for production of value-added product such as chitin and its deacetylated derivative chitosan.

Chitosan have been used as additive in the processing of fruit juices, for reducing the turbidity (Soto-Peralta et al., 1989), reduction of acidity (Imeri and Knorr, 1988), reduction of browning (Sapers,1992), and also demonstrated antimicrobial activity against bacteria, yeasts and molds, with low toxicity in mammalian cells (Martín-Diana et al., 2009), as antioxidant agent (Chien et al., 2007) as well as shelf life extender for selected fruit and fruit juice (Martín-Diana et al., 2009, Hossain and Iqbal, 2014).

Pineapple juice is very popular and abundantly consumed in many countries. Bangladesh produces a large amount of pineapple every year. Its popularity is based on attractive aroma and flavor characteristics and beneficial components that play a primary role in avoiding the risk of chronic diseases. Pineapple juice is one of the

fruits juices that contain high contents of antioxidant and phenolic compounds (Wen and Wrolstad, 2002). To prolong the juices shelf life, chemical additives are used. However, some countries limit their use because of possible health damage. These facts, combined with growing consumer demand for natural foods, encourages the study of the area of food science to gain new perspectives preservatives that meet market demands without neglecting the quality of products (Raybaudi-Massilia et al., 2009). In this context, chitosan has gained popularity to be applied widely in the pharmaceutical and food industries due to its unique features such as non-toxicity and biodegradability etc.

Processing of clarified fruit juices commonly involves the use of clarifying aids, including gelatins, bentonite, tannins or combinations of these compounds (Soto-Peralta et al., 1989). Chitosan with a partial positive charge has been shown to possess acid binding properties (Imeri and Knorr, 1988) and to be effective in aiding the separation of colloidal and dispersed particles from food processing wastes (No and Meyers, 2000), while thermal pasteurization of juice significantly reduces the risk of food born disease and can also reduce the nutrient content. For these reasons, the scientific community and food industry focus their attention on non-thermal emerging technologies and alternative novel treatments to control undesirable microorganisms with less adverse effects on quality.

Therefore, in this research work, it is attempted to extract and characterize chitosan from shrimp and crab shell and subsequently to study the feasibility of applying chitosan to improve the quality of pineapple fruit juice and to enhance the shelf life.

Materials and Methods

1. *Extraction of Chitosan*

The experiment has been conducted in the laboratory of the Department of Food Technology and Rural Industries, Bangladesh Agricultural University, Mymensingh. Fresh shrimp and crabs were collected from local market. Shell of shrimp and crab were separated from the whole body using a sharp knife. The collected wastes were then washed with tap water and crushed with mortar-pastel. Other essential reagents and utensils were used from the laboratory stock. Clean and crushed shrimp and crab wastes were kept in a polyethylene bags at ambient temperature (28 ± 2^0C) for 24 hours for partial autolysis to facilitate chemical extraction of chitosan and to improve the quality of chitosan (Toan, 2009). The isolation of chitosan was carried out following 3 (three) steps namely-demineralization, deproteinization and deacetylation as described by Toan (2009) and Hossain and Iqbal (2014). The resulting chitosan was then dried at cabinet dryer for 4 hours at 65 ± 5^0C and stored in polyethylene bag until they are used as a preservative in pineapple juice.

2. *Physicochemical and functional properties of chitosan*

Moisture and ash content, Solubility, Bulk density, intrinsic viscosity, Molecular weight, Color, Water binding capacity, Fat binding capacity, degree of deacetylation etc. of chitosan were measured as per the standard methods described by several researchers (AOAC, 2005, Wang et al., 2007, Knorr, 1982, Hossain and Iqbal, 2014).

3. *Application of chitosan to Pineapple juice*

Pineapple juice was prepared from mature and fresh pineapples. Clarification of pineapple juice is performed by addition of three different concentrations of shrimp and crab chitosan S1, C1 (0.2%), S2, C2 (0.4%), S3, C3 (0.6%) including a control sample P (0), where S and C indicates chitosan prepared from Shrimp and Crab, respectively. The clear juice was obtained after centrifugation at 5000 rpm for 10 min. Unclarified juice was used as a control for comparison among clarification treatments. The clarified juice was stored at 4^0C until further analysis (Oszminanski and wojdylo, 2007).

4. *Quality evaluation of Pineapple juice*

Total soluble solids (TSS), pH, potential browning etc were measured as per approved and standard methods.

Results and Discussion

1. *Physiochemical and functional Properties of shrimp and crab chitosan*

Properties of shrimp and crab chitosan are summarized at Table 1. Chitosan's moisture content, obtained from shrimp shells and crab was found as 4.23% and 3.78%, respectively which indicates shrimp chitosan has more moisture than the crab counterparts.

Ash content indicates that crab chitosan has more ash content compared to shrimp chitosan. Mohanasrinivasan et al. (2014) reported that commercial chitosan consists ash content around 2.28% which is very similar to the result obtained in this study, particularly for crab shell.

Shrimp chitosan was more soluble than crab

chitosan. Higher temperatures during the deacetylation process lead to a reduction in solubility. The quality of chitosan depends on the degree of deacetylation which in-turn affects its solubility (Madhavan and Nair, 1974). The degree of deacetylation of shrimp and crab was found to be 76% and 65% respectively. Because of low deacetylation of crab chitosan, solubility was found to be low whereas shrimp chitosan's solubility was more. Hossain and Iqbal (2014) reported that several critical factors affecting chitosan solubility including temperature and deacetylation reaction time, alkali concentration, the ratio of chitin to alkali solution, and particle size.

Table 1 Physiochemical and functional properties of chitosan

Parameter/properties	Chitosan from	
	Shrimp	Crab
Moisture content (%)	4.23	3.78
Ash content (%)	0.29	2.3
Yield (%)	16.0	20.2
Solubility (%)	91	70
Degree of deacetylation (%)	76	65
Bulk density (g/ml)	0.09	0.20
Intrinsic viscosity (dl/g)	11.5	8.20
Ave. molecular weight (Da)	6273	6267
Water binding capacity (%)	445	260
Fat binding capacity (%)	360	210

The bulk density found for chitosan from shrimp and crab indicates that shrimp chitosan is more porous than crab chitosan. The intrinsic viscosity of chitosan obtained from shrimp and crab in this study was found to be 11.5 dl/g and 8.20dl/g. The average molecular weight of chitosan derived from shrimp and crab was 6273 Dalton and 6267 Dalton, respectively. Crab chitosan has less average molecular compared to that of shrimp. Water binding capacity of chitosan derived from shrimp and crab was found to be 445% and 260%, respectively which indicated that water binding capacity of shrimp chitosan was better than that of crab chitosan. The fat-binding capacity of shrimp and crab chitosan was found to be 360% and 210% respectively. No et al., (1989) reported that fat binding capacity values of chitosan ranged from 314% to 535%, which indicates that the value obtained in this research is within the range.

2. *Effect of chitosan on pineapple juice quality*

The effect of chitosan at different concentration (0.2, 0.4, 0.6 g/L) on the clarification of pineapple juice has been investigated. The juices showed increased in luminosity with increasing chitosan concentration. At 90 min., the optical density of shrimp chitosan added juice (@0.6 g/L) was found less than that of crab chitosan added juice. Domingues et al. (2012) reported that treatments employing chitosan ensures a turbidity reduction of almost 100% regarding the raw juice or even to the juice centrifuged at 4000 rpm, similar behavior is observed regarding color removal.

The effect of chitosan on the TSS showed that chitosan reduced the TSS value of the pineapple juice and significant changes over storage time were observed. This result showed that the TSS reducing effect of shrimp chitosan is higher than Crab chitosan.

It is seen that pH was significantly affected by chitosan concentration and storage time. All the samples showed a similar pH increasing trend (from 3.7 to 4.18) over storage time and no interaction effect resulted from storage time and chitosan concentration.

An interactive effect between chitosan concentration and storage time on the browning potential (BP) was also observed. In samples with lower or no chitosan concentration, the BP increased rapidly over storage time, while it remained almost constant in samples with higher chitosan concentration.

3. *Sensory evaluation*

Results of the sensory (hedonic) evaluation of pineapple juice using chitosan as preservative are presented in Table 2. In all the treatments, the average score ranged between 7-9 for color, taste and overall acceptability on a 9-point hedonic scale, the data are the mean scores of 10 panelists selected randomly (Table 2). These data showed that there is significant increase in the degree of acceptance of each score with the increase of chitosan concentration (i.e., scores for color, taste and overall acceptability of the chitosan added samples were higher than the control sample). This result agrees with

Table 2 Sensory evaluation scores of pineapple juice enriched with chitosan

Parameter	P	*S1	S2	S3	*C1	C2	C3
Color	6.15^a	6.82^b	7.19^b	7.85^c	6.43^a	7.15^b	7.76^c
Taste	7.02^a	7.11^b	7.13^b	7.00^b	7.06^a	7.12^b	6.85^c
Overall acceptability	6.65^a	7.08^b	7.18^b	7.56^c	7.02^b	7.17^b	7.20^b

*S for samples treated with chitosan from Shrimp shell and
*C for samples treated with chitosan from crab shell;
P=control, S1=(0.2g/L), S2=(0.4g/L), S3=C1=(0.6g/L);
C1=(0.2g/L), C2=(0.4g/L), C3=(0.6g/L);

Chatterjee et al. (2004) who reported improvement of acceptability and appearance when treated with chitosan. The result showed that Shrimp chitosan added juice is more acceptable than crab chitosan added juice.

Conclusion

Comparative studies on chitosan extracted from shrimp and crab waste showed that shrimp shell is better choice for extraction of chitosan based on all physicochemical properties. Chitosan application on pineapple juice showed increased in luminosity with increasing chitosan concentration. Chitosan reduced the Brix value of the pineapple juice. The pH increased significantly with increasing chitosan concentration and shrimp chitosan added juice showed greater pH than crab chitosan added juice. Chitosan retarded potential browning of pineapple juice during storage. As the outcome of this research is promising and optimistic, it will not be confined only to pineapple, but also may be used for other fruits like apple, orange and litchi etc.

References

AOAC (2005) Official Methods of Analysis. 15th Edition. Association of Official Analytical Chemists. Washington, D.C.

Chatterjee, S., Chatterjee, S., Chatterjee, B.P., Guha, A.K. (2004) Clarification of fruit juice with chitosan. *Process Biochemistry*, 39(22), 2229–2232.

Chien, P., Sheu, F., Huang, W.T., Su, M.S. (2007) Effect molecular weight of chitosans on their antioxidative activities in apple juice. *Food Chemistry* 102, 1192–1198.

Domingues, R.C.C., Junior, S.B.F., Silva, R.B., Cardoso, V.L., Reis, M.H.M. (2012) Clarification of passion fruit juice with chitosan: Effects of coagulation process variables and comparison with centrifugation and enzymatic treatments. *Process Biochemistry*, 47, 467–471.

Hajji, S., Ghorbel-Bellaaj, O., Younes, I., Jellouli, K., Nasri, M. (2015) Chitin extraction from crab shells by Bacillus bacteria. Biological activities of fermented crab supernatants. *International journal of biological macromolecules*, 79, 167–173.

Hossain, M.S., Iqbal, A. (2014) Production and characterization of chitosan from shrimp waste. *Journal of the Bangladesh Agricultural University*, 12(1), 153–160.

Imeri, A.G., Knorr, D. (1988) Effect of chitosan on yield and compositional data of carrot and apple juice. *Journal of Food Science*, 53(3), 1707–1709.

Kaya, M., Baran, T., Asan-Ozusaglam, M., Cakmak, Y., Tozak, K., Mol, A., Mentes, A., Sezen, G. (2015) Extraction and characterization of chitin and chitosan with antimicrobial and antioxidant activities from cosmopolitan Orthopteran species (Insecta). *Biotechnology and Bioprocess Engineering*, 20(1), 168–179.

Knorr, D. (1982) Functional properties of chitin and chitosan. J*ournal of Food Science*, 47, 593-595.

Madhavan, P., Nair, K.G.R., (1974) Utilization of prawn waste-Isolation of chitin and its conversion to chitosan. *Fishery Technology*, 1, 50–53.

Martín-Diana, A.B.M., Rico, D., Barat, J.M., Barry- Ryan, C. (2009) Orange juices enriched with chitosan: Optimisation for extending the shelf life. *Innovative Food Science and Emerging Technologies*, 10(4), 590–600.

Mohanasrinivasan, V., Mishra, M., Paliwal, J.S., Singh, S.K., Selvarajan, E., Suganthi, V., Subathra Devi C. (2014) Studies on heavy metal removal efficiency and antibacterial activity of chitosan prepared from shrimp shell waste, *Biotechnology*, 4 (2), 167–175.

No, H.K., Meyers, S.P., Lee, K.S. (1989) Isolation and characterization of chitin from crawfish shell waste. *Journal of Agriculture and Food Chemistry*, 37, 575–579.

No, H.K., Meyers, S.P. (2000) Application of Chitosan for Treatment of Wastewaters. In: Ware G.W. (eds) Reviews of Environmental Contamination and Toxicology. *Reviews of Environmental Contamination and Toxicology*, vol 163. Springer, New York, NY.

Oszmianski, J., Wojdylo, A. (2007) Effects of various clarification treatments on phenolic compounds and color of apple juice. *Eur. Food Res. Technol.*, 224, 755–762.

Pérez Roda, M.A. (ed.), Gilman, E., Huntington, T., Kennelly, S.J., Suuronen, P., Chaloupka, M. and Medley, P. (2019). A third assessment of global marine fisheries discards. FAO Fisheries and Aquaculture Technical Paper No. 633. Rome, FAO. 78 pp.

Ramasamy, P., Shanmugam, A. (1885) Characterization

and wound healing property of collagen–chitosan film from Sepia kobiensis. *International journal of biological macromolecules*, 74, 93–102.

Raybaudi-Massilia, R.M., Mosqueda-Melgar. J., Soliva-Fortuny, R., Martih-Belloso, O. (2009) Control of pathogenic and spoilage microorganisms in fresh-cut fruits and fruit juices by traditional and alternative natural antimicrobials. Comprehensive *Reviews in Food Science and Food Safety*, 8, 157–180.

Sapers, G.M. (1992) Chitosan enhances control of enzymatic browning in apple and pear juice by filtration. *Journal of Food Science*, 57(5), 1192–1193.

Soto-Peralta, N.V., Mller, H., Knorr, D. (1989) Effects of chitosan treatments on the clarity and color of apple juice. *Journal of Food Science*, 54(2), 495–496.

Toan, N.V. (2009) Production of Chitin and Chitosan from Partially Autolyzed Shrimp Shell Materials. *The Open Biomaterials Journal*, 1, 21-24.

Wen, L., Wrolstad, R.E. (2002) Phenolic composition of authentic pineapple juice. *Journal of Food Science*, 67, 155–161.

Electrical Impedance Analysis for Evaluating Tissue Conditions of Processed Vegetables

Teppei IMAIZUMI[1*], Haruki ANDO[1], Satoshi IWAMOTO[1]

[1] Faculty of Applied Biological Sciences, Gifu University, Yanagido 1-1, Gifu city, 501-1112, Japan
[*] Corresponding Author: imaizmi@gifu-u.ac.jp

SUMMARY

Tissue conditions are strongly related to quality of processed vegetables. To establish a technique which enables to evaluate the tissue conditions, we applied electrical impedance analysis to heated vegetables such as carrot. Carrot samples were heated at 50 °C. Electrical impedance spectroscopy was performed over a frequency range of 50 Hz to 5 M Hz. The obtained impedance values were analyzed using an equivalent circuit model, then cell membrane capacitance, extracellular resistance and intracellular resistance were determined. The model was successfully fitted to the measured values. As expected, cell membrane capacitance decreased by long-time heating. By using a confocal laser scanning microscope, we observed cell membrane structure which stained with 0.05 % DiI. The images also indicated that cell damage appeared when the sample was heated. Our research confirmed that the changes of electrical properties were occurred by cell membrane damage.

Introduction

Recently, electrical impedance spectroscopy (EIS) is often used to know cell membrane soundness of vegetables. The advantage of this technique is that the measurement is completed easily and quickly, and there is almost no adverse effect on vegetables. Cell membrane of plant tissue, which is formed by lipid bilayer, has a dielectric function. When AC current is applied to healthy cellular tissue, a dielectric relaxation occurs due to the cell membrane structure in a specific frequency band. While, it is assumed that deteriorated or damaged cell membrane decrease the function. To date, researchers reported that the impedance value of fruit and vegetables changed under various situations such as drop shock (Watanabe et al., 2018) and decay (Euring, Russ, Wilke, & Grupa, 2011).

Equivalent circuit analysis is an effective technique for obtaining detailed tissue state information from impedance measurement results. In this method, models in which the tissue structure is regarded as electric circuits are used and the parameters are determined by complex nonlinear least square method. An equivalent circuit described in Fig.1a is popularly used in past studies (Wu, Ogawa, & Tagawa, 2008; Zhang & Willison, 1992). Recently, another circuit which substitutes constant phase element (CPE) for capacitance (Fig.1b) is also used for more accurate analysis (Imaizumi et al., 2015). The parameters are considered to be directly related to the tissue structure of vegetables. Because the tissue structure is strongly related to quality aspects including texture of vegetables, the equivalent circuit parameters of processed vegetables can be one of quality indexes. However, knowledge about changes in the parameters during processing and the relevance to actual tissue structures is not enough. The purpose of this study was to clarify the applicability of equivalent circuit analysis to heated vegetables and relationships between the parameters and cell membrane structure.

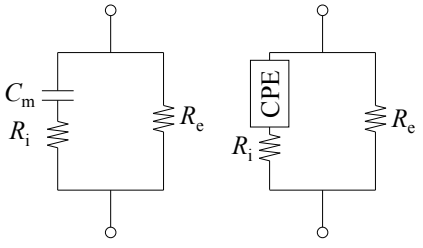

(a) Hayden's model (b) CPE model

Fig. 1 Equivalent circuit models for biological tissues.

Materials and Methods

1. *Sample preparation*

Carrot roots were cut into cylinders having 16 mm of diameter and 10 mm of height. The carrot cylinders were immersed into 150 mL of distilled water which kept at

50 °C, then immediately cooled in iced water after the heating.

2. *Electrical impedance measurement*

Two needle electrodes (diameter: 0.25 mm) connected to a LCR tester (3532-50, HIOKI, Japan) were inserted into the sample. The impedance $|Z|$, resistance R and reactance X of the sample were measured at 100 points over the frequency range from 50 Hz to 5 MHz at a measuring voltage of 1 V, and automatically recorded by a computer for analysis.

3. *Electrical impedance measurement*

In this study, equivalent circuit analysis using CPE model (Fig.1b) was conducted according to the past study (Imaizumi et al., 2015). The impedance of CPE was defined as following equations:

$$Z_{CPE} = \frac{1}{(j\omega)^p T} \quad (1)$$

$$= \frac{\cos(\frac{\pi}{2}p)}{\omega^p T} - j\frac{\sin\left(\frac{\pi}{2}p\right)}{\omega^p T} \quad (2)$$

where j is the imaginary unit, ω is angular frequency and T and p are constants ($0 \leq p \leq 1$). Thus, the impedance of CPE model is expressed as follows:

$$Z = \frac{R_e\left[1 + \omega^p T\left\{(2R_i + R_e)\cos\left(\frac{\pi}{2}p\right) + \omega^p T R_i(R_e + R_i)\right\}\right]}{\{\omega^p T(R_e + R_i)\}^2 + 2\omega^p T(R_e + R_i)\cos\left(\frac{\pi}{2}p\right) + 1}$$

$$-j\frac{\omega^p T R_e^2 \sin\left(\frac{\pi}{2}p\right)}{\{\omega^p T(R_e + R_i)\}^2 + 2\omega^p T(R_e + R_i)\cos\left(\frac{\pi}{2}p\right) + 1} \quad (3)$$

where R_e is extracellular resistance, R_i is intracellular resistance. The equivalent circuit parameters (R_e, R_i, T, p) were estimated using complex nonlinear least squares curve fitting (Macdonald, 1992). In addition, the cell membrane capacitance C_m was defined using the following equation (4) (Ando et al., 2014):

$$C_m = T^{1/p}(R_e + R_i)^{(1-p)/p} \quad (4)$$

4. *Confocal laser scanning microscopy*

The cell membrane structure of potato tissue was evaluated by confocal laser scanning microscopy (CLSM). Sections for observation were obtained from the central part of the cylindrical sample. Each section was stained with 0.05 % 1,1'-dioctadecyl-3,3,3',3'-tetramethyl-indocarbocyanine perchlorate (DiI) (Wako, Japan) and gently washed with distilled water. All confocal images were obtained and digitized using a confocal laser scanning microscope. A HeNe laser (543 nm) was used as the excitation source for the observation of DiI.

Results and Discussion

We measured impedance values from the heated samples with different heating time. The CPE model was successfully fitted to the measured values ($R^2 > 0.99$), and resistance R_e and intracellular resistance R_i. Figure 2A we obtained cell membrane capacitance C_m, extracellular shows that the C_m values of each heated sample. Cell membrane of plant tissue is formed by a lipid bilayer, which is thought to function as a capacitor. Since this value was lowered by heating for 40 min or more, it is considered that the membrane structure was damaged. Figure 2B shows the ratio of extra and intra cellular resistance R_e/R_i. Biological tissues maintain electrolyte concentration inside and outside the cell. It is assumed that R_e and R_i are

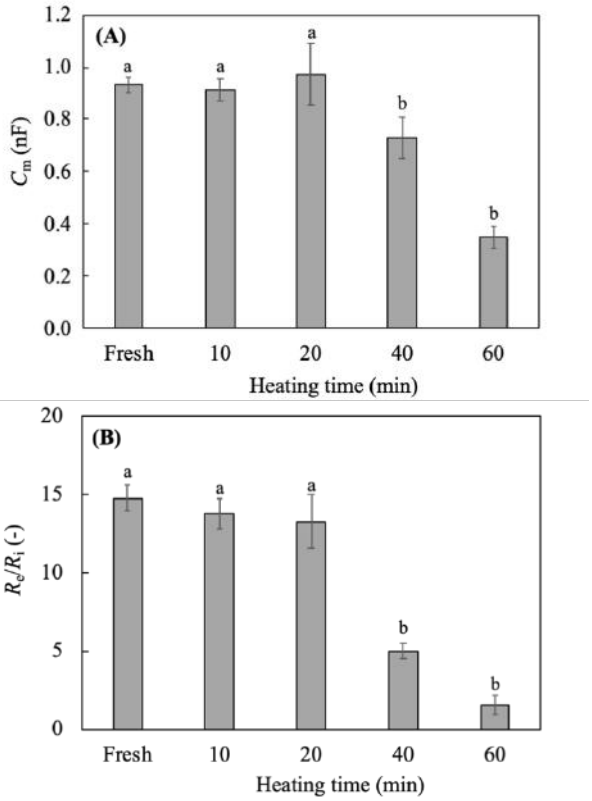

Fig.2 The values of cell membrane capacitance C_m (A) and ratio of extra and intra cellular resistance R_e/R_i (B) obtained from fresh and heated carrot samples. Bar: S.E. Different letters indicate significant difference ($p < 0.05$).

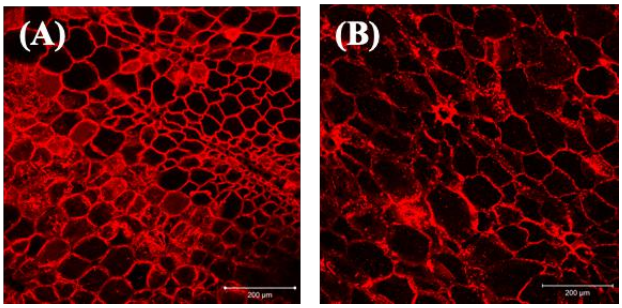

Fig. 3 CLSM images observed from fresh carrot sample (A) and sample heated at 50 °C for 40 min (B). Bar: 200μm

influenced by the electrolyte concentrations. Our result suggests that the function of adjusting electrolyte concentration was impaired after 40 min of heating. Thus, the R_e/R_i result also supported occurrence of cell membrane damage.

In our research, in order to confirm the cell membrane damage which was assumed from these electrical changes, we observed the structure with a confocal laser scanning microscope. Figure 3 shows that CLSM images of fresh and heated (40 min) samples. While cell membrane structure was clearly observed in the fresh tissue, the boundary formed by cell membrane lost its continuity. In this way, destruction of cell membrane structure was also indicated by CLSM observation.

Conclusion

Impedance measurement helps us to obtain some biological information without complicated procedure. In this study, it was indicated that electrical properties of carrot, which obtained by impedance analysis, greatly changed by heating treatment. Additionally, we also investigated that the relationships between the electrical properties and cell membrane structure. By CLSM observations, it was supported that the electrical properties changed due to cell membrane damage.

References

Ando, Y., Mizutani, K., & Wakatsuki, N. (2014). Electrical impedance analysis of potato tissues during drying. *Journal of Food Engineering*, 121(121), 24–31. https://doi.org/10.1016/j.jfoodeng.2013.08.008

Euring, F., Russ, W., Wilke, W., & Grupa, U. (2011). Development of an impedance measurement system for the detection of decay of apples. *Procedia Food Science*, 1, 1188–1194. https://doi.org/10.1016/J.PROFOO.2011.09.177

Imaizumi, T., Tanaka, F., Hamanaka, D., Sato, Y., & Uchino, T. (2015). Effects of hot water treatment on electrical properties, cell membrane structure and texture of potato tubers. *Journal of Food Engineering*, 162, 56–62. https://doi.org/10.1016/j.jfoodeng.2015.04.003

Macdonald, J. R. (1992). Impedance spectroscopy. *Annals of Biomedical Engineering*, 20(3), 289–305. https://doi.org/10.1007/BF02368532

Watanabe, T., Nakamura, N., Ando, Y., Kaneta, T., Kitazawa, H., & Shiina, T. (2018). Application and Simplification of Cell-Based Equivalent Circuit Model Analysis of Electrical Impedance for Assessment of Drop Shock Bruising in Japanese Pear Tissues. *Food and Bioprocess Technology*, 11(11), 2125–2129. https://doi.org/10.1007/s11947-018-2173-7

Wu, L., Ogawa, Y., & Tagawa, A. (2008). Electrical impedance spectroscopy analysis of eggplant pulp and effects of drying and freezing–thawing treatments on its impedance characteristics. *Journal of Food Engineering*, 87(2), 274–280. https://doi.org/10.1016/j.jfoodeng.2007.12.003

Zhang, M. I. N., & Willison, J. H. M. (1992). Electrical impedance analysis in plant tissues: The effect of freeze-thaw injury on the electrical properties of potato tuber and carrot root tissues. *Canadian Journal of Plant Science*, 72(2), 545–553. https://doi.org/10.4141/cjps92-068

-PART 2-

UGSAS-GU & BWEL JOINT POSTER SESSION

ON AGRICULTURAL

AND BASIN WATER ENVIRONMENTAL SCIENCES

2019

POSTER PRESENTATIONS

Thursday, 10th October 2019
13:00 pm - 15:00 pm

6th Floor, UGSAS Building, Gifu University

ORGANIZERS:
THE UNITED GRADUATE SCHOOL OF AGRICULTURAL SCIENCE,
GIFU UNIVERSITY
&
GIFU UNIVERSITY REARING PROGRAM
FOR BASIN WATER ENVIRONMENTAL LEADERS

Proceedings of International Symposium on a New Era in Food Science and Technology 2019
UGSAS-GU & BWEL Joint Poster Session on Agricultural and Basin Water Environmental Sciences 2019: P01

The effect of Japanese persimmon (*Diospyros kaki*) extract on the prevention of sarcopenia

Nayla Majeda Alfarafisa[1], Kohji Kitaguchi[1,2] and Tomio Yabe[1,2,3]
1. **The United Graduate School of Agricultural Science, Gifu University**
2. **Faculty of Applied Biological Sciences, Gifu University**
3. **G-CHAIN, Gifu University**

INTRODUCTION

Sarcopenia is an age-related syndrome which characterized by progressive loss of mass, strength, and function of skeletal muscle (Budui, et al., 2015). People with sarcopenia syndrome usually experienced a progressive and irreversible loss of body weight, followed by muscular atrophy, decreased muscle strength, and even death. Sarcopenia is a multifactorial syndrome. The exact underlying mechanisms and pathophysiology of sarcopenia remain unclear. As of now, there is no effective clinical strategies to overcome sarcopenia

Nowadays, the use of natural bioactive compound from plant extract as therapeutic agent had gained much attention. Various botanical compound proved to be effective in maintaining muscle health. Compared with conventional medicine, natural compound possessed lower physiological and psychological addiction among patients with relatively lower side effect. Japanese persimmon (kaki fruit persimmon), *Diospyros kaki*, is one of a well known and highly distributed fruits around the world. This fruit enriches with many bioactive compounds that have beneficial effect on human health (Yaqub, et al., 2016). It is suggested that bioactive compound in Japanese persimmon also had an effect to pathological condition of sarcopenia.

This study aims to investigate the effect of Japanese persimmon extract on skeletal muscle health. For mimicking real-life condition, co-culture system using a human Caco-2 intestinal cell as intestinal barrier model and a murine C2C12 skeletal muscle cell will be established for evaluating its possible effect on muscle cell proliferation, differentiation, and atrophic prevention. Therefore, each fraction was added into co-culture system, follow by the collection of culture media from the basolateral components and then C2C12 cell proliferation, cell differentiation, and its role on muscle protein turnover will be evaluated. Currently in this research progress, the extraction and fractionation steps have been done. Evaluation of each fractions in the form of antioxidant activity and total phenolic content showed different potentiality with hydrophobic fractions tend to show stronger antioxidant activity

MATERIALS AND METHODS

Materials

Diospyros kaki Nishimura cultivar was provided by Gifu Prefectural Agricultural Technology Center (Gifu, Japan) and used as a sample. (±)-6-Hydroxy-2,5,7,8-tetramethylchromane-2-carboxylic acid and Trolox (Sigma-Aldrich, St. Lois, USA) were used as a standard for measuring antioxidant activity, and 1,1-diphenyl-2-picrylhydrazyl (DPPH; Wako Pure Chemical Industries, Osaka, Japan) was used as a stable free radical which turns yellow when scavenged. 2,2-azobis-2-methyl-propanimidamide dihydrochloride (AAPH) was obtained from Wako Pure Chemical Industries. Cell Counting Kit-8 (CCK-8) were purchased from Dojindo Molecular Technologies Inc. (Kumamoto, Japan).

Japanese persimmon extraction

After washed and properly handled, the raw material of Japanese persimmons was freezed at –30ºC until it was ready to process. The samples were completely dried by lyophylization methods. After exclude the calyx and seeds, the remaining parts of the samples weighed and were recorded as dry weight. The samples then crushed using mortar in order to improve the efficiency of extraction by increasing their surface area. Powdered samples (42.5 g) were extracted in 420 mL of 98% aqueous ethanol for 30 min in boiled condition. After three cycles of extractions, the extract was mixed combined and filtered using a Buchner funnel. The solvents were vaporized using rotary evaporator and dried up using lyophylization methods. All crude extract was kept on –30ºC until further analysis.

Japanese persimmon fractionation

Japanese persimmon crude extract was fractionated using different concentrations of ethanol (25, 50, and 75%). The extracts (5.00 g) were dissolved in each solvent (50 mL) and homogenized using magnetic stirrer for 1 h at room temperature. When the crude extract completely dissolved in ethanol solvent, the samples were fractionated again using butanol (1:1) solvent until two different phases were obtained. Solvent were vaporized using rotary evaporator and dried up using lyophylization methods. All samples were kept on –30ºC until further analysis.

DPPH radical scavenging activity

The free radical scavenging activity of the extract was measured in terms of hydrogen donating or radical scavenging ability using the stable free radical DPPH. Gradient concentration (3.00-11.00 mg/mL) of Japanese persimmon fraction solutions in water was prepared. On the other hand, trolox solution was prepared by dissolving trolox in ethanol. Gradient concentration of trolox were used as a standard curve. 30 µL of Japanese persimmon fraction and trolox solutions were added to 96-well plate, followed by 240 µL of methanol. Water was used as a blank. 1 mM solution of DPPH in ethanol was prepared and added to each well of the samples. After 30 min of incubation in dark condition, the absorbance was measured at 540 nm. The assay was performed in triplicate. Percentage of inhibition of free radical DPPH was calculated by using equation bellows:

$$\text{DPPH Scavenging Activity (\%)} = \frac{(\text{Ab} - \text{As})}{\text{Ab}} \text{ x } 100$$

Ab = Absorbance of the blank
As = Absorbance of the sample

Oxygen Radical Absorbance Capacity (ORAC) Assay

Different concentration of Japanese persimmon fraction solutions in water, blank, and trolox standard solutions (50 µL) were added to 96-well plate. After that, 50 µL of fluorescein was added. Incubated the plate in dark condition at 37ºC. After 15 minutes, 25 µL of AAPH was added to each well. The fluorescence intensity was monitored every 5 min for 90 min by a micro plate reader in excitation 485 nm and emission 535 nm with 37ºC incubation temperature. The assay was performed in triplicate. ORAC value is the result of net area under the curve of the fluorescence decay (AUC) of standard or sample minus AUC of blank.

Determination of Total Phenolic Content

The total phenolic content of the extracts was determined by the Folin–Denis method. Briefly, 1 mL of the diluted sample extract was transferred to reaction tubes containing 1 mL of Folin-Denis reagent. After 3 minutes, 1 mL of sodium carbonate solution was added to the mixture. The tubes were then allowed to stand at room temperature for 1 hour before measuring absorbance at 760 nm. The total phenolic content of the extracts was calculated as catechin equivalents.

Cell Culture and Treatments

C2C12 cell lines were maintained in growth medium consisting of Dulbecco's Modified Eagle's Medium (DMEM) supplemented with 10% fetal bovine serum (FBS) and L-glutamine. On the other hand, Caco-2 cells were also maintained in DMEM supplemented with 10% fetal bovine serum and Non-Essential Amino Acid (NEAA). Cells are maintained under 70% confluency. After exceeds 70%, the cells were harvested with trypsin/EDTA and place to the new vessels. Both cells were incubated at 37 °C and 5% CO_2.

Cell Viability Assay

WST-8 that utilized in CCK-8 kit (2-(2-methoxy-4-nitrophenyl)-3-(4-nitrophenyl)-5-(2,4 disulfophenyl)-2H tetrazolium, monosodium salt) was used to evaluate cell viability and cytotoxicity. WST-8 solution (3%) in complete medium was added to the culture in 96 well plate. After 2 h incubation, the absorbance was measured at 450nm.

RESULTS AND DISCUSSION

Japanese persimmon extraction and fractionation

Table 1 showed an extraction yield of hot ethanol extraction from Japanese persimmon. Theoretically, the quantity of extractive yield was directly affected by the type of extraction methods/solvents and their extraction efficiency (Sharma & Cannoo, 2016). In this research, we conducted three cycles for each extraction step. Relatively high number of yield percentage from extraction step indicated the method of extraction which was chosen can be said sufficiently effective to isolate water soluble bioactive compound from Japanese persimmon.

Table 1. Japanese persimmon extraction yield

Dry Sample (g)	Crude Extract (g)	Yield (%)
42.5	27.8	65.3

Japanese persimmon fractionation

After underwent an extraction step, Japanese persimmon crude extract was fractionated. Table 2 showed total yield of fractionation from 5 g Japanese persimmon crude extract. There are six different fractions obtained from Japanese persimmon crude extract: ethanol (A) and butanol (B) phase from 25% ethanol fractionation, ethanol (C) and butanol (D) phase from 50% ethanol fractionation, ethanol (E) and filtrate (F) phase from 75% ethanol fractionation.

Table 2. Total yield fractions

Fraction	A	B	C	D	E	F
Yield (g)	1.75	2.85	3.53	0.92	4.30	0.64

To evaluate the extraction and fractionation methods of plant compound, several analytical procedures were carried out. Below are the results of qualitative and quantitative chemical analysis of Japanese Persimmon.

DPPH IC_{50} values of Japanese persimmon fractions

Figure 1 showed IC_{50} values of each fraction of Japanese persimmon. DPPH IC_{50} value is the capability of an antioxidant and necessary concentration to reach 50% of scavenging DPPH free radical activity. Therefore, this means that the fraction with lowest IC_{50} concentration have strongest antioxidant activity among others. In Figure 1, D fraction possessed the strongest antioxidant activity, followed by B or E, and then C or F. Meanwhile A fraction showed the lowest radical scavenging activity with the IC_{50} values was more than 11 mg/mL. These findings are almost in line with Jang, et al. (2011) which stated that Nishimura-wase persimmon hydrophobic extract has better DPPH IC_{50} values in compare with hydrophilic extract, except the fact that E sample as hydrophilic fraction gave a comparable value among others hydrophobic fractions.

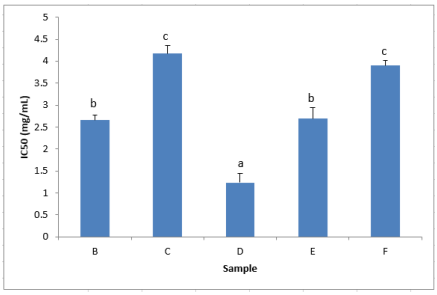

Figure 1: IC_{50} (mg/mL) values of persimmon fractions for DPPH radical scavenging activity. Values are means ± SD, n=7/group. Statistically significant difference of each group was determined by Tukey test.

ORAC Values of Persimmon Fractions

ORAC values of Japanese persimmon fractions can be seen in Figure 2. Compared with DPPH, ORAC measures the degree of inhibition of peroxy-radical-induced oxidation by the compounds of interest in a chemical milieu. The results showed slightly different pattern in compare with DPPH results. Among fraction B, D, E, and F, there were no significantly different results. On the other hand, fraction C and A are significantly lower among others. In general, hydrophobic fraction have better ORAC value compare to hydrophilic fraction, except for E fraction that again give a comparable value among others hydrophobic fractions.

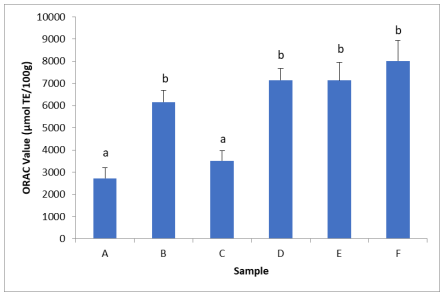

Figure 2: ORAC value (µmol/100 g TE) of persimmon fractions. Values are means ± SD, n=4/group. Statistically significant difference of each group was determined by Tukey test.

Total Phenolic Content of Persimmon Fractions

In line with ORAC value, fractions with higher antioxidant activity from ORAC analysis also possessed higher phenolic content. In Figure 3, F fraction had the highest phenolic content followed by D, B or E, and then A or C fractions. However, total phenolic content of F fraction was way too high compare to others. Otherwise, according to ORAC analysis, antioxidant activity from F fraction was not significantly different with fraction B, D, or E. It was suggested that the major antioxidant components in several fractions might not be phenolics compound. Therefore, among Japanese persimmon fractions with relatively high antioxidant activity only F fraction that showed high phenolic content.

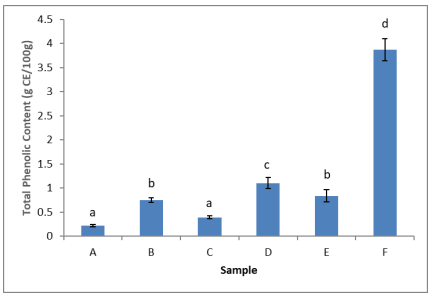

Figure 3: Total Phenolic Content (g/100 g CE) of persimmon fractions. Values are means ± SD, n=6/group. Statistically significant difference of each group was determined by Tukey test.

In general, hydrophobic fractions (B, D, F) from Japanese persimmon tend to have stronger antioxidant activity compare to hydrophilic fractions (A and C). On the other hand, E fraction always showed the highest antioxidant activity and phenolic content among other hydrophilic fractions, which even almost comparable with hydrophobic fractions. Several papers stated that there was a positive relationship between antioxidant activity and anti-atrophy potential for muscle cell *in vitro* (Hirasaka, et al., 2013). Therefore, we choose fractions B, D, E, and F for further analysis. As future plan, cytotoxicity of each fractions for C2C12 and Caco-2 cells will be analyzed to decided fractions ideal range of concentration. Furthermore, we will study the effect of each fractions on the physiological factor of myoblast, which are cell proliferation, differentiation, and finally its potential on preventing induced-muscular atrophy.

REFERENCES

Budui, S. L., Rossi, A. P. & Zamboni, M. (2015) The pathogenetic bases of sarcopenia. *Clin. Cases Mater. Bone Metab.,* 12, 22-26.

Hirasaka, K. et al. (2013) Isoflavones Derived from Soy Beans Prevent MuRF1-Mediated Muscle Atrophy in C2C12 Myotubes through SIRT1 Activation. *J. Nutr. Sci. Vitaminol.,* 59, 317-324.

Jang, I.-C.et al. (2011) Antioxidant Activity of 4 Cultivars of Persimmon Fruit. *Food Sci. Biotechnol.,* 20, 71-77.

Sharma, A. & Cannoo, D. S. (2016) Comparative evaluation of extraction solvents/techniques for antioxidant potential and phytochemical composition from roots of Nepeta leucophylla and quantification of polyphenolic constituents by RP-HPLC-DAD. *Food Measure,* 10, 658-669.

Yaqub, S. et al. (2016) Chemistry and Functionality of Bioactive Compounds Present in Persimmon. *J. Chem.* 2016, 3424025.

Proceedings of International Symposium on a New Era in Food Science and Technology 2019
UGSAS-GU & BWEL Joint Poster Session on Agricultural and Basin Water Environmental Sciences 2019: P02

Lipidomic profiling of cabbage stored at low temperature by liquid chromatography-tandem mass spectroscopy

Putri Wulandari Zainal[1], Daimon Syukri[2], Teppei Imaizumi[1], Masayasu Nagata[3] and Kohei Nakano[1]
1. **The United Graduate School of Agricultural Science, Gifu University, 1-1 yanagido, Gifu, 501-1193, Japan**
2. **Faculty of Agricultural Technology, Andalas University, Limau Manis, Padang, 20362, Indonesia**
3. **National Food Research Institute, NARO, 2-1-2 Kannondai, Tsukuba, Ibaragi, 305-8642, Japan**

INTRODUCTION

Fresh produce continues the biological activity after harvesting, and it is higher than the legume and grain because the fresh produce has a high moisture content around 95 % which relatively have high metabolic activity (Seymour, Taylor, & Tucker, 1993). The high metabolic causes rapid maturity and senescence, which lead to deterioration of chemical composition, texture, flavor, aroma, appearance, and color. This metabolic process is strongly influenced by temperature during storage (Lyons and Breidenbach, 1987), and low temperature is one of a method to reduce them. Give that, it has been used in preserving quality of fresh produce in market or transportation since long ago (Wismer, 2003).

The process of metabolism can be slowed down by the utilization of the low temperature, even the deterioration process still continues. Senescence has related to membrane deterioration caused by membrane lipids and proteins catabolism (Paliyath & Droillard, 1992). Lipid composition in plants is very diverse and have an essential function such as signaling (Munnik, Irvine and Musgrave, 1998) and energy storage (Meer, Voelker, and Feigenson (2008). Therefore, lipid profiling needs to know for learning about the senescence process, subsequently leads to the development of the novel assessment method for freshness of the postharvest products.

MATERIALS AND METHODS

Plant material and storage condition

The cabbage 'cv. Kinkei 201' was harvested at Kanagawa Prefecture Agricultural Technology Center on 25th April 2019 and stored at 5 °C for 0 and 16 days. The leaf was cut into small pieces using φ3-mm of cork-borer, and approx. 100 mg of sample was put into 2 ml cryotube with a piece of φ5-mm of zirconia ball. Then, it was rapidly frozen by liquid nitrogen and stored at -80 °C until lipid analysis.

Lipid extraction

Lipid was extracted using a methyl-tert-butyl ether (MTBE) method as described by Vitali et al. (2008) with some modifications. Each sample was homogenized with methanol and 0.01% Butylated Hydroxytoluene (BHT) for 1 minute by a beads crusher. The homogenates were centrifuged at 12,000 rpm for 10 minutes at 10°C, and 400 µl of supernatant was collected in 10 ml testing tube. Then, 50 µl of internal standard (a mixture of phosphatidylcholine; PC 17:0 and phosphatidylethanolamine; PE 17:0) were added and put 3ml of MTBE and was shaken in a water bath for 1 hour. After that, 400 µl of 1% potassium chloride was added and mixed thoroughly by a vortex mixer.

The suspension was centrifuged for 3 minutes at 2,000 rpm, and the supernatant was collected into a different testing tube. Then, the lipid extraction was evaporated by a centrifugal evaporator at 30°C for approx. 2 hours, and dissolve again in 600 µl of the solvent used for the mobile phase in HPLC separation (acetonitrile/20 mM ammonium acetate/isopropanol (27.3:9.1:63.6 v/v) with 0.01% acetic acid). The concentrate was filtrated using a membrane filter (pore size; 0.2 µm), and used for subsequent LC-MS/MS analysis. Lipids were extracted from each 5 cabbage sample.

LC-MS/MS condition

Lipids were separated by liquid chromatography in binary gradient mode with a C_{18} reversed-phase column and were ionized by electrospray ionization (ESI) using Turbo V ion source, then detected using multiple reaction monitoring (MRM) by a triple-quadrupole mass spectrometer (Q-TRAP 4500 AB-Sciex, Framingham, MA, USA). In detecting lipid species, total 900 channels were set in MRM transitions.

Data processing

The peak area of lipid from MRM chromatogram was processed using MultiQuant software (AB-Sciex, Framingham, MA, USA). Each peak area was normalized using that of the internal standard and the weight of the sample. Hierarchical clustering analysis (HCA) was conducted based on Pearson's correlation using Multiple experiment viewer (MeV 4.9.0). Moreover, principal component analysis (PCA) was applied to the auto-scaled data for finding out the most important lipid species.

RESULTS AND DISCUSSION

Around 555 kinds of lipid species were detected in the stored cabbage. The number of species in each lipid class was shown in Table 1. PC, PE and 3 kinds of glycolipids, namely MGDG, DGDG, and SQDG class have rich diversity compared to other ones. In membrane, lipid has 3 major class which classified into glycerophospholipids, sphingolipids, and sterols (Harayama and Riezman, 2018) and glycerophospholipids are the main constituent in membrane bilayer, for example, PC and PE are abundant content in plant membrane (Nakamura, 2017). On the other hand, especially in leaf, glycolipids are the main lipids which account for about 40% of total lipids, and MGDG is the major single component (Kates, 1970).

Figure 1 shows the difference of the lipid class distribution between non-stored and 16 days stored cabbage at 5 °C. HCA could separate into two main clusters in which several classes were increased, and the other ones were decreased during storage. Figure 2 (A) shows the PCA score plot between two samples and each group could be successfully separated into two on PC1 axis. Figure 2 (B) is box plots of top 6 important lipid species in the senescence process which were chosen from the loading plot of PCA. 6 lipid species in LGPL class shown here clearly increased in the cabbage stored at 5 °C for 16 days.

Several researchers have discussed the change of lipid composition in the plant under stress and postharvest conditions using LC-MS (Welti et al., 2002, Kong et al., 2017, Bustamante et al., 2018) and detected about 200 kinds of lipid species. However, in this study we successfully found 555 lipids species in stored cabbage using LC-MS/MS. Lipid profiling with a large number of species could give more accurate results for discussing the mechanism of bio-membrane deterioration during senescence of fresh produces.

The lipid profile obtained in this study will also contribute to the development of postharvest technology for assessing the degree of freshness in fruits and vegetables.

Table 1 Lipid profile in stored cabbage.

Lipid classes	Number of detected lipid species	
	0d	16 d
Phosphatidylcholine (PC)	63	54
Phosphatidic Acid (PA)	8	10
Phosphatidylethanolamine (PE)	75	69
Phosphatidylglycerol (PG)	40	34
Phosphatidylinositol (PI)	26	21
Phosphatidylserine (PS)	28	22
Lysoglycerophospholipids (LGPL)	15	16
Lysoglyceroglycolipids (LGGL)	19	19
Monogalactosyldiacylglycerol (MGDG)	66	63
Digalactosyldiacylglycerol (DGDG)	34	24
Sulfoquinovosyl Diacylglycerols (SQDG)	58	52
Diacylglycerol (DAG)	26	26
Triacylglycerol (TAG)	51	34
Fatty Acid	6	6
Ceramide	42	36
Acylated Sterylglucoside (ASG)	13	10
Steryl Glycoside (SG)	3	3
Steryl Ester (SE)	12	11
Total	592	517

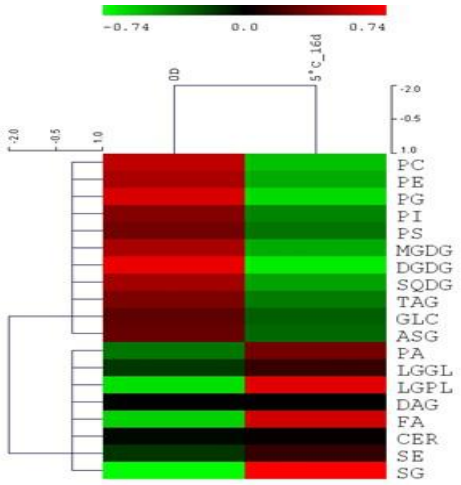

Fig. 1 Hierarchical clustering analysis (HCA) showing the differential of lipid classes between non-stored and stored cabbage at 5°C for 16 days.

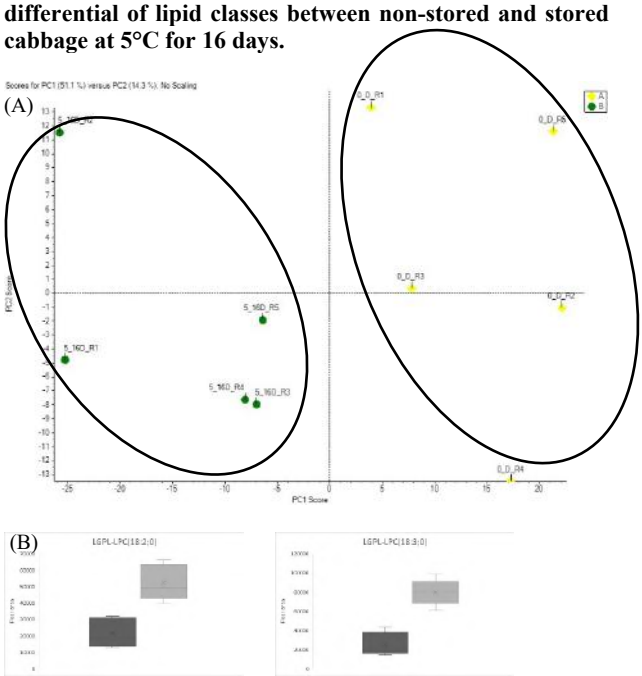

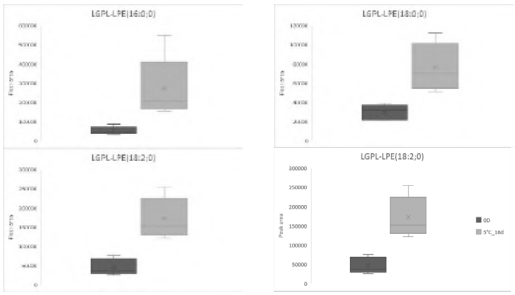

Fig. 2 Score-scatter plot of PCA (A) and six important lipid species selected by loading plot of PCA in stored cabbage for 0 and 16 days (B).

REFERENCES

Bustamante, C. A., Brotman, Y., Monti, L. L., Gabilondo, J., Budde, C. O., Lara, M. V., and Drincovich, M. F. (2018). Differential lipidome remodeling during postharvest of peach varieties with different susceptibility to chilling injury. Physiologia plantarum, 163(1), 2-17.

Harayama, T., & Riezman, H. (2018) Understanding the diversity of membrane lipid composition. Nature Reviews Molecular Cell Biology, 19(5), 281.

Kates, M. (1970). Plant phospholipids and glycolipids. In Advances in lipid research (Vol. 8, pp. 225-265). Elsevier.

Kong, X., Wei, B., Gao, Z., Zhou, Y., Shi, F., Zhou, X., & Ji, S. (2017) Changes in membrane lipid composition and function accompanying chilling injury in bell peppers. Plant and Cell Physiology, 59(1), 167-178.

Lyons, J.M., and R.W., Breidenbach. 1987. Chilling injury. In J. Weichmann (Ed.), Postharvest physiology of vegetables. Newyork: Marcel Dekker, Inc.

Nakamura, Y. (2017) Plant phospholipid diversity: emerging functions in metabolism and protein–lipid interactions. Trends in plant science, 22(12), 1027-1040.

Munnik, T., Irvine, R. F., & Musgrave, A. (1998) Phospholipid signaling in plants. Biochimica et Biophysica Acta (BBA)-Lipids and Lipid Metabolism, 1389(3): 222-272.

Matyash, V., Liebisch, G., Kurzchalia, T. V., Shevchenko, A., & Schwudke, D. (2008) Lipid extraction by methyl-tert-butyl ether for high-throughput lipidomics. Journal of lipid research, 49(5): 1137-1146.

Paliyath, G., & Droillard, M. J. (1992) The mechanisms of membrane deterioration and disassembly during senescence. Plant Physiology and Biochemistry, 30; 789–812.

Seymour, G. B., Taylor, J. E., & Tucker, G. A. (Eds.). (2012). Biochemistry of fruit ripening. Springer Science & Business Media, 454.

Van Meer, G., Voelker, D. R., & Feigenson, G. W. (2008) Membrane lipids: where they are and how they behave. Nature reviews Molecular cell biology, 9(2): 112.

Welti, R., Li, W., Li, M., Sang, Y., Biesiada, H., Zhou, H. E., & Wang, X. (2002) Profiling membrane lipids in plant stress responses role of phospholipase Dα in freezing-induced lipid changes in Arabidopsis. Journal of Biological Chemistry, 277(35), 31994-32002.

Wismer, W.V. (2003) Low temperature as a causative agent of oxidative stress in postharvest crops. In Hodges, M.D, Postharvest oxidative stress in horticultural crops. Binghamton: The Haworth Press, Inc.

First record of *wolbachia* infection in camellia spiny whitefly, *Aleurocanthus camelliae* (Hemiptera: Aleyrodidae), during their invasion stages in Japan

Eko Andrianto and Atsushi Kasai
1. **The United Graduate School of Agricultural Science (UGSAS)-Gifu University**
2. **Laboratory of Applied Entomology, Faculty of Agriculture, Shizuoka University**

INTRODUCTION

The camellia spiny whitefly (*Aleurocanthus camelliae* Kanmiya & Kasai) was decribed as a new species that closely related to the citrus spiny whitefly (*A. spiniferus*), the most serious pest of citrus plantation in Japan in 1920s (Kanmiya et al. 2011). The occurance of this whitefly firstly reported in Uji, Kyoto prefecture in 2004 and had rapidly spreads all around Japan (Kasai et al. 2010). This pest became serious by causing reduction of tree vigour, sap loss and sooty mould (Yamashita & Hayashida, 2006).

A huge number of sap feeding herbivore e.g. whiteflies harbour the bacterial symbionts to provide the essential nutrients. The one of most widely distributed endosymbiont in arthropods is *Wolbachia,* a group of rickettsial endocelluar bacteria, belonging to the α-proteobacteria. *Wolbachia* endosymbiont was suggested can affect the evolution of closely related insect host species by affecting the genetic structure and diversity of mitochondria of insect host (Narita et al. 2006).

Recently, the study that compare haplotype of the *Rhagoletis cerasi*, the European cherry fruit fly and its *Wolbachia* infection status revealed a strong association between the endosymbiont and the mitochondrial haplotype—individuals of haplotype 1 (HT1) are *Wolbachia*-uninfected, whereas *Wolbachia*-infected flies are associated with haplotype 2 (HT2) (Schuler et al. 2016). Similar with *R. cerasi*, In Japan, *A. camelliae* has a low genetic diversity, with only a single haplotype in mtCOI (haplotype B1) (Uesugi et al. 2016). We hypothesized that if this low genetic diversity caused by *Wolbachia* infection status, the population of *A. camelliae* in Japan would be either positively infected or uninfected by *Wolbachia*. The infection of *Wolbachia* in the *A. camelliae* are not yet reported. This study is trying to measure the frequency of *Wolbachia* infection and its diversity and assessing the mitochondrial genotypes of the host under natural conditions during the invasion stages of *A. camelliae*.

MATERIALS AND METHODS

Sample collection. Samples were collected from tea field in several cities in Japan during 2009-2011 and 2017-2018. In total, there are 14 specimen from 6 cities. Mostly samples are collection of Laboratory of Applied Entomology in Shizuoka University from previous study and reanalyzed for the infection of *Wolbachia*.

Table 1. Sampling locations including code, city, year and number of population samples

Code	City	Year	n
KKG	Kikugawa	2011	3
SZK1	Shizuoka	2010	1
SZK2	Shizuoka	2018	1
KNY	Kanaya	2017	1
SHG	Shiga	2010	2
MIE	Mie	2009	4
KYO	Kyoto	2009-2010	2

DNA extraction and PCR The DNA both of *Wolbachia* and their hosts were extracted using modified STE method. Ten of nymphs whiteflies were crushed in eppendorf tube contains 100 µl of STE buffer (100mM Nacl, 10mM tris-HCl, ImM EDTA,pH 8.0) using Biomasher. About 30µl of aliquot was transfered into PCR tube (0.2µL) and proteinase K (10mg/ml, 2µl) was added. And then it placed in the thermocycler at 95ºC for 15 and then temperature was reduced to 4ºC.

The polymerase chain reaction were performed in a total volume of 20µl GoTaq® Green Master Mix. PCR profile used was: Pre-denaturation (98ºC for 10 sec). Then followed by 35 cycles 98ºC for 10 sec, Annealing temperature (Table 2) for 50 sec and 72 ºC for 1 min. Extension period at 72 ºC for 4 min. PCR products were visualized after subjected to an agarose gel electrophoresis. The positive results of *Wolbachia* detection were sequenced. And to avoid false negative results of PCR we also performed the nested PCR using the primer WacF/WacR (Table 2) to confirm the results. This a set of primer were designed based on the sequence data of *Wolbachia* in *A. camelliae* from Shizuoka (2010).

Table 2. The set of primers in this study

Gene/ Primer name	Sequence (5'→3')	Annealing temperature/ product size	Reference
COI			
HCO2198	taaacttcagggtgaccaaaaaatca	52 ºC/710bp	Folmer et al. 1994
LCO1490	ggtcaacaaatcataaagatattgg		
wsp			
81F	tggtccaataagtgatgaagaaac	55 ºC/600bp	Braig et al. 1998
691R	aaaaattaaacgctactcca		
WacF	atagctggtggtggtgcatt	55 ºC/358bp	This study
WacR	aaccgaagtaacgagctcca		

Data analysis. The all sequences including the partial mtCOI sequences and *wsp* genes of 14 samples, which were representative ofthe genetics groups in each locality, were determined. Sequence similarity was analysed using BLAST on nucleotide sequences deposited in NCBI/GenBank databases. Sequences were aligned using MUSCLE using MEGA version X (Kumar et al. 2018). Phylogenetic analyses were performed using both the maximum likelihood (ML) and Neighbor Joining (NJ) methods, In both analysis, 1000 bootstrap replicates were performed.

RESULTS AND DISCUSSION

Infection of Wolbachia. The detection of *Wolbachia* infection are common using *wsp* gene as a target PCR. A standard PCR using 81F/691R as *wsp* gene primer in this study revealed the negative results of 6 samples or in other words there are more 40% samples were not infected by *Wolbachia*.

Considering the false negative results that also often found in *Wolbachia* detection, hence the nested PCR were performed to reconfirm the negative result samples using the second set of *wsp* primers. The target size of the second primer is shorter than the previous one. The results of nested PCR shows the positive infection in all samples of this study. This results indicate that the *A. camelliae* haplotype B1 might be infected by *Wolbachia*. However this results is not sufficient to proof the *Wolbachia* effect to the genetic diversity of *A. camelliae* since there are two other haplotypes of *A. camelliae* (B2 and B3) that exclude in this study. Haplotype B2 only detected in the populations of Chongqing (China) that might be native to that region.While haplotype B3 only detected on Theaceae plants in Japanese quarantine (China) (Uesugi et al. 2016).

Table 3. The infection rate of *Wolbachia* in *A. camelliae*

Code	n	Standard PCR		%	Nested PCR		%	Total (%)
		+	–		+	–		
KKG	3	3	0	100				100
SZK1	1	1	0	100				100
SZK2	1	1	0	100				100
KNY	1	1	0	100				100
SHG	2	0	2	0	2	0	100	100
MIE	4	1	3	25	3	0	100	100
KYO	2	1	1	50	1	0	100	100

***Wolbachia* diversity in the *A. camelliae* populations.** Based on the *wsp* sequences data, at least there are seven clades of *Wolbachia* in the *A. camelliae* population samples (I-VII). Those clades indicates the *Wolbachia* group which were separated into two supergroup (A and B). A supergroup is generally defined as a cluster of phylogenetically related strains, though type and number of genes used for phylogenetic inference are not set.

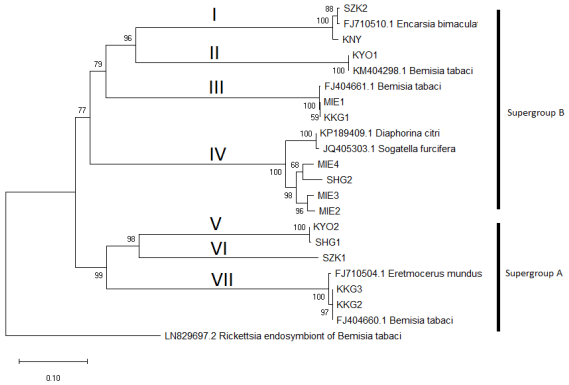

Fig.1. Neighbour-joining phylogenetic tree of *Wolbachia* infected *A. camelliae*. Taxa are labeled as the host from which *Wolbachia* isolated.

The supergroup B consisting the populations of *A. camelliae* that infected by *Wolbachia* group (I-IV), the rest groups (V-VII) clustered into supergroup A. This study is the first reveal the positive infection status of *Wolbachia* in all *A. camelliae* population samples. A modified nested PCR is an apporiate method to measure the infection status of *Wolbachia* using *wsp* gene target. This results supports the previous study that used a modified nested PCR to measure infection rates of *Wolbachia* in the *Bemisia tabaci* populations (Ji et al. 2015). However to conclude that *Wolbachia* infection affects the genetic diversity of *A. camelliae*, more samples data are needed. At this point, we noted that the populations of *A. camelliae* in Japan were infected by *Wolbachia* during the early invasion of this whitefly in Japan.

ACKNOWLEDGMENTS

We thank to Prof. Tsutomu Saito for the permission to use *A. camelliae* sample collections.

REFERENCES

Braig, H. R., Zhou, W., Dobson, S. L., and O'Neill, S. L. (1998). Cloning and characterization of a gene encoding the major surface protein of the bacterial endosymbiont *Wolbachia pipientis*. Journal of Bacteriology 180 :2373-2378.

Folmer O, Black M, Hoeh W, Lutz R, Vrijenhoek R (1994). DNA primers for amplification of mitochondrial cytochrome c oxidase subunit I from diverse metazoan invertebrates. Molecular Marine Biology and Biotechnology 3(5):294-299.

Ji, H.L., Qi, L.D., Hong, X.Y., Xie, H.F. & Li, Y.X. (2015). Effects of Host Sex, Plant Species, and Putative Host Species on the Prevalence of *Wolbachia* in Natural Populations of *Bemisia tabaci* (Hemiptera: Aleyrodidae): A Modified Nested PCR Study. Journal of Economic Entomology 108(1): 210-218

Kanmiya K., Ueda, S., Kasai, A., Yamashita, K., Sato, Y., and Yoshiyasu, Y. (2011) Proposal of new specific status for tea-infesting populations of the nominal spiny whitefly *Aleurocanthus spiniferus* (Homoptera: Aleyrodidae). *Zootaxa* 2979: 25-44

Kasai, A., K. Yamashita and Yoshiyasu, Y (2010) Tea infesting population of Citrus Spiny Whitefly, *Aleurocanthus spiniferus* (Homoptera: Aleyrodidae), Does not accept citrus leaves as host plants. *Japaese Journal of Applied Enomology and Zoology* 54: 140-143 (In Japanese)

Kumar S, Stecher G, Li M, Knyaz C, and Tamura K (2018) MEGA X: Molecular Evolutionary Genetics Analysis across computing platforms. *Molecular Biology and Evolution* 35:1547-1549.

Narita, S., Nomura, M., Kato, Y., and Fukatsu, T. (2006) Genetic structure of sibling butterfly species affected by *Wolbachia* infection sweep: Evolutionary and biogeographical implications. *Molecular Ecology 15*: 1095–1108.

Schuler, H., Kern, P., Arthofer, W., Vogt, H., Fischer, M., Stauffer, C., and Riegler, M. (2016) *Wolbachia* in parasitoids attacking native European and introduced Eastern cherry fruit flies in Europe. *Environmental Entomology 45*: 1424–1431.

Uesugi, R., Sato, Y., Han, B.-Y., Huang, Z.-D., Yara, K., & Furuhashi, K. (2016) Molecular evidence for multiple phylogenetic groups within two species of invasive spiny whiteflies and their parasitoid wasp. *Bulletin of Entomological Research*. 106(3):328-340.

Yamashita, K. and Hayashida, Y. (2006) Occurance and control of the citrus spiny whitefly, *Aleurocanthus spiniferus* (Quaintance), on tea tree in Kyoto Prefecture. Plant Protection 60:378-380

Physicochemical properties of chitosan films contained curcumin nanoemulsion

Fakfan Luangapai [1], Methavee Peanparkdee[2,3] and Satoshi Iwamoto[2,3]
1. **Graduate School of Natural Science and Technology, Gifu University**
2. **Faculty of Applied Biological Sciences, Gifu University**
3. **The United Graduate School of Agricultural Science, Gifu University**

INTRODUCTION

Chitosan is a derivative of chitin, which can be found in crustaceans, insects and fungi. Because of the effective biodegradability and antimicrobial activities, chitosan has been commonly applied as biopolymer in food, agricultural and pharmaceutical industries (Luangapai et al. 2019). Furthermore, the chitosan films provide as good barrier when compared to other polymers such as methylcellulose and corn starch (García et al. 2009). Chitosan films easily to interact with environmental moisture which changes physicochemical properties such as tensile strength, sorption ability and permeability of the films (Yoshida et al. 2009). Therefore, in order to prevent the undesirable changes in chitosan films, an addition of bioactive compounds into the films has been investigated (Mujtaba et al. 2019).

One of the remarkable bioactive compounds, turmeric has been used as food additive, food preservative and coloring agent for ages in Asian countries. Indeed curcumin, one of the main components of turmeric, has an excellence anti-oxidant and anti-microbial ability against *E. coli*, *B. subtilis* and *S. aureus* (Maheshwari et al. 2006), it exhibits low water solubility which leads to lower bioavailability (Manju and Sreenivasan 2011). To improve the solubility, a number of methods have been studied, including nanoemulsion method. Since, nanoemulsion technology has attracted wide attention in the food and pharmaceutical industry for years. The nanoemulsion can be to strengthen the solubility, stability and bioactivity of various oil-soluble chemical substance due to its small droplet size and high kinetic stability which this method widely accepted many industries (Mazzarino et al. 2012).

In the present work, the study on combining of chitosan films with nanoemulsion of bioactive compound such as curcumin in physicochemical perspective will be determined. Nevertheless, for the first step, the evaluation to find optimal condition of curcumin nanoemulsion on uniformity stability and size distribution need to be achieved. Thus, the aim of the study is to evaluate appropriate condition for curcumin nanoemulsion in order to be using for further study.

MATERIALS AND METHODS

Chitosan films preparation

Chitosan film-forming solution was prepared according to the procedure of Siripatrawan and Harte (2010) with slightly modification. Dissolved specific amount of chitosan powder into 1% acetic acid solution and glycerol, as plasticizer, was added to the film-forming solution at the constant concentration of 30% w/w of chitosan powder. The solution was heated at 60 °C in a water bath shaking incubator at 100 oscillation/minutes for 30 minutes. The solution was cooled to room temperature and the turmeric nanoemulsion were added. The film-forming solutions were homogenized for 2 minutes using a homogenizer (NS-60, Microtec, Japan) and removed air bubbles using ultrasonicator (ASU-10D, AS ONE, Osaka, Japan). The amount of films forming solution, 100 ± 1 g, were cast on a 12 × 28.5 cm on rubber plate and dried. The dried films were adjusted to proper conditioned in an environmental chamber at 25 °C and 50% relative humidity (RH) by using saturated Mg $(NO_3)_2 \cdot 6H_2O$ for 48 hours before measurement. All property measurements were performed immediately after removing film sample from the chamber to lessen moisture variances of these natural films.

Preparation and characterization of curcumin nanoemulsion

About 30 mg of curcumin was dispersed into 10 mL Medium Chain Triglyceride (MCT oil) as oil phase. The aqueous phase was prepared by mixing the surfactant (Tween 20) and water. The compositions of oil, surfactant, and water. The formulation of each curcumin nanoemulsion was varied by ultrasonication time, amount of curcumin and ratio of oil phase and aqueous phase. First, oil phase and aqueous phase were mixed and homogenized by a homogenizer followed Table 1 (NS-60, Microtec, Tokyo, Japan) at 13500 rpm for 15 minutes. Then, curcumin nanoemulsion was subjected to ultrasonic emulsification using 43 kHz ultrasonicator (ASU-10D, AS ONE, Japan) with a maximum power output of 500 W duration vary by Table 1. Then, the formulated nanoemulsion was characterized and the uniformity stability of the emulsion was investigated (Ghosh et al. 2013).

Table 1 formulation of curcumin nanoemulsion.

Curcumin nanoemulsion Sample	Curcumin (mg)	Ratio of oil phase and aqueous phase	Ultrasonic time (minute)
1	70	1:4	30
2	70	1:4	90
3	70	1:4	120
4	30	1:3	15
5	30	1:9	15

Determination of stability of nanoemulsion under processing conditions

Curcumin nanoemulsion was evaluated particle size distribution by dynamic light scattering method using Malvern Zetasizer Nano ZS (Malvern Instruments, UK). Then, zeta potential, an electrical charge on the oil droplets in the emulsions was evaluated at approximate temperature of 25°C and electrical voltage 3.9 V.

RESULTS AND DISCUSSION

Chitosan films was prepared in good condition. The appearance of the films shows smooth surface without air bubbles, yellowish color and transparency. The color of the films depends on quality and sources of chitosan powder, in this case, chitosan powder obtained from red snow crab. However,

chitosan isolated from squid pens provide perfectly white and shrimp or lobster sources provide highly pink color.

From Table 1, size and zeta potential value are analyzed by Dynamic Light Scattering (DLS) method. The Zetasizer shown that the particle size in the nanoemulsion in each sample are varied by amount of curcumin, ultrasonication time and ratio of oil phase and aqueous phase. The sample 1,2,3,4 and 5 have average size distribution, zeta potential and Polydisperse index (PdI) as shows in Table2. The sample 2 and 3 tend to have lower size distribution compare to other sample, however, ultrasonication time of both samples are 90 and 120 minutes which takes longtime for creating nanoemulsion. Perhaps, the longtime of ultrasonication generate heat which can increase temperature result in active substances such as phenolic compound is lessen during the ultrasonication process.

On the other side, sample 5 has size distribution resemble to sample 2 and 3 but using less ultrasonication time. Furthermore, in part of PdI value, which is a ratio of standard deviation to average of droplet size of nanoemulsion, so it indicates the ability of accumulation depended on droplet size distribution, the lower of size distribution means the lower in droplet accumulation. In addition, PdI value, the higher the PdI value shown the lower the potential on uniformity of the droplet whereas the lower values shown the higher. Therefore, from sample 5 exhibit notable lowest PdI values. This means that sample 5 illustrate higher stability on uniformity than other samples. From this result, sample 5 tend to has potential applying as optimal condition for further study according to size distribution and PdI value.

Table 2 size, zeta potential and polydisperse index of nanoemulsion samples.

Curcumin nanoemulsion Sample	Size distribution	Zeta potential (mV)	PdI
1	624.66±15.40	-0.025±0.12	0.482±0.032
2	360.66±2.29	-0.54±0.49	0.447±0.013
3	378.2±5.59	-1.54±0.48	0.509±0.012
4	680.06± 1.24	-0.64±0.34	0.46±0.029
5	410.67 ± 1.80	-2.45±0.087	0.23±0.027

FUTURE WORK

Following the results in this study, need to achieve for the further study. Firstly, the stability of nanoemulsion time will be determine by monitor the change of size and stability of nanoemulsion during longer storage time. Then, the optimal results of stability together with size distribution will be used to combine with chitosan film in order to create chitosan film incorporated curcumin nanoemulsion. The incorporated films will be examined the physicochemical properties to monitor inner structure change of films and incorporated films, for example, Thermal property by using Differential scanning calorimetry (DSC) measurements, Mechanical properties determined by tensile strength (TS), elongation at break (EAB) and Young's modulus, Water vapor permeability (WVP). In addition, as curcumin itself provide potential of antioxidant properties, in order to know the alteration of antioxidant properties need to be examined. The examination will be conduct by the technique of Total phenolic compound (TPC), analyzing phenolic content, and DPPH radical scavenging assay, analyzing antioxidant content.

REFERENCES

Aider, M. (2010) Chitosan application for active bio-based films production and potential in the food industry. Review LWT Food Science Technology 43 (6): 837–842.

Anton, N., Benoit, J., and Saulnier, P. (2008) Design and production of nanoparticles formulated from nano-emulsion templates. A review Journal of Controlled Release 128: 185-199.

Chattopadhyay, I., Biswas, K., Bandyopadhyay, U., and Banerjee, R. (2004) Turmeric and curcumin. Biological actions and medicinal applications 87: 44-53.

Ghosh, V., Mukherjee, A., and Chandrasekaran, N. (2013) Ultrasonic emulsification of food-grade nanoemulsion formulation and evaluation of its bactericidal activity. Ultrasonics Sonochemistry 20: 338-344.

García, A., Pinotti, A., Martino, N., and Zaritzky, E. (2009) Characterization of starch and composite edible films and coatings. Edible films and coatings for food applications 169-209.

López-Mata, A., Ruiz-Cruz, S., de Jesús Ornelas-Paz, J., Del Toro-Sánchez, L., Márquez-Ríos, E., Silva-Beltrán, P., Burruel-Ibarra, E. (2018) Mechanical, Barrier and Antioxidant Properties of Chitosan Films Incorporating Cinnamaldehyde. Journal of Polymers and the Environment 26: 452-461.

Luangapai, F., Peanparkdee, M., and Iwamoto, S. (2019) Biopolymer films for food industries: properties, applications, and future aspects based on chitosan. Reviews in Agricultural Science 7: 59-67.

Maheshwari, K., Singh, K., Gaddipati, J., and Srimal, C. (2006) Multiple biological activities of curcumin. Jounal of Life Sciences 78: 2081-2087.

Manju, S., and Sreenivasan, K. (2011) Conjugation of curcumin onto hyaluronic acid enhances its aqueous solubility and stability. Journal of Colloid and Interface Science 359: 318-325.

Martins, T., Cerqueira A., and Vicente, A. (2012) Influence of α-tocopherol on physicochemical properties of chitosan-based films. Food Hydrocolloids 27: 220-227.

Mazzarino, L., Travelet, C., Ortega-Murillo, S., Otsuka, I., Pignot-Paintrand, I., Lemos-Senna, E., and Borsali, R. (2012) Elaboration of chitosan-coated nanoparticles loaded with curcumin for mucoadhesive applications. Journal of Colloid and Interface Science 370: 58-66.

Mujtaba, M., Morsi, E., Kerch, G., Elsabee, Z., Kaya, M., Labidi, J., and Khawar, M. (2019) Current advancements in chitosan-based film production for food technology. International Journal of Biological Macromolecules 121: 889-904.

Siripatrawan, U., and Harte R. (2010) Physical properties and antioxidant activity of an active film from chitosan incorporated with green tea extract. Food Hydrocolloids 24: 770-775.

Yoshida, M., Oliveira Junior, N., and Franco, T. (2009) Chitosan tailor made films: the effects of additives on barrier and mechanical properties. Packaging Technology and Science 22: 161-170.

Identification of Plantaricin A on *Lactobacillus plantarum* IYO1511

Yolani Syaputri[1], Masanori Horie[2] and Hitoshi Iwahashi[1]
1 The United Graduate School of Agricultural Science, Gifu University, Yanagido 1-1, Gifu City, 501-1193, Japan
2 Health Research Institute, National Institute of Advanced Industrial Science and Technology (AIST), 2217-14, Hayashi-Cho, Takamatsu, Kagawa, Japan

INTRODUCTION

Lactobacillus plantarum is a gram-positive bacteria, commonly found in many fermented food products. *L. plantarum* has anti-microbial activity *in vitro* against potentially pathogenic species such as *Listeria monocytogenes, Bacillus cereus, Escherichia coli, Yersinia enterocolitica, Citrobacter freundii, Enterobacter cloacae, Enterococcus faecalis, Salmonella enterica subsp. Enterica,* and *Candida albicans* (Todorov, 2009). *L. plantarum* produced antimicrobial substances such as organics acids, fatty acid, and bacteriocins. Bacteriocins are defined as proteinaceous antibiotics which kill or inhibit the growth of bacterial species closely related to producer bacteria (Malik, Sumayyah, Yeh, & Heng, 2016).

Bacteriocin that produced by *L. plantarum* is plantaricin. *plnA* expressed by *L. plantarum* inserts in the cytoplasmic membrane of the target cell, thereby promoting membrane depolarization and cell death (Ahmad, et al., 2017). The genes encoding bacteriocin are located on operon clusters, which may be placed on the chromosome (such as PlantaricinST31), or plasmids (such as Plantaricin423) or transposons (such as Nisin A) (Wada, et al., 2009). *L. plantarum* IYO1511 was isolated from fresh tea leaf. This research aims to determine the existence of the bacteriocin biosynthetic cluster of *plnA* in *L. plantarum* and show the related structural cluster gene ORFs.

MATERIALS AND METHODS

Plasmid Isolation from L. plantarum IYO1511

Plasmids were extracted with the protocol based on *Lactobacillus spp. oriented* High-Quality methods (O'Sullivian & Klaenhammer, 1993) with modification. One hundred EDTA 1M was added into the solution.

Identification of Gene Encoding Bacteriocin Production from Lactobacillus plantarum Using Specific Primers

The identification of gene encoding bacteriocin was performed using PCR. The *plnA* specific primer F: (5`-TAGAAATAATTCCTCCGTACTTC-3`) and R: (5`-ATTAGCGATGTAGTGTCATCCA-3`). Polymerase chain reaction (PCR) was carried out in a Fast reaction Tube (Applied Biosystems, USA) in a total volume of 25 µl containing 12.5 µl 2 × Green Master Mix PCR (Promega, USA), 1.25 µL of each primer (concentration 0.05 pmol/µL), 9 µL nuclease free deionized water, and 1 µL template DNA, and was run under the following temperature program: initial denaturation of DNA for 5 min at 95°C, 30 cycles of 30sec at 94°C, 1 min at 55°C, and 1 min at 72°C; and final extension for 10 min at 72°C. Then, 5 µl aliquots of the PCR product were analyzed by electrophoresis using 1% (w/v) agarose gel in TAE 1X buffer at 100 V for 30 min. The gel was then placed in an Electronic U.V. Transilluminator to detect the presence a 1500 bp band. The size of the DNA fragments was estimated using a FastGene 100 bp DNA Ladder (Nippon Genetics, Germany). Fast Gene™ Gel/PCR Extraction kit (Nippon Genetics, Germany) was used for purification before sending the extracted DNA for sequencing, according to the manufacturer's instructions. An average of 500 bp nucleotides for each sequence from each side was read and compared against the NCBI database using BLAST (http://blast.ncbi.nlm.nih.gov/Blast.cgi).

RESULTS

Identification Plantaricin A on L. plantarum using Specific Primers

Identification of gene encoding bacteriocin was done to know the presence of plantaricin on plasmid. Specific primer of *plnA* was amplified on plasmid of *L. plantarum* IYO1511 using PCR method. The cell harvest at the early of stationary phase to reached maximum production of plantaricin (data not shown). The presence of *plnA* gene encoded on plasmid were confirmed (fig. 1) based on the observation of the PCR product using specific primers of *plnA* with size approximately ~550bp. Plasmid of *L. plantarum* COY-2906 isolated from Virgin Coconut Oil that had confirmed present *plnA* is used as positive control.

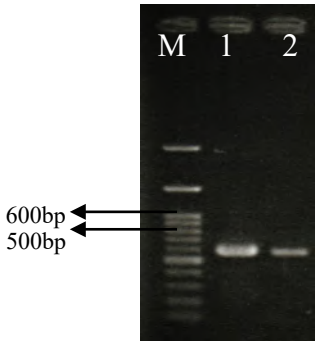

Fig. 1: Detection of *plnA* sequence in *L. plantarum* IYO1511 plasmid M: Molecular Weight Marker 100bp DNA Ladder. 1: Positive control, Amplification of plantaricin from *L. plantarum* COY2906 isolated from Virgin Coconut Oil; 2 Amplification of *plnA* from *L. plantarum* IYO1511.

Plantaricin A of L. plantarum IYO1511 on plasmid

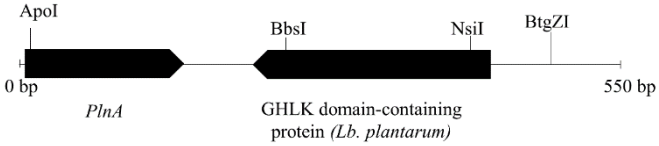

Fig. 2: Gene cluster *plnA* of *L. plantarum* IYO1511 on plasmid

L. plantarum IYO1511 DNA sequence analysis has high DNA sequence identity 100% that correspond to *plnA* from GenBank, the plantaricin gene was shown elsewhere. The cluster structure of plantaricin encoding region was not shown yet around plantaricin A gene region (fig. 2). Open Reading Frame 1 showed *plnA* from *L. plantarum* IYO1511 start on 4-152 bp and ORF2 showed GHLK domain-containing protein *(L. plantarum)* start on 268-519bp. Plantaricin A of *L. plantarum* IYO1511 encoded a protein consisting of 48 amino acid residues, followed by a TAA stop codon. The start codon *plnA* followed by 4-152 bp, ATG start codon.

DISCUSSION

L. plantarum IYO1511 is one of the potential lactic acid bacteria (LAB) isolated from fresh tea leaf. Plantaricins were encoded on plasmid and chromosome. This study, we focus on plasmid of *L. plantarum* IYO1511. *PlnA* of *L. plantarum* IYO1511 encoded a protein consisting of 48 amino acid residues, followed by a TAA stop codon. The sequence analysis showed 100% that correspond to *plnA* GenBank. Many bacteriocins are produced by Lactic Acid Bacteria (LAB) and the bacteriocins are mostly active against Gram-positive bacteria and foodborne pathogens such as *Listeria monocytogenes* (Azizi, Najafi, & Dovom, 2017) (Malik, Sumayyah, Yeh, & Heng, 2016) (Reenen, Zyl, & Dicks, 2006) (Cho, Hanak, Huch, Holzapfel, & Franz, 2010) (Gautam, Sharma, & Ahlawat, 2014). The bacterial pathogens included *Staphylococcus aureus, Clostridium botulinum, Campylobacter jejuni* and *Escherichia coli 0157:H7* (Gautam, Sharma, & Ahlawat, 2014). This *plnA* has potential to kill or inhibit pathogen bacteria.

In conclusion, plantaricin A has due role to their potential to kill or inhibit pathogen bacteria. The most attractive feature of plantaricin A in this study is improved potential as role in fermentation process. Although, the antimicrobial activity of plantaricin is relatively well understood, the used of p*lnA* as a key role for fermentation food is still limited to study in the process of product.

REFERENCES

Ahmad, V., Khan, M. S., Jamal, Q. M., Alzohairy, M. A., Karaawi, M. A., & Siddiqui, M. U. (2017) Antimicrobial potential of bacteriocins: in therapy, agriculture and food preservation. International Journal of Antimicrobial Agents, 49, 1-11.

Azizi, F., Najafi, M. B., & Dovom, M. R. (2017) The biodiversity of Lactobacillus spp. from Iranian raw milk Motal cheese and antibacterial evaluation based on bacteriocin-encoding genes . AMB Express, 1-10.

Cho, G.-S., Hanak, A., Huch, M., Holzapfel, W. H., & Franz, C. M. (2010) Investigation into the Potential of Bacteriocinogenic Lactobacillus plantarum BFE 5092 for Biopreservation of Raw Turkey Meat. Probiotics & Antimicro. Prot, 241-249.

Gautam, N., Sharma, N., & Ahlawat, O. P. (2014) Purification and Characterization of Bacteriocin Produced by Lactobacillus brevis UN Isolated from Dhulliachar: a Traditional Food Product of North East India. Indian J Microbiol, 185–189.

Horie, M., Sato, H., Tada, A., Nakamura, S., Sugino, S., Tabei, Y., . . . and Toyotome, T. (2019) Regional characteristics of Lactobacillus plantarum group strains isolated from two kinds of Japanese post-fermented teas, Ishizuchi-kurocha and Awa-bancha. Bioscience of Microbiota, Food and Health, 11-22.

Malik, A., Sumayyah, S., Yeh, C.-W., & Heng, N. C. (2016) Identification and sequence analysis of pWcMBF8-1, a bacteriocin-encoding plasmid from the lactic acid bacterium Weissella confusa . FEMS Microbiology Letters, 1-8.

Møller, S. A., Jensen, P. Ø., Høiby, N., Ciofu, O., Kragh, K. N., Bjarnsholt, T., & and Kolpen, M. (2019) Hyperbaric oxygen treatment increases killing of aggregating Pseudomonas aeruginosa isolates from cystic fibrosis patients. Journal of Cystic Fibrosis , 1-9.

O'Sullivian, D., & Klaenhammer, a. T. (1993) Rapid Mini-Prep Isolation of High-Quality Plasmid DNA from Lactococcus and Lactobacillus spp. Applied and Environmental Microbiology , 2730-2733.

Reenen, C. A., Zyl, W. H., & Dicks, L. M. (2006) Expression of the Immunity Protein of Plantaricin 423, Produced by Lactobacillus plantarum 423, and Analysis of the Plasmid Encoding the Bacteriocin. Applied and Environmental Microbiology, 7644–7651.

Renois, F., Jacques, J., Guillard, T., Moret, H., Pluot, M., Andreolettu, L., & and Champs, C. d. (2011) Preliminary Investigation of a Mice Model of Klebsiella pneumoniae subsp. ozaenae Induced Pneumonia. Microbes and Infection , 1045-1051.

Todorov, S. D. (2009) Bacteriocins from Lactobacillus plantarum - Production, Genetic Organization and Mode of Action. Brazilian Journal of Microbiology , 209-221.

Wada, T., Noda, M., Kashiwabara, F., Jeon, H. J., Shirakawa, A., Yabu, H., . . . Sugiyama, M. (2009) Characterization of four plasmids harboured in a Lactobacillus brevis strain encoding a novel bacteriocin, brevicin 925A, and construction of a shuttle vector for lactic acid bacteria and Escherichia coli. Microbiology, 1726–1737.

Proceedings of International Symposium on a New Era in Food Science and Technology 2019
UGSAS-GU & BWEL Joint Poster Session on Agricultural and Basin Water Environmental Sciences 2019: P06

Genome-wide association study for understanding aluminum signaling genes expression in the shoots of *Arabidopsis thaliana*

Raj Kishan Agrahari[1], Yuriko Kobayashi[1, 2], Ayan Sadhukhan[2], Sanjib Kumar Panda[3] and Hiroyuki Koyama[1, 2]
[1]The United Graduate School of Agricultural Science, Gifu University
[2]Faculty of Applied Biological Sciences, Gifu University, Gifu 501- 1193, Japan
[3]Department of Biochemistry, Central University of Rajasthan, Rajasthan 305817, India

INTRODUCTION

Aluminum (Al) toxicity in acid soils (pH < 5.5) is a severe global problem that affects greater than 30% of the world's arable land. Physiologically Al toxicity includes severe root growth inhibition coupled with reduction in shoot biomass and crop yield (Kochian, 1995).

Accumulating evidence suggests that the cell wall plays important roles in the perception and manifestation of Al toxicity in plants (Horst *et al.*, 2010; Kochian *et al.*, 2015). The cell wall is the first point of contact when plants are exposed to Al, and serves as a major pool for the metal. Al bound to the cell wall negatively affects wall structure and function by increasing the rigidity and reducing cell expansion and mechanical extensibility, thus affect plant growth (Van *et al.*, 1994; Ma *et al.*, 2004; Yang *et al.*, 2010). The major Al binding site in cell walls is generally the pectin, because their negatively charged carboxylic groups have a high affinity for Al (Chang *et al.*, 1999; Schmohl and Horst, 2000).

It was reported that ALS3 *ALUMINIUM-SENSITIVE 3* (*ALS3*) & *PGIP1* (POLYGALACTURONASE INHIBITING PROTEIN 1), regulated by *STOP1* (SENSITIVE TO PROTON RHIZOTOXICITY1) are Al biomarker genes induced in shoot (Sawaki et al., 2016), *ALS3* encodes a half type ATPase is involved in the Al-translocation process (Larsen et al., 1996, 1997) where as *PGIP1* stabilizes the cell wall (Kobayashi et al., 2014), But the detailed regulatory mechanisms leading to the induction of *STOP1*-regulated genes under Al stress in shoot remain unclear. Recently we identified involvement of phospholipids upstream to *STOP1* in *ALS3* signaling. Here we present our work regarding the new signaling molecule upstream to *PGIP1*.

MATERIALS AND METHODS

Plant Materials

Seeds of natural *A.thaliana* accessions and KO lines were obtained from the Arabidopsis Biological Resource Center (Columbus, OH, USA), the Nottingham Arabidopsis Stock Center (Nottingham, UK), and the RIKEN BioResource Center (Tsukuba, Japan), We treated 85 *A.thaliana* accessions with 25 μM Al for the GWAS. Progeny lines were obtained by controlled self-pollination method. The homozygocity of KO lines was confirmed by PCR using SALK recommended methods.

Plant Growth Condition

Germinated *A.thaliana* seedlings were grown on mesh and transferred to to modified 2% MGRL (pH was 5.6) culture solution (Fujiwara et al., 1992). The solution was changed every 2 days, and grown under controlled environmental conditions for 10 days (Sawaki et al., 2016).

Gene Expression Analysis

10 days old seedlings were then transferred to the treatment solution containing 25 μM Al. after a 24-h stress treatment, the shoots were collected and freeze in liquid nitrogen, and crushed using tissue homogenizer. Total RNA was extracted from the shoot and used for cDNA. *PGIP1* expression level was determined by real-time qPCR.

Genome-wide Association Study

The GWAS calculations were completed using the compressed mixed linear model of the TASSEL program as previously described (Sadhukhan *et al*. 2017). The genome-wide SNPs used in this study were obtained from a public database. Missing data or a minor allele frequency below 10% was removed. Genes nearest to the most significantly associated SNPs were annotated according the TAIR 10 database.

PGIP1 expression analysis in KO line

Total RNA was extracted from a 24-h stress (25 μM Al) treated shoot sample, and used for cDNA. *PGIP1* expression level was determined by real-time qPCR.

RESULTS & DISCUSSION

From a GWAS on *PGIP1* expression we found 16 SNPs ($P<10^{-3.5}$) to be strongly associated to *PGIP1*expression. Role of the genes, linked to the most significant SNPs, in regulating *PGIP1 was* validated by reverse genetics.

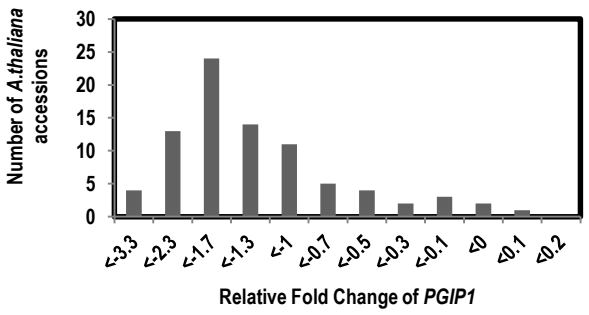

Fig 1. Histogram of *PGIP1* expression in *A. thaliana* accessions.

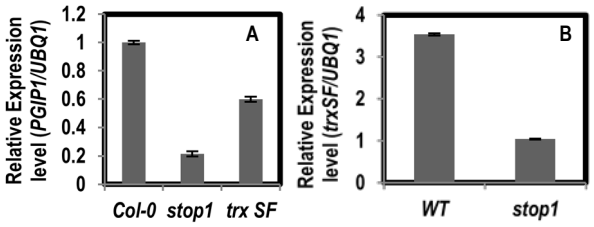

Fig 2. (A) Expression of *PGIP1* in T-DNA insertion mutants of GWAS detected genes. (B) Expression of trx SF in WT and *stop1*

As *PGIP1* encodes a POLYGALACTURONASE INHIBITING PROTEIN 1 responsible for cell wall stability under Al stress, though it's signaling is unclear. We did GWAS to identify a signaling cascade regulating *PGIP1* expression under Al stress. From the GWAS we identified thioredoxin (Trx) superfamily protein downstream of *STOP1* that involved in *PGIP1* signaling.

REFERENCES

Chang, Y.C., Yamamoto, Y., Matsumoto, H. (1999). Accumulation of aluminium in the cell wall pectin in cultured tobacco (*Nicotiana tabacum*L.) cells treated with a combination of aluminium and iron. Plant, Cell and Environment 22,1009– 1017.

Fujiwara, T., Hirai, M.Y., Chino, M., Komeda, Y., and Naito, S.(1992). Effects of sulfur nutrition on expression of the Soybean seed storage protein genes in transgenic petunia. Plant Physiol. 99:263–268.

Horst ,W.J., Wang, Y., Eticha, D. (2010) The role of the root apoplast in aluminium-induced inhibition of root elongation and in aluminium resistance of plants: a review. Annals of Botany 106, 185–197.

Kochian, L.V. (1995) Cellular mechanisms of aluminum Toxicity and resistance in plants. Annu. Rev. Plant Physiol. Plant Mol.Biol. 46, 237–260.

Kochian, L.V., Pineros, M., Liu, J., Magalhaes, J. (2015) Plant adaptation to acid soils: the molecular basis for crop aluminum resistance. Annual Review of Plant Biology 66, 23.1–23.28.

Kobayashi, Y., Ohyama, Y., Kobayashi,Y., Ito,H., Iuchi,S., Fujita, M., Zhao, C.R., Tanveer, T., Ganesan, M., Kobayashi, M. and Koyama,H. (2014) STOP2 activates transcription of several genes for Al- and low pH-tolerance that are regulated by STOP1 in *Arabidopsis* Mol. Plant, 7 (2014), pp. 311-322.

Larsen, P.B., Kochian, L.V. and Howell, S.H. (1997) Al inhibits both shoot development and root growth in als3, an Al-sensitive Arabidopsis mutant. Plant Physiol. 114, 1207–1214.

Ma, J.F., Shen, R., Nagao, S., Tanimoto, E. (2004) Aluminum targets elongating cells by reducing cell wall extensibility in wheat roots. Plant and Cell Physiology 45, 583–589.

Schmohl, N., Horst, W. (2000). Cell wall pectin content modulates aluminium sensitivity of *Zea mays* (L.) cells grown in suspension culture. Plant, Cell and Environment 23, 735–742.

Sadhukhan A., Kobayashi Y., Nakano Y., Iuchi S., Kobayashi M., Sahoo L. & Koyama H.(2017) Genome-wide Association Study Reveals that the Aquaporin NIP1;1 Contributes to Variation in Hydrogen Peroxide Sensitivity in *Arabidopsis thaliana*. *Molecular Plant* 10, 1082–1094.

Sawaki,K.,Sawaki.Y.,Zhao,C.R.,Kobayashi,Y., and Koyama,H.(20 16) Specific transcriptomic response in the shoots of Arabidopsis thaliana after exposure to Al rhizotoxicity: - potential gene expression biomarkers for evaluating Al toxicity in soils. Plant Soil. 409:131–142.

Van, H.L., Kuraishi, S., Sakurai, N. (1994) Aluminum-induced rapid root inhibition and changes in cell-wall components of squash seedlings. Plant Physiology 106, 971–976.

Yang, Z.B,, Eticha, D., Rao, I.M., Horst, W.J. (2010) Alteration of cellwall porosity is involved in osmotic stress-induced enhancement of aluminium resistance in common bean (*Phaseolus vulgaris* L.). Journal of Experimental Botany 61, 3245–3258.

Proceedings of International Symposium on a New Era in Food Science and Technology 2019
UGSAS-GU & BWEL Joint Poster Session on Agricultural and Basin Water Environmental Sciences 2019: P07

Annual characterization and variations of airborne insect

Panyapon Pumkaeo[1], Junko Takahashi[1,2] and Hitoshi Iwahashi[1]

1. **Division of Science of Biological Resources, The United Graduate School of Agricultural Science, Gifu University, 1-1 Yanagido, Gifu, 501-1193, Japan**
2. **National Institute of Advanced Science and Technology (AIST), 1-1, Higashi, Tsukuba, Ibaraki, 305-8566, Japan**

INTRODUCTION

Bioaerosols are atmosphere particles, mists or dust of µm range, associated with metabolically active or inactive viable particles. They contain living organism's included microorganisms such as viruses, bacteria, and fungi also plant material as well as pollen.

The presence of microorganism in aerosols has been known for centuries, However, most studies have only focus on bacteria to have a potential impact on public health and ecosystems. Therefore, in this study, insect abundance and community composition were determined by cytochrome oxidase I (COI region) using Next generation sequencing and compared on particle size distribution.

MATERIALS AND METHODS

The Aerosol samples collected on the filter membrane using Anderson's air sampler at the rooftop of Gifu Field Science Center building, Gifu University.

The sample was divided into three subgroup and two subgroups total 6 samples according to the size of its bioaerosols, large subgroup contains bioaerosols whose diameter is bigger than 3.3µm, and small subgroup contains those smaller than 3.3µm. (during 2017–2018; 24 samples over four seasons)

The DNA was extracted by using soil DNA extraction kits. and PCR amplication of cytochrome oxidase I (COI region) using mlCOIintF and HCO2198 primers and followed by high-throughput sequencing.

RESULTS

The seasonal distribution in insect abundance of large particle size (> 3.3 µm) were not observed. About 530 OTUs were Identified to the species level as they showed more than 98% sequences similarity with GENBANK sequences.

Hemiptera sp. remained the dominant insect species in all samples.(Fig 1 and 2) Potentially of fungal plant pathogen strain were found using mlCOIintF and HCO2198 primers such as *Calonectria colhounii* strain H125.

The insect community composition on smaller size particle was rather stable seasonally and did not differ from that on large size particle.

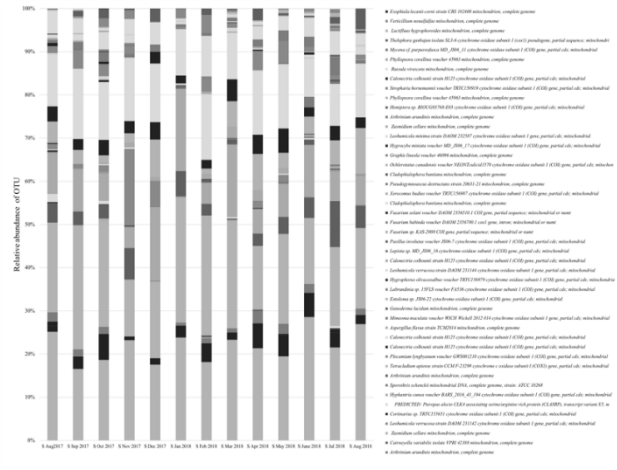

Fig. 1: Taxonomic composition of each sample of outdoor airborne insect communities. (size <3.3 µm)

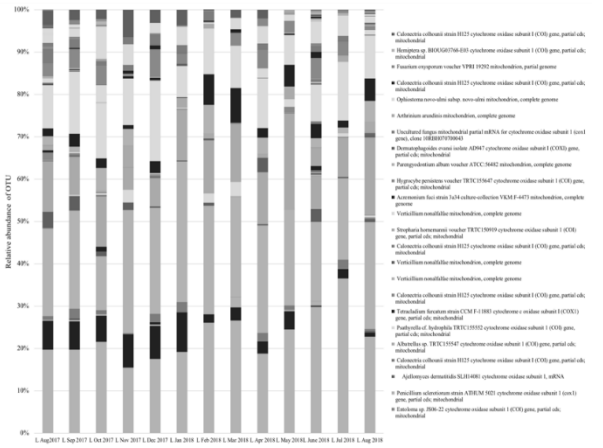

Fig. 2: Taxonomic composition of each sample of outdoor airborne insect communities. (size >3.3 µm)

DISCUSSION

The Heteroptera (Insecta: Hemiptera), or true bugs, are one of the major insect groups with respect to the very diverse habitat preferences. Due to the high habitat diversity and the relatively high environment specificity, Hemiptera can be a useful bio-indicator of various environmental parameters, such as habitat structure and vegetation coverage.

Our findings suggest that aerosol sampling might be helpful for early warning screening of species and also plant pathogen detection.

ACKNOWLEDGMENTS

This study is acknowledged for Gifu Field Science Center building, Gifu University as the sampling place.

REFERENCES

Park. J, Ichijo. T, Nasu. M, Yamaguchi. N. (2016) Investigation of bacterial effects of Asian dust events through comparison with seasonal variability in outdoor airborne bacterial community. Scientific Reports | 6:35706

Ishikawa. T, Masayuki U. Saito , Keiko Kishimoto-Yamada, Toshihide Kato , Osamu. (2015) Inventory of the Heteroptera (Insecta: Hemiptera) in Komaba Campus of the University of Tokyo, a highly urbanized area in Japan. Biodiversity Data Journal 3: e4981

Srivastava, A., Singh, M., & Jain, V. K. (2012). Identification and characterization of size-segregated bioaerosols at Jawaharlal Nehru University, New Delhi . *Nat Hazards* , 485-499.

Proceedings of International Symposium on a New Era in Food Science and Technology 2019
UGSAS-GU & BWEL Joint Poster Session on Agricultural and Basin Water Environmental Sciences 2019: P08

The relationship between major chemical components and genomic structures in tea accessions

Hiroto Yamshita[1,2], Tomoki Uchida[1], Hideyuki Katai[3], Lina Kawaguchi[4], Atsushi J. Nagano[4], Akio Morita[1] and Takashi Ikka[1]

1. **Faculity of Agriculture, Shizuoka University, Ohya, Shizuoka, Japan**
2. **United Graduate School of Agricultural Science, Gifu University, Yanagito, Gifu, Japan**
3. **Shizuoka Prefectural Research Institute of Agriculture and Forestry, Tea Research Center, Kurasawa, Kikugawa, Shizuoka, Japan**
4. **Faculty of Agriculture, Ryukoku University, Yokotani, Seta Oe-cho, Otsu, Shiga, Japan**

INTRODUCTION

Tea is one of the most popular beverages worldwide. Tea plant (*Camellia sinensis* (L.) O. Kuntze) contains many functional ingredients such as theanine and catechins. Consequently, the production area and yield of tea are increasing worldwide, but especially in Asia. Tea is a woody plant in the Theaceae family of angiosperms. The origin of tea plants is considered to be southwestern China and surrounding regions (Tanaka, 2012). In general, there are two varieties of tea plants; var. *sinensis* (Chinese type), and var. *assamica* (Assam type). These two varieties have different phenotypic characteristics and different origins (Yang et al., 2016). For example, *C. sinensis* var. *sinensis* has small leaves and is able to withstand colder climates, while *C. sinensis* var. *assamica* has large leaves and is sensitive to cold temperatures. *C. sinensis* var. *sinensis* is mainly cultivated in China and Japan for green tea production and *C. sinensis* var. *assamica* is mainly cultivated in India and Sri Lanka for black tea production. Assam hybrids, which are crosses between var. *sinensis* and var. *assamica*, have larger leaves and are more cold-tolerant than var. *assamica*, and so these hybrids are mainly utilized for breeding and for black tea production in Japan and China. However, the relationship between genetic differentiation and phenotypic characteristics such as major chemical components traits in these tea varieties is still unclear. And, it is important for tea breeding to control the content of chemical components, which contribute tea quality, in tea young shoots. Here, we performed the phenotyping of major chemical components of first flush and genotyping by double-digest restriction site-associated DNA sequencing (ddRAD-seq) in tea accessions, and genome wide association study to identify these locus associated with these traits.

MATERIALS AND METHODS

Plant materials and the measurement of major chemical components for tea—Tea accessions were obtained from the Tea Research Center, Shizuoka Prefectural Research Institute of Agriculture and Forestry, Kikugawa city, Shizuoka, and the Botanical Research Gardens of the ICHIMURA Foundation for New Technology, Atami city, Shizuoka. The 167 accessions comprised three subspecies: 96 Japanese var. *sinensis*, 42 exotic var. *sinensis* (originating from China and Taiwan); and 29 Assam hybrids (introduced from India and Nepal to Japan). To measure the content of major chemical components, young leaves at the same developmental stage in the first flush season were harvested from 150 accessions grown under the same cultivation environment at the Tea Research Center. 11 Free amino acids, 8 catechins, caffeine and chlorophyll as major chemical components for tea were measured by HPLC system (unpublished) and absorption spectrometry (Porra et al., 1989).

Genotyping by ddRAD-seq — Genomic DNA was extracted from young leaves of each tea accession using a DNeasy Plant Mini Kit (Qiagen) following the manufacturer's instructions, and then ddRAD-seq was conducted as described elsewhere (Sakaguchi et al., 2015). Genomic DNA was digested with *Bgl* II and *Eco*RI-HF. Sequencing of 50-bp single-end reads and the index sequences of the library was conducted using one lane of Hiseq2500 (Illumina, San Diego, CA, USA). Reads were preprocessed using Trimmomatic-0.33. After preprocessing, the remaining reads were mapped to the tea reference draft genome (Wei et al., 2018) using Bowtie2, and then the SNPs were called using Stacks (ver. 1.37). These raw SNPs data were filtered against the following thresholds: SNP call rate within a locus ≥ 0.7 and minor allele frequency (MAF) ≥ 0.05. The filtered SNP data were imputed using R package missForest and used for subsequent population analyses. The RAD-Seq data have been deposited in the DDBJ Sequence Read Archive (Accession number: DRA008166).

Population analysis — To clarify the genetic structure, we used the Bayesian clustering algorithm, hierarchical cluster analysis (HCA), and principal component analysis (PCA). The Bayesian clustering analysis was performed using STRUCTURE ver. 2.3.4 (Pritchard et al., 2000). In this analysis, we evaluated one to eight genetic subgroups (K) with ten runs per K value. For each run, the initial burn-in period was set to 50,000 with 20,000 Markov chain Monte Carlo iterations. The values of ΔK (Evanno et al., 2005) were calculated to infer the optimum number of subgroups. The components of each subgroups, i.e., ancestral components determined by this STRUCTURE analysis, were compared with the origin and pedigree information for the accessions.

Genome Wide Association Study — Genome wide association analysis (GWAS) was performed by using mixed linear model (MLM) implemented in the "GWAS" function of the R package rrBLUP ver. 4.6. In total, 10,943 SNPs among 150 accessions were used for the GWAS after selected SNPs without missing rates ≥ 0.3 and MAF < 0.05. The principal components and a kinship matrix were included in the GWAS calculation based on MLM. A principal component analysis (PCA) was conducted using the prcomp function of R to estimate the population structure. The first eight principal components from the plot explaining the total variation among SNPs were selected. The kinship matrix was computed by using the "A.mat" function of the R package rrBLUP ver. 4.6. To illustrate the localization of associated SNPs by GWAS, we created Manhattan plots of all anchored to linkage groups for each traits.

RESULTS AND DISCUSSION

SNPs identification by ddRAD-seq and genetic structures of world tea accessions — To acquire high-resolution genotypic information for the 167 tea accessions, we conducted SNPs genotyping by the ddRAD-seq method. After preprocessing the data, 1,269,648 SNPs were initially identified by the Stacks pipeline. Further filtering (SNP call rate within a locus ≥ 0.7, MAF ≥ 0.05) returned 13,715 in all 167 accessions To verify the locations of the detected SNPs on linkage groups, scaffolds with these SNPs were mapped to the reference tea genetic map (Wei et al., 2018). In total, 11,257 of the detected SNPs in all accessions were anchored across 15 linkage groups. To clarify the genetic structure and the degree of relatedness among tea accessions with different genetic backgrounds, we first used the Bayesian clustering approach with high-density SNP markers. To infer the optimal number of subgroups (K), we calculated ΔK values. We obtained the highest ΔK values in the order of $K = 2$ and $K = 3$. At $K = 2$, the 167 worldwide tea accessions were divided into var. *sinensis* and Assam hybrids, reflecting the two main subspecies of tea plants. The ΔK method of Evanno et al. (2005) often results in $K = 2$, because there is a very low likelihood of $K = 1$ in all analyses. Accordingly, there was a very low likelihood of $K = 1$ in our analyses, and the changes of likelihood values based on K also became moderate at $K = 3$. Therefore, we regarded $K = 3$ as the optimal classification in the genetic structure analysis of worldwide tea accessions. This classification of $K = 3$ more accurately reflected the genetic background of the tea accessions and was supported by the results of PCA and HCA. Comparisons of the accessions with the three ancestral components at $K = 3$ revealed the main composition of each subgroups: (1) Japanese var. *sinensis*; (2) Japanese and exotic var. *sinensis*; and (3) Assam hybrids and exotic var. *sinensis*. In a previous study, genotyping of tea accessions by SSR markers revealed marked genetic differentiation between Japanese var. *sinensis* and exotic accessions including var. *assamica* (Taniguchi et al., 2014). A possible reason for this result was that there was a bias in the SSR markers that were identified based on polymorphisms between the Japanese and Chinese accessions. Our analyses clarified the genetic structure of each accession without biases from their genetic backgrounds by using high-density SNPs markers.

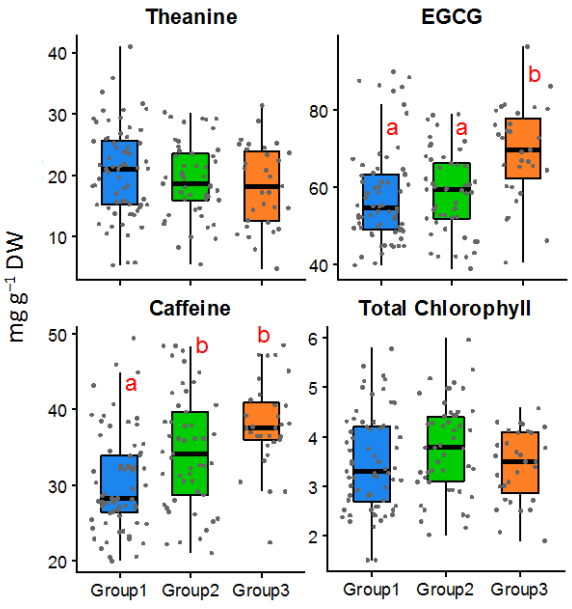

Fig. 1 The boxplots of major chemical components among three genetic subgroups. Different letters indicates significantly difference (Steel-Dwass test, $P < 0.05$).

Genetic variation of major chemical components in tea shoots and GWAS — The variation of each major chemical components in the tea first flush were widely observed; the content of theanine, epigallocatechin gallate (EGCG), caffeine and total chlorophyll ranged from 4.7 to 41.0 mg g^{-1} D.W., 38.9 to 96.4 mg g^{-1} D.W., 20.0 to 49.4 mg g^{-1} D.W. and 1.5 to 6.0 mg g^{-1} D.W (Fig.1). When compared the content of major chemical components among three genetic subgroups, the content of EGCG and caffeine in Group3 (subgroup of Assam hybrids) was higher than Group1 and Group2 (subgroup of var. *sinensis*) (Fig.1). Finally, GWAS based on each major chemical components identified some candidate locus. These results suggested that these locus may contain the gene(s) controlling the content of chemical components in tea shoots.

ACKNOWLEDGMENTS

We thank Satoko Kondo, technical assistant, from Ryukoku University for conducting the ddRAD-seq analyses in this study.

REFERENCES

Evanno G, Regnaut S and Goudet J. (2005) Detecting the number of clusters of individuals using the software STRUCTURE: A simulation study. Mol Ecol.14(8):2611–2620.

Porra RJ, Thompson WA and Kriedemann PE (1989) Determination of accurate extinction coefficients and simultaneous equations for assaying chlorophylls a and b extracted with four different solvents; verification of the concentration of chlorophyll standards by atomic absorption spectroscopy. Biochim Biophys Acta 975: 384–394

Pritchard JK, Stephens M and Donnelly P. (2000) Inference of Population Structure Using Multilocus Genotype Data. Genetics. 155(2):945–959.

Sakaguchi S, Sugino T, Tsumura Y, Ito M, Crisp MD, Bowman DMJS, Nagano AJ, Honjo MN, Yasuji M, Kudoh H, Matsuki Y, Suyama Y and Isagi Y (2015). High-throughput linkage mapping of Australian white cypress pine (Callitris glaucophylla) and map transferability to related species. Tree Genet Genomes.11(6).121

Tanaka J. (2012) Japanese tea breeding history and the future perspective. In: Chen L, Apostolides Z, Chen ZM. Grobal tea breeding Springer, berlin. 227–239.

Taniguchi F, Kimura K, Saba T, Ogino A, Yamaguchi S and Tanaka J. (2014) Worldwide core collections of tea (*Camellia sinensis*) based on SSR markers. Tree Genet Genomes. 10(6):1555–1565.

Yang H, Wei C, Liu H, Wu J, Li Z. (2016) Genetic Divergence between Camellia sinensis and Its Wild Relatives Revealed via Genome-Wide SNPs from RAD Sequencing. 1–21.

Proceedings of International Symposium on a New Era in Food Science and Technology 2019
UGSAS-GU & BWEL Joint Poster Session on Agricultural and Basin Water Environmental Sciences 2019: P09

Screening and molecular breeding of amylose utilizing yeast for bioethanol production

Annisyia Zarina Putri and Tomoyuki Nakagawa
The United Graduate School of Agricultural Science, Gifu University, 1-1 Yanagido, Gifu City 501-1193, Japan

INTRODUCTION

Amylases have a significant commercial importance and they employed about 25–33% of the world enzyme market (Nguyen et al., 2003). Because of the importance of amylases, isolation of new microorganisms, which are suitable for amylase production, could provide potential new sources of the enzyme (Aullybux and Puchooa, 2013). Recently, the hydrolysis of starch by α-amylase has been increasingly used as a key step to produce carbohydrate substrate for bio-ethanol production. Starch is the best substrate for production of yeast cells in a large scale due to its low price and easily available raw material in most regions of the world. Because most of yeasts from environments are generally recognized as safe compared to bacteria, interest in amylolytic yeasts has increased in recent years as their potential value for conversion of starchy biomass to single-cell protein and ethanol has been recognized (Gupta R et al., 2003).

In recent years, the interest in production of enzymes has increased due to several potential applications, such as the production of bioenergy and biofuels, and application in textile and paper industries (Soccol et al., 2003). Many studies have been published seeking new microorganisms to produce enzyme with higher specific activity and efficiency. Several strategies are available for improving the production and efficiency of cellulases, including optimization of the fermentation process, genetic difications and mutagenesis.

The purpose of this study is to screen, and breeding amylase producing yeast from different sources for bioethanol production and also describe some of the biochemical properties of the α-amylase purified from the culture broth. Total of around 190 strain yeast isolates were obtained from soil, fruits, vegetables, etc. on the starch agar medium.

MATERIALS AND METHODS

Screening of Amylase Producing yeast strains:

YNB medium containing 2% amylose (Amy/YNB medium) was used for cultivation of amylolytic yeast strains. Screening of the yeast strain was done by enrichment static or shaking culture at 30ºC.

Amylolytic activity of the strains was observed on Amy/YNB plate. Yeast cultures were incubated at 30ºC for 24-36hrs. After incubation of the yeast strains, Iodine vapor was used to detect degradation of amylose. The degradation of amylase was indicated by the clear zone of starch hydrolysis surrounding the colony.

Determination of Amylase Activity:

Amylase activity was carried out by measuring the amount of sugar released using DNSA method. Amylase activity was determined by incubating a mixture of 1 ml of each enzyme source and 1% soluble starch dissolved in 0.5 M phosphate buffer, at pH 5.5, at 30°C for 10 min. The reaction was stopped by adding 1 ml of 3, 5-dinitro salicylic acid, and then followed by boiling for 10 min. The final volume was made up to 12 ml with distilled water and the reducing sugar released was measured at 540 nm. One unit of amylase activity was defined as the amount of enzyme that releasing 1μmole glucose equivalent per minute under the standard assay conditions. Reducing sugar (Glucose or maltose) concentration was determined from a standard curve under same condition using glucose

Determination of Ethanol Activity:

The fermentation samples were analyzed by high-performance liquid chromatography. To monitor the fermentation, about 2 mL of sample was drawn at 144-216 hours, centrifuged at 10,000 rpm for 10 min. The liquid was immediately filtered through 0.2 μm into HPLC vials.

RESULTS

Screening of amylase producing yeast strains

In this work, we screened amylolitic yeast strains from yeast strains stocked in our laboratory. As a result, 7 yeast strains, GY 16, GY 73, GY 74, GY 76, GY 169, GY 183 and GY 184, could grow on Amy/YNB medium. Moreover, they showed clear zones on the Amy/YNB plate (Fig. 1). Especially,

the two yeast strains (GY 16 and GY 73) exhibited the largest clear zones (Fig. 1).

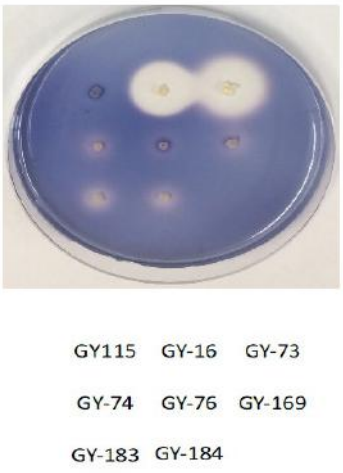

Fig. 1 Amylolytic activity of yeast transformants in plate assays.

Moreover, we identified these strains using 16S rRNA sequences. Strain GY 16 was identified as *Cryptococcus flavus*, strain GY 73 was *Ustilago trichophora*, and other strains were classified in *Papiliotrema laurentii*.

Determination of Amylase Activity:

In this research, amylase activities of the strains grown on Amy/YNB medium at 30ºC for 24 hours were mesured. All strains had enough levels of amylase activity (Fig. 2). Among these strains, GY 73 had the highest activity (Fig. 2).

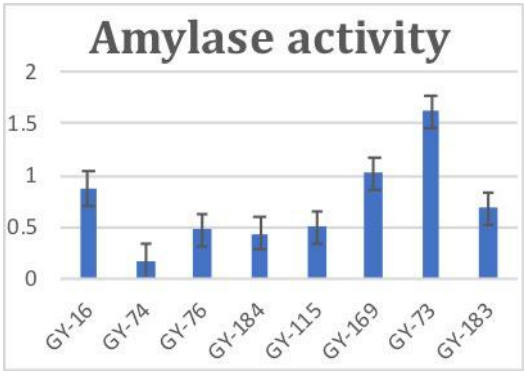

Fig. 2 Amylase activities of the amylolitic yeast strains.

Determination of Ethanol Activity:

Finally, we observed ability of ethanol production of the amylolitic yeast strains. As a result, all strains did not show the ethanol production during fermentation steps for 144-216 hours (Fig. 3).

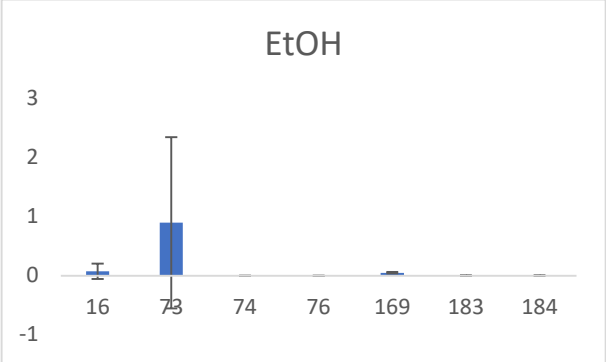

Fig. 3 Ethanol level from HPLC

DISCUSSION

In this work, we identified 7 strains of the amylolitic yeasts, GY 16, GY 73, GY 74, GY 76, GY 169, GY 183 and GY 184, and these strains belongs to *C. flavus*, *U. trichophora*, and *P. laurentii*. Moreover, the strains had enough amylase activities. In the next work, we will purify amylases from these yeast strains and will identify *amy* genes of the strains.

REFERENCES

Aullybux, A., & Puchooa, D. (2013). α-Amylase Productioon Low-Cost Substrates by *Naxibacter* sp. Isolated from Mauritian Soils. Microbiology Research Journal International, 3(4), 478-491.

Gupta R, Gigras P, Mohapatra H, Goswami VK, Chauhan B. Microbial α-amylases: a biotechnological prospective. Process Biochem. 2003; 38: 1599–1616. doi: 10.1016/ S0032-9592(03)00053-0.

Nguyen, C.V.; Smulikowska, S.; Mieczkowska, A., 2003. Effect of linseed and rapeseed or linseed andrapeseed oil on performance, slaughter yield and fatty acid deposition in edible parts of the carcass in broiler chickens. J. Anim. Feed Sci., 12:27-288

Soccol C R, Luciana P S, Vandenberge (2003). Overview of applied solid state fermentation in brazil. Biochem. engg. 13: 205-218

Proceedings of International Symposium on a New Era in Food Science and Technology 2019
UGSAS-GU & BWEL Joint Poster Session on Agricultural and Basin Water Environmental Sciences 2019: P10

The influence of particle size distribution on the mechanical properties of wood plastic composite

Arif Delviawan, Yoichi Kojima, Hikaru Kobori, Shigehiko Suzuki and Kenji Aoki
Faculty of Agriculture, Shizuoka University, Japan

INTRODUCTION

Wood plastic composite (WPC) is one of bio-composite product that made from wood-based materials and polymers (Gardner et al. 2015). It is made by a variety of production techniques (Najafi and Eslam 2011) under the specific heat and pressure conditions (Rahman et al. 2013). WPC has advantages such as lower maintenance requirement, better in thermal properties and durability compared other wood-based materials (Garcia et al. 2009). One of the largest commercial applications for WPC is exterior use, such as outdoor decking applications (Gardner et al. 2015), automotive interior substrates, furniture, packaging, housing (English and Falk. 1995), and cladding applications (Friedrich and Luible 2016).

The characteristics of wood flour (WF) as a raw material are important in the manufacturing of WPC. The quality and functionality of WPC should be improved to meet the increasing public demand. The wet ball milling process fibrillates the surface fibers of WF. The degree of fibrillation increased with increasing wet milling time (Isa et al. 2014). Although various studies have been conducted, there are still unsolved factors such as the particle size distribution as a function of wet milling time. It is also necessary to consider the relationship between this factor and the properties of WPC. The objective of this study is to evaluate the influences of particle size distribution due to different wet milling times and the mechanical properties of WPC.

MATERIALS AND METHODS

Commercial WF of Japanese red pine (*Pinus densiflora*), Polypropylene (PP, J107G, Prime Polymer Co., Ltd., Japan) and maleic anhydride-grafted PP (MAPP, Kayabrid 006PP-N, Kayaku Akzo Co., Ltd., Japan) were used as a filler, matrix and compatibilizer, respectively. WF (13.5 g) was milled with 200 ml of water by a ball mill (Pulverisette 5, Fritsch, Germany). A rotating speed of 200 rpm was applied with the different wet milling times (0, 10, 20, 30, 40, 60, and 120 min). After wet milling, two kinds of drying conditions were applied; seven days of freeze-drying at a temperature of −45 °C by a freeze dryer (FDU-1200, Eyela, Japan) and 24 h of heat drying by an oven dryer (SOFW-450S, Ettas, Japan) at a temperature of 80 °C. Then, dried WF was refibrillated for 1 min by a blender (IFM-800DG, Iwatani, Japan) and screened by mesh to be classified into 90–180 µm of mesh size. A vibrational acceleration of ± 20 G was applied for 30 min for each condition by a compact vibrating shaker (VSS-50D, Tsutsui, Japan). The micro-structure of WF was investigated through a scanning electron microscope (JSM-6510LV, JEOL, Japan) examination. The particle size distribution of WF after milling, drying, and screening was analyzed by a laser diffraction particle analyzer (LA-950S2, Horiba, Japan).

The ratio of the weight of WF, PP, and MAPP in the compound was 25:74:1, respectively. PP and MAPP were mixed by a kneader under 190 °C with 30 rpm for 3 min. Then, WF was added to mix them for 10 min with an extruder machine (Laboplast Mill 30 R 150, Toyo Seiki Seisakusho Ltd., Japan). After kneading, the WPC compound was crushed by a crusher machine (Pulverizer SA-23, Stolz Co. Ltd., Japan). Melt kneading was carried out for 5 min at a temperature of 190 °C and a screw rotation speed of 50 rpm by a twin-screw small kneader (Micro 5 cc Twin Screw Compounder, DSM Xplore, Netherlands). After that, the injection molding machine (Micro 5.5 cc Injection Moulding Machine, DSM Xplore, Netherlands) was used to make WPC test specimens. The dimensions of a bending test specimen were 50 mm in length, 2 mm in thickness, and 6 mm in width. The specimens were conditioned for 5 days or more in a constant temperature and humidity room (20° C, RH 65%) before testing. The bending and tensile tests were conducted to evaluate the performance of WPC according to the JIS A-5741 standard. The three-point bending flexural test was conducted using a universal testing machine (BT-805, Yasui Kikai, Japan). The speed of the test was 5 mm/min, and the span was 32 mm. The number of replications for each condition was 5.

RESULTS AND DISCUSSION

The particle distribution of dried-WF after the screening process is shown in Fig. 1. The WF obtained with heat drying condition can be seen in Fig. 1(a) and the dried WF under the freeze-drying condition can be seen in Fig. 1(b). Deviation of particle size distribution of the produced WF depends on the milling conditions. The particle size distribution for the freeze-drying condition was wider than that for the heat drying condition.

At 0 to 30 min of wet milling time, there was no peak for the larger particle size near 1000 µm. However, from 40 up to 120 min, the peak intensity decreased with increasing the wet milling time. Under those conditions, the peak intensity for the freeze-drying condition was higher than that for the heat drying condition. For the particle size near 100 µm, the intensity decreased as the wet milling time increased up to 30 min. However, the intensity for a particle size near 100 µm from 40–120 min increased with increasing the wet milling time. The highest intensity of milled WF for the heat drying condition was observed at 120 min, which might be due to aggregation. In the case of the smaller particle size near 20 µm, heat and freeze-drying conditions showed the same trend. As the wet milling time increased, the intensity near 20 µm increased. Under this condition, the intensity for freeze-drying was higher than that for the heat drying condition.

The correlation coefficient (R) between the intensity at any particle size (Ip) and mechanical properties (M) are calculated as the following Equation,

$$R_{M,Ip} = \frac{\sum(M_t - \overline{M})(Ip_t - \overline{Ip})}{\sqrt{\sum(M_t - \overline{M})^2 \sum(Ip_t - \overline{Ip})^2}}$$

where $M_t, \overline{M}, Ip_t,$ and $\overline{Ip}$ are any mechanical property at wet milling time t, mean mechanical property, intensity at p µm on the particle size distribution of wet milling time t and its mean intensity, respectively. R is calculated for the intensity at any particle size versus flexural modulus. Because the particle size distribution pattern on freeze-dried and heat-dried WF were different, R for freeze-drying and heat drying were separately calculated. Note that R is the parameter to evaluate

only the 'linear' relationship between intensity and mechanical properties.

The correlation vector of flexural modulus for each WF size was observed. The results showed that the flexural modulus at a particle size smaller than 100 µm had negative correlation. Inversely, particle size from 100 – 900 µm had positive correlation for these flexural modulus. For heat dried WF, correlation vector for flexural modulus at smaller particle less than 30 µm had a negative correlation. However, particle size around 40 – 100 µm and around 200 µm showed positive and negative correlation, respectively. The highest correlation between flexural modulus was observed at a particle size 77.3 µm as a representative of the smaller size of WF. The intensity at 678.5 µm, which also indicated a higher correlation between flexural modulus, decreased with increasing wet milling time.

Figure 2 shows the relationship between the flexural modulus and the intensity of small and large particles. As shown in Fig. 2(a), an excessive percentage of small particles resulted in the decrease of flexural modulus. In the case of large particle, as shown in Fig. 2(b) the flexural modulus decreased during decreasing the intensity The lowest flexural modulus was observed under the condition of heat drying with a wet milling time of 120 min. the wet milling condition is the same for both freeze and heat drying.

Therefore, the actual amounts of smaller particles for the same milling time must be identical. It is suggested that the aggregation of smaller particles during heat drying reduces the apparent intensity for the small particles. The fact that the flexural modulus for a wet milling time of 120 min with heat drying showed a similar value as that for freeze-drying, indicating that the aggregation of smaller particles did not strongly influence the flexural modulus of WPC.

ACKNOWLEDGMENTS

The authors are grateful to the Toclas corporation for all of collaborating, supporting, and providing the materials for this research.

REFERENCES

English, B. W., and Falk, R. H. (1995) Factors that affect the application of woodfiber-plastic composites. In: Proc of Woodfiber-plastic composites: Virgin and recycled wood fiber and polymers for composites, May 1–3, 1995, Madison, WI, pp 189–194.

Friedrich, D., and Luible, A. (2016) Investigations on ageing of wood-plastic composites for outdoor applications: A meta-analysis using empiric data derived from diverse weathering trials. Constr Build Mater 124:1142-1152.

García, M., Hidalgo, J., Garmendia, I., and Jaca, J. G. (2009) Wood–plastics composites with better fire retardancy and durability performance. Composites Part A 40:1772-1776.

Gardner, D. J., Han, Y., and Wang, L. (2015) Wood–Plastic Composite Technology. Springer Int Pub 1(3):139-150.

Isa, A., Toyoda, T., Suzuki, S., Kojima, Y., Ito, H., Makise, R., and Okamoto, M. (2014) The effects of wet-milled wood flour on the mechanical properties of WF/polypropylene composites. J Wood Chem Technol 34:20-30.

JIS A5741–2016 (2016) Wood-plastic recycled composite (in Japanese). Japanese Standards Association, Tokyo, pp 1172–1191.

Najafi, A., and Eslam, H. K. (2011) Lignocellulosic filler/recycled HDPE composites: Effect of filler type on physical and flexural properties. Bioresources 6(3):2411-2424.

Rahman, K. S., Islam, M. N., Rahman, M. M., Hannan, M. O., Dungani, R., and Khalil, H. P. S. A. (2013) Flat-pressed wood plastic composites from sawdust and recycled polyethylene terephthalate (PET): physical and mechanical properties. SpringerPlus 2(629):1-7.

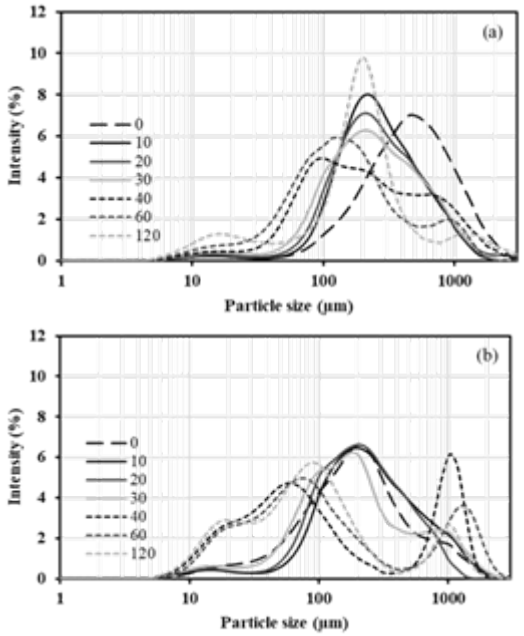

Fig. 1: The particle size distribution after the screened process for 90 to180 µm obtained by (a) heat drying condition and (b) freeze-drying condition.

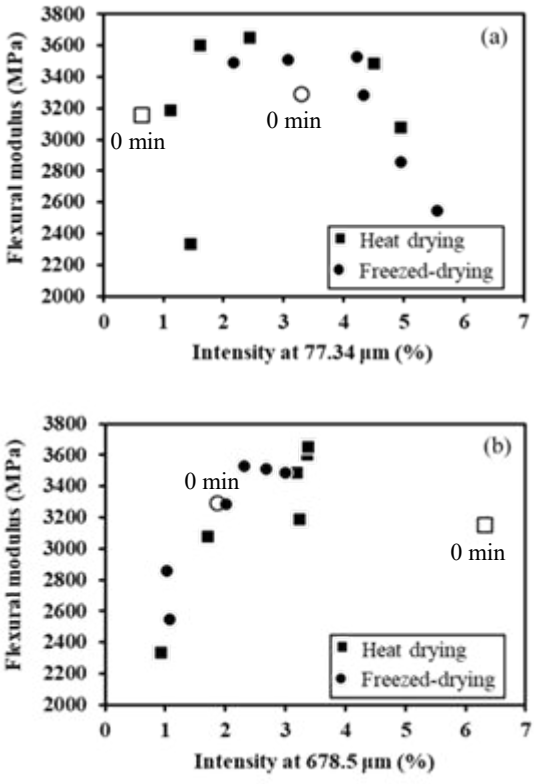

Fig. 2: The relationship between flexural modulus and intensity at (a) 77.3 µm and (b) 678.5µm.

Proceedings of International Symposium on a New Era in Food Science and Technology 2019
UGSAS-GU & BWEL Joint Poster Session on Agricultural and Basin Water Environmental Sciences 2019: P11

A novel peptide derived from rice α-globulin decreased cholesterol micellar solubility in vitro and inhibited cholesterol absorption in rats

Maihemuti Mijiti, Wang Jilite, Huang Bingyu and Satoshi Nagaoka
Gifu University, Gifu Japan

INTRODUCTION

It is well known that the appearance of coronary heart disease depends on the serum cholesterol level. To diminish the risk of such lifestyle related diseases, early prevention through chronic treatment with low-cost medicines have attracted increased attention. Numerous studies have focused on the beneficial effects of soy protein on hypercholesterolemia and cardiovascular disease. On the other hand, remarkably fewer reports have focused on the atheroprotective effects of rice protein. Rice α-globulin reduces serum cholesterol concentrations in rats fed a hypercholesterolemic diet by promoting excretion of fecal neutral sterols (1). This experiment was designed to identify the peptides which have bile acid-binding activity and inhibit the cholesterol absorption from rice α-globulin.

MATERIALS AND METHODS

Peptide array— In this study, we used a peptide array to evaluate the bile acid-binding activity of peptide derived from rice α-globulin. A peptide array was constructed using previously reported methods (2, 3). In the peptide array, bile acid-binding ability was evaluated by the binding ability of taurocholic acid and fixed peptides on cellulose membrane, then binding peptides with taurocholic acid were detected by immunoassay.

Bile acid binding— The abilities of selected peptides, SPH (soybean protein peptic hydrolysate), CTH (casein tryptic hydrolysate), and cholestyramine (Sigma, St. Louis, USA) to bind with taurocholate were measured by a method described previously. (13) Mixtures containing 1.85 kBq of tauro[carbonyl-^{14}C] cholic acid (sodium salt) (Amersham International, Buckinghamshire, UK), 0.1 mol/l sodium taurocholate in 2ml of 0.1 mol/l Tris-HCl buffer (pH 7.4), and binding substance (selected peptides, SPH, CTH or cholestyramine, 5 mg/ml) were incubated at 37℃ for 2 h, and the radioactivity in the supernatant (15.000×g for 15 min) was measured by liquid scintillation counting.

Micellar solubility— The micellar solubility of cholesterol with the selected peptides, SPH, CTH, and cholestyramine in vitro was measured by previously described method. (13) [^{14}C]-labeled micellar solutions (1.0 ml) were prepared at the following concentrations, and were mixed by sonication: 0.74 kBq [4-^{14}C]-cholesterol (2.1 Gbq/mmol, NEN, Boston, MA), 0.1 mmol/l cholesterol (Sigma), 6.6 mmol/l sodium taurocholate (Sigma), 1 mmol/l oleic acid (Sigma), 0.6 mmol/l phosphatidylcholine (Sigma), 0.5 mmol/l monoolein (Sigma), and 15 mmol/l sodium phosphate (pH 7.4). After incubation at 37 ℃ for 24 h, selected peptides, SPH, CTH, or cholestyramine (5 mg/ml) was added to the micellar solution, dispersed by sonication, incubated at 37 ℃ for 1 h, and centrifuged at 100.000×g for 60 min at 37 ℃. The supernatant was collected for determination of [^{14}C]-cholesterol by a liquid scintillation counter.

Intestinal cholesterol absorption in rats. Selected candidate peptide (MRFRDR) were synthesized with purity greater than 95% and remaining trifluoroacetic acid was removed. 7-week-old Wistar male rats (Japan SLC, Hamamatsu, Japan) were deprived of food for 48 h, without restriction of their access to water. Next, the rats received the test solutions by intragastric intubation with a polyethylene catheter. One hour later. Blood was collected by cardiac puncture for separation of the serum, and the liver and intestines were quickly excised. The test solutions were MRFRDR, or control. The [^{3}H]-cholesterol incorporated into the serum, liver, and intestine was extracted with hexane.

RESULTS

Analysis of the 6-mer peptides derived from s rice α-globulin with bile acids binding affinity by using the peptide array— To find the peptide derived from rice α-globulin with bile acid binding capacity, we constructed 6-mer peptides, the array consisting of 181 sequences plus positive control sequence (VAWWMY) plus negative control sequence (GGGGGG). Using the peptide array, 15 spots (quintuplicate x3 arrays) were evaluated for each unique sequence. So, there are some peptides with higher bile acid binding activity than positive control peptide (VAWWMY) **(Fig.1)**.

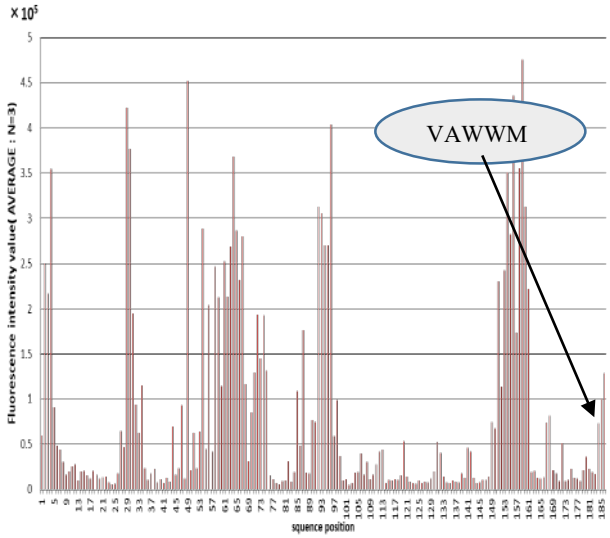

Fig.1 Fluorescent intensity of taurocholic acid binding to overlapping peptides 6 residues in length, covering globulin. The sequence is in descending hydrophobicity order from left to right. The sequence VAWWMY described in the figure is the positive control, GGGGGG is the negative control.

Bile acid binding capacity— MRFRDR had a significantly greater ability to bind bile acid than CTH in vitro. Among the five candidates, the binding capacity of MRFRDR was greater than the other peptides.

Micellar solubility— The micellar solubility of cholesterol was significantly lower in the presence of MRFRDR, of SPH, and of cholestyramine than in the presence of CTH.

Cholesterol absorption in vivo— Incorporation of [^{3}H]-cholesterol into the serum, liver, and intestines was significantly lower in the MRFRDR than in the control group (**Fig.2**).

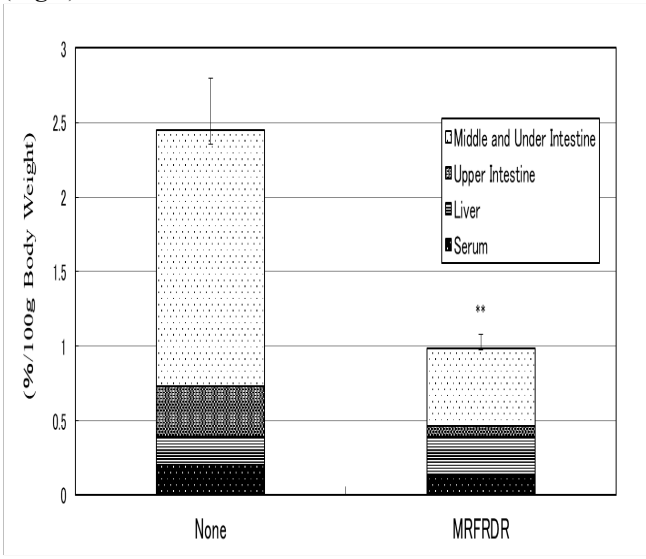

Fig.2 Effect of MRFRDR on the distribution of ^{3}H-cholesterol in serum, liver and intestine.
Statistical significance compared to control by Student's t-test (**: P<0.01)

DISCUSSION

Rice protein consumption with modulation of plasma cholesterol level has been demonstrated in some studies (5). And also rice α-globulin reduces serum cholesterol concentrations in rats fed a hypercholesterolemic diet by promoting excretion of fecal neutral sterols (1). The bile acid binding 6-mer peptide VAWWMY (Val-Ala-Trp-Trp-Met-Tyr) was previously reported as the soystatin obtained from the soybean glycinin (11S globulin) A1aB1b subunit of soybean protein (6, 7). In this study, we screened the peptide library covering all possible those peptide. As a result, we succeeded in finding novel peptides with high bile acid binding capacity. Unfortunately, all candidates' peptides didn't showed good results in the bile acid binding capacity and micellar solubility *in vitro*. But some of them showed good results, like MRFRDR showed higher bile acid binding ability and disruption of bile acid micelles so peptide can lower micellar solubility of cholesterol. The lowering of micellar solubility of cholesterol in small intestine is known as one of the effective strategies to inhibit cholesterol absorption. Cholesterol forms micelles with fatty acids, 2-monoglycerides and bile acids. The mixed micelle cholesterol passes through the unstirred water layer (UWL) to reach the small intestinal epithelium. Mixed micelles are integral to the process of passing cholesterol UWL. It was thought that MRFRDR could inhibit the passage of UWL and reduce cholesterol absorption in the small intestine by reducing cholesterol micelle solubility. Therefore, MRFRDR is considered to have the potential to exhibit cholesterol absorption inhibitory effect even in in vivo tests using animals. For that reason we examined the effects of MRFRDR on cholesterol absorption in rats (*in vivo*) using ^{3}H-cholesterol. The result indicated, MRFRDR significantly suppresses cholesterol absorption in the blood, upper small intestine and all over the small intestine compared with the control group containing no peptide in the administration solution, and significantly suppresses the total cholesterol absorption as well (**Fig.2**) .

In conclusion, starting from the peptide array screening, we were successful in finding novel bile acid binding peptides (MRFRDR) that interact with bile acid in soluble-form and strongly lower to micellar solubility of cholesterol. And the peptide (MRFRDR) significantly inhibited cholesterol absorption in rats. Our results are consistent with Iwami et al. (8) where they report successful inhibition of bile acid re-absorption in the ileum with bile acid binding peptides.We would also like to note that this is the first report of peptide array screening technology applied to the optimization of bile acid binding peptides. We believe these findings could contribute to the future investigation and design of therapeutic peptides and functional food constituents for the early prevention of life style related diseases.

REFERENCES

1. Tong, LT., Fujimoto, Y., Shimizu, N., Tsukino, M., Akasaka, T., Kato, Y., Iwamoto, W., Shiratake S., Imaizumi, K., Sato, M. (2012) Rice α-globulin decreases serum cholesterol concentrations in rats fed a hypercholesterolemic diet and ameliorates atherosclerotic lesions in apolipoprotein E-deficient mice. Food Chem., 132: 194–200.
2. Kato, R., Noguchi, H., Honda, H., and Kobayashi, T. Hidden markov model-based approach as the first screening of binding peptides that interact with MHC class II molecules. (2003) Enzyme Microb. Technol., 33: 472-481
3. Kato, R., Kaga, C., Kunimatsu, M., Kobayashi, T., and Honda, H. Peptide array-based interaction assay of solid-bound peptides and anchorage-dependant cells and its effectiveness in cell-adhesive peptide design. (2006) J. Biosci. Bioeng., 101: 485-495.1.
4. Nagaoka, S., Miwa, K., Eto, M., Kuzuya, Y., Hori, G., and Yamamoto, K., Soy Protein Peptic Hydrolysate with Bound Phospholipids Decreases Micellar Solubility and Cholesterol Absorption in Rats and Caco-2 Cells. J. Nutr., 129, 1725–1730 (1999).
5. Morita, T., Oh-hashi, A., Kasaoka, S., Ikai, M., Kiriyama, S. (1996) Rice protein isolates produced by the two different methods lower serum cholesterol concentration in rats compared with casein. J. Sci. Food Agric., 71:415–424.
6. Choi, S. K., Adachi, M., and Utsumi, S., Identification of the Bile Acid-binding Region in the Soy Glycinin A1aB1b Subunit. (2002) Biosci. Biotechnol. Biochem., 66: 2395-2401
7. Nagaoka, S., Nakamura, A., Shibata, H., Kanamaru, Y., Soystatin (VAWWMY), a Novel Bile Acid-Binding Peptide, Decreased Micellar Solubility and Inhibited Cholesterol Absorption in Rats (2010) Biosci. Biotech. Biochem., 74: 1738-1741.
8. Iwami, K., Kitagawa, M., and Ibuki, F., Effect of dietary proteins and/or their digestive products on intestinal taurocholate absorption. (1990) J. Nurt. Sci. Vitaminol. 36, S141-S14

Proceedings of International Symposium on a New Era in Food Science and Technology 2019
UGSAS-GU & BWEL Joint Poster Session on Agricultural and Basin Water Environmental Sciences 2019: P12

The effect of frozen storage on textural quality of cooked pasta

Rachmad Adi Riyanto and Takahisa Nishizu
The United Graduated School of Agricultural Science, Gifu University, Japan

INTRODUCTION

Pasta is popular worldwide and considered as a staple food of many nations. It is a simple product, traditionally, the primary ingredient of pasta is wheat semolina, where durum wheat semolina and water are mixed and kneaded to obtain a dough that is then shaped and, most commonly, dried (Carini, Curti, Minucciani, Antoniazzi, & Vittadini, 2014). Dry pasta is consumed mainly around the world because of its secure storage and cooking, long shelf-life and versatility when combined with other ingredients to yield a variety of final products (Hager, Zannini, & Arendt, 2012; Lucisano, Cappa, Fongaro, & Mariotti, 2012; Marti & Pagani, 2013). However, nowadays, consumers pay more and more attention to ready-to-eat convenience and healthy food (Diez et al., 2009). Therefore, frozen cooked pasta offer a feasible alternative.

Olivera and Salvadori (2009) investigated the influence of freezing on the quality of cooked organic pasta and found that fast-frozen pasta quality was closer to the fresh pasta than the slow frozen one. However, quite a few literature are available concerning the detailed evaluation of products by different precooking methods. The effects of freezing and storage life of frozen foods have been studied for several years (Fellows, 1997). Recently starch-based food products have been analyzed during freezing and frozen conditions (Giannou, Kessoglou, & Tzia, 2003; Gormley, Walshe, Hussey, & Butler, 2002; Ribotta, Leon, &An˘on, 2001), but there are few pieces of information about the relationship between the quality of cooked and frozen pasta as in ‘‘ready-to-eat’’ meals (Kobs, 2000).

One of the critical parameters to assess cooked pasta quality, concerning consumer acceptability, is textural properties (Carini, Vittadini, Curti, & Antoniazzi, 2009). The texture is a parameter that could imitate the sensory as of the critical quality attributes that determine consumer acceptance of the product (Luo et al. 2015; Ajila et al. 2010; Olivera and Salvadori, 2009). The texture of foods is mostly determined by the moisture and fat contents and the types and amounts of structural carbohydrates (cellulose, starch, and pectic materials) and proteins that are present. Changes in texture are caused by loss of moisture, fats, formation or breakdown of emulsions and gels, hydrolysis of polymeric carbohydrates, and coagulation or hydrolysis of proteins (Fellows, 1997). The retention of texture similar to that of the fresh product is an essential criterion for acceptance of a frozen convenience pasta by the consumer (Hatcher, 2004). The quality of the frozen cooked pasta was evaluated via texture profile analysis (TPA).

The effect of frozen storage on the textural quality of cooked pasta has not been fully investigated, especially for long-term storage. Therefore, the aims of this study were to determine the texture properties of cooked pasta during frozen storage for 6 weeks and observe microstructure changes by SEM.

MATERIALS AND METHODS

The commercial dried pasta “Ma Ma” with diameter size 1.6mm from Nisshin Foods Inc was used as the sample. The dried pasta was cut into 11cm length and boiled in the water bath with polypropylene reaction tube size 15ml at 100ºC for 7 minutes. After boiling, pasta was drained and wiped using tissue paper to reduce the water on the surface for 1 minute, and then kept on the freezer at -20ºC before being analyzed.

Moisture analysis Frozen cooked pasta was kept outside the freezer for 10 minutes before moisture analysis. Samples were dried in the oven at 121ºC for 72 hours. The moisture content was determined using the oven-drying method.

Texture analysis Frozen cooked pasta was kept outside the freezer for 10 minutes before texture analysis. Texture properties were measured by a TA-XT2i Texture Analyzer (Stable Micro Systems, London, England). The texture analyzer was equipped with a light knife blade (A-LKB) probe and the measurements were carried out at room temperature using a 5 kg compression cell. A sample of pasta was placed onto the measurement plate of the texture analyzer. The measurement assay parameters were: pretest speed: 1.0 mm/s; test speed: 1.0 mm/s; posttest speed: 1.0 mm/s. The strain was 100%, so the sample was cut completely.

Scanning electron microscopy (SEM) The section profile of frozen cooked noodles with different frozen storage were analyzed using SEM (S-4300, Japan Electron Optics Laboratory CO., Ltd., Tokyo, Japan). Firstly, the frozen cooked pasta were soaked in glutaraldehyde with a solution of 2.5% (w/w) for 90 minutes for chemical fixation. Then rinsed with distilled water. After that, the samples were immersed in Osmium 50% for 60 minutes then rinse with distilled water and continue eluted in graded ethanol series (30%, 50%, 60%, 70%, 80%, 90%, 95%, and 100%) for 15 min at each gradation. After that, remove the ethanol and immerse the sample on the t-butyl alcohol for 15 minutes. The pasta was freeze-dried afterward and the dehydrated samples were coated with osmium gas for 15 seconds. The images of pasta were observed at 60 times and 250 times respectively at an accelerating voltage of 5.0 kV.

Statistical analysis All the determinations and analysis were performed in triplicate at least. One-way ANOVA (analysis of variance) and Duncan’s test were conducted by using the software SPSS 16.0 for windows (SPSS Inc., Chicago, IL, USA). Significance was defined at $P < 0.05$.

RESULTS

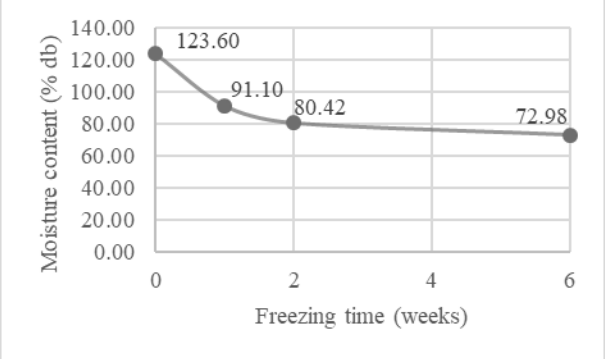

Fig. 1: Moisture content (% db) of cooked pasta after freezing

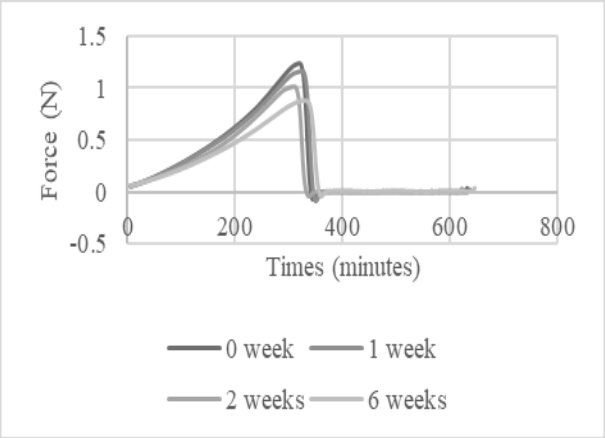

Fig. 2: Textural properties of cooked pasta after freezing

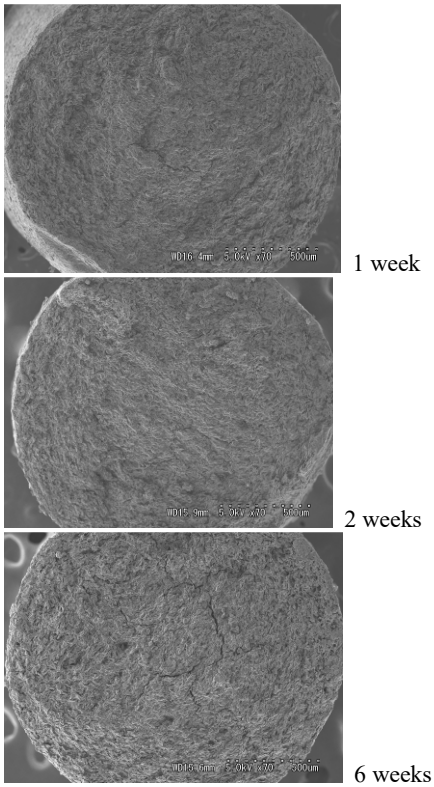

Fig. 3: Scanning electron microscope images of cooked pasta after freezing

DISCUSSION

Water, playing as an active substance, is regarded as a critical role in the quality of food, especially for frozen food. As frozen cooked pasta possess a high water content of over 60%, and most of the water can transform into ice crystals (Carini et al., 2010). In this study, the moisture content was analyzed using the oven-drying method, as presented in Fig. 1. The results showed that the moisture content decrease during frozen storage. This is because the water was transformed into ice crystals, and during the frozen storage, the ice crystal could be sublimated into the gas as known as freezer burn phenomena. These phenomena affect the textural properties of frozen cooked pasta.

The texture characteristics of frozen cooked pasta play an essential role in quality, which determines the acceptance of consumers on the product (Olivera & Salvadori, 2009). In this study, textural profile analysis (TPA) was used to evaluate the quality of cooked pasta. The textural parameters of cooked pasta during frozen storage were measured and summarized in Fig. 2. The results showed that during the frozen storage the texture of cooked pasta gradually decreased, the lowest force was at the 6 weeks of freezing storage.

To have tangible evidence of microstructure changes of frozen cooked pasta during the frozen storage visually, the scanning electron microscopy (SEM) was employed. The cross-section of frozen cooked pasta with different storage time were exhibited in Fig. 3. The cross-section of frozen cooked pasta stored after 1 week presented a smooth and continuous status. However, clear differences can be noticed after 6 weeks, when the surface became rougher along with large pores, which may be related to the ice crystals formation.

ACKNOWLEDGMENTS

I would like to thank the MEXT scholarship for sponsoring my study and thank Food Processing and Chemistry Laboratory at the University of Gifu for the use of equipment and in particular Prof. Takahisa Nishizu for his guidance on this project.

REFERENCES

Carini, E., Vittadini, E., Curti, E., & Antoniazzi, F. (2009). Effects of different shaping modes on physico-chemical properties and water status of fresh pasta. Journal of Food Engineering, 93, 400–406.

Carini, E., Curti, E., Minucciani, M., Antoniazzi, F., & Vittadini, E. (2014). Pasta. In R. D. P. F. Guine, & P. M. dos Reis Correia (Eds.). Engineering aspects of cereal and cerealbased products (pp. 211–238). Boca Raton: CRC Press.

Fellows, P. (1997).Food processing technology—principles and practice.London: Woodhead Publishing Ltd.

Hatcher, D. W. (2004). Influence of frozen noodle processing on cooked noodle texture. Journal of Texture Studies, 35(4), 429–444.

Hager, A. S., Zannini, E., & Arendt, E.,K. (2012). Gluten-free pasta: Advances in research and commercialization. Cereal Foods World, 57, 225–229.

Luo, L. J., Guo, X. N., & Zhu, K. X. (2015). Effect of steaming on the quality characteristics of frozen cooked noodles. LWT – Food Science and Technology, 62(2), 1134–1140.

Olivera, D. F., & Salvadori, V. O. (2009). Effect of freezing rate in textural and rheological characteristics of frozen cooked organic pasta. Journal of Food Engineering, 90(2), 271–276.

Proceedings of International Symposium on a New Era in Food Science and Technology 2019
UGSAS-GU & BWEL Joint Poster Session on Agricultural and Basin Water Environmental Sciences 2019: P13

Effect of forest age on slope stability evaluated by a distributed landslide model

Vany Fadhilah[1], Al Nuriza Rahmadania[1] and Fumitoshi Imaizumi[2]
1. **Graduate School of Integrated Science and Technology, Shizuoka University, Japan**
2. **Faculty of Agriculture, Shizuoka University, Japan**

INTRODUCTION

Since ancient times, people have suffered numerous landslide disaster. Landslide can be simply described as the movement of a mass of rock, earth or debris down a slope. Landslides, specifically in Japan, generally occur along gently to moderately sloping ground which is also important as these areas include residential and agricultural use. Additionally, landslide also frequently occurred after clearcutting forest on steep area (Imaizumi, 2008). Because of these conditions, landslide disaster is harmful for human. Therefore, the study of landslide phenomenon is necessary to protect the slopes from future land sliding and failures.

In preventing landslide, the stability of slope is an important issue to be concerned. There are some natural factors that responsible for slope stability, those are geomorphic factors, soil properties, hydrology, vegetation and seismicity (Sidle et al. 1985). However, vegetation has been widely recognized that it plays an important role in increasing slope stability. through root (Stokes et al. 2008; Kreng et al. 2015).

Previous studies have tried to evaluate contribution of vegetation on the slope stability by interpreting spatial distribution of underground roots and physical test of individual root. However, such studies cannot evaluate contribution of vegetation on the slope stability in hillslope-scale, because of difficulty in interpretation of root network in wide areas.

The overall aim of this study is to evaluate effect of forest age on slope stability. The specific objectives of this study are (i) to interpret temporal changes in landslide ratio and (ii) to evaluate temporal changes in root cohesion after harvesting, through GIS analysis and back calculation of a physical parameter using a distributed landslide model.

STUDY SITE

The study area is about 17.6km^2 located in the Ikawa University Forest catchment, southern side of the Southern Japanese Alps, central Japan (Fig.1). Geologically, characteristic of the study area is sedimentary rocks with alternate strata of sandstone and shale of the late Cretaceous period (Maita, 2001). The range of topography is from 900 m a.s.1 in the south to the 2406 m a.s.1 peak of Mt. Aonagi in the northwest, leads to gradient of 35-40o comprising about 50% of the entire catchment. The study area is hilly covered by brown forest soil and podzol. Also, it has high average annual precipitation calculated approximately 2800 mm from 1993 to 2002. The most abundant rainfall events mainly occur from the early summer in June through the typhoon season in August to early October. In this study area, forest practice such as forest harvesting specifically clear-cutting is frequently occurred in artificial forest which cover 17% of area, while the rest area is natural forest. This artificial forest is comprised by Cryptomeria japonica (Japanese cedar, sugi), Chamaecyparis obtusa (Japanese cyprus, hinoki) and Larix kaempferi (karamatsu). A significant proportion of the trees in the secondary growth forest was harvested in the 1950s and 1960s. After clear-cutting, branches and leaves of harvested trees were left on the ground to protect the slopes from surface erosion. These harvesting operations conducted in the Ikawa University Forest are common in Japanese forestry (Tsukamoto 1987; Imaizumi et al. 2017).

METHODOLOGY

1. Aerial Photograph Interpretation

Assessing the location and area of landslide in the Ikawa University Area was obtained by using monochrome aerial photographs for two different years (1980 and 1984). New occurrences of landslide were identified by comparing those successive aerial photographs. In this study, landslides were identified as all mass movement from hillslopes to channels, while other mass movements move down channels were excluded. Landslide area ratio was calculated through dividing landslide area that occurred in every forest age by forest area in every forest age.

2. Back Calculation of Root Cohesion

The model framework of slope stability used for this study is a distributed landslide model. This model proposed by Okimura et al. (1985) which are consisted of groundwater level calculation and infinite slope analysis. Groundwater level is calculated using Darcy's law (Shuin et al. 2014). Darcy's law possibly calculates groundwater flow through aquifer to the cross-sectional area perpendicular. While infinite slope analysis is calculated as used by Shuin et al. (2014) which defines that a safety factor of 1.0 as unstable slope. In this study, we used cohesion, which is a parameter representing root and soil strength, as varied parameter when calculating the safety factor. Therefore, slope stability generated by various root cohesion would be obtained, and by back-calculation derived value for root cohesion of real landslide occurrences in every forest age class (O'Loughlin CL, 1974).

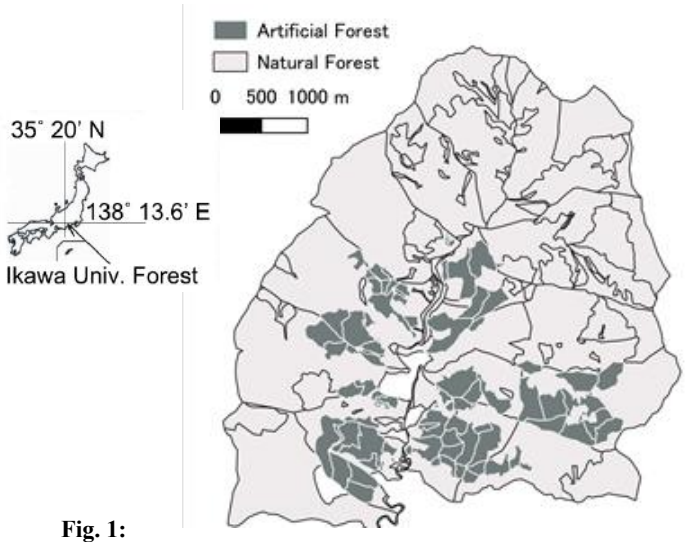

Fig. 1:
Location and forest type of the Ikawa University Forest

RESULT AND DISCUSSION

1. Temporal changes in landslide ratio after harvesting

New landslide occurrences were identified in the study area specifically in artificial forest on series of aerial photographs taken from 1980-1984 with total 29 new landslides. A total of 29 landslides occurred in the various forest age. Relationship between landslide ratio and forest age as shown in the Fig. 2 shows that the immediate effect of landslide occurrence in forest age less than 10 years after harvesting was the largest. However, the effect significantly decreased in the forest age more than 10 years. It was probably caused by root decay of harvested trees that existed in the area. Roots begin to decay a few years after cutting, with the most strength disappearing within 10 years. Consequently, root decay in 1–10 years old forests accelerates the occurrence of landslides (Tsukamoto, 1987). It is in accordance with prior study in Sanko catchment Japan (Imaizumi et al. 2008) that forest stands age 1 to 10 years after harvesting impact greatly on landslide occurrence. In addition, Fig. 2 also shows that no landslide occurrence founded in the forest age more than 15 years old. This shows that the stability of the slope in this area almost entirely recovers within 15 years.

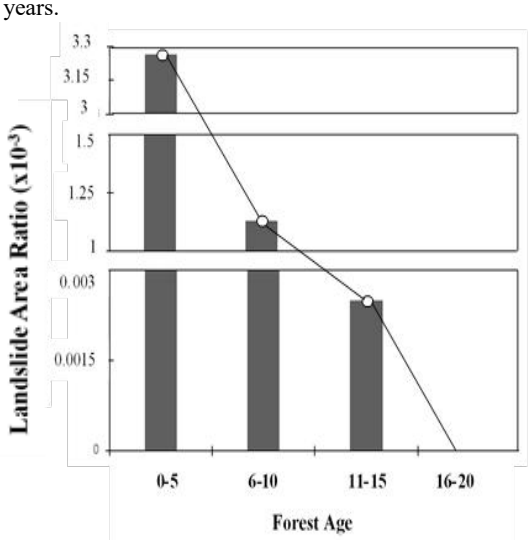

Fig. 2: Landslide area ratio obtained by aerial photograph interpretation

2.Temporal changes in root cohesion after harvesting

Relationship between root cohesion and estimated landslide area shows that estimated landslide area decreased with increased cohesion. It is in accordance with prior study that increasing effective soil cohesion will decrease potential of landslide area (Shuin, 2014).

To clarify how gradual increased root cohesion on forest age which impact on real landslide occurrence, back calculated of root cohesion was conducted as shown as Fig. 3. It shows that root cohesion gradually increased with increasing age of forest. However, the result of this study also shows that root cohesion for artificial forest age 5 years and 10 years after harvesting was not very distinct. It is in accordance with prior study (Imaizumi et al, 2008) that root re-growth and total root strength were not so evolved yet in the early 10 years. While, root cohesion significantly increased when forest age more than 10 years and slowly increased when forest age more than 16 years after harvesting. It is probably the effect of the dynamic root strength values in Imaizumi et al. (2008) that regrowth of newly planted was described by a sigmoid relationship. Therefore, the root strength will so weak in the early, significant in the middle time and being stagnant when

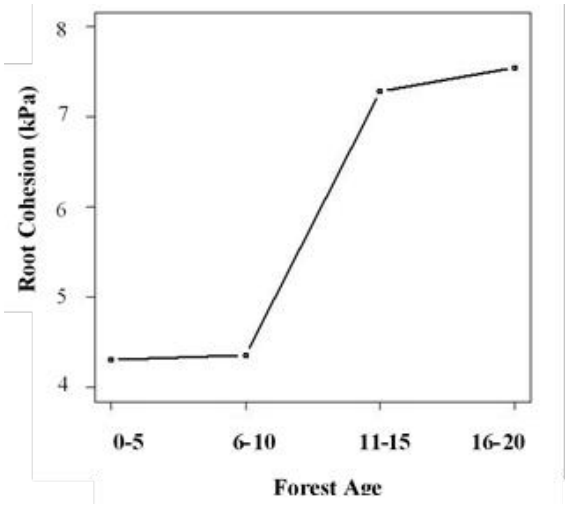

Fig 3: Root cohesion of obtained by back calculation

reaching certain time. This study could adequately predict root cohesion calculated by landslide model without field measurements which are time consuming and regional coverage is difficult to obtain. This result of this study could contribute to help predict and mitigate landslide disaster specifically around the artificial forest industry on steep terrain. Furthermore, it could also be used as consideration in establishing forest management.

ACKNOWLEDGMENTS

This study was supported by the Ministry of Education, Culture, Sports, Science and Technology, Japan.

REFERENCES

Imaizumi, F., Sidle, R.C. and Kamei, R., 2008. Effects of forest harvesting on the occurrence of landslides and debris flows in steep terrain of central Japan. Earth Surface Processes and Landforms: The Journal of the British Geomorphological Research Group, 33(6), pp.827-840.

Imaizumi, F., Suzuki, O. and Togari‐Ohta, A., 2017. Seasonal changes in the sediment flux on steep hillslopes in a humid diurnal frost environment. Earth Surface Processes and Landforms, 42(3), pp.389-398.

Kreng Hav Eaba, Suched Likitlersuangc,n, Akihiro Takahashi. 2015. Laboratory and modelling investigation of root-reinforced system for slope stabilization. Soils and Foundations 2015;55(5):1270–1281

Maita H, Shizuoka River Work Office. 2001. Ohi River. Source-to-sink sedimentary cascades in Pacific Rim Geo-systems. 36-43

O'Loughlin CL (1974) The effects of timber removal on the stability of forest soils. J Hydrol NZ 13:121–134

Shuin, Y., Otsuka, I., Matsue, K., Aruga, K., Tasaka, T. And Hotta, N., 2014. Estimation of Shallow Landslides Caused by Heavy Rainfall Using Two Conceptual Models. International Journal of Erosion Control Engineering, 7(3), pp.92-100.

Sidle, R.C., Pearce, A.J. and O'Loughlin, C.L., 1985. Hillslope stability and land use. American Geophysical Union.

Stokes, A., Norris, J.E., Van Beek, L.P.H., Bogaard, T., Cammeraat, E., Mickovski, S.B., Jenner, A., Di Iorio, A. and Fourcaud, T., 2008. How vegetation reinforces soil on slopes. In Slope stability and erosion control: ecotechnological solutions (pp. 65-118). Springer, Dordrecht.

Tsukamoto Y. 1987. Evaluation of the effect of tree roots on slope stability. Bulletin of the Experiment Forests, Tokyo (In Japanese with English abstract).

Proceedings of International Symposium on a New Era in Food Science and Technology 2019
UGSAS-GU & BWEL Joint Poster Session on Agricultural and Basin Water Environmental Sciences 2019: P14

Evaluation and characterization of carotenoids and β-carotene in rice landraces from Northeast India

Devendra Kumar Maravi[1], Muthuvel Jothi[1], Gundimeda Jwala Narasimha Rao[1,2], Lingaraj Sahoo[1]

1. **Department of Biosciences and Bioengineering, Indian Institute of Technology Guwahati, Guwahati, Assam, 781039, India**
2. **Crop Improvement Division, ICAR-National Rice Research Institute, Cuttack, Odisha, 753006, India**

INTRODUCTION

Carotenoids are one of the most diverse classed of natural compounds. Plant carotenoids are composed of C40 isoprenoids skeleton with or without epoxy, hydroxyl and keto groups. Carotene, such as α- and β- carotene and lycopene are hydrocarbons, whereas xanthophyll are oxygenated derivatives of carotenes and includes the compounds β-cryptoxanthin, lutein and zeaxanthin (Giuliano et al. 2008; Stanley and Yuan, 2017). They have fundamental roles in human nutrition as antioxidant and precursor of vitamin A and their consumption is associated with protection from a range of diseases. Vitamin A deficiency is one of the leading causes of micronutrient malnutrition in developing countries. Carotenoids carrying list on unsubstituted beta-ionone ring, such as alpha and beta-carotene, are nutritional vitamin A precursor. This is prompted as series of efforts to evaluate and breed high provitamin-A levels into staple crops.

Biosynthesis of carotenoids in plants take place within the plastids, chloroplast of photosynthetic tissues and chromoplast of fruits and flowers. Chlorophyll, tocopherols, plastoquinone, gibberellins and carotenoids all share a common biosynthetic precursor geranyl geranyl-diphosphate (GGPP) which is derived from plastid isoprenoid metabolism. It has been established that four enzymes in plant mainly involves in β-carotene biosynthesis (Jourdan et al. 204). Phytoene synthase, phytoene desaturase, ζ-carotene desaturase and lycopene cyclase catalyzes the β-carotene synthesis from GGPP (**Fig. 1**). The first step in carotenoid biosynthesis is the condensation of two molecules of GGPP to produce phytoene by the enzyme phytoene synthase (PSY). PSY is firmly associated with the chromoplast membrane in its active form (Yao et al. 2018). The cyclization of lycopene by two different lycopene cyclases specific for ⟨- and ∑-ionone end-groups of LCY marks a branching point in the pathway where one branch leads to β-carotene and its oxygenated derivative lutein, while the other forms ®-carotene and the derived xanthophylls, such as zeaxanthin, antheraxanthin, violaxanthin and neoxanthin.

Carotenoids are very minor constituents in cereal grains. Besides their nutritional and health benefits, they are responsible for the attractive yellow to pale yellow colors of durum wheat (Roncallo et al. 2012). Rice grains are known to devoid of carotenoids in their endosperms. Rice, an important staple crop, is produced around the world and consumed by half of the world's population. Asian countries are much more dependent on rice for food energy and protein intake than other countries. Evaluation and characterization of important carotenoids from rice landraces is necessary. North-East (NE) India, the probable origin of rice has diverse genetic resources. Many rice landraces of NE India were not yet characterized for sourcing of pro-vitamin.

We explored the possibility of finding β-carotene in grains of rice landraces of Northeast India in order to use in conventional plant breeding or biofortification programs, aiming to increase the total carotenoids and β-carotene contents. We determined the total carotenoid and β-carotene in rice landrace samples. Our results found β-carotene in few rice landraces of Northeast India.

MATERIALS AND METHODS

Chemicals: HPLC grade methanol, tetrahydrofuran, acetonitrile, water were purchased from Merck (Germany). The β-carotene standard were purchased from Sigma (USA).

Carotenoid extraction and HPLC analysis: Indigenous rice cultivar were collected from Northeast Region of India (Assam). Rice were de-howled manually and milled using mortar pestle in liquid nitrogen. The carotenoids were extracted from 500 mg of seed powder with acetone (2 ml the first time and 1 ml the second time). Half the proportion of petroleum ether was added to combined extract. The phase extraction was performed by adding the water, upper clear phase eluted and evaporated under vacuum.

Spectrophotometer absorbance was measured at 470 nm. The total carotenoid (µg/g) was calculated based on the spectrophotometer reading, taking the extinction coefficient (2592) in petroleum ether.

The petroleum ether is evaporated in vacuum and extract were re-dissolved in chloroform and 20µl were used for HPLC analysis (Perkin Almer). For HPLC, C18 reverse-phase column were used with following solvent system: solvent A= acetonitrile (ACN): Tetrahydrofuran (THF): water (H2O), 10:4:6; solvent B= ACN: THF: H2O, 10:8.8:1.2 with a linear gradient of 100% A for first 3 min and slowly to 100% B for 10min, with the total run time of 25min.

Nuclear Magnetic Resonance - the rice carotenoids samples were analyzed on Bruker AVANCE III 600 MHz NMR instrument using 1D -1H and 13C spectroscopy in $CDCL_3$. Fatty acid compositional analysis from rice endosperm were also analyzed based on the NMR spectra.

RESULTS

Quantification of total carotenoids and β-carotene: Rice endosperm from individual landraces were analyzed quantitatively by spectrophotometry and qualitatively for β-carotene by high performance liquid chromatography (HPLC). Estimation of carotenoids from rice seeds showed total carotenoids level ranging from 2.24- 6.79 µg/g (Table 1). The rice variety B and SS showed lower carotenoid content in endosperm while GS showed high content of carotenoids (Table). The HPLC revealed the β-carotene content in difference rice varieties collected from northeast India. Among all rice varieties MS and BA showed lower quantity, 1.325, 2.713 µg/g respectively (Table 2) and in SS has high content of β-carotene (4.221 µg/g).

Table 1 Total carotenoid content in rice endosperm.

Rice Variety	λ450	Concentration (µg/g)
GS	0.088	6.790
B	0.031	2.392
BS	0.064	4.938
MZ	0.075	5.695
SS	0.064	2.237
NB	0.088	6.685

Table 2 β-carotene content in rice endosperm

Varieties	**RT**	Peak Area	**Conc. (µg/g)**
GS	18.705	9.696	3.992
B	18.628	6.589	2.7127
BS	18.601	23.800	9.8007
MZ	18.688	3.219	1.3255
SS	18.443	10.252	4.2206
NB	-	-	-

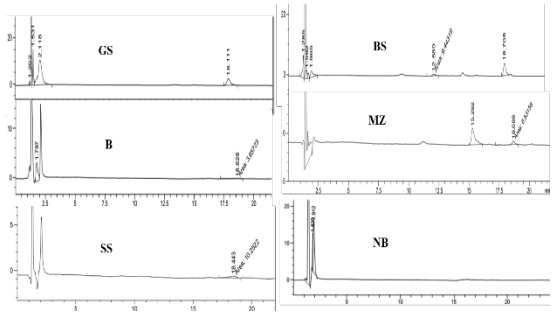

Fig.1 HPLC chromatogram showing the β-carotene peaks in the carotenoid extracts from rice varieties in of Northeast India.

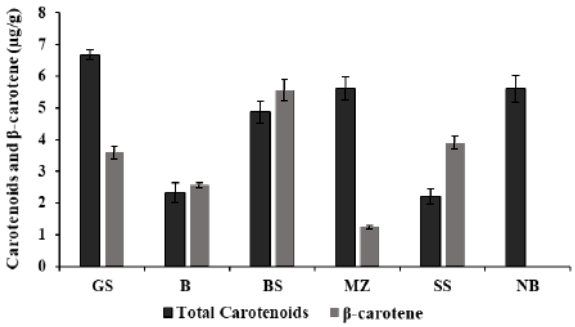

Fig. 2 Comparison of total carotenoids and β-carotene content in rice verities

Table.3 Fatty acid profiling in rice varieties

	Linoleneic acid	Linoleic acid	Oleic acid	Stearic acid
GS	2.0	24.57	**48.52**	24.91
B	2.11	26.18	47.92	23.28
BS	4.78	24.1	**46.02**	25.88
MZ	2.12	31.97	39.026	26.18
SS	1.75	29.8	44.61	23.84
NB	3.4	28.5	44.35	24.72

1H NMR spectroscopy- Fatty acid composition were measured with peak integration. GS and BS showed higher oleic acid 48.52, 46.02% respectively (**Table 3**). The ^{1}H NMR spectra of the six rice variety revealed characteristics features of carotenoid spectra. The spectra of all samples revealed a number of resonances in the region o 6.0-7.0 ppm, which represent different olefinic proton along the conjugated chains (**Fig. 3**). ^{1}H NMR spectra confirm the presence of β-carotene in all rice varieties however signal intensities are significantly low.

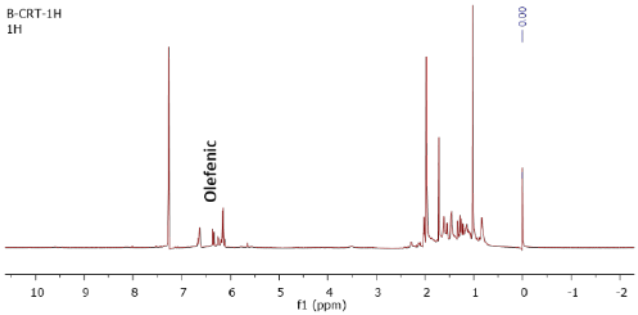

Fig. 3 Representative 1H NMR spectra of β-carotene standard.

DISCUSSION

Carotenoids are one of the most diverse natural compounds. Carotenoids are very minor constituents in cereal grains. Carotenoids are not reported in rice endosperm yet. Several genetic engineering approaches has been reported in rice and other crop to enhance the β-carotene content in rice grains. In present study, we observed carotenoids and β-carotene in rice landrace endosperms. The BS and GS rice variety showed higher β-carotene content as well carotenoids. Breeding of these rice landraces with high yielding rice variety can augment biofortification programs. Further metabolomics approaches will be done to reveal the metabolomics pathway involves in β-carotene biosynthesis.

ACKNOWLEDGMENTS

We acknowledge the Department of Biotechnology (DBT), New Delhi, India for Program Support Project funds for carrying out the research work. GJN Rao thank DBT-NERBPMC for funding Visiting Research Professor at IIT Guwahati.

REFERENCES

Giuliano, G., Tavazza, R., Diretto, G., Beyer, P., Taylor, M.A. (2008) Metabolomic engineering of carotenoid biosynthesis in plants. Trends in Biotechnology 26: 3.

Stanley, L. and Yuan, Y.W. (2017) transcriptional regulation of carotenoid biosynthesis in plants: so many regulators, so little consensus. Frontiers in Plant Science 10:1017.

Jourdan, M., Gangne, S., Laurent, C.D., Maghraoui, M., Huet, S., Suel, A., Hamama, L., Briard, M., Peltier, D., Geoffriou, E. (2014) Carotenoid content and root color of cultivated carrot: a candidate-gene association study using an original broad unstructured population. PLOSone 0116674.

Yao, D., Wang, L., Li, Q., Ouyang, X., Li, Y., Wang, C., Ding, L., Hou, L., Luo, M., Xiao, Y. (2018) Specific upregulation of a cotton phytoene synthase gene produces golden cottonseeds with enhanced provitamin A. Scientific Reports 8:1348.

Roncallo, P.F., Cervigni, G.L., Jensen, C., Miranda, R., Carrera, A.D., Helguera, M., Echenique, V. (2012) QTL analysis of main and epistatic effects for flour color traits in durum wheat. Euphytica 185:77–92

Proceedings of International Symposium on a New Era in Food Science and Technology 2019
UGSAS-GU & BWEL Joint Poster Session on Agricultural and Basin Water Environmental Sciences 2019: P15

Magnetic cellulose nanofibers/chitosan based edible nano-coating with curcumin loading: Influence of filler materials on perishable food products

Tabli Ghosh[1], Yoshikuni Teramoto[2], Kohei Nakano[3] and Vimal Katiyar[1]
1. **Department of Chemical Engineering, Indian Institute of Technology Guwahati, Guwahati, Assam-781031, Assam, India**
2. **Faculty of Applied Biological Sciences, Gifu University, Gifu 501-1193, Japan**
3. **The United Graduate School of Agricultural Science, Gifu University, Gifu 501-1193, Japan**

INTRODUCTION

From very early days, edible coating based postharvest management system has attained significant attention as a commercially viable mode of produce deliverables. The application of edible coating is generally applied as a thin layer of materials on food products for improved shelf life, and quality. For edible coating, cellulose, starch, chitosan, and gum arabic based polysaccharides are generally used for enhanced food property. However, chitosan obtained from deacetylation of chitin, is very effective in maintaining the quality of food materials during the product life for its antimicrobial property. Moreover, the biocomposites and blend preparation from available biopolymers can provide additional benefits.

Among available bionanomaterials, cellulose nanofiber (CNF) is considered as a remarkable candidate in the multifaceted application for their multifunctional properties such as surface property, aspect ratio, mechanical property, etc. which further make them a better candidate for stringent food packaging sectors. The specific material is considered as one of the emerging bionanomaterials to be used in the development of edible nano-coating in addition to various biopolymers (Ghosh et al., 2019).

Moreover, the noteworthy properties of CNF and other available biopolymers such as non-toxicity, biodegradability, biocompatibility, are utilized to obtain the tailor-made properties to improve shelf life of perishable food products. Further, CNF can be modified through the incorporation of iron particles to offer iron fortified products as edible coating materials. In this regards, the work investigates the development of non-toxic magnetic CNF (mgCNF) and chitosan based edible nano-coating materials with loading of curcumin for tailored administration of nutraceuticals and for improved properties of cut pineapple fruits, where the fabrication of mgCNF can be obtained following several methods.

MATERIALS AND METHODS

The fabrication of mgCNF is obtained through single step coprecipitation method, which is used as a nanofiller material for the fabrication of edible coating materials. The development of edible nano-coating on cut pineapple was obtained through following dip coating method. The developed materials are further taken for various property analysis such as mechanical, transparency, color properties, and others.

RESULTS

The modified nanofiller mgCNF are used as effective fillers for iron fortification of food products. Further, the fabrication of filler materials can be confirmed via FETEM micrograph as shown in **Fig. 1.** The neat CNF (Trade name: BiNFi-s CNF) have a cloudy appearance when dispersed in water, whereas the fabricated mgCNF provide spherical shaped particles attached on CNF molecules.

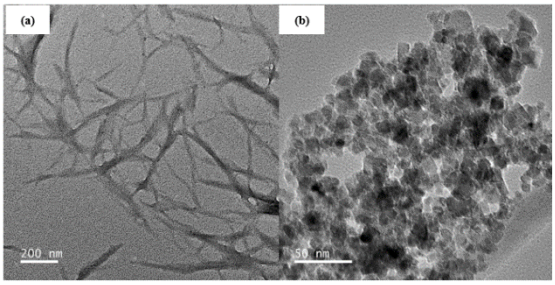

Fig. 1: FETEM micrograph of (a) BiNFi-s CNF and (b) mgCNF

In the present study, the nanofiller materials are utilized to develop chitosan based biocomposites for improved properties. The mechanical properties (tensile strength, and Young's Modulus), thermal properties in terms of temperature at which 50% of sample weight get degraded (T_{50}), transparency (UV and visible region), and color properties are shown in Table 1. The color properties are expressed in terms of L values (brightness to darkness), a* values (+a* is red and –a* is green), and b* values (+b* is yellow and –b* is blue).

Characteristics	Components
Mechanical Property	Tensile strength = ~ 57 MPa Young's Modulus = ~2348 MPa
Thermal Properties	T_{50}= ~ 340 °C
Transparency	~ 18% (UV Region) ~ 45% (Visible Region)
Color Properties	L = ~28.69 a*= ~3.34 b*= ~2.48

Table. 1: Properties of 1.5% mgCNF/Chitosan based biocomposites materials

Table. 1 represents the properties of 1.5% mgCNF/chitosan based biocomposites materials, where, the tensile strength has been found to improve by ~89% in comparison to neat chitosan. Further, Young's modulus is also improved by ~80% when compared with neat chitosan. The observed transparency of neat chitosan is ~85% which is reduced to ~ 18% in the UV region. In the same way, transparency has been reduced to ~45% from ~89% (neat chitosan) in the visible region (Ghosh et al., 2019).

Further, Fig. 2 represents the surface morphology of 1.5% mgCNF/Chitosan based biocomposites materials with curcumin loading, where the uniform dispersion of mgCNF nanofiller in chitosan matrix has been observed.

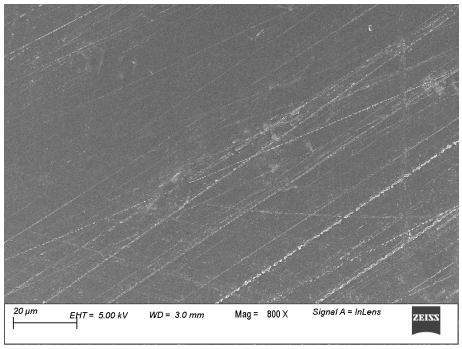

Fig. 2: FESEM micrograph of 1.5% mgCNF dispersed chitosan with curcumin loading for edible coating.

Interestingly, the developed edible nano-coating materials are applied on cut pineapple, where various properties are analyzed to check the quality of stored food products in terms of respiration rate, total soluble solids, microbial count, etc.

DISCUSSION

The investigation shows that the developed mgCNF dispersed chitosan based edible nano-coating materials are very effective to be acted as commercially viable mode of produce deliverables. The used postharvest management system with the targeted materials are very beneficial for offering improved packaging properties. The formulated materials as edible nano-coating for food products provide improved tensile strength, young's modulus, thermal stability, optical properties and others. As well known the perishable food products such as fruits and vegetables have very less product life, so the used materials are beneficial to prolong the shelf life of cut pineapple.

ACKNOWLEDGMENTS

The authors are thankful to Centre of Excellence for Sustainable Polymers (CoE-SusPol) for the experimental facilities. Further, the authors are thankful to central instrument facility and IIT Guwahati for the research facility. The authors are very grateful to Gifu University, Japan. Miss Ghosh is very much thankful to the department of science and technology, Government of India, for awarding INSPIRE Fellowship for persuing doctoral degree.

REFERENCES

Ghosh, T., Teramoto, Y., and Katiyar, V. (2019). Influence of Nontoxic Magnetic Cellulose Nanofibers on Chitosan Based Edible Nanocoating: A Candidate for Improved Mechanical, Thermal, Optical, and Texture Properties. Journal of agricultural and food chemistry 67:4289-4299.

Proceedings of International Symposium on a New Era in Food Science and Technology 2019
UGSAS-GU & BWEL Joint Poster Session on Agricultural and Basin Water Environmental Sciences 2019: P16

Poly (L-lactic acid)/modified gum arabic biocomposites for targeted food packaging applications

Purabi Bhagabati, Tabli Ghosh and Vimal Katiyar
Department of Chemical Engineering, Indian Institute of Technology Guwahati, North Guwahati, Assam, India-781039

INTRODUCTION

Poly (L-lactic acid) (PLLA) is an aliphatic polyester which is derived from renewable resources such as potato, Corn sugar, and sugarcane. It has played a central role in replacing fossil-based polymers for certain applications. It is a biodegradable thermoplastic which can be used as a packaging materials including the area of foods and is also a hygienic product because of its good biodegradability, compatibility and environmental friendly (Lim et al. 2008, Auras et al. 2004). Gum Arabic (GA) or Acacia gum is the exudates from the Acacia Senegal and Acacia Seyal trees. It is widely used for industrial purposes such as stabilizer, emulsifier, thickener and an encapsulating in the food industry, and to a lesser extent in ceramics, lithography, cosmetics, textiles and other application (Verbeken et al. 2003). The prime motivation of the work is to develop tough and flexible films of PLA/mGA biocomposites for specified food packaging applications. Chemical modification of Gum Arabic via in-situ polymerization of lactic acid would form oligomeric lactic acid grafted Gum Arabic (OLLA-g-GA) (Tripathi et al. 2016). Effect of the modified GA of varying grafting percentage would affect the hydrophilicity of the GA and so about the dispersion within the PLLA matrix in the biocomposites. The work reports the effect of the chemical modification of GA on crystal morphology, thermal, mechanical and optical properties of its PLLA biocomposites responsible for its potential candidacy for food packaging applications.

MATERIALS AND METHODS

L-lactic Acid and poly(lactic acid) (PLLA) (granular form; 2003D) were procured from Jiaan Biotech and Nature Works, respectively. Gum Arabic(GA) from Acacia tree, HPLC Chloroform (SPECTROCHEM PVT. LTD) were purchased from Sigma Aldrich. StartSYNTH Microwave Synthesis Labstation, Magneto Rheometer, Analytical Balance, Sonicator, Magnetic hot plate stirrer, UTM, Color Spectrophotometer, DSC, POM, TGA.

Fabrication of LA-g-GA in STARTsynth Microwave Synthesis Labstation.

Preparation of LA-g-GA

Table. 1: Composition of Lactic Acid and Gum Arabic

Modified GA (mGA) samples	L-lactic Acid	Gum Arabic
1% LA-g-GA	25ml	0.25 g
3% LA-g-GA	25ml	0.75 g
5% LA-g-GA	25ml	1.25 g

Chemical modification GA to synthesize OLLA-g-GA was carried out in StartSYNTH Microwave Synthesis Labstation. Lactic acid and Gum Arabic were taken in three neck round bottom flask as per the composition presented in Table 1.

The temperature of the heating tape connected between glass rod outlet and condenser was maintained at 100ºC in order to avoid condensation of byproducts. The amount of oligomer formed and the water collected was measured.

Preparation of PLLA/LA-g-GA Nanocomposite films

PLLA/LA-g-GA nanocomposite films with 2, 5 and 7 wt% of LA-g-GA filler (1%, 3%, 5%), and 1 neat PLLA film were prepared by solution casting method. The solution of LA-g-GA was prepared by dissolving LA-g-GA with PLLA granules in chloroform with vigorous stirring magnetically at room temperature for 5-6 hours. The composition of PLLA granules, LA-g-GA and chloroform for different films is given in Table 2. The solution was poured into Teflon petri dishes to obtain the film after evaporation of chloroform. The formed films were peeled off from the Petri dishes after 12 hours and further dried in a vacuum oven for 12 hours to remove the remaining chloroform from the films.

Table. 2: Composition of PLLA, oligomer, chloroform

Designation	Concentration	PLA granules	Oligomer	Chloroform
1% LA-g-GA	2%	1.96 g	0.04 g	60 ml
	5%	1.90g	0.10 g	60ml
	7%	1.86g	0.14g	60ml
3% LA-g-GA	2%	1.96g	0.04g	60ml
	5%	1.90g	0.10 g	60ml
	7%	1.86g	0.14g	60ml
5% LA-g-GA	2%	1.96g	0.04g	60ml
	5%	1.90g	0.10 g	60ml
	7%	1.86g	0.14g	60ml
NPLA	-	2g	-	60ml

RESULTS AND DISCUSSION

Trans-crystallization phenomenon

The crystallinity of a semi-crystalline polymer like PLLA has a tremendous impact upon other physio-mechanical properties. Addition of fillers of varying size and shape as additive of PLLA instinctively affects its crystallinity. While nanoparticles are more effective in altering the crystalline morphology of base polymer matrix, addition of microparticles in unmodified form has no significant impact. However, a strategic covalent modification of microparticles may act as a great way to cause alteration of these properties.

Trans-crystallization phenomenon was observed at the interphases of these mGA particles, which can be interpreted from the second image of each sample. Further crystal growth from these nucleating sites led to formation of a single large spherulite of diameter >800 μm and at 30 minutes, which superficially looks like a single spherulite that was nucleated by a single mGA particle. However, there is a distinct variation in the rate of crystallization in the samples and they are as follows: GA1>GA3>GA5. This indicates that a higher grafting concentration of OLLA enhances rate and degree of crystallization in the composite. It is noteworthy to mention that no such nucleation phenomenon was observed in case of PLLA composites with unmodified GA. The loosely bound particles are incapable to transfer load to the polymer matrix and this promotes stress initiation under mechanical testing of respective samples. For detailed understanding, mechanical

performance is evaluated by a destructive mechanical test under tensile mode.

Mechanical properties

The tensile strength of the fabricated films sample represents the ability for its load bearing capacity and ultimate tensile strength and % elongation at break values of the samples are presented in Fig 2. While, NPLLA samples show maximum UTS of 29 MPa, its composites with GA1, GA3 and GA5 show relatively closer UTS of 26.7, 28.1 and 26.8 MPa, respectively. In each case of the PLA/mGA composites, the lowest concentration of each set of mGA (i.e. 2wt%) showed a better tensile property in comparison to its higher concentration counterparts.

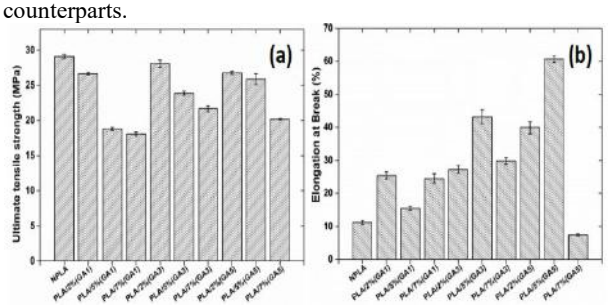

Fig 2: Ultimate tensile strength (MPa) and percentage elongation break of NPLA and its biocomposites of mGA samples

PLLA is highly brittle in nature and showed percentage elongation at break of NPLA close to 11%. However, incorporation of the mGA into PLLA matrix caused a significant increment in the values of percent elongation at break. A maximum of 60% elongation at break was achieved in PLA/5%(GA5) sample, which infers a significant increment in value from NPLA samples. The PLA/2%(GA5) sample render great improvement in its percentage elongation by 263% from NPLA, which also showed UTS value apparently close to NPLA, i.e. 26.8 MPa. An approximately 7.5% reduction in the tensile strength value and the appreciable 263% increment in ductility may logically be supported as the optimized composition for the composites.

Thermal analysis

The DSC analysis of NPLA and its composites may throw light into the in-depth understanding on the thermal properties upon addition of mGA in PLA matrix. The second heating thermograms of all sample consisted of a single inflection peak corresponding to Tg, two melting endotherm peak (Tm1 and Tm2) and a cold crystallization exothermic peak (Tcc) that lied between Tg and Tm. While a decrease in Tg of composite with 2wt% mGA caused little to insignificant reduction in Tg, appreciable reduction in Tg was observed in case of composites with 5wt% and 7wt% mGA concentration.

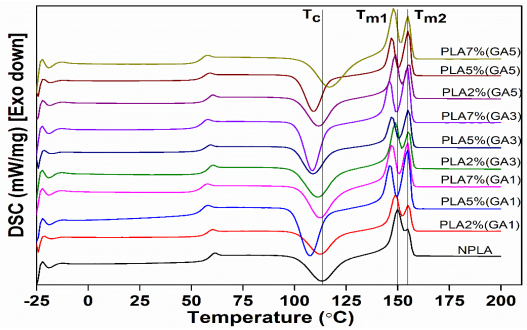

Fig. 3: DSC second heating thermograms of NPLA and its biocomposites of mGA samples

While the low molecular weight OLLA is capable to plasticize the brittle PLA matrix, the covalently attached OLLA-g-GA particles offer good reinforcement to the matrix, which represents anti-plasticization effect. Existence of good interphase interaction between the polymer matrix and the mGA is the responsible factor for the reduced Tcc of the composites over NPLA. The seemingly higher percentage crystallinity and Tcc value in most of the composites over NPLA support the nucleation phenomenon as observed in the POM analysis.

The heat sealing property of the PLA/mGA biocomposites with higher mGA content is relatively higher than the NPLA, which is much beneficial for food packaging applications.

Optical properties

The optical characteristics of NPLA and biocomposites were characterized with the UV-vis spectrophotometer and the datacolor to understand the effect of mGA onto the PLLA films. Excellent transparency and color of films endorse its application in the packaging of food items.

ACKNOWLEDGMENTS

The authors sincerely acknowledge the Department of Chemicals and Petrochemicals, Ministry of Chemicals and Fertilizers, Government of India funded Centre of Excellence for Sustainable Polymers (CoE-SusPol) at IIT Guwahati for research facilities to perform this research work.

REFERENCES

Auras, R., Harte, B., &Selke, S. (2004). An overview of polylactides as packaging materials. Macromolecular bioscience, 4(9), 835-864.

Lim, L. T., Auras, R., &Rubino, M. (2008). Processing technologies for poly (lactic acid). Progress in polymer science, 33(8), 820-852.

N. Tripathi & V. Katiyar, Journal of Applied Polymer Science, 133, 21 (2016).

Verbeken, D., Dierckx, S., &Dewettinck, K. (2003). Exudate gums: occurrence, production, and applications. Applied Microbiology and Biotechnology, 63(1), 10-21

Proceedings of International Symposium on a New Era in Food Science and Technology 2019
UGSAS-GU & BWEL Joint Poster Session on Agricultural and Basin Water Environmental Sciences 2019: P17

Controlling the molecular architecture to tailor the thermal and mechanical properties and water vapor transmission rate of the biodegradable block copolymers: Versatile materials for food packaging

Neha Mulchandani[1], Kazunari Masutani[2], Shinichi Sakurai[2,] Yoshiharu Kimura[2] and Vimal Katiyar[1]
1. **Department of Chemical Engineering, Indian Institute of Technology Guwahati, Kamrup, Assam, India**
2. **Department of Biobased Materials Science, Kyoto Institute of Technology, Matsugasaki, Sakyo-ku, Kyoto, Japan**

INTRODUCTION

Biodegradable aliphatic polyesters such as poly(lactic acid) (PLA) and poly(ε-caprolactone) (PCL) have received significant attention in the past decades owing to their remarkable characteristics and end-use applications (Pisani et al., 2018). PLA is widely recognized as a biobased material with a significant potential to replace the petroleum derived plastics. However, the inferior thermal resistance and the brittle nature of PLA have restricted its use in widespread commodity and engineering applications(Hirata, Masutani, & Kimura, 2013). On the other hand, PCL is known to be a flexible polymer possessing high impact strength, while having a relatively lower tensile strength (Rojo, Martín, Calvo, & Cocero, 2009). In order to improve the thermal resistance of PLA, stereocompelxation (crystalline form between the enantiomeric PLA chains) has been widely adopted, which improves the melting temperature of stereocomplex crystallites to ~230 °C. Stereocomplexation may be achieved by blending the enantiomeric chains i.e. poly(L-lactic acid) (PLLA) and poly(D-lactic acid) (PDLA) or by stereoblock formation (Gupta & Katiyar, 2017).

To develop the materials with tailored properties, PLA and PCL are used in combination. Blending of PLA and PCL often leads to the macro-phase separation resulting in the inferior overall mechanical properties (Lv et al., 2016). In this regard, block copolymerization of PCL and PLA has been regarded as an effective approach to develop the materials with intended properties.

With the aim of designing biodegradable polymers for versatile food packaging applications, the current research focuses on synthesizing triblock and pentablock copolymers consisting of soft middle segments and hard end segments, incorporating the concept of stereocomplexation to improve the overall material properties. The triblock copolymers (BCB) are synthesized by two-step ring opening polymerization (ROP) and the pentablock copolymers (ABCBA) are synthesized by three-step ROP by using PCL as a macro-initiator. The thermal and mechanical properties along with the water vapour permeability have been detailed underlying the impact of molecular architecture on the properties of the material indicating their potential for versatile food packaging applications.

MATERIALS AND METHODS

L- and D-Lactides (99% purities) were acquired from Musashino Chemical Laboratories Ltd., Tokyo, Japan. ε-caprolactone was purchased from Nacalai Tesque, Kyoto, Japan, and distilled prior to use. 1,12-Dodecanediol was obtained from Wako Pure Chemical Industries Ltd., Tokyo, Japan. Tin octoate (Sn(Oct)2, 95%) was purchased from Sigma Aldrich and used after distillation under high vacuum. Dichloromethane and methanol were procured from Nacalai Tesque, and 1,1,1,3,3,3-Hexafluoro-2-propanol (HFIP) was obtained from Central Glass Co. Ltd., Yamaguchi, Japan.

Synthesis of BCB/ACA and ABCBA/BACAB type copolymers: In the first step, PCL-doil was synthesized which was then used as a macroinitiator to synthesize PLLA-b-PCL-b-PLLA and PDLA-b-PCL-b-PDLA by adding L-and D-lactides respectively. The block copolymers were synthesized such that the block length of PLLA/PDLA terminal segments was 20 kDa and that of PCL was 10 kDa. The triblock copolymers were further used as macroinitiators to form ABCBA/BACAB type pentablock copolymers where the block length of all the segments was ~10 kDa. The molecular weight of the block copolymers was confirmed by ^{1}H-NMR measurements. The enantiomeric block copolymers were then blended (50:50) in order to form enantiomeric blends designated as BCB/ACA blends and ABCBA/BACAB blends.

Additionally, PLLA was synthesized (Mn ~ 50 kDa) to compare the properties of the block copolymers with the homopolymer.

^{1}H-NMR spectra were determined using AV600 spectrometer (Bruker, Germany) where the samples were dissolved in deuterated chloroform ($CDCl_3$).

Differential Scanning Calorimetry measurements were conducted using DSC 214 Polyma (NETZSCH).

The mechanical properties of the samples were determined using a universal testing machine (Kalpak Instruments and Controls) equipped with a load cell of 500 N and the cross head speed being 5 mm/min.

The water vapor permeability was measured using PERMATRAN-W by using the ASTM standard E398-03 where the relative humidity (RH) was 90%.

RESULTS

Differential Scanning Calorimetry: The thermal transitions in the synthesized block copolymers are ascertained by differential scanning calorimetry (DSC) measurements. The heating profile indicates the presence of individual melting peaks of PCL and PLLA/PDLA designating the presence of individual crystalline domains. Further, the stereocomplex crystallites are present in the enantiomeric triblock blend as well as the pentablock copolymer and its blend which leads to the improved T_m of the resulting copolymers. The cold crystallization temperature (T_{cc}) of the pentablock copolymer is found to be ~76 °C as compared to the triblock copolymer (T_{cc} ~ 84 °C). This indicates the relatively faster crystallization in case of pentablock copolymers.

Mechanical Properties: The tensile strength and elongation at break of the synthesized homo/block copolymers are shown in Fig. 1. The ultimate tensile strength is found to improve in case of the stereoblock copolymers. However, the elongation (at break) of stereoblock copolymer is reduced pertaining to its brittle nature. The elongation at break of the triblock copolymer is significantly enhanced to (~300%) with approximately

similar tensile strength. The improvement in elongation is attributed to the presence of soft (PCL) segments.

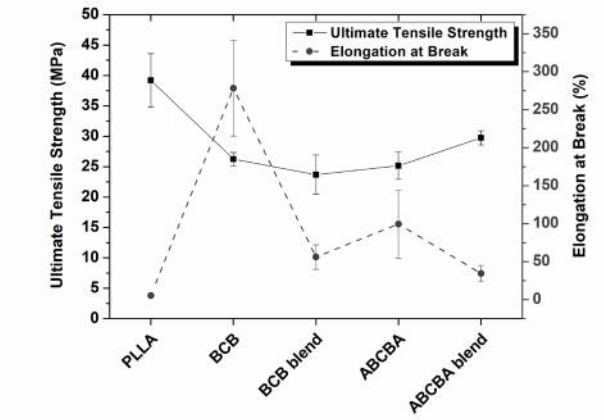

Fig. 1: Ultimate tensile strength and elongation at break of the synthesized homo/block copolymers

Water Vapor Transmission Rate: The water vapor transmission rate of the homopolymer and block copolymers is shown in Table 1. The WVTR of the synthesized PLLA is 3.77 which is increased by incorporating PCL segments as seen in the case of triblock and pentablock copolymers. Further, the WVTR is reduced on blending the enantiomeric block copolymers which may attributed to the increasing crystallinity of the materials due to the stereocompelxation creating a tortuous pathway for the water vapor to pass through.

Table 1: Water vapor permeability of the synthesized homo/block copolymers

Identity	WVTR ($gm.mm.m^{-2}.day^{-1}$)
PLLA	3.77 ± 0
BCB	7.9 ± 2.6
BCB blend	4.7 ± 1.0
ABCBA	7.8 ± 0.3
ABCBA blend	4.9 ± 2.9

DISCUSSION

The thermal and mechanical properties along with the water vapor transmission rate are found to be significantly influenced by the molecular architecture of block copolymers. The elongation (at break) is found to be enhanced upon the addition of PCL segments into the chains of PLLA/PDLA which may be exploited for the flexible biodegradable food packaging applications. Further, the fresh produce requires relatively higher water vapor transmission rate in order to respire whereas the packaged food requires low water vapor permeability, and the developed biodegradable block copolymers may serve as candidates for these applications possessing versatile characteristics.

ACKNOWLEDGMENTS

The authors acknowledge the Centre of Excellence for Sustainable Polymers (CoE-SusPol) funded by the Department of Chemicals and Petrochemicals (DCPC); Central Instruments Facility (CIF) at Indian Institute of Technology Guwahati (IIT Guwahati); Kyoto Institute of Technology (KIT), Japan for providing the research and analytical facilities; and Department of Science and Technology (DST) for providing the INSPIRE fellowship (IF 160861) for the doctoral research.

REFERENCES

Gupta, A., & Katiyar, V. (2017) Cellulose Functionalized High Molecular Weight Stereocomplex Polylactic Acid Biocomposite Films with Improved Gas Barrier, Thermomechanical Properties. ACS Sustainable Chemistry & Engineering 5(8):6835-6844.

Hirata, M., Masutani, K., & Kimura, Y. (2013) Synthesis of ABCBA Penta Stereoblock Polylactide Copolymers by Two-Step Ring-Opening Polymerization of l- and d-Lactides with Poly(3-methyl-1,5-pentylene succinate) as Macroinitiator (C): Development of Flexible Stereocomplexed Polylactide Materials. Biomacromolecules 14(7):2154-2161.

Lv, Q., Wu, D., Xie, H., Peng, S., Chen, Y., & Xu, C. (2016) Crystallization of poly(ε-caprolactone) in its immiscible blend with polylactide: insight into the role of annealing histories. RSC Advances 6(44):37721-37730.

Pisani, S., Dorati, R., Conti, B., Modena, T., Bruni, G., & Genta, I. (2018) Design of copolymer PLA-PCL electrospun matrix for biomedical applications. Reactive and Functional Polymers 124:77-89.

Rojo, S. R., Martín, Á., Calvo, E. S., & Cocero, M. J. (2009) Solubility of Polycaprolactone in Supercritical Carbon Dioxide with Ethanol as Cosolvent. Journal of Chemical & Engineering Data 54(3):962-965.

Proceedings of International Symposium on a New Era in Food Science and Technology 2019
UGSAS-GU & BWEL Joint Poster Session on Agricultural and Basin Water Environmental Sciences 2019: P18

Fabrication of nano cellulose from marine green algae residue and their effects as filler in developing biodegradable polymer composite

Kona Mondal[1], Shinichi Sakurai[2], Purabi Bhagabati[1], Vaibhav. V. Goud[1] and Vimal Katiyar[1]
1. **Department of Chemical Engineering, Indian Institute of Technology Guwahati, India**
2. **Department of Biobased Materials Science, Kyoto Institute of Technology, Kyoto, Japan**

INTRODUCTION

Green algae are widely available around the world and its exploitation for the production of biodiesel, bioethanol, and agar has become an important industry in recent years aiming to conserve the fossil fuels and minimizing global warming. Also, it became the alternative source for third generation biodiesel production. Furthermore, petroleum-based plastics are reason for occurring global warming, plastic waste, and many other hazards. Contrariwise, biodegradable polymers with identical properties have been found as a great research outcome for substitution of petroleum-based plastics. Thus, the green or sustainable polymer would be the best possible replacement for conventional plastics to protect our globe from the environmental hazard. However, the industrial processing of green algae generates a large quantity of solid wastes, which constitutes a source of serious environmental problems. Further, these algae wastes contain polysaccharide such as cellulose which is a natural biodegradable polymer with some unique characteristics of renewability, biodegradability, high tensile strength and stiffness, cost effectiveness and light weight (Sucaldito and Camacho 2017). Although, other lignocellulosic biomass sources are available in environment for extractions of cellulose, in spite of those algae are of special interest, ideally suitable for a variety of applications, including polymer reinforcement (Guo et al. 2017). Additionally, algae derivatives consist of several valuable components such as a polysaccharide, antioxidants, pigments, fatty acids, proteins and vitamins, and minerals. On the otherside, the demand of food packaging is increasing more with the growing population.

Nano Cellulose (NC) has emerged as a biobased material that has captured considerable research and industrial interest. They feature a high aspect ratio, low density, high mechanical strength, and low coefficient of thermal expansion. In addition, they display abundant hydroxyl groups that facilitate NC functionalization and allow strong inter fibrillar hydrogen bonding.

In the present work, utilization of green algae waste as a raw material to produce value added nano celluloses (NC) has been investigated, and the effect of the as-isolated NC as a filler material in biodegradable polymers (poly(Lactic acid) (PLA) and poly(ε-caprolactone)(PCL)) have been studied. Further, washed algae biomass residue (WABR) is also used as filler in both the polymer matrix to check the effect of WABR.

MATERIALS AND METHODS

PLA granules (grade: 4032D, with weight average molecular weight (Mw) ~200 kDa and content of L-lactic acid/D-lacticacid: 98.6/1.4) have been purchased from Nature Works® LLC., USA. Further, PCL has been synthesized in the laboratory with Mw ~80 kDa. Algae biomass residue (ABR) has been subjected to washing for removal of dirt and extraneous matter followed by drying and grounding which is supplied by TERI, India. Fabrication of NC has been done through acid hydrolysis (sulphuric acid) method. Both the fillers WABR and NC loading amount in polymer matrix are 0, 0.5, 1 and 2wt% respectively. WABR composite and NC nanocomposite specimens have been developed by solution casting. Thermal properties and crystalline behaviour of the specimens have been examined using a differential scanning calorimeter (DSC) and a polarized optical microscope (POM). The DSC isothermal and non-isothermal study has been done for both composite specimens. The isothermal crystallization of PLA and PCL composite specimens are conducted at 110˚C and 45˚C respectively. The POM observations have been conducted with the isothermal condition at 125˚C for PLA and at 45˚C for PCL composite specimens. To observe the spherulite growth behavior in both of the polymer composite specimens POM study has been done.

RESULTS AND DISCUSSIONS

It has been observed that NC acts as a good nucleating agent in both types of polymer composite specimens as compared to WABR. It has also been found that WABR can act as a nucleating agent. Non-isothermal DSC study has shown the reduction in cold crystallization temperature in PLA/NC nanocomposite specimens (in the second heating process) from 135.8˚C to 119.3˚C (Fig.1a) whereas NC helped to increase the crystallization temperature in the PCL/NC nanocomposite specimens from 29.4˚C to 35˚C (in the cooling process from melt) (Fig.2a&b). Both results indicate the improvement of crystallization in the nanocomposite specimens. The DSC isothermal crystallization study confirms the improved crystallization in PLA/NC nanocomposite specimens (Fig.1c) whereas in case of PCL/NC crystallinity decreased after addition of NC (Fig.2c). It also been observed that with increasing the filler loading percentage crystal formation occurs rapidly (Fig.1b). The POM study has also shown accelerated crystallization for both of the polymers. Overall, we successfully demonstrated a high-end utilization of a bioresource from the marine green algae residue.

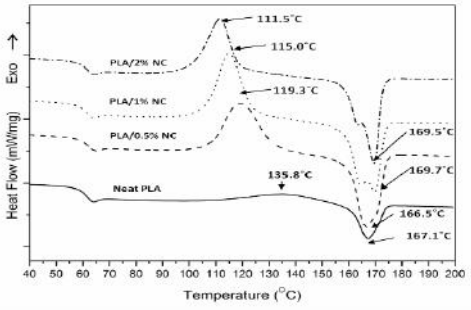

Fig.1a:Non-isothermal DSC thermogram of PLA/NC nanocomposites

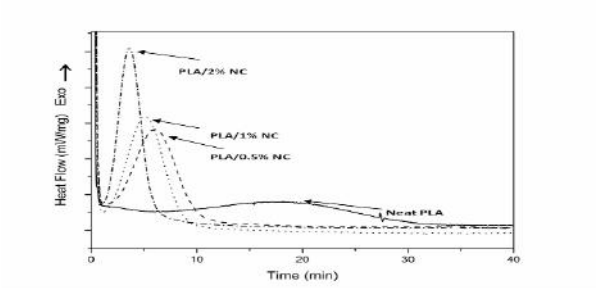

Fig.1b: Isothermal DSC thermogram of PLA/NC nanocomposites at 110˚C

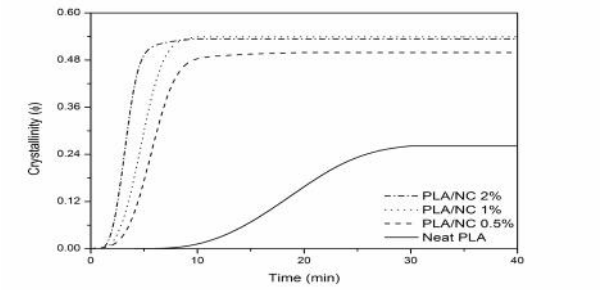

Fig. 1c: Crystallinity curve of PLA/NC anocomposite

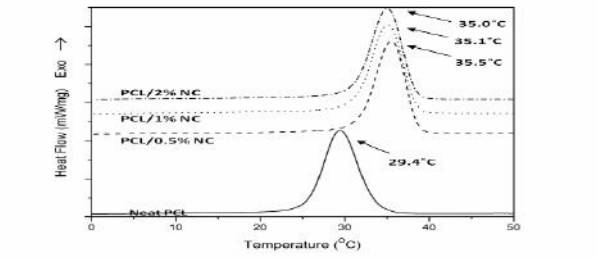

Fig.2a: Non-isothermal DSC thermogram of PCL/NC nanocomposites

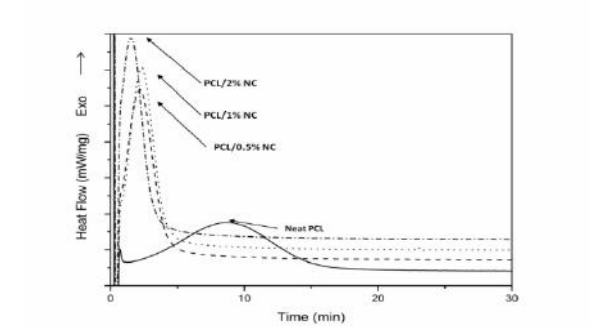

Fig.2b: Isothermal DSC thermogram of PCL/NC nanocomposites at 45˚C

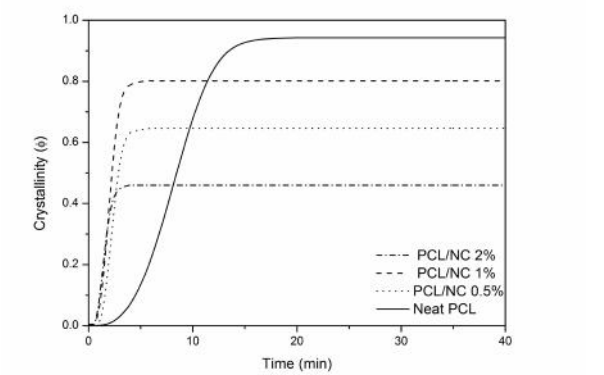

Fig. 2c: Crystallinity curve of PCL/NC anocomposite

ACKNOWLEDGEMENT

The authors are very grateful to Excellence of Sustainable Polymers (CoE-SusPol), CIF at IIT Guwahati and Kyoto Institute of Technology, Japan for providing research facilities. We also thankful to TERI (The energy and Resource Institute)-DBT (Department of Biotechnology, Gov. of India) Centre of Excellence on Biofuels and Biocommodities for funding the project.

REFFERENCES

Sucaldito, M. R., & Camacho, D. H. (2017). Characteristics of unique HBr-hydrolyzed cellulose nanocrystals from freshwater green algae (Cladophora rupestris) and its reinforcement in starch-based film. Carbohydrate polymers 169: 315-323.

Guo, J., Uddin, K. M. A., Mihhels, K., Fang, W., Laaksonen, P., Zhu, J. Y., & Rojas, O. J. (2017). Contribution of residual proteins to the thermomechanical performance of cellulosic nanofibrils isolated from green macroalgae. ACS Sustainable Chemistry & Engineering 5(8): 6978-6985.

Proceedings of International Symposium on a New Era in Food Science and Technology 2019
UGSAS-GU & BWEL Joint Poster Session on Agricultural and Basin Water Environmental Sciences 2019: P19

A sensitivity analysis of Piano Key Weir discharge capacity based on 3D numerical modeling

Le Anh Tuan[1, 2] and Ken Hiramatsu[3]
1. **The United Graduate School of Agricultural Science, Gifu University**
2. **Gifu University Rearing Program for Basin Water Environmental Leaders**
3. **Faculty of Applied Biological Sciences, Gifu University**

INTRODUCTION

Piano key weirs (PKW) are new cost-effective free-flow spillways, designed to substantially increase the discharge capacity of dams. However, their structure involves a lot of geometrical parameters and the hydraulic behavior is complex. Physical modeling usually offers different characteristics to derive adequate hydraulic design and gain insight into the hydrodynamics (Novak, et al. 2010). However, design, building and operation of physical models may take long periods of time. With the improvement of computational power, 3D numerical modeling turned out to be an interesting opportunity as it could enable to model various geometries within a reasonable delay. However, the accuracy of computational fluid dynamics (CFD) is an important matter of concern. The objective of the current study is to evaluate the accuracy of CFD to predict the head-discharge behavior of PKW, including a discussion regarding model setup and the influence of different turbulence closure methods on solution results.

EXPERIMENTAL DATA

In this study, 28 simulations were performed using a commercially available CFD solver (FLOW-3D) for Escouloubre PKW in France (Epricum, et al. 2013). The PKW of Escouloubre, operated by "Electricite de France (EDF)" is situated in the Aude River in the Pyrenees in the south of France. It is used as a spillway on the rest lake of the hydropower plant of Escouloubre and is currently used as a by-pass for the penstock of the hydropower plant of Nentilla. The PKW is composed of a central inlet key, two outlet keys and, on both weir sides, two rectangular labyrinth inlet keys without overhang or bottom slope. Additional details regarding the PKW geometries are contained within Machiels (2012).

NUMERICAL MODEL

The majority of simulations utilized the Reynolds Average Navier-Stokes (RANS) equations by means of the finite volume method, coupled with RNG k-ε turbulence modelling, being k the turbulent kinetic energy and ε the turbulent dissipation rate, both modelled by their respective transport equations. However, within the RNG model, there are two options for the user to control the maximum turbulence mixing length (MTML), one is to allow for dynamical control by the solver, the other is for the user to prescribe a set value. For the latter a common rule of thumb is to choose 7% of the channel depth. Besides, the upstream head used in the head-discharge relationships corresponds to a subcritical flow condition with relatively low turbulence, the simulations were also conducted with no turbulence model to decrease the calculation times. FLOW-3D® uses an advance algorithm for free surface tracking, TruVOF, developed by Hirt and Nichols (1981). After defining both geometry and a Cartesian, staggered grid, the software uses FAVOR™ method to generate area fractions for each cell face in the grid by determining which corners of the face are inside of a defined geometry and reconstructing the geometry based on these parameters. Therefore, the process is significantly dependent on the mesh resolution. For the numerical approximation of the advection terms, a first order scheme was employed for an initial period of time, follow by an explicit second order scheme with gradient preserving using a *Restart* simulation.

RESULTS

In this study, a sensitivity analysis of the main configurations in FLOW-3D based on the prototype discharge results was carried out. They were:

- Momentum advection model (1st order vs 2nd order with monotonicity preserving)
- VOF method (automatic vs split Lagrangian method);
- Maximum turbulence mixing length (MTML);

The numerical results are presented in Table 1. In order to evaluate if the flow rate obtained in the numerical simulations corresponded to those of the experimental tests, the relative differences between prototype and numerical discharges were evaluated (δ) (Fig. 1).

DISCUSSION

In general, the model has demonstrated a good correlation with the prototype results. However, there are discrepancies in the numerical results with the low head water over weir (i.e. $H = 0.11; 0.19m$), where the region near the weir will be characterized by sharp changes in momentum (especially at the overflow nappe) and thin geometry (the overhang crests are only centimeter thick). This will require a fine mesh to resolve. Some other main conclusions were obtained:

- The transition from a laminar regime model to a turbulence had influence on the discharge results. It is the least accurate simulation based on discharge capacity.
- The second order momentum advection with monotonicity preserving did not show more accurate results but with more computational effort. This is contrast to studies of (Miguel, et al. 2014) and (Crookston, et al. 2017).
- The sensitivity analysis for the RNG k-ε turbulence model for dynamically computed and constant (7% of P and of H) MTML found a better agreement using dynamically computed MTML when estimating Q for PK weirs. In contrast, Savage et al. (2016) employed constant MTML values to estimate Q for labyrinth weirs.
- The results of this PK weir CFD validation study indicated that the 3 dimensional CFD simulation, employing either LES or RNG k-ε turbulence models are suitable for the discharge estimation of PK weirs with mean relative errors of 2 to 5% (in condition of refined enough cell size).
- The obtained discharges were highly dependent on cell size.

REFERENCES

Crookston, B.M, Anderson, R.M, and Tullis, B.P. 2017. "Free-flow discharge estimation method for Piano Key weir geometries."

Epricum, S, Silvestri, A, Dewals, B, Arcchambeau, P, Pirotton, M, Colombie, M, and Faramond, L. 2013. "Escouloubre Piano Key Weir: Prototype versus scale models." *Labyrinth and Piano Key Weir II - PKW 2013.* London: Taylor&Francis Group.

Hirt, C.W., and B.D. Nichols. 1981. "Volume of fluid (VOF) method for the dynamics of the free boundaries." *Journal of Hydraulic Engineering* 138 (9): 796-802.

Machiels, O. 2012. "Experimental study of the hydraulic behaviour of Piano Key Weirs." PhD Thesis, University of Liege (Belgium).

Miguel, R.Silva, Lucia, T.Couto, and Antonio, N.Pinheiro. 2014. "Complementary spillway of Salamonde dam. Physical and 3D numerical modelling." *3rd IAHR Europe Congress.* Porto - Portugal.

Novak, P, Guinot V, Jeffrey A, and Reeve D.E. 2010. *Hydraulic modelling - An Introduction.* London and New York: Spon Press.

Savage, B, Crookston, B.M, and Paxon, G. 2016. "Physical and numerical modeling of large headwater ratios for a 15 degree labyrinth spillway."

Table 1. PK weir numerical simulations results

Head over PKW (m)	0.11		0.19		0.26		0.48	
$Q_{prototype}$ (m^3/s) (Q_1)	**1.2**	*δ(%)*	**2.8**	*δ(%)*	**5**	*δ(%)*	**10**	*δ(%)*
$Q_{RNG\ k\text{-}e\ dynamic\ -\ automatic\ -\ 1st\ order}$ (Q_2)	**1.49**	*24.16*	**3.27**	*16.79*	**4.98**	*-0.4*	**10.07**	*0.7*
$Q_{RNG\ k\text{-}e\ dynamic\text{-}split\ Lagrangian\ -2nd\ order\ with\ monotonicity\ preserving}$ (Q_3)	**1.53**	*27.5*	**3.28**	*17.14*	**5.03**	*0.6*	**10.39**	*3.9*
$Q_{RNG\ k\text{-}e\ (0.07P)\ -\ split\ Lagrangian\ -\ 2nd\ order\ with\ monotonicity\ preserving}$ (Q_4)	**1.51**	*25.83*	**3.28**	*17.14*	**5.01**	*0.2*	**10.47**	*4.7*
$Q_{RNG\ k\text{-}e\ (0.07H)\ -\ split\ Lagrangian\ -\ 2nd\ order\ with\ monotonicity\ preserving}$ (Q_5)	**1.53**	*28*	**3.28**	*17.14*	**5.01**	*0.2*	**10.69**	*6.9*
$Q_{LES\ -\ split\ Lagrangian\ -\ 2nd\ order\ with\ monotonicity\ preserving}$ (Q_6)	**1.52**	*26.67*	**3.28**	*17.14*	**5.04**	*0.8*	**10.19**	*1.9*
$Q_{Laminar\ -\ automatic\ VOF\ -\ 1st\ order}$ (Q_7)	**1.5**	*25*	**3.32**	*18.57*	**4.99**	*-0.2*	**10.46**	*4.6*

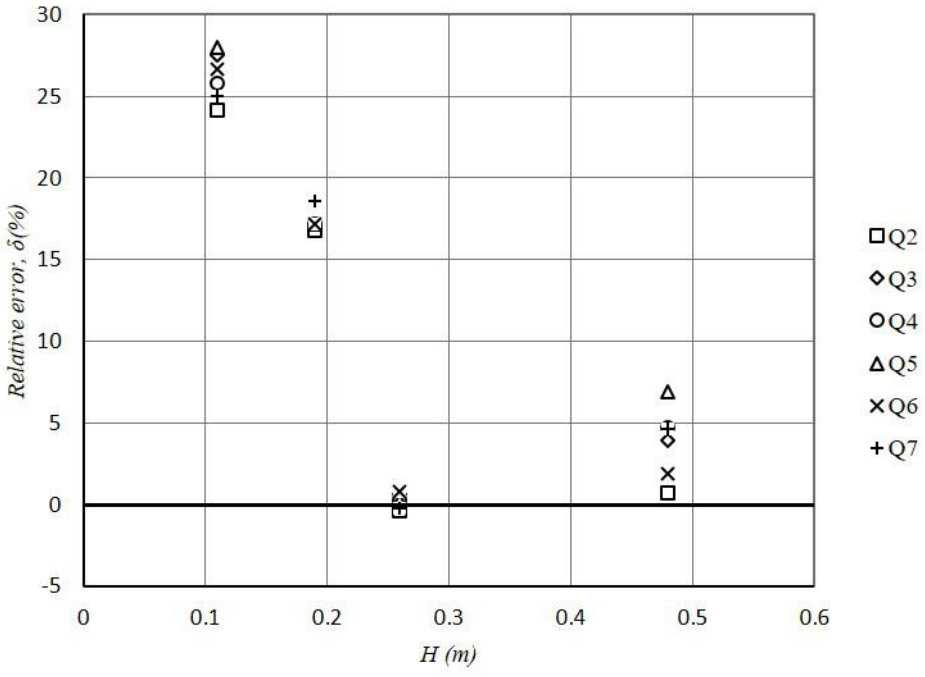

Fig. 1. Relative error between prototype and numerical flow rates

Proceedings of International Symposium on a New Era in Food Science and Technology 2019
UGSAS-GU & BWEL Joint Poster Session on Agricultural and Basin Water Environmental Sciences 2019: P20

Nitrogen deposition of bulk precipitation, throughfall and stemflow in a Lucidophyllous forest near Gifu Park in Central Japan

Ruoming Cao[1,2], Siyu Chen[2], Shinpei Yoshitake[2] and Toshiyuki Ohtsuka[2]
1. **The United Graduate School of Agricultural Science, Gifu University**
2. **River Basin Research Center, Gifu University**

INTRODUCTION

Atmospheric nitrogen (N) deposition inputs into forest ecosystems by wet deposition (rainfall and snowfall), dry deposition (gases) and cloud deposition (cloud or fog). It was reported that cloud deposition usually occurred in high-elevation forest ecosystems and was often neglected in most forest ecosystems with low elevation. N deposition (wet and dry deposition) can originate from various natural sources (lightning, forest fires and lava flows) and anthropogenic sources (energy combustion, agricultural activities and biomass burning). It was gradually increased at the global scale mainly due to considerable fossil fuel combustion (NO_x emission) and agricultural activities (NH_3 emission). Chronic N deposition significantly alters N cycle of forest ecosystems with beneficial or detrimental ecological effects, such as, promotion of plant growth, or soil acidification and N leaching via seepage water or runoff.

The role of precipitation in transferring nutrients to forest ecosystems has long been recognized. From the perspective of the hydrological cycle of forest ecosystems, precipitation is routed to the forest floor by throughfall (TF) and stemflow (SF). TF is defined as the precipitation that directly passes through a canopy or intercepted by plant surfaces and subsequently drips from a canopy. SF is defined as the part of precipitation that flows along leaves and branches and then is channeled to the bole of plants. TF and SF represent the ultimate N deposition to the forest floor.

Many studies about bulk precipitation (BP), TF and SF on natural forest ecosystems that is far from N emission sources were reported. However, studies of TF and SF on urban forest ecosystems exposure to intensive human activities are rare. The ecology of a natural forest can't be simply applied to urban forests. Net TF (TF + SF – BP) can indirectly mirror wash-off of dry deposition gathered on the canopy surface and canopy exchange (uptake or leaching) of N deposition. It was reported that wash-off of dry deposition at the pollution exposed site contributed a lot compared with sheltered site using net TF approach (Rodrigo et al., 2003). Effects of human activities on N fluxes in biogeochemical cycle of urban forest ecosystems were still unclear.

The present study was designed to estimate the concentrations and fluxes of dissolved N in BP, TF and SF over three years in the Mt.Kinka forest site, central Japan, which is an evergreen broad-leaved forest site of exposure to pollution of human activities. The study site is near Gifu Park and surrounding with mountain trails. We hypothesized that dry deposition would have substantial effects on N fluxes in the study site. We attempted to address the following questions to test the hypothesis: (1) What are the dynamics and characteristics of the concentrations and fluxes of dissolved N in BP, TF and SF? (2) What are the temporal variations of dissolved N fluxes in net TF?

MATERIALS AND METHODS

Study site—The study site is a subtropical evergreen broad-leaved forest located at Mt.Kinka near Gifu Park, Gifu city in central Japan. A 0.7 ha study plot (70 m × 100 m) was established on the lower slopes of Mt. Kinka (ca. 60 m a.s.l., 35°26′ N, 136°47′ E) in 1989. The annual mean temperature is 15.8 °C and the annual mean precipitation is 1827.5 mm during the period from 1981 to 2010. Dominant species in this study site is *Castanopsis cuspidata* (91.9 % of basal area in 2017).

Experimental setup—we set up samplers to collect BP (3 replicates), TF (9 replicates), and SF (15 replicates) from July 2016 to June 2019. BP was collected in bottles (20 L) equipped with funnels (collection area: 0.0346 m^2) that were set up in areas near the study plot without a tree canopy. The TF collectors were the same as those for BP, except for the volume of the bottles (12 L) and the fact that they were evenly distributed within the study plot. An SF collector consisted of a polyethylene film surrounding a tree trunk (like a collar), a tube connecting the film to a rain gage (HOBO RG3), and a reservoir tank (24 L). SF collectors were set up on evergreen dominant tree species according to different diameter at breast height (DBH) classes of *Castanopsis cuspidata* (DBH > 20 cm, DBH > 30 cm, DBH > 40 cm, and DBH > 50 cm) and deciduous tree species (3 replicates each). The volumes of water samples were measured by cylinder or rain gauge and water subsamples were collected by 100 ml bottles at twice per month.

Chemical analysis—After being filtering by 0.45μm membrane filter, we measured the concentrations of total dissolved nitrogen (TDN), NH_4^+–N and NO_3^- + NO_2^-–N (DIN) by a QuAAtro 2-HR nutrient analyzer using a colorimetric method and continuous flow analysis. In each analysis run, standard solutions with 0.5 mg L^{-1} concentration (NO_2^-–N and NO_3^-–N) were used to check the recovery of NO_3^- during the oxidation process, with the oxidation efficiency kept over 90%. The concentration of DON was calculated by difference between TDN and the sum of NH_4^+–N and NO_3^- + NO_2^-–N (DIN).

Calculation—N fluxes were calculated based on the average concentration (mg L^{-1}) and water depth (mm) in each sampling time. Annual N fluxes were calculated by the sum of N fluxes in each sampling time during whole year. Net TF was used to evaluate the interactions of canopy to N deposition. Net TF was performed in terms of flux data in each sampling time: Net TF = TF + SF – BP.

RESULTS AND DISCUSSION

For net TF, DIN fluxes in each sampling time followed a clear seasonal pattern in each sampling year, with the highest positive net fluxes in summer. And DON fluxes revealed negative value in some sampling time (Fig. 1).

In this study site, the positive DIN fluxes in net TF indicated that dry deposition played a vital role in DIN fluxes

for tree canopy interactions. Generally, DIN is easy to be consumed by the tree canopy reported by many studies (e.g. Aguillaume et al., 2017). Direct foliage or bark uptake, epiphyte uptake, and microbial action can cause the consumption of DIN. Enrichment of DIN by the canopy also was reported possibly due to wash-off of dry deposition gathered by the surface of canopy (e.g. Izquieta-Rojano et al., 2016). The positive DIN fluxes in net TF in this study coincided with the previous study (Rodrigo et al., 2003), which reported the more importance of wash-off of dry deposition in pollution exposed site. The possible source of dry deposition in the study site may come from transportation and energy consumption around the study site. Clear seasonal pattern of DIN fluxes in net TF was in accordance with emission from considerable electricity production during summer in Gifu city.

Negative value of DON fluxes in net TF indirectly implied that there was consumption of DON in canopy exchange process. Leaching of DON from a canopy is a common phenomenon (Lovett and Lindberg, 1993). In contrast, it was also reported that plants can consume some organic N directly from solution without microbial mineralization (e.g. Izquieta-Rojano et al., 2016).

REFERENCES

Aguillaume, L., Izquieta-Rojano, S., García-Gómez, H., Elustondo, D., Santamaría, J.M., Alonso, R., Avila, A., 2017. Dry deposition and canopy uptake in Mediterranean holm-oak forests estimated with a canopy budget model: A focus on N estimations. Atmospheric Environment 152, 191–200.

Izquieta-Rojano, S., García-Gomez, H., Aguillaume, L., Santamaría, J.M., Tang, Y.S., Santamaría, C., Valiño, F., Lasheras, E., Alonso, R., Àvila, A., Cape, J.N., Elustondo, D., 2016. Throughfall and bulk deposition of dissolved organic nitrogen to holm oak forests in the Iberian Peninsula: Flux estimation and identification of potential sources. Environmental Pollution 210, 104–112.

Lovett, G.M., Lindberg, S.E., 1993. Atmospheric deposition and canopy interactions of nitrogen in forests. Canadian Journal of Research.

Rodrigo, A., Àvila, A., Rodà, F., 2003. The chemistry of precipitation, throughfall and stemflow in two holm oak (Quercus ilex L.) forests under a contrasted pollution environment in NE Spain. Science of the Total Environment 305, 195–205.

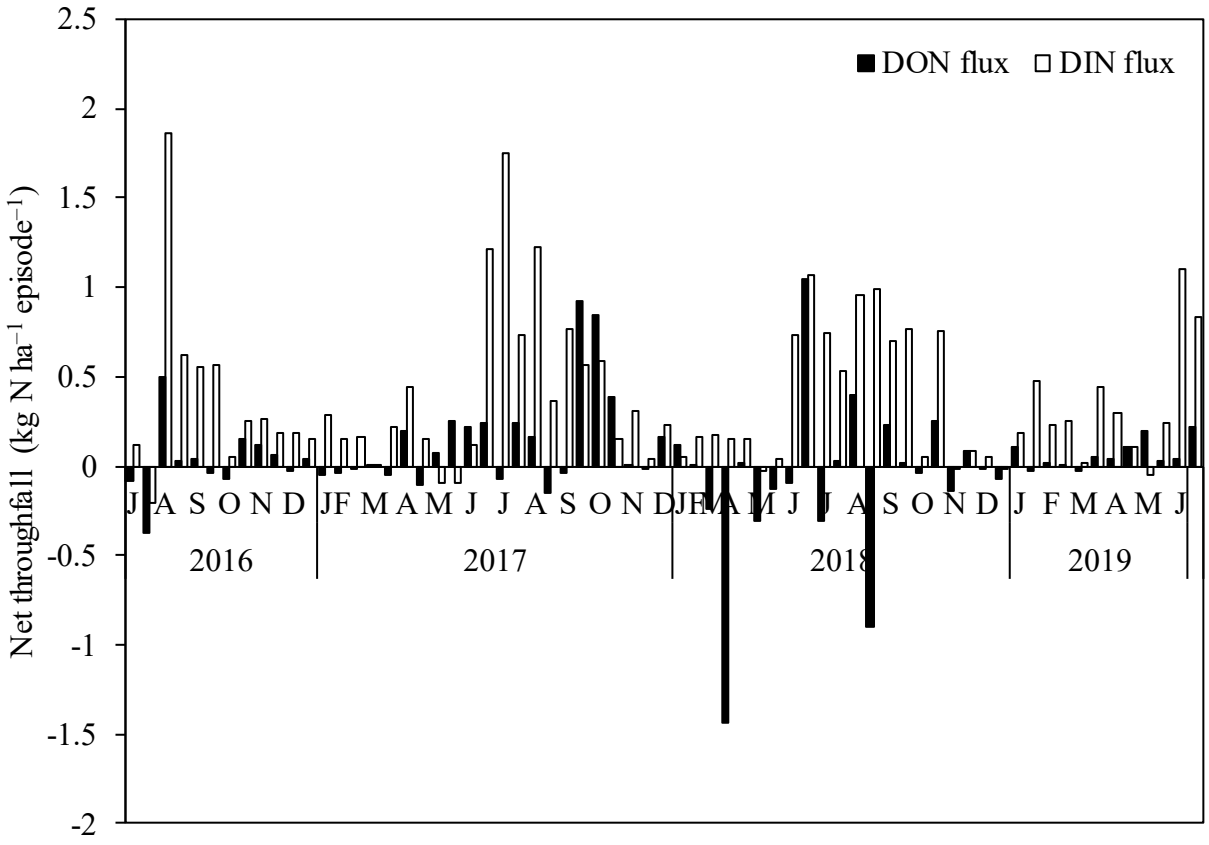

Fig. 1: Dissolved organic nitrogen (DON) and dissolved inorganic nitrogen (DIN) fluxes (kg N ha^{-1} episode^{-1}) in net throughfall from July 2016 to June 2019. Net throughfall = throughfall + stemflow – bulk precipitation.

Proceedings of International Symposium on a New Era in Food Science and Technology 2019
UGSAS-GU & BWEL Joint Poster Session on Agricultural and Basin Water Environmental Sciences 2019: P21

Various swidden activities play complementary roles for local food security in montane northern Laos

Cahyo Wisnu Rubiyanto[1] and Isao Hirota[2]
1. **The United Graduate School of Agricultural Science, Gifu University, Japan**
2. **Faculty of Applied Biological Sciences, Gifu University, Japan**

INTRODUCTION

In Laos, agricultural and forestry plays important role in economic sector. The farming system in Laos decided into two major practices; lowland farming (rain-fed or irrigated farming) and upland farming (Shifting cultivation or swidden system). Shifting cultivation is the most common agriculture practice in Laos because the landscape of Laos about 80% is mountainous.

One of the landmark policies in Laos during 1990s to clarify the the shifting cultivation in village forest, the village boundary, classifying the villages forest and land to mitigate illegal logging activities is The Land and Forest Allocation (LFA) (Fujita, 2008). LFA was used to control shifting cultivation because shifting cultivation is one of the factor of deforestation. Shifting cultivation must be eliminated by the year 2000 because the objectives of this policy are to alleviate poverty and to introduce more sustainable management of agricultural resources. In fact, in 2019, the indigenous people in northern Laos are continuing shifting cultivation to get sufficient in rice.

Sifting cultivation practice have been decline in some area of Laos. However, there are negative impacts of replacing shifting cultivation to other stable ecological system; changes in the patterns of forest–field landscapes (Castella, 2013), and also to the social and human capital (Vliet, 2012). Whereas, shifting cultivation provides a lot of products and livelihood activities. Rice crop in swidden field is typically mixed with vegetables and some fruits that it could be covered their food security in household level. In addition, to understand the food security in northern Laos, this study has main objective to conduct local food security of indigenous people in four villages of Sone District, Houaphan Province.

MATERIALS AND METHODS

The livelihood change is described based on statistic data and by interviewing head of household in study site. The collection of both quantitative and qualitative data were collecting through individual interviews. To gain an understanding of the village context and to support the interview findings, the study area was documented through direct observation and photographs of the village. In addition to participatory observation relating to research objectives, one hundred twenty-five households were chosen and interviewed with semi-structured questionnaire. The quantitative data were processed using simple statistics (in excel) to support the qualitative data.

RESULTS

Average rice production per household are shown in table. 1, and the value of various swidden activities in the study area is shown in table.2 and fig.1.

Table 1. Average rice production per household and its sufficiency in the four villages of Sone District, Houaphan Province.

Items	Bong	Houay Su	Houay Sanguan	Houay Lao
Paddy				
Household engaged (%)	40.62	15.79	45.71	0.00
Production (kg/HH/y)	574.38	98.31	1028.57	0.00
Estimated price of produced rice (USD/HH/y)*	172.31	29.49	308.57	0.00
Upland				
Household engaged (%)	87.50	92.11	65.71	95.00
Production (kg/HH/y)	1813.75	2500.26	1521.00	3222.00
Value (USD/HH/y)*	544.13	750.08	456.30	966.60
Sufficiency Rice				
Self-sufficiency ratio in rice	68.75	92.10	57.14	85.00
Insufficient value in rice (USD/HH/y)*	223.89	61.59	327.82	144.99
Swidden activities				
NTFPs	1293.17	1403.51	1397.31	606.09
Commercial crops	118.74	353.93	76.35	897.84
Livestock	500.38	465.77	655.13	1275.30

Source: Field Survey 2019
Note:
Total sample: Bong (35), Houay Su (38), Houay Sanguan (35), Houay Lao (20)
*price (0.3USD/kg)

Table 1. shows that upland rice in swidden field is the most common agricultural practice for the local people in northern Laos. However, some household, like in Houay Sanguan village tried to replace the swidden to the paddy field and others activities. Overall, more than 50% the households at the village had enough sufficiency in rice and the others not. The range insufficient value of rice between 60 US dollars to 327.82 US dollars per household per year. It indicates that the household with less activities on swidden has a risk to vulnerability to the food security for each household in the village.

The value of various swidden activities in the study area are different in each village. These indicates the strategy for each household at the village level to encounter the sufficiency rice. Almost in the all villages, non-timber forest products (NTFPs) have significant value to cover their food security. However, the value from livestock and commercial crop in Houay Lao village more significant than value from NTFPs (Fig.2). It examines the market and road access in Houay Lao village are well available. Otherwise, the household in remote village with poor access are still depending on NTFPs products for their main activities to get cash income and make ends meet.

DISCUSSION

This study clarified that shifting cultivation can provide a lot of products for their food security. Upland rice activity is still important for the household to get rice sufficiency in each household. Generally, paddy is the backbone of food security to the household (Castella and Erout, 2002). However, increasing of landowner of paddy field in the study area are not significantly related to the rice sufficiency in each household.

They who replacing the upland field (shifting cultivation) to lowland field (paddy) could not fulfill their rice needs. Household that have met their rice needs begin to diversify their livelihood with cash crops and cattle and buffalo raising like in Houay Lao and Houay Su village. However, household that have not met their rice needs begin to collecting NTFPs as the best way to get cash income and cover their rice needs in advance like in Bong and Houay Sanguan village. In the end, this study need further research in livelihood strategies and its diversity to understand the strategy for the poor people to survive and met their needs.

ACKNOWLEDGMENTS

The authors would like to express sincere gratitude to all villagers and officers of Sone district, Houaphan province. This research could not be done without their cooperation

REFERENCES

Castella, J-C., Erout, A. 2002. Montane paddy rice: the cornerstone of agriculture production system in Bac Kan Province, Viet Nam. The Agriculture Publishing House (book): Doi Moi in the Mountain, Vietnam.

Castella, J-C., Lestrelin, G., Hett, C., Bourgoin, J., Fitriana, Y.R., Heinimann, A. & Pfund, J-L. 2013. Effects of landscape segregation on livelihood vulnerability: moving from extensive shifting cultivation to rotational agriculture and natural forests in northern Laos. Human Ecology, 41: 63–76.

Fujita, Y. and Phanvilay, K. (2008). Land and Forest Allocation in Lao People's Democratic Republic: Comparison of Case Studies from Community-Based Natural Resource Management Research. Society and Natural Resources, 21(2), pp. 120-133.

Vliet, N.V., Mertz, O., Heinimann, A., Langanke, T., Pascual, U., Schmook, B., Adams, C., Schmid-Vogt, D., Messerli, P., Leisz, S., Castella, J-C., Jorgensen, L., Birch-Thomsen, T., Hett, C., Bech-Brunn, T., Ickowitz, A., Vi, K.C., Yasuyuki, K., Fox, J., Padoch, C., Dressler, and W., Ziegler, A.D. 2012. Trends, drivers, and impacts of changes in swidden cultivation in tropical forest-agriculture frontiers: A global assessment. Global Environmental Change, 22: 418-429.

Proceedings of International Symposium on a New Era in Food Science and Technology 2019
UGSAS-GU & BWEL Joint Poster Session on Agricultural and Basin Water Environmental Sciences 2019: P22

Dynamics of dissolved organic carbon (DOC) and soil carbon sequestration in a deciduous forest

Islam Md Rashidul[1, 3], Yasuo Iimura[2], Takeo Onishi[1], Shinpei Yoshitake[3], Ashik Tahmidul[1, 3] and Toshiyuki Ohtsuka[3]

1. **Faculty of Applied Biological Science, Gifu University, Japan.**
2. **School of Environmental Science, The University of Shiga Prefecture, Japan**
3. **River Basin Research Centre, Gifu University, Japan.**

INTRODUCTION

Growing concern about climate change evoked interest in the role of dissolved organic matter (DOM) in the global C balance (Hedges, 2002). DOC is often considered the most labile portion of organic matter in soil and these fluxes are small compared to the C fluxes due to primary productivity and heterotrophic respiration in terrestrial ecosystems. DOC is one of the most actively cycling soil organic pools and its significance is translocation and stabilization of organic matter in forest soils (Fujii et al. 2009) whereas the DOC export fluxes with runoff might represent a substantial contribution to the net C budget of ecosystems (Kindler et al. 2011). We studied in the Takayama Forest, is a part of the Asia Flux network, the carbon fluxes and budgets within it have been measured regularly since October 1993. Biometric-based carbon flux measurements have been conducted intensively in the Takayama Forest, so that where and how the forest stores C is well known (Ohtsuka et al. 2007). Yet there are no previous studies about the contribution of DOC fluxes to the carbon accumulation in the soil of this study site, and the contribution of DOC fluxes to the large soil organic carbon pool remains unknown. Although, the 1–2 m depth snow generally has melted at the end of April, the study of melt water draining dynamics during the snowmelt period was insufficient. Plot based Biometric NEP measurement has some uncertainty due mainly to the model estimation error of annual soil respiration and root respiration. Errors in measuring or estimating any one of these fluxes can lead to relatively large errors in the net exchange. Therefore, we need to measure other fluxes such as C in precipitation, and losses of C such as elution of DOC by soil water flow. However, we used small watershed techniques which has been extremely useful for quantitative study of element fluxes and cycling with appropriate hydrologic control and precise estimates of chemical inputs and outputs can be obtained. Watershed based aquatic C dynamics is not only measuring C sequestration in soil organic matter but also for aquatic C export from forests, (Bormann and Likens, 1967). The investigations of linking the DOC fluxes in temperate forest ecosystems to the soil organic carbon in Japan were limited (Shibata et al. 2001). Laboratory experiment found that added to a subsoil was retained 60–90% of DOC by sorption (Kaiser and Zech, 1997). However, in field level accumulation of carbon in soil by DOC fluxes and their leaching loss from different forested ecosystem is rare and their contribution to net C balance is uncertain.

The present study focuses with the objectives are:

1. To estimate soil C accumulation and aquatic C export using water-shed technique.

MATERIALS AND METHODS

Study site: Takayama forest is located in the central region of the main island of Japan, far from the heart of city, a permanent plot of 1 ha (100 m * 100 m) was set on a west-facing slope is in forest belonging to the river basin research center, Gifu university, Japan.

1. Lysimeters: We set small free tension lysimeters of each 137 cm^2 in 7 July, 2018 at 0 cm (litter layer) and 60 cm depth with five points each in three different place viz. Ridge, middle and down slope respectively. Lysimeters have been used to measure DOC dynamics in litter layer (0cm) and deep soil layer (60cm) of three soil profiles to quantity of DOC input to construct C accumulation at certain depth of soil.

2. Small watershed techniques: To construct runoff dynamics (daily discharge) in both growing and snow melting period a par shall flume type flow meter was setup in the 4-hectare watershed on 29 August, 2018 and first water Samples were collected in 25 September, 2018. An auto sampler was up for daily water sample collection in order to measure daily DOC.

3. Laboratory analysis: EC, pH, DOC, C and N density, Bulk density: samples are filtered by 0.45um filter (Whatman, GF/C), the concentrations of DOC were measured with a total organic carbon analyzer (TOC-V, Shimadzu, Japan). Total carbon and nitrogen contents of soil (dry weight base) were measured with a CN-analyzer (SUMIGRAPH NC-22F).

4. Statistical analyses: All data are presented as arithmetic means. One-way ANOVA was used to detect significant differences ($P < 0.05$). Analyses were performed with Statistics 10.

RESULTS AND DISCUSSION

Soil chemistry: The soil at the study site has a very thick and dark colored A horizon with high C content, particularly in the 2A horizon, (FAO 2014) is used as a criterion for andisol (a soil order that is rich in soil carbon and allophane and/or organo-aluminum) along with Japanese volcanic ash soils.

a. Difference between three soil profiles: Slope position at watershed scale varies greatly. Thickness of black soil layer is lower in ridge portion but gradually increases to middle and down slopes (>60cm) and large surface layer (A) around 32 cm in down slope was found. Soil organic carbon at 5-10 cm depth is higher in ridge slope and gradually decreases to down slopes (151.9, 142.4 and 113.3 C g kg^{-1}). Higher C: N ratio
(High N content) and high moisture contents was found in down slope than ridge and middle slopes (Table, 1). 60 cm depth reaches both surface and subsurface soil of Ridge and middle slopes but down slope within surface soil due to large A and 2A soil horizon. Litter leachates DOC production, sorption and water volume is significantly higher in ridge and middle slopes than down slope profile.

1. Water dynamics: Inter annual and seasonal variability is higher among three soil profiles. In 2018, monthly water found in litter leachate 0.87±0.16, 1.06±0.16 and 0.64±0.08 litter in ridge, middle and down respectively. But in contrast the in 2019 growing season (3 month) water volume was found 1.97±0.29, 2.65±0.63 and 2.08±0.44 litter respectively. No significant difference was found among soil profiles in case of deep soil layer (60cm). Monthly water depth was around 3-10 cm among them.

2. DOC dynamics: DOC concentration in Growing season (2018) 2 fold and (2019) 3 fold larger than winter season but in both year Ridge and middle was significantly different from down slopes. Mean concentration in growing season 2018 was found 16.86±0.0.83, 15.56±1.49 and 10.11±0.74 mg L^{-1} and

2019 was found (25.01±3.81, 23.25±1.38 and 14.81±1.41 mg L^{-1}) and winter season (Dec, 2018-april 2019) was found 10.18±1.47,10.64±0.64 and 7.07±0.42 mgL^{-1}. No significance difference was found in deep soil layer both in seasonality and inter-annual variation. Average monthly concentration was found 5.04±0.54, 4.93±0.42 and 3.19±0.42 mg L^{-1}.

3. DOC input to soil: DOC fluxes of ridge and middle in litter leachates were also significantly different from down slopes in both year (2018 and 2019). 2018, monthly DOC input to soil was 8.52±2.22, 10.93±2.35 and 3.91±0.608 and 2019 was found 37.68, 49.48 and 21.16 $kgha^{-1}$. But no significance difference at 60 cm depth, where the monthly flux (2018) was found 0.618±0.246, 0.4528±0.22 and 0.317±0.076 and 2019 was 0.2215, 0.2652 and 0.7147 $kgha^{-1}$ respectively.

4. DOC adsorption: DOC storage at 60 cm depth of ridge and middle was significantly different from down slopes in both year (2018 and 2019). But the no significant different was found for sorption rate (92%) for three sites. DOC accumulation was lower in 2018 may- 2019 April around 60 $kgha^{-1}$ and 2019 (may- July) was found 107 $kgha^{-1}$.

5. Stream water dynamics: Water year (August 2018 - 2019 July), we found irregular discharge in studied watershed. Discharge was only found during high rainfall occurred during July to September. During dry periods and Snow melt period we found no discharge in par-shall flow meter.

6. Stream DOC dynamics: Stream DOC concentration was 10 fold smaller than the DOC input to litter leachate. Monthly DOC concentration was found 2.08 mg L^{-1} and DOC flux was found 5.33 kg ha^{-1} 7 $month^{-1}$.

Table. 1 Chemical properties of three soil profiles (0-90 cm)

	Zones	C (g kg^{-1})	N (g kg^{-1})	C:N ratio	Bulk density (g cm^{-3})
Soil depth	**Ridge**				
5-12	**A1**	**151.9**	**9.9**	**15.34**	**0.5**
12-22	A2	93.7	6.1	15.36	0.48
22-42	AB	49	3.2	15.31	0.57
42-80	B1	21.1	1.7	12.41	0.77
80+	B2C	2.9	2.1	1.38	0.89
	Middle				
5-11	**A1**	**142.4**	**9.7**	**14.68**	**0.41**
11-25	A2	84.9	4.9	17.33	0.48
25-47	**2A**	**67.5**	**3.4**	**19.85**	**0.5**
47-58	2AB	63.9	3.3	19.36	
58-80	B1	21.8	1.8	12.11	0.62
80+	B2C	16.7	1.5	11.13	0.8
	Down				
5-32	**A1**	**113.3**	**6.6**	**17.17**	**0.43**
32-73	**2A**	**100.8**	**4.4**	**22.91**	**0.47**
73-80	2AB	55.9	3.1	18.03	0.62
80+	B1	20.6	1.8	11.44	0.74

Table. 2 Monthly mean litter leachate DOC conc. (mg L^{-1}), water volume (L) and Flux; Storage (kg ha^{-1}) at three profiles

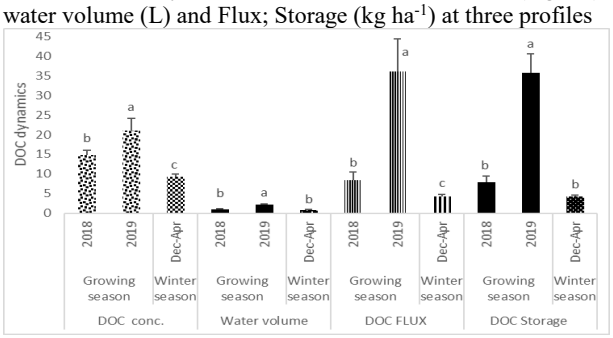

b. Soil profiles at watershed scale: Soil heterogeneity and thickness of A horizon variability, we used three soil profile in watershed scale. The distinct soil layers and their SOC contents signifies the importance of slope position in hilly areas. The C: N ratios at three sites were strongly positively correlated. Slope wise variation not only for decomposition but also for temperature, pH, EC, plant litter, root exudates, hydrological inputs and other chemical properties of soils. With pH and EC both SOC and DOC production at surface soil was strongly correlated. Thus it indicates SOC and DOC production at three site largely depends on the slope position (Fig.1) but the sorption of DOC at 60 cm depth is uniform around >90% at three site indicates variability of Sorption rate (%) in Takayama andisol soil is negligible. At watershed scale, upper and middle portion contains much C due to high input of DOC than lower position (down) but C stability is more than upper sites due to lower decomposition. DOC retention in mineral sub-soils within the ranges of 0-90 cm depth in 17 sites around 40-370 kg ha^{-1} $year^{-1}$ (Currie et al. 1996). Moreover, Kawahigashi (2011) reported that andisols, adsorbing more than 90% of DOC, and that DOC rarely leaches from andisols to stream. In growing season (2018 and 2019) we found 65 $kgha^{-1}$ 5$month^{-1}$ and 107 $kgha^{-1}$ 3$month^{-1}$ (May-July) and in winter season 20 $kgha^{-1}$ 5$month^{-1}$. Amount of DOC fluxes is vital for much C accumulation (Fig.1). Therefore, at watershed scale, DOC plays a critical role in C sequestration in surface and subsurface soils due to its high sorption capacity and DOC concentration is very lower in lateral flow compared to litter leachate probably high adsorption in surface soil thus aquatic export is negligible (5.33 $kgha^{-1}$ 7$month^{-1}$) compared to heterotrophic respiration.

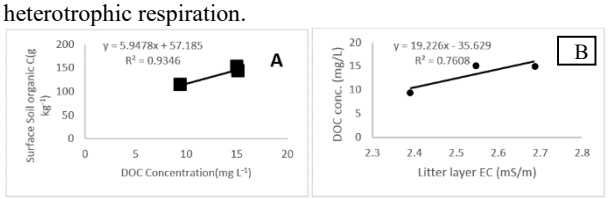

Fig.1, Relationships between (A) DOC concentration and Surface C content (B) EC (mS/m) and DOC flux of three soil profiles.

REFERENCES

Bormann, FH., Likens, GE., (1967) Nutrient cycling, Science, 177: 424-9.

Currie, W. S., Aber, J. D., McDowell, W. H., Boone, R. D., and Magill, A. H. (1996) Vertical transport of dissolved organic C and N under long-term N amendments in pine and hardwood forests. Biogeochemistry, 35(3), 471-505.

Fujii, K., Uemura, M., Hayakawa, C., Funakawa, S., Kosaki, T., and Ohta, S. (2009) Fluxes of dissolved organic carbon in two tropical forest ecosystems of East Kalimantan, Indonesia. Geoderma, 152(1-2), 127-136.

Hedges, J. I., (2002) Why dissolved organic matter?, Biogeochemistry of Marine Dissolved Organic Matter. Academic Press, San Diego, pp. 1–33.

Kaiser, K., and Zech, W., (1997) Competitive sorption of dissolved organic matter fractions to soils and related mineral phases. Soil Science Society of America Journal, 61(1), 64-69.

Kindler, R., Siemens, J. A. N., Kaiser, K., Walmsley, D. C., Bernhofer, C., Buchmann, N., and Heim, A. (2011) Dissolved carbon leaching from soil is a crucial component of the net ecosystem carbon balance. Global Change Biology, 17(2), 1167-1185.

Ohtsuka, T., Mo, W., Satomura, T., Inatomi, M., and Koizumi, H. (2007) Biometric based carbon flux measurements and net ecosystem production (NEP) in a temperate deciduous broad-leaved forest beneath a flux tower. Ecosystems, 10(2), 324-334.

Shibata, H., Mitsuhashi, H., Miyake, Y., & Nakano, S. (2001) Dissolved and particulate carbon dynamics in a cool temperate forested basin in northern Japan. Hydrological Proceses, 15(10), 1817-1828.

Proceedings of International Symposium on a New Era in Food Science and Technology 2019
UGSAS-GU & BWEL Joint Poster Session on Agricultural and Basin Water Environmental Sciences 2019: P23

A paired catchment study of nitrogen dynamics in a cool-temperate mixed deciduous broad-leaved and coniferous evergreen forest, central Japan

Tahmidul Ashik[1, 2], Takeo Onishi[2], Rashidul Islam[1, 2], Cao Ruoming[1, 3] and Toshiyuki Ohtsuka[1]

1. **River Basin Research Centre, Gifu University**
2. **Faculty of Applied Biological Science, Gifu University**
3. **The United Graduate School of Agricultural Science, Gifu University**

INTRODUCTION

Nitrogen (N) which is considered an essential nutrient for plants, can be deposited into forest ecosystem from the atmosphere via the hydrological pathway or dry deposition process. Plant can uptake nitrogen for growth by root absorption from soil (NH_4^+ and NO_3^-) and from atmosphere (NO_2^- and NH_3^+) (Rennenberg and Gessler, 1999). Paired catchment studies involve the use of two catchments with similar characteristics in terms of slope, aspect, soils, geology, area, climate and vegetation located adjacent or in close proximity to each other. Following a calibration period, where both catchments are monitored.

In previous studies, the annual runoff of two types of forests at the same basin was measured by long-term observation while the forest was being converted from a deciduous broadleaf type to an evergreen coniferous type (Swank, and Douglass, 1974).

In Kuraiyama forest biogeochemistry studies area is divided into two catchment, viz. A (Deciduous forest type) and B (Coniferous forest type). Catchment area for deciduous (0.71km^2) and coniferous forest (0.61km^2) is about same, average slope (21.1°), maximum and minimum elevation, geological type, soil type (Nohi rhyolite), precipitation and maximum and minimum temperature are also same for both type of forest. The difference of two catchments is only vegetation difference, one catchment is artificially planted coniferous type and another is broad leaved deciduous type. The deciduous forest floor is covered with a high density of bush, sasa bamboo grass and a little layer and coniferous forest floor is uncovered.

In Kuraiyama forest hydrological characteristics studies of runoff water under watershed had indicated that annual discharge in deciduous forest (5.39mm/day) is higher than the coniferous forest (4.76mm/day) because of no leaves in broadleaf deciduous forests during winter season, the more snow can reach the ground (Rahmat et al. 2019). But peak discharge is higher in coniferous forest (1.69m^3/s/km^2) than the deciduous forest (1.61m^3/s/km^2) during rainy season and after rainfall ended the discharge in coniferous forest decreased very rapidly. According to Komatsu et al. (2011) it can be concluded that the annual runoff in broadleaf deciduous is higher than the coniferous evergreen in the region with high winter precipitation. It also estimate that organic matter in coniferous forest was concentrated only in surface soil due to the accumulation of hardly decomposable fallen leaves and in deciduous forest organic matter was distributed to the whole soil profile due to the dead and decomposed understory. And soil permeability is higher in deciduous forest.

In Kuraiyama the EC in watershed water is higher in deciduous forest because of ionic character (Higher amount of Na^+, K^+, Ca^{2+} and Mg^{2+} ion present in water). And nitrate nitrogen concentration is higher in coniferous forest. In broad leaved deciduous forest mineralization rate is higher than the coniferous forest because we found that the NH_4^+ concentration is higher in deciduous forest. The rate of NO_3^- leaching depends on soil drainage, rainfall, nitrate present in the soil, and plant uptake. There is no previous studies on nitrogen deposition by throughfall and NO_3^-N (mg/l) leaching from forest soil. It is the first time to study nitrogen dynamics in Kuraiyama forest. The present study shows the quantity of leaching of N from soils to streams in the pair catchment and pathways and reasons of higher N leaching from planted coniferous forests than secondary deciduous forests.

MATERIALS AND METHODS

Study site— The study site is the Kuraiyama experimental forest at Gifu University (137°11′-137°14′E and 35°58′-36°01′N), which is located in Gero City, Gifu Prefecture, Japan. Experimental plots are divided in two catchments (deciduous and coniferous evergreen). Two permanent plot (20m x 20m) have set in both catchments.

River water sample collection—Auto sampler had set up along the watershed in each catchment for collecting river water sample.

Field survey—For estimating the Nitrogen inputs into the forest through water flux, we have set up sampler in 9th April 2019 to collect water.

1. Lysimeter for collecting litter leachate (horizontal area 0.0144m^2)
2. Throughfall collector, consists of a funnel (horizontal area 0.0346m^2)
3. Bulk precipitation collector, consists of a funnel (horizontal area 0.0346m^2)

Observing soil mineralization—It will be observed during the growing season (May – November) and snow season (December – April)

Observing soil and air temperature—Stow Away Tidbit Temp. Logger have been set up for soil and air temperature.

Chemical analysis—pH and EC were measured by using a pH and EC meter (Horiba, D-54) after collecting the runoff and water sample. The concentrations of NH_4^+, NO_3^-, NO_2^- were measured using a ion chromatograph analyzer and total dissolve nitrogen (TDN) were measured using nutrient analyzer (QaAAtro 2-HR) by colorimetric methods.

RESULTS

Soil observation— Soil sample were collected from the four sample site from broadleaved deciduous and evergreen coniferous forest catchment. Soil pH, bulk density, NO_3^-N concentration and NH_4^+ concentration had been measured. The pH of evergreen forest soil and deciduous forest soil is 5.62 ± 0.18a and 5.45 ± 0.091a respectfully which are almost same. There are significant difference in bulk density between evergreen forest soil (0.679 ± 0.043a g/cm^3) and deciduous forest soil (0.410 ± 0.011b g/cm^3). The NO_3^-N and NH_4^+ concentration are almost same in both catchment. The NO_3^-N concentration in evergreen forest is 0.075 ± 0.024a mg/l and

deciduous forest is 0.096 ± 0.008a mg/l and for NH_4^+ concentration in evergreen forest is 0.099 ± 0.015a mg/l and for deciduous forest is 0.146 ± 0.041a mg/l. There is no significant difference among them.

River water hydrological characteristics— Auto sampler had been set previously in the both catchment for collecting river water sample every day. PH and EC is higher in broadleaved deciduous forest than the evergreen coniferous forest. All the nutrient conc. (Na^+, K^+, Ca^{2+}, Mg^{2+}, Cl^-) are higher in deciduous forest than the evergreen forest river water. Only NO_3^-N (Fig. 1) and SO_4^{2-} concentration is higher in the evergreen forest river water.

Dynamics of nitrogen in forest—In throughfall the concentration of NO_3^-N and NH_4^+ is higher in evergreen forest than the deciduous forest (Table 1). For average NO_3^-N fluxes, in evergreen forest (0.137±0.047 ka/ha/month) which is higher than the deciduous forest (0.089±0.055 kg/ha/month) flux. And for average NH_4^+ fluxes, in evergreen forest (0.935±0.533 kg/ha/month) which is lower than the deciduous forest (1.171±0.653 kg/ha/month) flux from May to July 2019 (Fig. 2). In litter leachate the concentration of NO_3^-N and NH_4^+ is higher in deciduous forest than the evergreen forest (Table 1). For average NO_3^-N and NH_4^+ fluxes, in evergreen forest (NO_3^-N = 0.129±0.054 kg/ha/month and NH_4^+ = 0.731±0.376 kg/ha/month) which is higher than the deciduous forest (NO_3^-N = 0.105±0.041 kg/ha/month and NH_4^+ = 0.610±0.238 kg/ha/month) fluxes from May to July 2019 (Fig. 2).

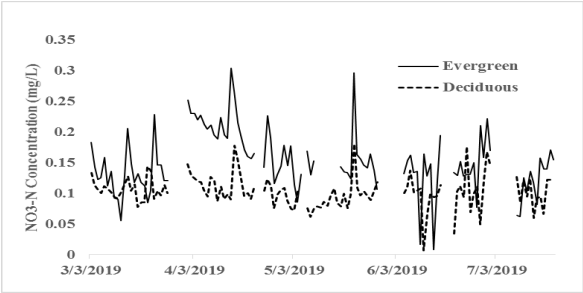

Fig. 1: NO_3^-N concentration in evergreen and deciduous Forest river water.

	NO_3^- (mg/L)		NH_4^+ (mg/L)	
	Evergreen	Deciduous	Evergreen	Deciduous
Through-fall	0.086±0.033a	0.061±0.0460a	0.495±0.245a	0.382±0.232a
Litter leachate	0.117±0.053a	0.206±0.029a	0.574±0.243a	0.734±0.206a
Bulk precipitation	0.115±0.037		0.219±0.073	

Table 1: Monthly NO_3^-N and NH_4^+ conc. of Evergreen and Deciduous forest from May to July 2019.

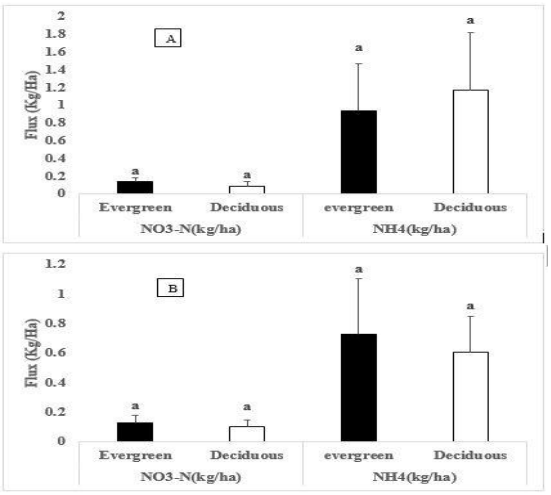

Fig. 2: Monthly flux (kg/ha) in evergreen and deciduous Forest (A) Throughfall Flux and (B) Litter Leachate Flux

DISCUSSION

Soil characteristics are same among the broadleaved deciduous and evergreen coniferous forest catchment. The pH, NO_3^-N and NN_4^+ concentration is almost same in the both catchment. Only the bulk density is higher in evergreen forest than coniferous forest, and higher bulk density indicates the low soil porosity and soil compactness. In river water in deciduous forest catchment the presence of Na^+, K^+, Ca^{2+}, Mg^{2+} ion are higher than the evergreen forest and for that the EC is higher in deciduous forest. NO_3^-N concentration is higher in evergreen forest. The annual NO_3^-N and NH_4^+ deposition is higher in evergreen forest than the deciduous forest with a high seepage of NO_3^-N and NH_4^+ compared to deciduous forest (Matson et al. 2002). In my experiment I only get 3 month data and I found that the throughfall deposition of NO_3^-N and NH_4^+ are almost same in both catchment. And for litter leachate the NO_3^-N and NH_4^+ flux is higher in evergreen coniferous forest. It is higher because the evergreen forest floor is uncovered and the deciduous forest floor is covered with sasa bamboo and bush and these understory needs extra nutrient for survive. Now my research is still running.

REFERENCES

Komatsu, H., Kume, T., and Otsuki, K. (2011) Increasing annual runoff-broadleaf or coniferous forests?. Hydrological Process 25, 302-318.

Matson, P., Lohse, K.A., and Hall, S.J. (2002) The globalization of nitrogen deposition: consequences for terrestrial ecosystems. Ambio 31, 113-119.

Rahmat, A., Ariyanto, D.P., Noda, K., Onishi, T., Ito, K., and Senge, M. (2019) Hydrological characteristics under deciduous broadleaf and evergreen coniferous forests in central Japan. International Journal of GEOMATE 16, 217-224.

Rennenberg, H., and Gessler, A. (1999) Consequences of N deposition to forest ecosystems-Recent results and future research needs. Water Air Soil Pollution 116, 47-64.

Swank, W.T., and Douglass, J.E. (1974) Streamflow greatly reduced by converting deciduous hardwood stands to pine. Science 185, 857-859.

Proceedings of International Symposium on a New Era in Food Science and Technology 2019
UGSAS-GU & BWEL Joint Poster Session on Agricultural and Basin Water Environmental Sciences 2019: P24

Evaluation of wave power generation potential in coastal area using wave model

Ryota Matsuura[1], Tomonao Kobayashi [2] and Jun Yoshino [2]
1. **Department of Energy Engineering, Graduate School of Natural Science and Technology, Gifu University**
2. **Environmental and Renewable Energy Systems Division, Graduate School of Engineering, Gifu University**

INTRODUCTION

In accordance with the basic energy plan, the amount of renewable energy introduced is increasing at an accelerating rate (METI, 2018). Japan is considered an island country and has a high abundance of marine energy, which is one of the renewable energies (NEDO, 2014). The ocean basic plan is also promoting the use of ocean energy (Cabinet Office, 2018). The introduction of wave power generation is delayed compared to other renewable energy. The reason is that energy density is low and it is difficult to extract energy, which is a big hurdle to commercialization.

Therefore, in this study, the wave energy potential in the coastal area was estimated, and the appropriate land of wave power generation and profitability of wave information was calculated.

Attempts to use ocean energy have existed for a long time. Maeda and Kinoshita et al. (1979) estimate the wave energy around Japan, and Katayama et al. (2014) rearranged the wave energy along the coast of Japan by increasing the number of target sites and the statistical period. These wave energies are ideal physical quantities that do not take into account the characteristics of the generator. Therefore, various wave characteristics required from the viewpoint of mechanical engineering and naval engineering were evaluated and arranged.

POTENTIAL OF WAVE POWER GENERATION ALONG JAPANESE SHORELINE

(1) Computational method

First, tried to select a suitable site for wave power generation throughout Japan. In this selection of suitable locations, the wave power at each point was calculated, and points with high wave power were extracted. The wave power was estimated using the significant wave height and the significant wave period every two hours of the nationwide ocean wave information network (NOWPHAS) (MLIT, 2018). The target period was five years from 2012 to 2016. The wave power used for the evaluation was an Omni-directional wave power that represents the amount of power that can be generated at that point. This is the amount of power generation on the premise that wave power can be received for waves coming from all directions without taking the wave direction into consideration. This wave power WE (kW / m) is expressed by the following formula.

$$\mathrm{WE} = \frac{\rho g^2}{64\pi} {H_{1/3}}^2 T_{1/3} = 0.492 {H_{1/3}}^2 T_{1/3} \quad (1)$$

Where ρ: seawater density (kg/m^3), g: gravitational acceleration (m/s^2), $H_{1/3}$: significant wave height (m), $T_{1/3}$: significant wave period (s).

(2) Results and discussions

The Fig.1 shows the average value and standard deviation of Omni-directional wave power estimated at the NOWPHAS observation point. As shown in this figure, the coastal area of the Sea of Japan, such as Sakata, generally has large average wave energy, but its standard deviation is also large. On the other hand, the standard deviation of wave energy is relatively small on the Pacific side, and the wave state is stable. Comparing the wave energy at each point, the points with the highest wave power are Sakata 11.9 kW / m, Kashima 9.85 kW / m, and Wajima 9.74 kW / m, respectively. However, Sakata and Wajima have large seasonal variations of waves as indicated by the standard deviation. From the viewpoint of wave power generation, it is desirable that the amount of power generation is large and there is no seasonal variation. From this point, Sakata and Wajima are not suitable for wave power generation due to large seasonal variations. On the other hand, Kashima has large wave energy and small standard deviation. Therefore, large capacity and stable power generation can be expected. From this result, it was found that the suitable site for wave power generation is the area around Kashima.

ESTIMATION OF ENERGY DISTRIBUTIONS AROUND HIGH-POTENTIAL AREA

(1) Computational method

a) Target area

In the previous section, the area around Kashima was selected as a suitable site for wave power generation from the coastal area

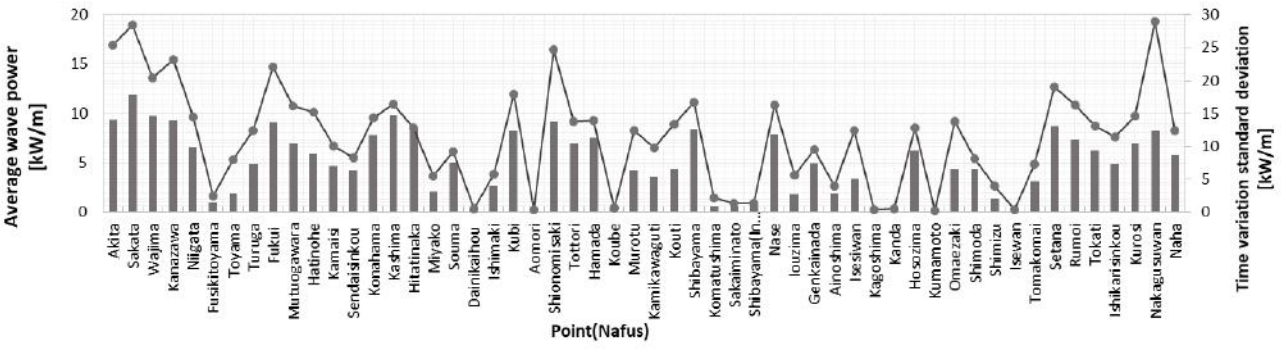

Fig.1 Average value of Omni-directional wave power at each point and time variation standard deviation (2012~2016year)
The bar graph shows the average wave power (left axis), and the line graph shows the standard deviation (right axis).

Table.1 Calculation condition

	Large area	medium area	small area
Lattice spacing	1/2°	1/8°	1/20°
longitude	115～180°	138～143.5°	140～142°
latitude	0～65°	33～38°	35.5～37°
Number of lattices	130×130	44×40	40×30

of Japan due to the magnitude of wave energy and seasonal stability. Here estimated how the wave energy is distributed in this area. Table.1 shows the conditions in each calculation area when conducting wave estimation. In the estimation, the calculation was performed by nesting three areas from the western Pacific (large area) to the Kashima area (small area). The target period was one year in 2016. Sea surface wind data were GSM-JP and MSM objective analysis data from the Japan Meteorological Agency (MLIT, 2016).

b) Wave prediction model

In this study, the third generation wave model, SWAN (version40.91ABC) was used. Output parameters were added to the small area based on this SWAN (The SWAN Team, 2013). The reason is to find the wave parameters from the viewpoint of mechanical engineering and ship engineering.

Here, as new wave parameters, the Omni-directional wave power, WE(Maximum directionally resolved wave power), $WE_{\theta WEmax}$ (maximum wave power direction), θ_{WEmax} (Direction of maximum directionally resolved wave power), SW (Spectral width), and d(Directionality coefficient) are calculated in accordance with IEC standard TS62600-101 (Wave Energy Resource Survey and Evaluation).

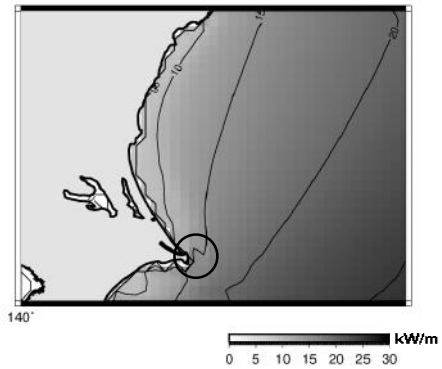

Fig.2 One-year-averaged Omni-directional power distribution (small area, 2016)

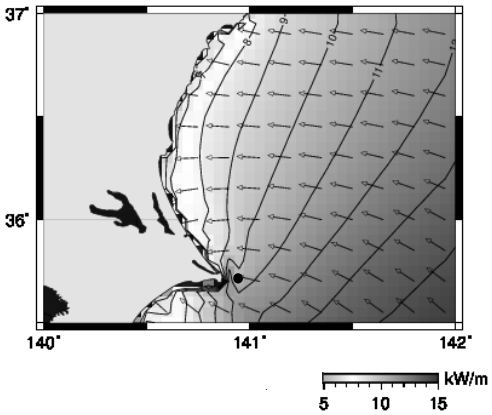

Fig.3 One-year-averaged Maximum directionally resolved wave power distribution (small area, 2016)

(2) Results and discussions

a) Omni-directional wave power

Fig.2 shows the average Omni-directional wave power distribution in 2016 for a small area. In Kashima and Hitatinaka, the Omni-directional wave power is 10～15 kW/m along the coast. From equation (1), the wave energy is proportional to the period. In this region, the wave energy is large because the swell generated in the Pacific is easy to reach. In particular, the point indicated by the black circle (the sea area around Choshi) has an energy of 13～20 kW/m. Therefore, the sea around Choshi is a promising area for wave power generation.

b) Maximum directionally resolved wave power

Maximum directionally resolved wave power imposes direction restrictions on the Omni-directional wave power. Therefore, it can be evaluated as a more realistic power generation amount. The Fig.3 shows the distribution of the annual average Maximum directionally resolved wave power and the Direction of maximum directionally resolved wave power in a small area. The black circle is 140.9 ° east longitude and 35.7 ° north latitude, the Omni-directional wave power is 15.8 kW / m, and the Maximum directionally resolved wave power is 11.2 kW / m. By limiting the wave direction, energy was reduced by 29%.

CONCLUSIONS

In this study, the appropriate location was selected using wave parameters required from the viewpoint of mechanical engineering and ship engineering. First, the wave energy of the whole country was calculated using NOWPHAS, and high energy areas were extracted. As a result, the area around Kashima with high annual average wave energy and little seasonal variation was suitable for wave power generation. Next, wave estimation was made around Kashima and a wave potential map was created. From this potential map, the sea around Choshi was promising for wave power generation. When the maximum wave energy direction was taken into account, the energy was reduced by 29% in this sea area due to direction restrictions.

REFERENCES

Ministry of Economy Trade and Industry (METI): Fifth Energy Basic Plan, 2018

New Energy Industrial Technology Development Organization (NEDO): NEDO Renewable Energy Technology White Paper Second Edition, Chapter 6, 2014

Cabinet Office: Basic Ocean Plan, 2018

Hisada Maeda, Ken Kinoshita: Wave Power Generation, Production Research Vol. 31, No. 11, 1979

Hiroyuki Katayama, Haruo Yoneyama, and Kenichiro Shimosako: Evaluation of wave power along the coast of Japan for selection of suitable locations for wave power generation, Journal of Japan Society of Civil Engineers B3 (Ocean Development), vol.70, No.2, I_73-I_78, 2014.

Port Bureau, Ministry of Land, Infrastructure, Transport and Tourism (MLIT): National Oceanographic Information Network 「 https://nowphas.mlit.go.jp/prg/pastdata/ 」 2018.10.10 Search

Ministry of Land, Infrastructure, Transport and Tourism Meteorological Operations Support Center: Objective Analysis Data, 2016

The SWAN Team : SWAN USER MANUAL SWAN Cycle Ⅲ version40.91ABC,2013

Proceedings of International Symposium on a New Era in Food Science and Technology 2019
UGSAS-GU & BWEL Joint Poster Session on Agricultural and Basin Water Environmental Sciences 2019: P25

A new *Pythium* species causing lettuce crown rot

Akihiro Hayano[1, 2], Kensuke Yamada[2], Ayaka Hieno[2], Haruhisa Suga[3] and Koji Kageyama[2]
1. **Graduate School of Natural Science and Technology, Gifu University, Gifu 501-1193, Japan**
2. **River Basin Research Center, Gifu University, Gifu 501-1193, Japan**
3. **Life Science Research Center, Gifu University, Gifu 501-1193, Japan**

INTRODUCTION

In 2016, the lettuce showing in the above-ground and root rot was observed in a lettuce field in Kagawa prefecture (Fig. 1a). The crown was rotted. (Fig. 1b) This disease occurred from October to December, and multiple species of *Pythium* and *Phytophthora* were detected. Among the isolated *Pythium* species one isolate did not match any existing *Pythium* species in BLAST search of the rDNA-ITS region. This study reveals that the isolate will be a new species causing lettuce disease.

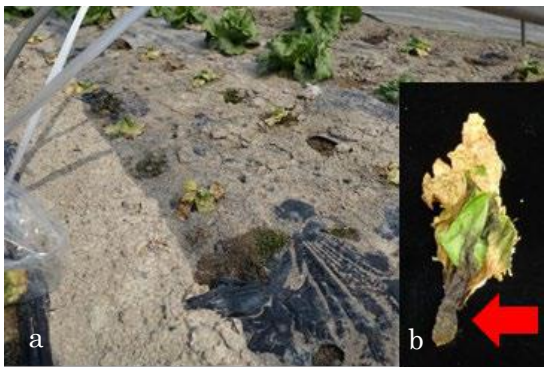

Fig. 1. Wilting and crown rot in of lettuce Kagawa prefecture.
a. wilting.
b. rotted crown.

MATERIALS AND METHODS

The crown of diseased lettuce was placed on *Pythium* genus selective medium to isolate this pathogen. The pathogenicity test was carried out at 20 ° C by placing a mycelial agar disc on a section of crown of lettuce. Molrcular phylogenetic analyses were conducted based on the sequencing the rDNA-ITS region, *cox* I, *cox* II, and β-tubulin. In morphological observation, a piece of turf grass infected with the isolate was put in water to induce the formation of reproductive structures.

RESULTS

Isolation
An isolate with fast-growing and non-septate hyphae like *Pythium* species was obtained from the root.

Pathogenicity test
The inoculated crown of lettuce developed a brown water-soaked lesion. Moreover, this isolate was re-isolated from the lesion.

Molecular phylogenetic analyses
When the sequence of the rDNA-ITS region was analyzed, it belonged to the molecular phylogenetic clade J of *Pythium* species classified by Lévesque and de Cock (2004). Additionally, the sequences of *cox* I, *cox* II and β-tubulin were examined, and multigene phylogenetic tree was constructed with the other members of clade J, resulting in a single lineage. (Fig. 2)

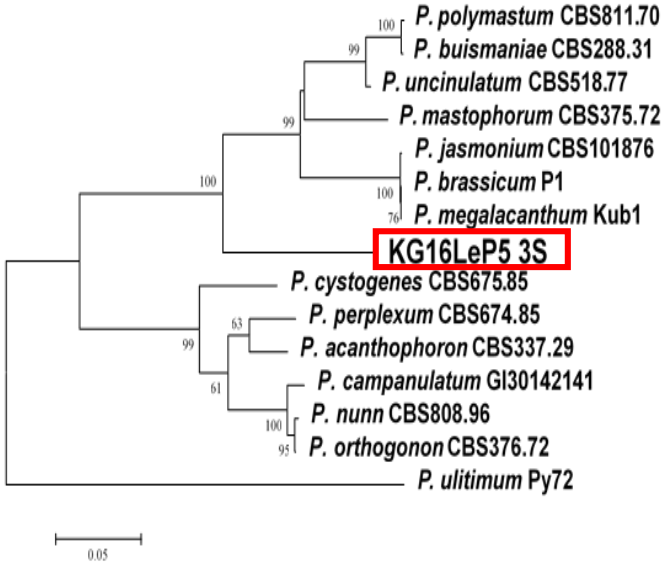

Fig. 2. Neighbor-joining phylogenetic tree based on the sequences of *cox* I, *cox* II and β-tubulin and rDNA-ITS region of *Pythium* clad J.

Morphological characterization and growth temperature
The morphological characteristics were confirmed; sporangia were spherical, average 27.3µm (18.7-35.6µm) (Fig. 3a), oogonium were smooth, spherical, 32.5µm (25.6-37.2µm) (Fig. 3b), and aplerotic oospores were unfilled, 27.6µm (21.0-30.2µm) (Fig. 3c). The antherdia were diclinous and the antheridial cells were clavate and crook-necked. (Fig. 3b) One to three the antheridia were attached per oogonium. Mycelial growth was observed between 5℃ and 25℃. (Fig. 4)

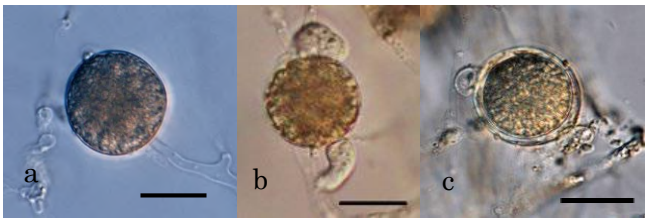

Bars=20µm

Fig. 3. Morphological characteristics.
a. Spherical sporangia.
b. Crook-necked antheridial cells and spherical oogonium.
c. Aplerotic oospore.

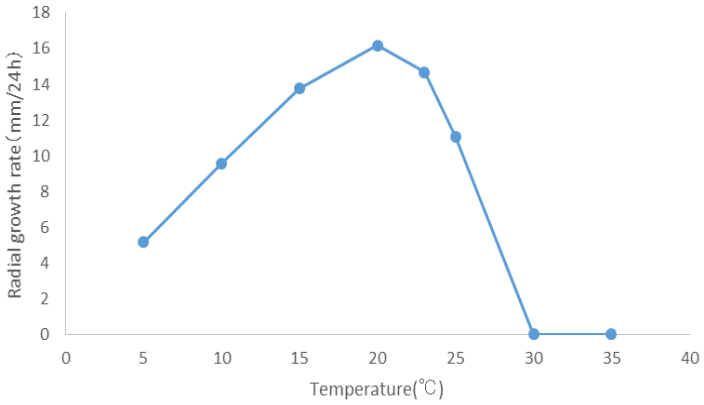

Fig. 4. Growth temperature reaction.

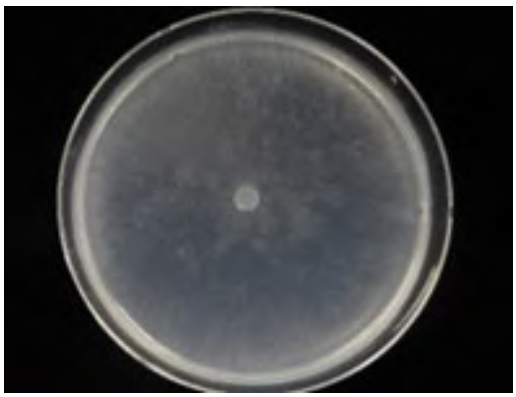

Fig. 5. Growth pattern on PCA.

DISCUSSION

The isolate from the rotted lettuce medulla showed pathogenicity to the crown of lettuce, and re-isolated from the lesioned part, suggesting that it would be a pathogen in lettuce. *P. irregulare* and *P. uncinatum* have been reported as pathogens that cause similar disease of lettuce. In molecular phylogenetic analyses, it belonged to molecular clade J of the geuns *Pythium* and showed a phylogenic monophyly. In addition, comparing to *P. perplexum*, which is a morphologically related species, the isolate was differed by diclinous antheridia, larger size of the reproductive structures and lower growth temperature. These results indicate that the isolate will be a new *Pythium* species causing lettuce disease.

REFERENCES

Lévesque C.A and Cock W.A.M.D (2004) Molecular phylogeny and taxonomy of the genus *Pythium*. Mycol. Res. 108 : 1363 – 1383.

Feng W., Hieno A., Kusunoki M., Suga H. and Kageyama K. (2019) LAMP Detection of Four Plant-Pathogenic Oomycetes and Its Application in Lettuce Fields. Plant Dis. 103 : 298 – 307.

Proceedings of International Symposium on a New Era in Food Science and Technology 2019
UGSAS-GU & BWEL Joint Poster Session on Agricultural and Basin Water Environmental Sciences 2019: P26

Future climate projections for storm surge associated with typhoon Jebi (2018) by a pseudo global warming downscaling

Masaya Toyoda, Jun Yoshino and Tomonao Kobayashi
Environmental and Renewable Energy Systems Division, Graduate School of Engineering, Gifu University

INTRODUCTION

Typhoon Jebi (2018), which attacked Japan in 2018, was a category 5 super typhoon (Fig. 1). The maximum wind speed was 55 m/s, breaking the previous wind speed record of 45 m/s. It caused a storm surge of 329 cm in Osaka and 233 cm in Kobe (Japan Meteorological Agency (JMA), 2018). Both storm surges exceeded the existing highest tide, which was recorded during Typhoon Nancy (1961). The total damage caused by Jebi was estimated to exceed 1 trillion yen (Mori et al., 2018), and there were numerous destructive events such as storm surge induced flood damage to the runway of Kansai International Airport (Mori et al., 2018) among recent typhoon disasters in Japan, Jebi produced remarkable storm surge destruction. In the future, as global warming progresses, coastal disasters caused by intensifying typhoons are likely to be also intensified.

In this research, future climate experiments for Typhoon Jebi (2018) are conducted, based on the pseudo- global warming downscaling technique using a storm surge model coupled with a high-resolution typhoon model. The purposes of this research are to evaluate the impacts of global warming on typhoon intensity (central pressure, maximum wind speed) and structure (radius of maximum wind speed), and to quantitatively assess the impact of global warming on maximum potential storm surges in Osaka Bay. In addition, the worst-case track scenario under the future climate is also investigated, taking into consideration typhoon intensity and the radius of maximum wind speed.

COMPUTATIONAL METHOD

(1) High-resolution typhoon model (HTM)

The high-resolution typhoon model (hereafter HTM) is used to simulate the intensity and size changes of overall life of typhoons. HTM is based on the mesoscale meteorological model MM5. The automatic movable nesting technique and the several kinds of physical parameterizations (e.g. the ocean mixed layer, dissipative heating, and sea-spray processes) are introduced into MM5 to express realistic typhoon intensity and structure accurately (Yoshino et al., 2013). The triply nested computational domains used in this study have a horizontal grid spacing of 27-km (D1), 9-km (D2), and 3-km (D3), respectively. The movable nesting technique is applied to both D2 and D3.

(2) Storm surge model (SSM)

The storm surge model (SSM) used in this study is composed of the nonlinear long-wave equation system, which predicts 2-dimensional distributions of sea-level anomalies and ocean current vectors. The typhoon atmospheric fields estimated by the ETM are inputted as the boundary conditions every 15 min. Computational domains for the SSM are set with a horizontal resolution of 1 km located around Osaka Bay. The topography data is sourced from the global earth surface relief

dataset ETOPO1 (produced by NOAA) with a horizontal grid of 1 min, and the global land use dataset, with a horizontal grid of 30 sec, is provided by the USGS. The SSM computation covers a time period of 1 day (24 hours) from 15:00 UTC on 3 September 2018 to 15:00 UTC on 4 September 2018.

(3) Present climate and future climate experiments

In this study, first of all, present climate experiments are carried out using NCEP FNL data as initial, boundary and assimilation conditions. We conduct future-climate experiments by applying the method of pseudo-global warming experiments (PGWE; Sato et al., 2007) to estimate future changes of intensity and structure of typhoons in comparison with present climate observations. The input conditions for the pseudo-global warming experiment are created by adding monthly average global warming difference (GWDs) to NCEP FNL. The GWDs are the difference of monthly mean fields between the future climate present climates. Temperature, Sea surface temperature, geopotential height, east-west wind speed, north-south wind speed and relative humidity are used as the3D monthly mean fields derived from the general circulation model GCMs. In this study, the monthly mean fields in the future climate are averaged during 2080-2099 by a total of 8 GCMs of the CMIP5 RCP8.5 scenario. In addition, the monthly mean fields in the present climate are averaged during 2000-2019 by 15 GCMs of the CMIP5 historical scenario (2000-2005) and 8 GCMs of the CMIP5 RCP8.5 scenario (2006-2019).

RESULTS AND DISCCUSION

(1) Present-climate experiment (CNTRL)

First, we will discuss the results of the present-climate experiment for Typhoon Jebi (Fig. 2) before discussing the

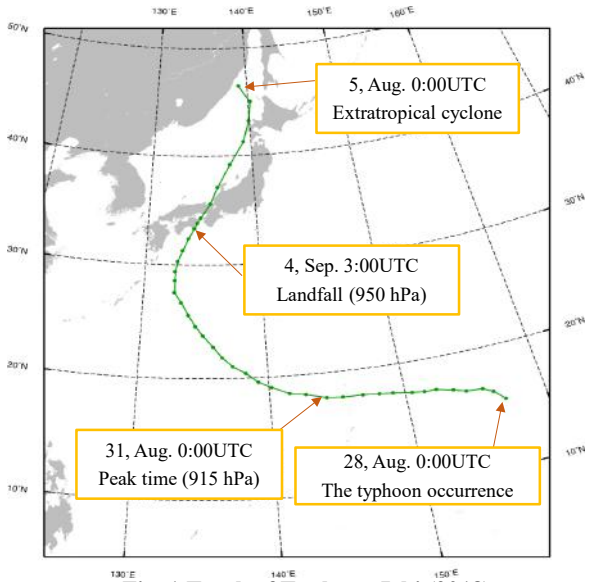

Fig. 1 Track of Typhoon Jebi (2018)

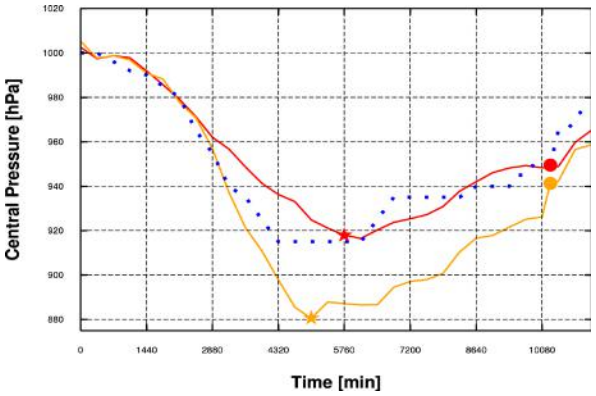

Fig. 2 Time series of the central pressure of Typhoon Jebi simulated by the HTM (present: red line, future: orange line), derived by the JMA best track (blue dotted line), the star is the peak time and the circle is the landfall time.

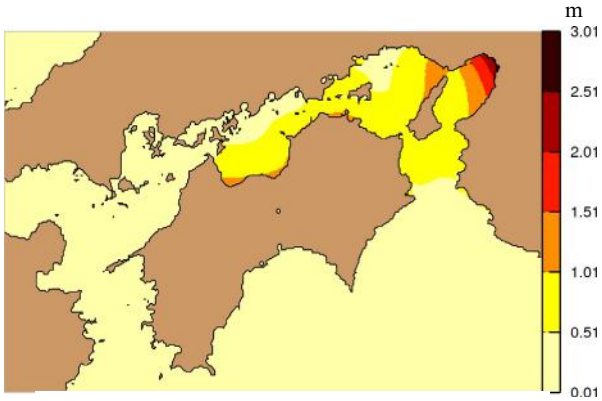

Fig. 3 Distribution of the storm surge caused by Typhoon Jebi simulated by present climate

results of the pseudo-global warming experiment (PGWE).

According to the JMA best track (Fig. 3; blue dotted line), the observed central pressures at peak time (5,760 min) and at landfall time to Japan (10,260 min) are 915 hPa and 950 hPa, respectively; the HTM results are 916 hPa and 948 hPa, respectively (Fig. 2; red line). The simulated typhoon intensities during the whole life cycle shows a good agreement with the observed values. The RMW at the time of storm surge was estimated to be 77.9 km, and the HTM simulated value was 70.0 km. The HTM results reproduced the observed structures in Jebi with a high accuracy.

The result for maximum sea level anomaly in Osaka Bay from the SSM is 282 cm (Fig. 2), which is close to the observed value of 277 cm at Osaka. Our numerical simulation technique can reproduce the mature intensity and structure of Super Typhoon Jebi and the storm surge at landfall time with high accuracy, which leads us to expect a certain precision for the PGWE.

(2) Maximum potential storm surge in the future climate

We will discuss the result of storm surge in the worst case (Figs. 3). The maximum sea level anomaly reached the highest value (328 cm) at Osaka when the typhoon followed a course0.3° further to the west than the actual typhoon course. In this time, the future change is +46.0 cm. Moreover, as the sea level anomaly increased in the Osaka bay, the area with a maximum sea level anomaly of 150 cm or more extended to the northern part of Shikoku Island. This suggests that the damage caused by future typhoons would be more widespread than under the present climate conditions. In addition, we

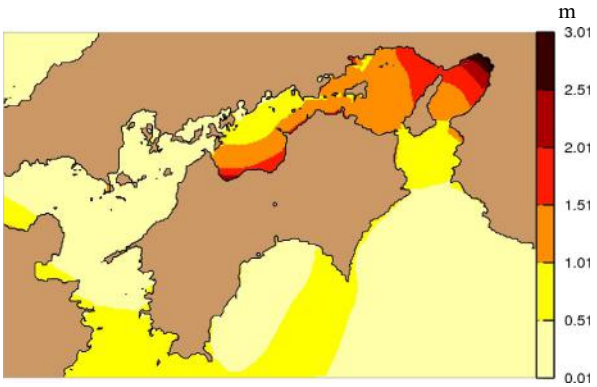

Fig. 4 Distribution of the worst storm surge caused by Typhoon Jebi simulated by PGWE.

investigated the reason of this typhoon course became the worst course for Osaka bay (Fig.4). The worst storm surge course is located about 80 km from Osaka Bay, and this distance will be consistent with the value of the RMW of Jebi (80.9 km) under the future climate. Therefore, in this case, Osaka and Kobe are considered to be just within the area of maximum wind speed, as a result, sea-level anomaly becomes the largest in all tracks of typhoon.

CONCLUSION

In this study, a pseudo-global warming experiment using a coupled high-resolution typhoon and storm surge model was performed for the case of Typhoon Jebi (2018). Results show that global warming causes typhoon intensity to increase at both peak and landfall times; typhoon associated storm surges also increase at Osaka Bay. Although the increase of the typhoon intensity at the time of landfall is small compared with the peak time, it needs to be careful because it is higher than the present climate. In addition, the worst case storm surge would be about 50 cm larger, and the worst course for a typhoon to take would be 0.3° west of the actual course. By applying the method of this research to other bays (e.g. Tokyo bay, Ise bay), it is expected that it will be possible to assess the global warming impact on storm surges in each coastal area considering typhoon intensity and structure.

ACKNOWLEDGEMENTS

This study was supported by JSPS Research Fellow (No.17J04771) and JSPS KAKENHI Grant (18H01542).

REFERENCES

Mori, N., T. Yasuda, T. Arikawa, T. Kataoka, S. Nakajo, K. Suzuki, Y. Yamanaka (2018): Typhoon Jebi Post-Event Survey of Coastal Damage in the Kansai Region, Japan. Coastal Engineering Journal, submitted

Yoshino, J., S. Arakawa, M. Toyoda, and T. Kobayashi (2015): Inter-comparison of global warming scenarios for typhoon intensity change using a High-Resolution Typhoon Model, JJSCE B2 (Coastal Engineering), Vol.71, No.2, 1519-1524 (in Japanese).

Sato, T., F. Kimura, and A. Kitoh (2007): Projection of global warming onto regional precipitation over Mongolia using a regional climate model, Journal of Hydrology, 333, 144-154.

Proceedings of International Symposium on a New Era in Food Science and Technology 2019
UGSAS-GU & BWEL Joint Poster Session on Agricultural and Basin Water Environmental Sciences 2019: P27

Prediction of object-movement by image processing with spectrum analysis

Takanori Ishii[1] and Rina Takada [2]

1. **Department of Energy, Engineering, Graduate School of Natural Science and Technology, Gifu University**
2. **Department of Civil Engineering, Faculty of Engineering, Gifu University**

INTRODUCTION

In recent years, the amount of photovoltaic power generation has increased worldwide in order to realize a recycling-oriented society. On the other hand, photovoltaic power generation is subject to adverse effects on the power system because the amount of power generation varies greatly depending on the weather conditions[1]. In particular, solar radiation is attenuated by the generation, development and annihilation of clouds, the movement of the clouds, and dust in the atmosphere such as aerosols, resulting in large temporal and spatial fluctuations[2]. Improving the accuracy of cloud movement prediction has the potential to bring about further development of stable power supply. Currently, there are two main types of cloud movement prediction: long-term and short-term. Long-term fluctuations throughout the year and throughout the day have periodicity and are relatively easy to predict. However, short-term fluctuations in the tens of minutes to several hours ahead have not yet reached a technique for predicting with high accuracy[3]. In the future, if a short-term prediction of cloud movement can be realized, it will be possible to adjust the power generation more delicately and take a step closer to the solution to the instability of renewable energy. In this study, we focused on short-term cloud movement prediction, and tried to develop the technology of cloud movement prediction using the time evolution method. In this paper, as a preparation stage, we created pseudo data of cloud images and made predictions. Furthermore, we compared and considered the cloud movement prediction with the original pseudo images.

CONTENTS

(1) Pseudo-data of cloud images

We investigate the characteristics about the forecast analysis of cloud movements by making the pseudo-data of the cloud images and analyzing its. The number of pixels about the pseudo-data image is 256×256. Make 24 pseudo-data images (a and b) in total, and 24 forecast images (c) by time development of original pseudo-data. After that, the motion of the pseudo image and the predicted image was synthesized (d).

(2) Forecast method

In this research, the forecast of cloud movements is performed based on the pseudo-data which I described in 2.1. Clouds move horizontally, develop and decay gradually. This spatiotemporal fluctuation is analyzed and forecasted on the spectral space. The image data uses 3D parameters in the x, y, and z directions defined in the .dat file. The intensity of the image data and the advection in the horizontal direction are represented by converting the image data to the spectral space. We try to forecast the image data by time development of them and converting spectral space to the image.

(3) Transformation and inverse transformation to spectral space

In this research, Fourier transform is performed on the image plane in order to analyze the intensity of the image data and the advection in the horizontal direction. The amplitudes and the phases in the spectral space which has the wave number plane (kx-ky plane) are calculated. If one-dimensional Fourier transform is extended to 3 dimension, Fourier transform for images can be similarly defined.

$$\mathrm{F}(\mathrm{u},\mathrm{v},\omega) = \frac{1}{2\pi}\int_{-\infty}^{\infty}\int_{-\infty}^{\infty} f(x,y,t)e^{-j(ux+vy+\omega t)}dxdydt \qquad (1)$$

where, $\mathrm{F}(\mathrm{u},\mathrm{v},\omega)$ is an arbitrary tertiary signal, imaginary unit is $\mathrm{j} = \sqrt{-1}$ and ω is angular frequency. u and v are wave number. Spectral space data can be converted to image data by performing inverse Fourier transform to the wave number plane of spectral space data.

(4) Extrapolation method

We try to forecast the images by extrapolating amplitudes and phases into the time direction on the spectral space after Fourier transform. Least squares method (LSM) is used in the time series direction as extrapolation method.

RESULTS

Location change of the cloud, intensity change of the cloud and size change of the cloud about the pseudo-data were analyzed. These clouds are considered as the state change of the actual clouds. Each forecast result was shown as (1) to (3).

(1) Pseudo-data forecast about location change of the cloud

Fig. 1 shows the forecast result of the pseudo-data about location change of the cloud. Location change of the pseudo-cloud can be accurately forecasted according to **Fig. 1**. It is considered that the linear approximation by LSM was able to accurately forecast location change of the pseudo-cloud because the pseudo-data changes regularly and linearly.

(2) Pseudo-data forecast about intensity change of the cloud

Fig. 2 shows the forecast result of the pseudo-data about intensity change of the cloud. Intensity change of the pseudo-cloud can be accurately forecasted according to **Fig. 2**. It is also considered that the linear approximation by LSM was able to accurately forecast intensity change of the pseudo-cloud because the pseudo-data changes regularly and linearly.

(3) Pseudo-data forecast about size change of the cloud

Fig. 3 shows the forecast result of the pseudo-data about size change of the cloud. Size change of the pseudo-cloud cannot be

accurately forecasted according to **Fig. 3**. Size change of the pseudo-cloud means that a nonzero value enters into a new region that was previously zero on the spectral space. The amplitude at the point where it was originally zero continues to be zero even in the subsequent forecast. For this reason, size change of the pseudo-cloud cannot be accurately forecasted and noise is added.

DISCUSSION

We knew that this method can cope with location change of the cloud and intensity change of the cloud in the pseudo-data analysis. However, it cannot cope with size change of the cloud.

Introducing a method to reduce noise or a new extrapolation method is cited as future issues and prospects. It is expected that image analysis will lead to the development of comprehensive system which can quantitatively understand various information such as a cloud amount, a cloud type and a cloud movement. If it becomes possible to combine these forecast methods with information from meteorological models or information from solar power generation measurement data, the forecast for the amount of solar power generation will be more accurate. First of all, after confirming that the behavior of the pseudo-data of the cloud images works correctly, we would like to use it for the meteorological satellite image obtained from Himawari-8. We would like to verify the accuracy of the prediction technology by comparing the predicted images with the actual cloud motion.

ACKNOWLEDGMENTS

The writing of this article was completed with great cooperation from teachers, members of the Renewable Energy Laboratory, and past seniors. We would like to express my gratitude to the people concerned and work hard for future research results.

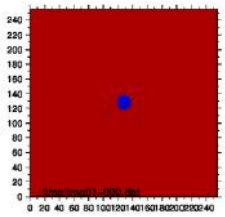

Fig.1(a) 1st image

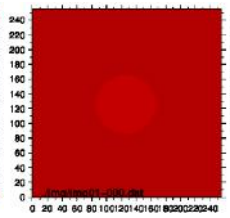

Fig.2(a) 1st image

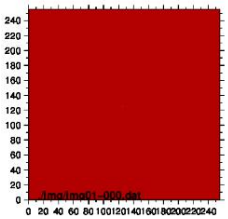

Fig. 3(a) 1st image

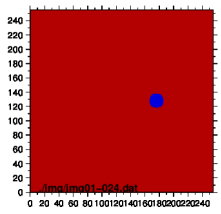

Fig. 1(b) 24th image

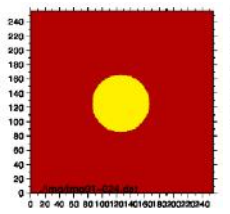

Fig. 2(b) 24th image

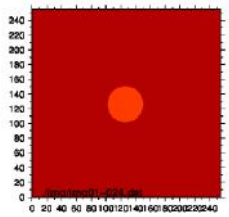

Fig. 3(b) 24th image

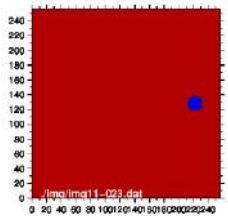

Fig. 1(c) 48th image

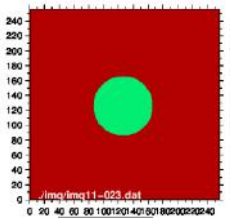

Fig. 2(c) 48th image

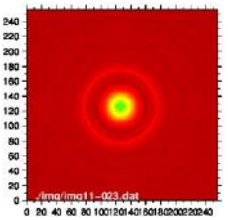

Fig. 3(c) 48th image

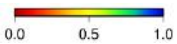

: Relative strength

REFERENCES

1) Naoto Ishibashi, Tatsuya Iizaka, Tohru Katsuno : Photovoltaic Power Generation Forecasting Technology for Supporting Energy Management Systems, Fuji Electric Technical Report (2013).
2) Hideaki Ohtake, Takumi Takashima, Takashi Oozeki : Forecast of Solar Irradiance obtained from a Local Forecast Model and its Validation of Forecast Errors, Journal of Japan of Energy and Resources, Vol.36, No.4(2015).
3) Japan Meteorological Agency : Widespread use of numerical forecasts, https://www.jma.go.jp/jma/kishou/know/whitep/1-3-10.html(Viewed August 2019).

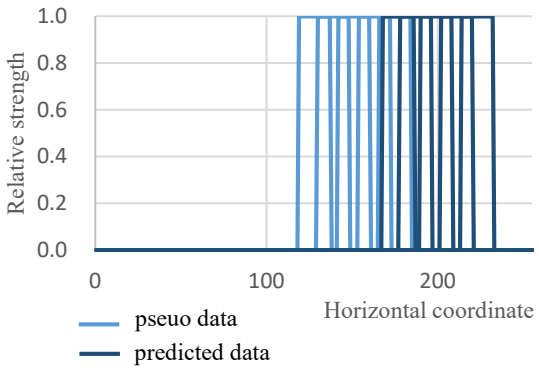

Fig.1(d) Object shifting

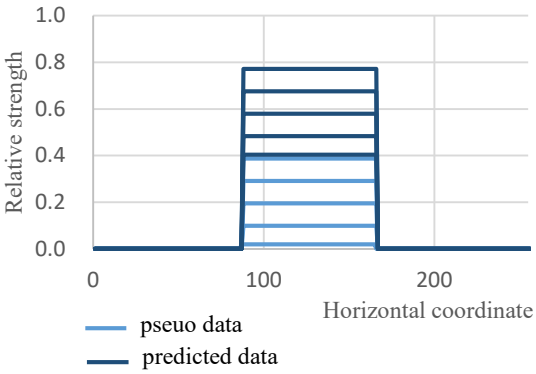

Fig.2(d) Object increasing its intensity

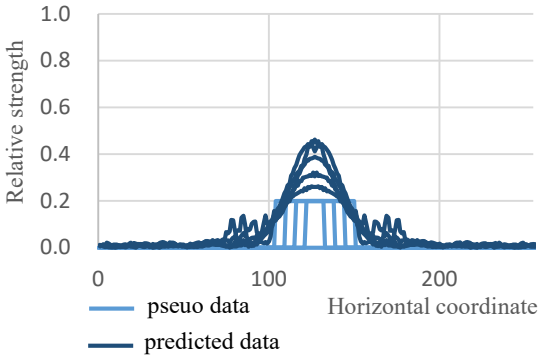

Fig. 3(d) Object becoming bigger

Proceedings of International Symposium on a New Era in Food Science and Technology 2019
UGSAS-GU & BWEL Joint Poster Session on Agricultural and Basin Water Environmental Sciences 2019: P28

A new idea of energy-saving activated sludge wastewater treatment process by promoting co-growth of algae and bacteria

Faisal Arsyad[1] and Fusheng Li[2]
1. **Graduate School of Natural Science and Technology, Gifu University, Japan**
2. **River Basin Research Center, Gifu University, Japan**

INTRODUCTION

The primary pollutant of domestic wastewater is organic matter, including proteins, amino acids, peptides, carbohydrates, fats, and fatty acids. Other pollutants in domestic wastewater include nutrients such as phosphorus and nitrogen. In domestic wastewater, the ratio of carbon, nitrogen, and phosphorous is generally suitable for the growth of activated sludge bacteria (Davies, 2005). Activated sludge process is dependent on oxygen availability because aerobic heterotrophic bacteria require oxygen to degrade the biodegradable organic matter. According to Bennett (2011), about 54%-90% of total supplied energy for WWTP is used in the aeration process. For energy saving, it is necessary to find new methods that could minimize the oxygen supply for the activated sludge process.

Promoting co-growth of algae and bacteria is a possible method for energy-saving in the activated sludge process. Algae, through their photosynthetic action, release oxygen that can probably be used by aerobic heterotrophic bacteria. Bacteria also release CO_2 that can probably be useful for algae in the photosynthesis process. Hence, the energy requirement for air supply can be lowered. The idea of algae photosynthesis application can be used as a pretreatment before the activated sludge process or combined in the process. However, the co-growth of algae and bacteria still have some significant problems. The main problem is the competition for nutrient uptake.

In this study, we investigated the growth and oxygen production potential of algae in the mixed liquid of the aeration tank. This research includes two specific items: determination of the growth of algae and dissolved oxygen (DO) production potential during co-growth of algae and bacteria, and the clarification of the relationship between algae, heterotrophic bacteria, and nitrifying bacteria during the process of co-growth of algae and bacteria.

MATERIALS AND METHODS

Activated sludge and the reactors

The mixed liquid in the aeration tank was collected from Hokubu Wastewater Treatment Plant in Gifu, Japan. The activated sludge in the liquid was allowed to settle to separate from the supernatant. The supernatant was used as a liquid medium, whereas the settled sludge was used for preparing a culturing medium with different suspended solid (SS) concentrations.

300 mL Erlenmeyer flasks, each with a working volume of 250 mL, were used as reactors. The first set of reactors were used to evaluate the effect of SS concentrations on co-growing of algae and bacteria. The concentrations of SS were 0 mg/L (R1), 500 mg/L (R2), 1000 mg/L (R3), 2000 mg/L (R4) and 5000 mg/L (R5), respectively. The second set of reactors were designed with the same SS concentration (2000 mg/L) but with different glucose concentrations: 0 mg/L (G0), 150 mg/L (G1) 300 mg/L (G2) and 600 mg/L (G3). These reactors were used for evaluation of the effect of biodegradable organic source on the co-growth of algae and bacteria.

Operation and analysis

All the reactors were placed on a shaker at 70 rpm installed in an incubator (Eyela FLI-2000). The incubation conditions for temperature, illumination, and dark/light cycle were 25°C, 13000 lux, and 12/12 hours, respectively. The liquid from each reactor was sampled twice a week for measurement of pH, DO, EC, chlorophyll-a, DOC, nitrate, nitrite, and ammonium.

pH and DO were measured by using a digital pH meter and DO meter, respectively. Chlorophyll-a was measured by following the trichromatic method. Dissolved Organic Carbon (DOC) was measured by a total organic carbon analyzer (Shimadzu, Japan). Nitrate, nitrite, and ammonium were measured by liquid chromatography-mass spectrometry (LC-MS) (Shimadzu, Japan).

RESULTS AND DISCUSSION

Effect of SS concentration on co-growth of algae and bacteria

Chlorophyll-a is generally used as a measurement index for quantification of algae concentration. As shown in Fig. 1 there were no significant increase of chlorophyll-a in all reactors from day one to day seven. This indicates a lag phase for algae to grow. Algae in R2, R3, R4, and R5 reactors showed significant increases for chlorophyll-a. The chlorophyll-a concentrations in the R1, R2, R3, R4, and R5 reactors at the end of the incubation period was 0.014, 0.088, 0.089, 0.280, and 0.404 μg/L, respectively. The concentration of chlorophyll-a changed along with SS concentrations and more chlorophyll-a was generated for the reactors with higher SS concentrations.

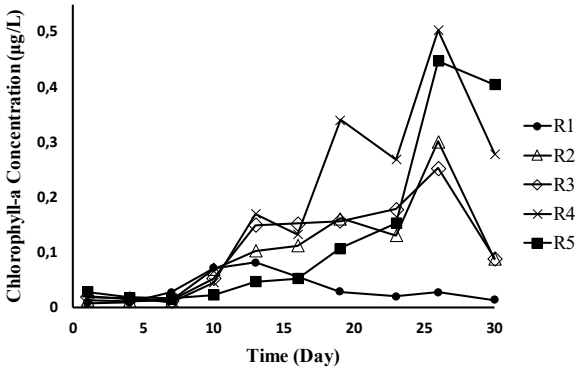

Fig. 1 Time profile of chlorophyll-a

The average of DO concentration during incubation in R1, R2, R3, R4, and R5 reactors was 6.29, 5.62, 4.98, 3.97, and 1.65 mg/L, respectively (Fig. 2). In the R5 reactor with the highest SS concentration (5000 mg/L), DO was the lowest and vice versa in the reactor R1 without SS (0 mg/L). The negative relationship between SS concentration and DO is probably due to the fact that more SS may contain a large number of aerobic heterotopic bacteria. The measured DO was the sum of DO released by algae and DO consumed by aerobic heterotrophic bacteria. Therefore, it is highly conceivable that more aerobic heterotrophic bacteria existing in the higher SS concentration reactors consumed more released oxygen from algae, thus leading to lower concentrations of DO detected in the reactors.

The significant growth of algae in the R1 reactor elevated the pH value as shown in Fig. 3, which may be due to the over-utilization of CO_2 by algae photosynthetic process that induced the conversion of HCO_3^- to CO_2. According to the reaction: $H^+ + HCO_3^- \rightleftharpoons CO_2 + H_2O$, H^+ consumed on HCO_3^- to CO2 conversion. The decrease of H^+ in the liquid led to an increase in pH (Zhang et al., 2014).

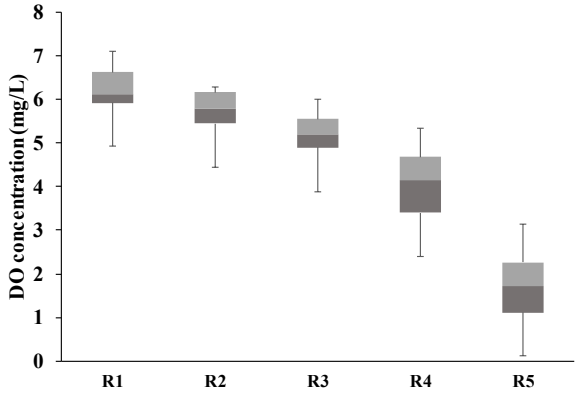

Fig. 2 Average DO concentration during incubation.

Effect of biodegradable organic matter concentration on co-growth of algae and bacteria

Different concentrations of glucose were added to observe the effect of biodegradable organic matter concentration on co-growth of algae and bacteria. A lag phase in G1, G2, and G3 reactors occurred until day 13 of incubation (Fig. 4). The lag phase was longer compared to G0, the reactor without glucose addition where algae started to grow after ten days of incubation. The longer lag phase in G1, G2, and G3 reactors occurred probably due to that the higher concentration of biodegradable organic matter promoted aerobic heterotrophic bacteria to grow and dominate in the reactors. The existence of aerobic heterotrophic bacteria in G1, G2, and G3 were reflected with the observed lower DO concentrations in these reactors as compared to G0 (Fig 5). The competition for nutrients between heterotrophic bacteria and algae might be a major reason behind the observed lag time difference.

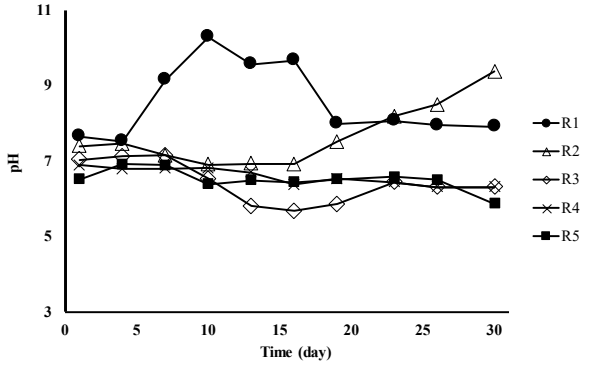

Fig. 3 pH during incubation.

Algal diversity was observed roughly by microscopic observation. *Chlorella sp*. was found to be the dominant species in all reactors. The diversity was obviously higher in the reactors added with higher concentrations of SS. It is thus conceivable that sludge in the mixed liquid of the aeration tank may contain more diversified algal species than those in the supernatant.

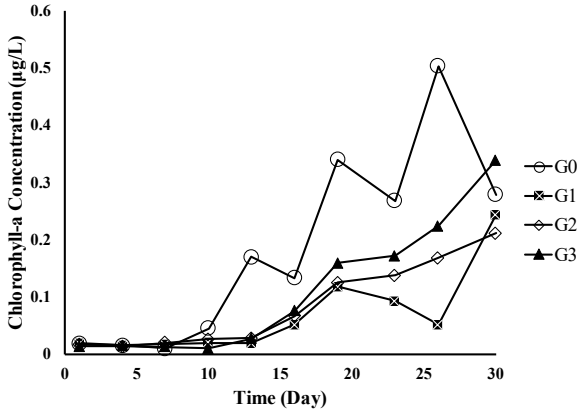

Fig. 4 Time profile of chlorophyll-a in the reactors added with glucose.

The results of the present study indicated algal growth in the mixed liquid connected from the aeration tank of a biological wastewater treatment plant was confirmed. The co-growth of algae allowed maintenance of DO at certain levels even without aeration. The co-growth of algae seemed to be inhibited by promoted growth of heterotrophic bacteria when a biodegradable substrate is supplied.

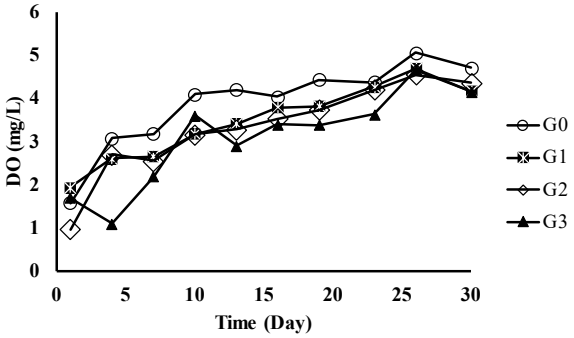

Fig. 5 DO time profile in the reactors added with glucose.

REFERENCES

Bennett, A. (2011). Wastewater treatment: Bubbling up for major energy saving. Filtration and Separation 48:42–43.

Davies, P. S. (2005). The biological basis of wastewater treatment. West of Scotland: Strathkelvin instruments Ltd.

Zhang, Q., Wang, T., Hong, Y. (2014). Investigation of initial pH effects on growth of an oleaginous microalgae Chlorella sp. HQ for lipid production and nutrient uptake. Water Science and Technology 70:712-719.

Proceedings of International Symposium on a New Era in Food Science and Technology 2019
UGSAS-GU & BWEL Joint Poster Session on Agricultural and Basin Water Environmental Sciences 2019: P29

A new species of *Pythium* with spiny oogonia isolated from forest soil in Japan

Daichi Iijima[1], Ayaka Hieno[1], Haruhisa Suga[2] and Koji Kageyama[1]
1. River Basin Research Center, Gifu University
2. Life Science Research Center, Gifu University

INTRODUCTION

The genus *Pythium* belongs to the Pythiaceae of the oomycetes which is different from true fungus. The genus is diployd and aseptate in vegetative hyphae and form zoospores in a vesicle that extends from the sporangium. Kirk et al. (2008) reported that there are about 150 species of *Pythium* reported in the world, but the number of species has been increasing year by year due to the recent reports of new species. Observation of the characteristics of asexual and sexual reproductive organs in order to clarify the characteristics of new species to be not found in known species in the genus *Pythium* and molecular phylogenetic analyses based on the sequence of *cox* 1 gene, rDNA ITS region and other regions are essential. A taxonomic key provided by van der Plaats Niterink (1981) is used to compare morphological features between species. The spine on the surface of oogonium are one of the important morphological features. In molecular phylogenyetic analysis, clades based on r DNA ITS region by Lévesque and de Cock (2004) are always used. Among the *Pythium* genus divided into 10 (A-K) clades, there are 6 species belonging to clade H, of which 5 species except for *P. undulatum* have spines in the oogonium. Therefore, clade H is a clade representing the genus *Pythium* which has spines in oogonium. In this study, we report a new species of a strain that has spines on oogonium isolated from a forest soil.

MATERIALS AND METHODS

The genus *Pythium* was isolated from a forest soil in Tosashimizu City, Kochi Prefecture by the bait isolation by Kenton et al. (2018). We analyzed the rDNA ITS region and *cox* 1 gene of the isolated strain, and created a molecular phylogenetic tree. We also observed the morphological characteristics of the sporangium, oogonium, antheridium and oospore.

RESULTS

Phylogenetic analyses

The total size of the rDNA ITS region of the isolate was 776bp, and BLAST search revealed that it belonged to the molecular strain clade H of the genus *Pythium* classified by Lévesque and de Cock (2004). The strain was shown to be closely related to *P. anandrum* by the molecular phylogenetic tree of the rDNA ITS region, but showed monophyly different from *P. anandrum* (Fig. 1). The phylogenetic tree combining the rDNA ITS region and the *cox* 1 gene was also monophyly (Fig. 2).

Morphological characteristics

Mature sporangia are ellipsoid, lemon-shaped, and egg-shaped with papilla at the apex (Fig. 3a-b). Occasionally, externally proliferating spores were seen (Fig. 3c). The size of the sporangia was 23.2-85.4 × 25.2-30.1 µm, with an average of 40.1 × 22.5 µm. There were no chlamydospore. Oogonium

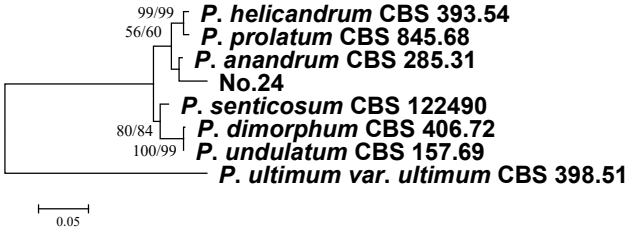

Fig. 1 Maximum Likely phylogenic tree based on the sequence of rDNA ITS region. Numbers over branches represent MP (left) and ML (right) bootstrap values (1000 replicates).

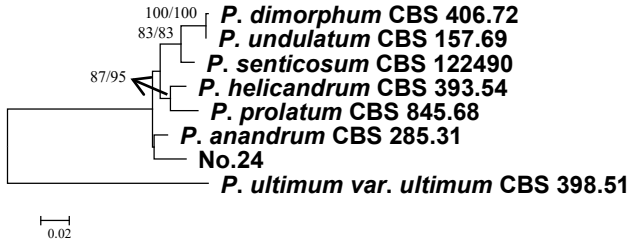

Fig. 2 Maximum Likely phylogenic tree based on combined sequence of the rDNA ITS region and *cox* 1gene. Numbers over branches represents MP (left) and ML (right) bootstrap values (1 000 replicates).

is spherical and has conical spines on the surface (Fig. 3e-h). The diameter of the oogonium was 19.3-30.2 (average 25.3) µm, and the length of the spines was 3.2-7.3 (average 4.6) µm. The antheridium is monoclinous, and one antheridium to oogonium (Fig. 3e). The antheridium just before bonding is inflated (Fig. 3e). Antheridum stlak is curved.Oospore is aplerotic (Fig. 3f-g). Rarely, two oospores are formed in the oogonium (Fig. 3g). The diameter of the oospore was 17.5-24.5 (average 21.0) µm. The mature oogonium is empty (Fig. 3h).

DISCUSSION

The isolated strain was molecularly phylogenetic monophyly with the rDNA ITS region and *cox* 1 gene. In addition, *P. anandrum*, which is closely related in molecular phylogeny, did not form an antheridum, and *P. senticosum*, which is morphologically similar, did not form a proliferating sporangium. These results indicate that the isolate will be a new species

REFERENCES

Kenton, S., Tyler J, D., Ellen, C., Chris, B. (2018) Detection of *Phytophthora cinnamomi* in Forest Soils by PCR on DNA Extracted from Leaf Disc Baits. Plant Health Progress 19(3):193-200.

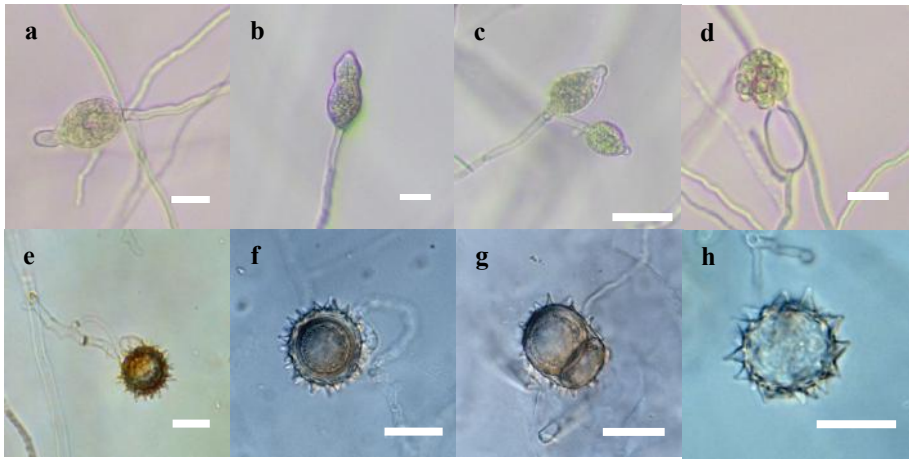

Fig. 3. Morphological characters of the isolate. a, mature lemon-shaped sporangium with papilla; b, ellipsoid sporangium ;c, externally proliferating sporangium; d, sporangium and vesicle with zoospores ; e, broad contact monoclinous antheridium on ornamented oogonium; f, aplerotic oospore in ornamental oogonium; g, two oospores in an oogonium ; h, abative oospore.

Bars=20 μ m

Kirk PM, Cannon PF, Minter DW, Stalpers JA （2008） Ainsworth & Bisby's Dictionary of the Fungi, tenth edition. CAB International, Wallingford, pp.771.

Lévesque CA, de Cock AWAM （2004） Molecular phylogeny and taxonomy of the genus Pythium. Mycol Res 108: 1363－1383.

van der Plaats-Niterink AJ. 1981. Monograph of the genus *Pythium*. Study Mycol 21:1–242.

Proceedings of International Symposium on a New Era in Food Science and Technology 2019
UGSAS-GU & BWEL Joint Poster Session on Agricultural and Basin Water Environmental Sciences 2019: P30

Bacterial community structure in fixed-bed activated carbon adsorbers treating Nagara River Water

Hiroki Maruyama[1], Wenjiao Li[2], Yasushi Isiguro[3], Toshiro Yamada[4] and Fusheng Li[3]
1. **Graduate School of Natural Science and Technology, Gifu University, Japan**
2. **Graduate School of Engineering, Gifu University, Japan**
3. **River Basin Research Center, Gifu University, Japan**
4. **Faculty of Engineering, Gifu University, Japan**

INTRODUCTION

In order to provide safe drinking water, the use of fixed bed granular activated carbon (GAC) as an advanced water purification unit is increasing in drinking water treatment plants (DWTP). GAC is effective in adsorbing a wide range of hazardous organic compounds, taste and odors, and precursors of chlorination and ozonation by-products. The application of GAC without pre-chlorination for surface water treatment allows microorganisms to develop on the GAC surface, thence changing GAC adsorbers into biological ones (BAC). In addition to the function of adsorption, we can also expect organic matter degradation as well as ammonia nitrification. However, little is known about the microorganism species in the biofilm of BAC, so with their roles and contributions to the risk relating to some newly emerging microbial agents of great health concern, such as bacterial and viral pathogens and antibiotic resistance bacteria and genes. The main objective of this study was to identify the structure and composition of bacterial community in the biofilm of BAC adsorbers treating surface water for a long term. The changes of bacterial density and species along the fixed bed depth and with GAC types were also investigated.

MATERIALS AND METHODS

A long-term down-flow mode experiment was conducted using GAC columns packed with five types of GAC, namely F400, F600, GL830, CW130 and GM830, respectively. The empty bed contact time (EBCT) was controlled identical for all five adsorbers as 20 minutes and the total run time was 13,000 hours. The raw water used in this study was sampled from Nagara River that contained low concentration of organic matter and various minerals necessary for the formation of BAC. Sampling from adsorber was conducted from three difference bed levels: top, middle and bottom, respectively. After sampling, water was filtered through 0.2μm membrane filter along with the raw water, and the filtrate was analyzed for dissolved organic carbon (DOC), UV absorbance at 260nm (UV260), fluorescence spectrum (EEM).

At the end of water feeding, three layers of BAC were taken out gently from each adsorber based on the designed three water sampling levels and, from each layer, DNA was extracted from the detached biofilm based on mechanical stirring. In addition to bacterial density and structure, gene *Intl 1* involved in the transmission of antibiotic resistance bacteria and genes (ARGs) in the biofilm was also quantified, together with four types of targeted ARGs (*tet G*, *tet X*, *tet M*, *sul* 1). The community structure of bacteria was analyzed through high throughput sequencing (Huang et al., 2018).

Table 1 Characteristics of all five GACs used in this study

GAC	F400	GM830	GL830	F600	CW130
Origin	Coal-based				Wood-based
Pore size	Pore volume (cm^3/g)				
~0.8 (submicro)	0.248	0.246	0.253	0.284	0.387
0.8~0.2 (micro)	0.194	0.162	0.215	0.031	0.091
2~ (meso)	0.162	0.161	0.100	0.037	0.002
Surface area (m^2/g)	1168	1140	1163	1619	1112
Pore volume (cm^3/g)	0.6037	0.569	0.568	0.351	0.351

RESULTS

The largest accumulative adsorption amount for dissolved organic matter was found with F400 and the smallest with F600 (Fig. 1). F400 has more micro-pores and meso-pores than F600 and the pore volume in these two size regions were reduced due to adsorption (Fig. 2).

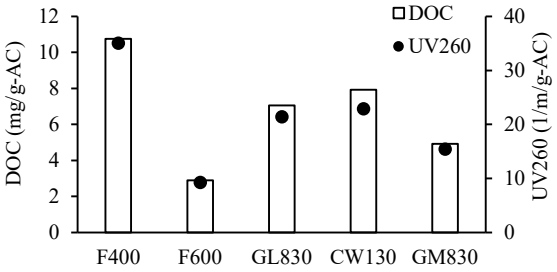

Fig. 1 Accumulative adsorption amounts of dissolved organic matter on five GACs. (The accumulative adsorption amount is calculated based on flow rate and the influent and effluent concentrations over the total runtime of 13,000 hours)

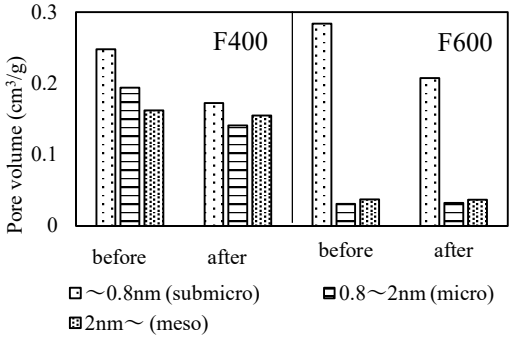

Fig. 2 Changes in pore volume of three different pore size ranges of F400 and F600 before and after use.

In the treated water from the outlet of the adsorbers, Gammaproteobacteria, unidentified_Actinobacteria, and Alphaproteobacteria were detected (Fig. 3a). Following the direction of water flow in the fixed bed, the relative abundance of Gammaproteobacteria was found getting higher (Fig. 3a). In the biofilm detached from BAC, Alphaproteobacteria, Gammaproteobacteria, Deltaproteo-bacteria and Nitrospira were detected for all three targeted BAC adsorbers (Fig. 3b). Deltaproteobacteria and Nitrospia, their relative abundance was obviously higher for the adsorber of F400 (Fig. 3b). This class includes the bacterial species of purple sulfur bacteria widely distributed in natural environments such as soil was well reported. The class of Unidentified-Actinobacteria generally refers to actinomycete, a group of bacterial species including those necessary for industrial production through their role in decomposing various organic compounds such as antibiotics and amino acids. In addition to various genera, Alphaproteobacteria also include many purple non-sulfur photosynthetic bacteria.

DISCUSSION

In the biofilm of all targeted BAC adsorbers and also the treated water, the presence of Alphaprobacteria, reported to be mainly consisted of purple non-sulfur photosynthetic bacteria that may be capable of decomposing organic matter, was confirmed, which probably contributed to the performance of BAC. Deltaproteobacteria were detected in the biofilm but not in the water after BAC treatment. Higher abundance of Nitrospira (nitrifying bacteria) was found in the BAC of F400, which showed the best performance in the uptake of dissolved organic matter.

REFERENCE

Huang K., Xia H., Wu Y., Chen J., Cui G., Li F., Chen Y., Wu N., Effects of earth-worms on the fate of tetracycline and fluoroquinolone resistance genes of sewage sludge during vermicomposting. Bioresource Technology, 259:32–39, 2018.

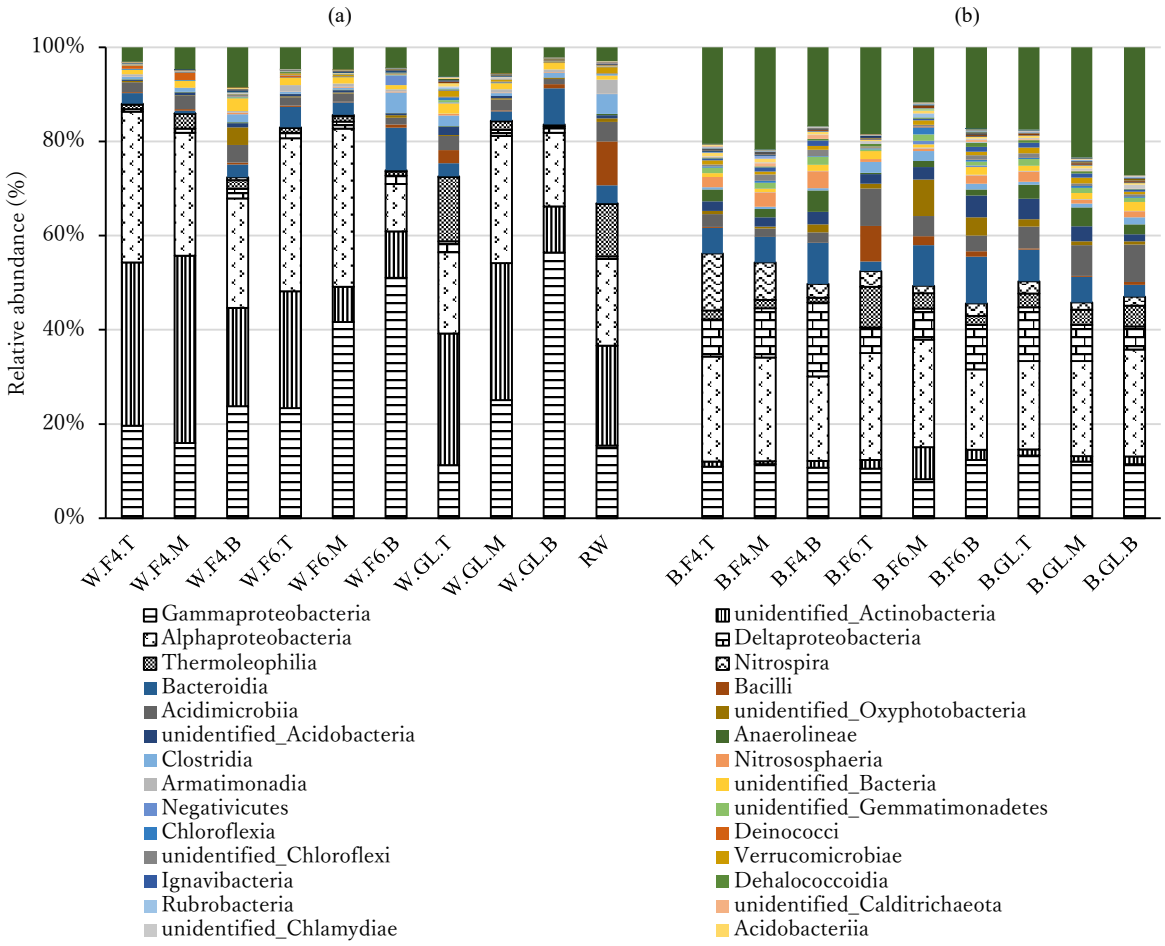

Fig. 3 Relative abundance of bacterial community structure in the treated water (a) and biofilm (b) of BAC at the class level (W: water, B: biofilm; F4: F400, F6: F600; T: top layer, M: middle layer, B: bottom layer)

Proceedings of International Symposium on a New Era in Food Science and Technology 2019
UGSAS-GU & BWEL Joint Poster Session on Agricultural and Basin Water Environmental Sciences 2019: P31

Efficient multi-site operation of optical communication between satellite and ground

Naoki Akiyama[1] and Akane Kusabuka[2]
1. **Gifu University**
2. **CHUBU Electric Power Co.,Inc.**

INTRODUCTION

In space communication, in addition to the conventional communication using electromagnetic waves, the establishment of communication technology using laser light has been promoted in recent years. In this space optical communication, the frequency of the carrier wave is high. It is excellent in terms of miniaturization and weight reduction of equipment, and high speed and large capacity communication. However, when this technology is applied to satellite-to-ground communications, the effects of clouds blocking the laser beam cannot be avoided. Asai et al.(2017) estimated the transmittance of laser light by reproducing clouds in the atmosphere using a weather forecast model. Their estimation results reproduce the actual measurements with high accuracy.

Therefore, in this study, we estimated the atmospheric transmittance for the whole area of Japan using their method. Furthermore, by making the ground station multi-site, we study to improve the probability of stable communication and evaluate the efficiency improvement effect.

MATERIALS AND METHODS

In this research, first, the meteorological field is reproduced by meso-meteorological model WRF. Using the result obtained from the calculation, the atmospheric transmittance is output by the atmospheric transmittance estimation model. The target period is one year from January to December 2016. The horizontal resolution of the estimation model is 0.05° × 0.05° and the target wavelength of the laser beam is 1550 nm.

RESULTS AND DISCUSSION

Figure 1 shows the distribution of annual average atmospheric transmittance in Japan in 2016. This figure shows that there is a clear difference in the distribution of atmospheric transmittance between the Sea of Japan and the Pacific Ocean. This is thought to be due to the difference between the Sea of Japan climate and the Pacific Ocean climate. The regions with high annual average atmospheric transmittance are the Okazaki Plain in Aichi Prefecture, Yamanashi Prefecture, a part of Nagano Prefecture, the Osaka Plain, and the remote islands in Okinawa Prefecture, which are about 60% to 70%. Comparing the results of 2016 and 2011, the first candidate for the standard for multi-site conversion was Hokuto City, Yamanashi Prefecture.

Laser light is attenuated by clouds. Therefore, the efficiency improvement of the system by multi-site (installing multiple ground sites) is examined.

Figure 2 shows the results of calculating the correlation coefficient around Hokuto City using the estimated atmospheric permeability. The site switching cycle is 1 hour. In this figure, a region with a high correlation coefficient spreads in the vicinity of Hokuto City, and the correlation coefficient decreases with increasing distance. In other words, the greater the distance between each ground site, the higher the efficiency improvement effect can be expected. In Obihiro City, Miyazaki Prefecture, Miyazaki City, and Miyakojima City, Okinawa Prefecture, the correlation coefficient is small and the annual average atmospheric permeability is high. Establishing a site at such a point is thought to lead to higher efficiency.

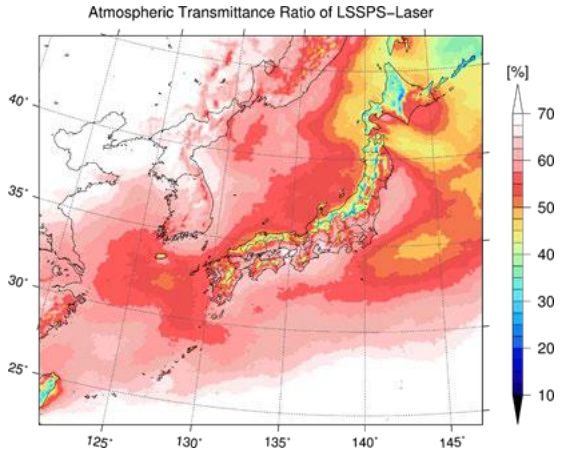

Fig. 1: Annual average atmospheric transmittance distribution throughout the Japanese archipelago

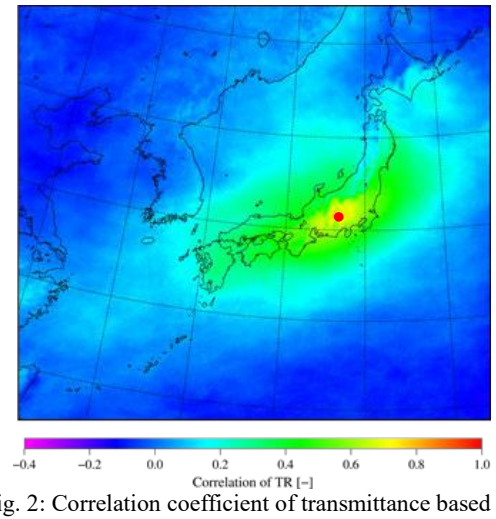

Fig. 2: Correlation coefficient of transmittance based on Hokuto City (Red-dotted point)

In order to evaluate the probability that communication can be performed stably, it is necessary to set the atmospheric transmittance that allows stable communication. However, the estimated atmospheric transmittance does not take into account all communicable states such as momentary cloud breaks. Therefore, using the observation result of the solar radiation intensity by the PV module sensor, we investigated the relationship between the probability of actual communication being possible and the atmospheric transmittance, and derived the "atmospheric transmittance that can be considered as stable communication". .

Fig. 3 is a CI (clear index) graph showing the degree of solar radiation intensity. For ideal clear weather, the CI is 1.0. Figure 4 shows a scatter plot that plots the annual average air permeability using this result on the horizontal axis and the probability that the CI exceeded the threshold value of 0.6 per

hour on the vertical axis. Regarding solar radiation fluctuations, data from April 2016 to March 2017 was used, and the target time was 9:00 to 15:00.

In order to perform satellite-to-ground optical communication smoothly, it is required that the threshold excess rate is at least 50%. From Fig. 4, when the probability that the CI exceeds the threshold value of 0.6 is 0.5, that is, 50%, the maximum value of hourly average atmospheric transmittance is 0.7. In addition, when the hourly average atmospheric transmittance is 70% or more, the probability that CI per hour exceeds 0.6 is plotted in a range where all points except two are higher than 50%. In other words, the condition required for atmospheric transmittance for stable communication is that the probability that the CI exceeds 0.6 is 50% or more, and it means that the hourly average atmospheric transmittance is 70% or more on the model. Therefore, in this study, we evaluate the actual efficiency improvement effect of multi-site by setting the condition that the stable communication is possible as "atmospheric permeability 70% or more".

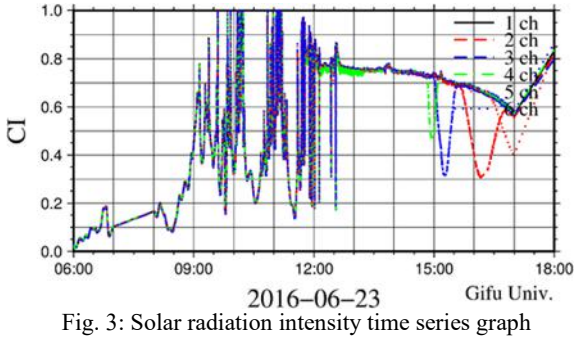

Fig. 3: Solar radiation intensity time series graph

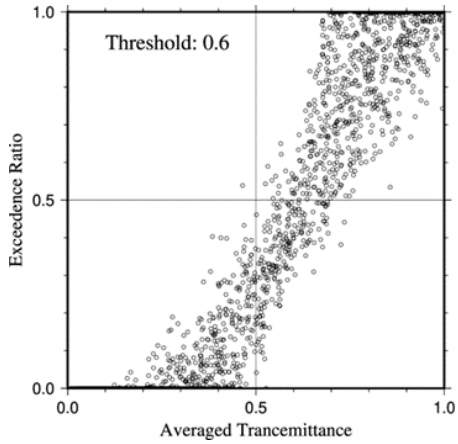

Fig. 4: Atmospheric transmittance and excess of CI 0.6

Figure5 shows how many hours the atmospheric transmittance exceeds 70% in one year (24 hours x 366 days = 8784 hours) at any point. In Hokuto City, Yamanashi Prefecture, the excess rate is as high as the atmospheric permeability shown in Figure1, which is considered to be appropriate for the multi-site standard.

Figure 6 shows the distribution of excess rate of 70% air permeability when multi-sites are established based on Hokuto City. In the case of only one point in Hokuto City, the ratio that can be said to be able to communicate stably in a good communication environment is about 0.61. On the other hand, it was found that multi-sites were improved at two points, and when combined with Obihiro City, it improved to about 0.78, combined with Miyazaki City, about 0.79, and combined with Miyakojima City, it improved to about 0.86. This is 223.3 days a year at one point in Hokuto City when converted to the number of days in a year (366 days). When combined with Obihiro City, 285.5 days a year, when combined with Miyazaki City, 289.1 days a year, and when combined with Miyakojima City, 314.8 days a year.

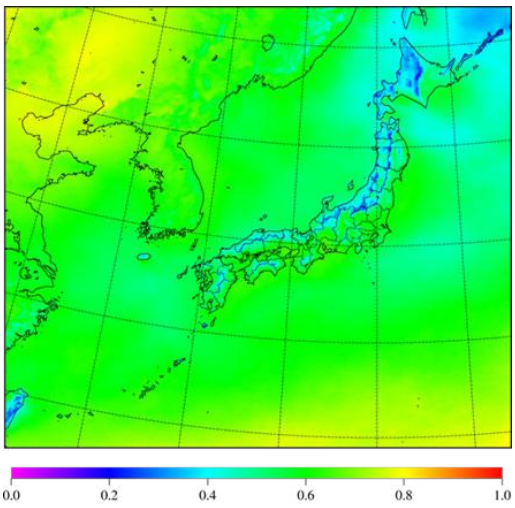

Fig. 5: Excess rate of 70% atmospheric transmittance at any point

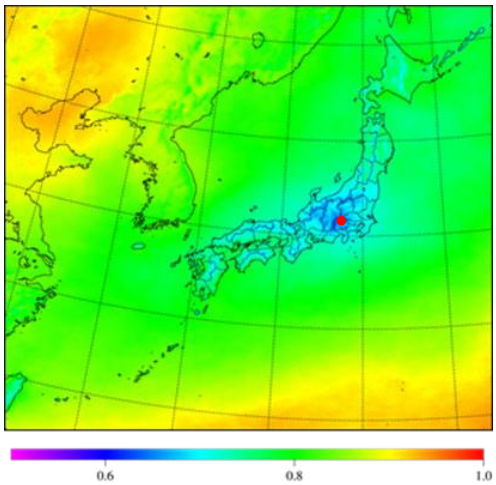

Fig. 6: Distribution of excess rate of 70% atmospheric transmittance when multi-site is made based on Hokuto City (Red-dotted point)

REFERENCES

・WRF Model Users Page:http://www.mmm.ucar.edu/wrf/

・Stephens, G. L.: Radiation Profiles in Extended Water Clouds. II: Parameterization Schemes. J Atmos Sci, 35, 2123-2132, 1978.

・Asai, J., T. Kobayashi, J. Yoshino, H. Yoshida, Y. Takayama: Estimation of atmospheric transmittance for optical communications between satellites and ground, Proc. of 61st Space Sciences and Technology Conf., 2A06, 2017 (in Japanese)

・Akiyama, N., T. Kobayashi, J. Yoshino, H. Yoshida, Y. Takayama: Estimation of atmospheric transmittance for optical communications between satellites and multi-sites on ground, Proc. of 62nd Space Sciences and Technology Conf., 1G06, 2018 (in Japanese))

Proceedings of International Symposium on a New Era in Food Science and Technology 2019
UGSAS-GU & BWEL Joint Poster Session on Agricultural and Basin Water Environmental Sciences 2019: P32

Vermicomposting of fruit and vegetable waste with the addition of excess activated sludge: A feasible approach leading to final products of higher utilization value

Wenjiao Li [1] and Fusheng Li [2]
1. **Graduate School of Engineering, Gifu University, Gifu, Japan**
2. **River Basin Research Center, Gifu University, Gifu, Japan**

INTRODUCTION

Fruit and vegetable waste (FVW) are generated in large quantity during production, processing and consumption. Several conventional methods are used for treatment and/or recycling of FVW, such as incineration, landfill, anaerobic digestion, feeding and composting. Compared to these methods, vermicomposting has the advantages of effective stabilization of the organic wastes through the joint function of earthworms and microorganisms in decomposition of easily decaying organic constituents, and of high utilization value for its final product as fertilizer. On the other hand, excess activated sludge (EAS), as the main byproduct of sewage treatment process, is also an organic waste. However, since EAS is mainly consisted of microorganisms and can be also treated by vermicomposting, it is reasonable to consider that the wide variety of microorganisms contained in EAS may enhance the microbial activities and contribute positively to the decomposition of FVW since the complex microbial communities are reported to play a key role during the vermicomposting (Chen et al., 2018). In addition, the rich content of proteins contained in EAS may promote the growth of earthworms and specific bacterial species, thus improving the stabilization efficiency of FVW and also may improve the utilization value of the final product.

Accordingly, the overall objective of this study was to investigate the effect of EAS on vermicomposting of FVW, which included the following specific aims: 1) to clarify the effect of EAS on earthworms; 2) to evaluate the effect of EAS on decomposition efficiency of FVW; 3) to clarify the effect of EAS on the utilization value of final product.

MATERIALS AND METHODS

Materials

The epigeic earthworm species *Eisenia foetida* was chosen for this experiment due to its wide tolerance against environmental variables. Five types of FVW, namely banana peels, cabbage, lettuce, carrot and potato, were cut into pieces with a width about 1 cm (and a thickness of 2 mm for carrot and potato) before experiment. In order to avoid the threat to earthworms from leachate generated during vermicomposting, a supporting bed was designed. The bed material was a mixture of soil and the final product from previous vermicomposting of FVW. For EAS, dewatered sludge from a slaughterhouse wastewater treatment plant in Gifu, Japan was used.

Experimental set up

Eleven plastic containers were used as vermicomposting reactors. Each reactor was formed with two compartments, namely a substrate compartment and a bed compartment. The two compartments were separated by a plastic plate opened with eight holes for earthworms to move freely between the two compartments. For the bed compartments, 100 g (wet basis) bed material was added and then 10 earthworms with an individual weight of 350-500 mg were invited. For the substrate compartments of six reactors, 100 g (wet basis) of banana peels, cabbage, lettuce, carrot, potato, and EAS were added respectively. For the remaining five substrate compartments, 100 g (wet basis) of the mixed substrates of each type of FVW with the EAS (FVW:EAS = 3:2, wet basis) were added respectively. All reactors were kept in dark and were run under 25 °C.

Analysis

The earthworms were taken out by hand and weighted every three days after washing with pure water and wiping with tissue. Dehydrogenase activity (DHA), a parameter reflecting the overall activity of existing bacteria, was determined by using the triphenyl tetrazolium chloride (TTC) method. Total carbon and total nitrogen were measured using a nitrogen and carbon analyzer (SHIMADZU, Japan). Total phosphorus was measured by using the molybdenum blue-absorption method with a spectrophotometer at the wavelength of 880 nm.

RESULTS AND DISCUSSION

Effect of EAS on earthworms

The body weight of earthworms increased in the initial period and then declined gradually in the end of vermicomposting for most treatments. Such a decline was corroborated by other studies and can be explained as the ageing of substrate materials. In general, earthworms in the treatments for FVW with the addition of EAS exhibited a distinct trends of weight gain, as compared to the earthworms in the treatments for FVW alone (data not shown). The growth rate of earthworms differed with the types of FVW during the vermicomposting. There was a negative growth rate occurred in the treatment for banana peels, cabbage, potato and its mixture with EAS but a positive growth rate in the treatment for others. The maximum growth rate was found in the treatment for lettuce with the addition of EAS (27.7 mg/worm/day), which is about twice the value of the treatment for lettuce alone (14.3 mg/worm/day). In addition, mixing EAS also promoted the cocoon production in treatment for banana peels, cabbage, carrot and potato as the number of cocoons in the reactors treating banana peels, cabbage, carrot and potato mixed with EAS (2, 2, 3, and 3, respectively) was larger than that treating respective FVW alone (0, 0, 0, and 2, respectively).

Effect of EAS on pH and electrical conductivity

The pH value in the substrate compartments increased from the initial range of 5.51 - 6.07 to the final range of 6.13 - 8.65 at the end of vermicomposting. For the bed materials, where the initial pH was 5.76, a variation of pH in the range of 5.41 - 7.80 was recorded. The variation of pH is probably in reflection of the changes in the processes of organic acid production and mineralization during vermicomposting.

The changes in the electrical conductivity (EC) before and after vermicomposting are showed in **Table 1**. EC decreased substantially in the substrate compartments of all reactors after vermicomposting. The maximum decreasing rate was measured in the treatment for lettuce and photo as 76.1%, followed by the treatment for carrot as 75.5%. The minimum decreasing rate was found in the treatment for EAS as 36.7 %. The decrease of EC during vermicomposting could be explained by reason that

the decomposition of organic substrates can lead to a great loss of dissolved ions (Huang et al., 2017). In contrast, the EC in all bed compartments increased from the initial level of 72.6 mS/m to 77.2 - 173.0 mS/m after vermicomposting. It is worthy of special notice that the increasing percentage of EC in the treatment for FVW with the addition of EAS was higher than that in the treatment for FVW alone except for cabbage. For the treatments of lettuce and carrot with or without the addition of EAS, the increasing percentage was a little bit lower compared to other treatments. The lower increasing percentage may be in association with the higher growth rate of earthworms in these two treatments (27.7 and 21.0 mg/worm/day). A larger amount of leachate was released from the treatments for lettuce and carrot due to their higher water content and was transferred to the bed compartment where some ions in the leachate were consumed by earthworms for their body growth.

Table 1 Changes of electrical conductivity in all substrate compartments and bed compartments. The positive values mean increasing percentages, and the negative values mean decreasing percentages.

	Electrical conductivity (mS/m)					
	Substrate compartment			Bed compartment		
	Initial	Final	Changes (%)	Initial	Final	Changes (%)
Banana peels	455	146.8	-67.7	72.6	159.4	119.6
Banana peels + EAS	589	161.2	-72.6	72.6	162.4	123.7
Cabbage	347	86.1	-75.2	72.6	162.2	123.4
Cabbage + EAS	308	134.9	-56.2	72.6	162.3	123.6
Lettuce	258	61.6	-76.1	72.6	77.2	6.3
Lettuce + EAS	244	67.9	-72.2	72.6	124.0	70.8
Carrot	420	102.9	-75.5	72.6	114.5	57.7
Carrot + EAS	311	89.4	-71.3	72.6	127.2	75.2
Potato	529	126.6	-76.1	72.6	159.6	119.8
Potato + EAS	387	131.8	-65.9	72.6	173.0	138.3
EAS	197	124.7	-36.7	72.6	157.8	117.4

Effect of EAS on decomposition efficiency

The total carbon decreased in all reactors except the treatment for banana peels, lettuce and carrot. The total carbon was lost as CO_2 during vermicomposting owing to the consumption of the available carbon as a source of energy for earthworms and microorganisms. A higher decreasing rate in the substrate compartment was observed in the treatment for FVW with the addition of EAS (data not shown). This may be contributed to the better growth of earthworms in the treatment with the EAS.

Looking into the decomposition efficiency from a view of microbial activity, a lower DHA was observed in the treatment for FVW except for carrot, but a higher DHA in the treatment for FVW with the addition of EAS (data not shown). An extremely higher DHA was found in the treatment for carrot and a lowered DHA was found in treatment for its mixture with EAS. Different types of FVW probably related to different decomposition efficiencies of phenolic compounds during vermicomposting, thus causing the different values of DHA. All results indicated that the EAS enhanced the decomposition efficiency of FVW by improving the microbial activities of FVW or by providing higher nutrients for earthworms.

Effect of EAS on utilization value of final product

As displayed in **Fig. 1**, a significantly higher total nitrogen was observed in both the substrate and bed compartments of the treatment for FVW with the addition of EAS after vermicomposting, except the bed compartment of the treatment for carrot. It may imply that earthworms were provided with a favored condition for nitrification and/or nitrogen mineralization. The loss of organic carbon, reduction in dry mass of the substrates, and the addition of nitrogenous substances etc. could be the major causes for the increase of nitrogen during the vermicomposting. The total phosphorus showed similar results with the total nitrogen, as could be seen from **Fig. 2**. The higher phosphorus concentrations can be assumed as the result of the reason that the added EAS encouraged the abundance of enzymes from earthworms and the activity of microorganisms, thus enhanced the mineralization and mobilization of phosphorus.

In summary, all data revealed that adding EAS into the vermicomposting of FVW could be a feasible option to enhance the decomposition efficiency of FVW and to enrich the utilization value of the final product of vermicomposting.

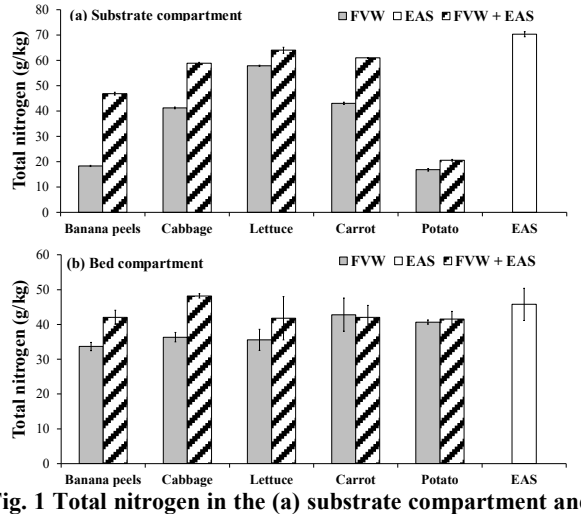

Fig. 1 Total nitrogen in the (a) substrate compartment and the (b) bed compartment after vermicomposting. Data are presented as mean and standard deviation (n = 3).

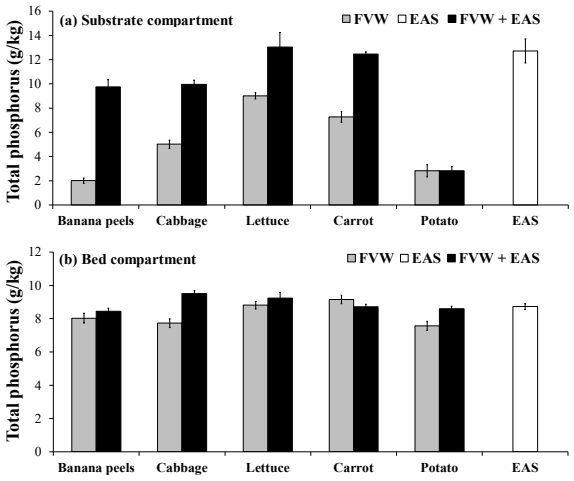

Fig. 2 Total phosphorus in the (a) substrate compartment and the (b) bed compartment after vermicomposting. Data are presented as mean and standard deviation (n = 3).

REFERENCES

Chen, Y., Chang, S.K.C., Chen, J., Zhang, Q., Yu, H. (2018) Characterization of microbial community succession during vermicomposting of medicinal herbal residues. Bioresour. Technol. 249, 542–549.

Huang, K., Xia, H., Cui, G., Li, F. (2017) Effects of earthworms on nitrification and ammonia oxidizers in vermicomposting systems for recycling of fruit and vegetable wastes. Sci. Total Environ. 578, 337–345.

Proceedings of International Symposium on a New Era in Food Science and Technology 2019
UGSAS-GU & BWEL Joint Poster Session on Agricultural and Basin Water Environmental Sciences 2019: P33

Inhibition of Arsenic transfer from contaminated soil to vegetation by wood ash

Shiamita Kusuma Dewi[1], Huijuan Shao[2], Shunichiro Mitsunaga [3] and Yongfen Wei[2]
1. **Graduate School of Natural Science and Technology, Gifu University, Japan**
2. **River Basin Research Center, Gifu University, Japan**
3. **Faculty of Engineering, Gifu University, Japan**

INTRODUCTION

Arsenic (As) is a toxic metalloid which is ubiquitous in nature. Because of its wide abundance, humans are always exposed to it that exists in food, water, air, and soil. Especially, Arsenic in the soil can be transferred to plants and hence threaten human health via food chain. In Japan, it is reported that there were 14 Areas (391 ha) of soils contaminated with As over 15 mg kg^{-1} (Ministry of the Environment, 2010).

Wood ash is the residual powder left after the combustion of wood, such as burning wood in a home fireplace or an industrial power plant. Since wood ash is composed of organic matter, Ca, Mg, Fe and other minerals, while Smith et al (2002) reported that the presence of Ca^{+} and Na^{+} led an increase in the retention of As and also Fe-oxides represented the role major sink for As sorption in soil; and Gadepalle et al (2007) also indicated that application of organic matter reduced the mobility of arsenic in soil, therefore wood ash is considered to be an effective material to influence the behavior of As in the soil-vegetation system by changing soil chemical/physical characteristics.

In this study, to investigate the inhibition effect of wood ash on As transfer from soil to vegetation, indoor pot experiment was designed and carried out. At the same time, the distribution of As in different parts of vegetation was also examined.

MATERIALS AND METHODS

Soil and additive samples – The mixture of two commercial products: Gardening soil and Decomposed granite soil with ratio of 3:2 by dry-weight, as shown in **Fig. 1** is used as soil media. Two different shapes of wood ash, namely powder and granular shape, were used in the study. Wood ash are made from Cryptomeria or Japanesse red-cedar wood. The properties of soil and wood ash are summarized in **Table 1.**

A B C

Fig.1 Soil sample (B: mixture of gardening soil and decomposed granite soil) and Gardening soil A and Decomposed granite soil C

Experimental design (**Fig. 2)** – Na_2HAsO_4 was used since arsenate was the main As species in the aerobic soil. The soil sample was in advance adjusted to four different As contamination levels with Na_2HAsO_4 (0, 50, 150, and 300 mg kg^{-1}), and then powder ash and granular ash were separately added to the soil at three different ratios (0, 1%, 5% and 10%, w/w). 600 g of soil was placed in each plastic pot, having a height about 10 cm and a perimeter about 15 cm. No additive applied soil was used as control for comparison. Each treatment had two replicates. Totally, 56 pots were prepared.

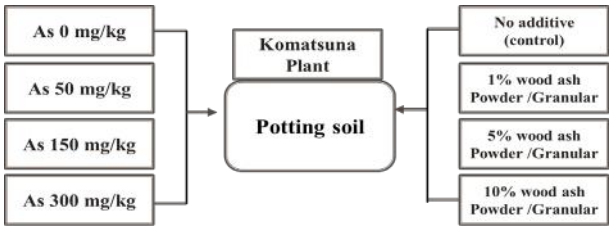

Fig. 2 Experimental design

Pot experiment and analysis – Komatsuna (*Brassica rapa* var. *perviridis*) was used in the pot experiment since it is a leaf vegetable that grow very fast and can actually be cultivated year round. Komatsuna was cultivated inside the room with constant temperature 25° C in Gifu University from Dec. 14, 2018 to April 2, 2019, and no additional fertilizer was added during this period. After harvest, the vegetation was washed and separated into three parts including leaf, stem and root, then further hot-dried in oven at 80°, followed by shattering by crusher and digested with nitric acid in autoclave. As concentrations of the digested samples from different parts were measured using inductively coupled plasma mass spectrometry (ICP-MS, Agilent 7700X).

7 days 21 days 35 days 60 days

Fig. 3 Komatsuna in different growth stages

Table 1 Properties of soil and wood ash used in this study

Sample	pH	Electrical Conductivity (mS/m)	Organic Matter (%)	Specific surface area (m^2/g)
Soil	6.08	81.2	12.361	4.014
Powder Wood Ash	12.78	457	0.743	17.418
Granular Wood Ash	10.15	214.3	7.202	0.082

All values represent the mean for each sample. pH and EC were measured using pH and EC meter (sample: water = 1:5). Organic matter was measured by Loss-on-Ignition method. Specific surface area was measured using 3Flex micrometrics.

RESULTS AND DISCUSSION

Komatsuna growth status – As shown in **Fig. 4 (**Granular wood ash was taken as an example**)**, the addition of wood ash seemed to be promoting the growth of Komatsuna cultivated in

soil with As concentration of 50 mg/kg. However, in the case of higher As contamination (150 mg/kg and 300 mg/kg), it looked like that the addition of the ash conversely suppressed the growth of the Komatsuna. On the other hand, no obvious difference was found between the influences of two different ashes on Komatsuna growth.

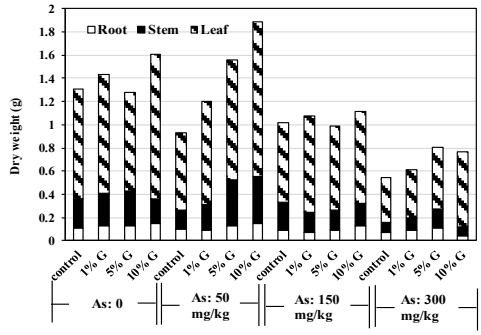

Fig. 4 Dry weight of different parts of Komatsuna under different addition ratio of granular wood ash (G) and different contaminated As level

Arsenic amount accumulated in different parts of vegetation – As shown **(Fig. 5, Fig. 6)**, As amount accumulated in root was the highest, followed by leaf and stem follow each As contaminated level. And obviously, the addition of powder wood ash decreased As accumulation in Komatsuna as compared to that of control, except the addition of 1% powder ash at 50 mg/kg

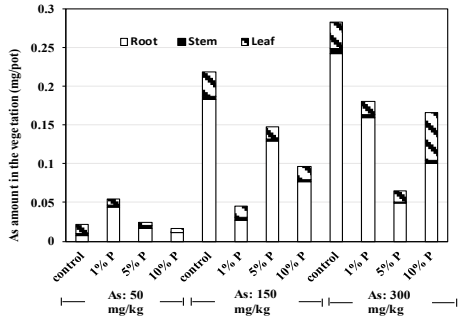

Fig. 5 Arsenic Amount of different parts of Komatsuna under different addition ratio of powder wood ash (P) and different contaminated As level

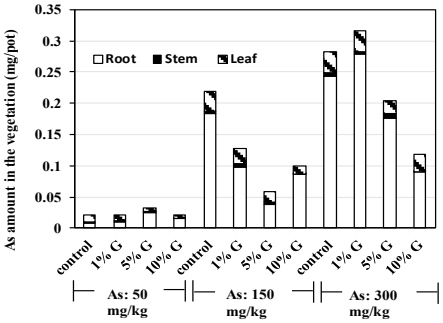

Fig. 6 Arsenic Amount of different parts of Komatsuna under different addition ratio of granular wood ash (G) and different contaminated As level

As contamination level (**Fig. 5**) and the additions of 5% granular ash at 50 mg/kg, 1% granular ash at 300 mg/kg As contamination levels, respectively (**Fig. 6**). The minerals included in the wood ash such as Fe, Al, K, Ca and Mg (data not shown) is considered to be a responsible reason for causing an increase in the As retention in the soil. Similarly, Stachowicz et al. (2008) described that Ca^{2+} and Mg^{2+} can induce the adsorption of phosphate and arsenate in soil.

Competition between Arsenic and Phosphorus – As shown in Fig. 5-6, arsenic addition showed a positive effect on As transfer to Komatsuna. But according to **Fig. 7**, we found that arsenic addition had a negative effect on phosphorus transfer to Komatsuna from soil; the lowest phosphorus transfer corresponded to the highest contamination level of As (300 mg/kg). This might be due to arsenate is a structural analogue of phosphate, replacing phosphate arsenic entered plant cells via phosphate transporters and also interfered phosphate's metabolism (Zhao, 2010).

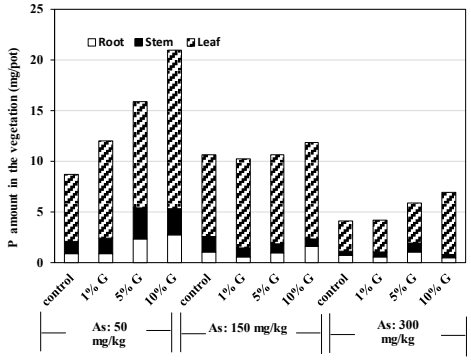

Fig. 7 Phosphorus amount accumulated of different parts of Komatsuna under different addition ratio of granular wood ash (G) and different contaminated As level

CONCOLUSION

In this study, the inhibition effect of wood ash on As transfer from soil to Komatsuna was investigated via an indoor pot experiment. The obtained results showed that wood ash had the capacity to reduce the amount of As accumulated in Komatsuna.

REFERENCES

Gadepalle VP, Ouki SK, Van HerwijnenR, Hutchings T (2007) Immobilization of heavy metals in soil using natural and waste materials for vegetation establishment on contaminated sites. Soil Sedim Contam 16:233-251

Ministry of the Environment (2010) Enforcernent Status of Agricultural Land-Soil Pollution Prevention Law in fiscal 2008, Ministry of the Environment ,Japan, http:llwww.enugo.jplpre$s/fleviewLphp?serial=16311&hou-id=12979

Smith E, Naidu R,Alston AM (2002) Chemistry of inorganic arsenic in soils. II. Effect of phosphorous, sodium, and calcium on arsenic sorption. J Environ Qua l31:557–563

Stachowicz M, Hiemstra T, van Riemsdijk WH (2008) Multi-competitive interaction of As (III) and As(V) oxyanions with Ca^{2+}, Mg^{2+}, $PO^{3-}{}_4$, and $CO^{2-}{}_3$ ions on goethite. J Colloid Interf Sci 320: 400-414

Zhao FJ, McGrath SP, Meharg AA (2010) Arsenic as a Food Chain Contaminant: Mechanisms of Plant Uptake and Metabolism and Mitigation Strategies. The Annual Review of Plant Biology 61:535-59j

The United Graduate School of Agricultural Science, Gifu University
1-1 Yanagido, Gifu 501-1193, Japan
Tel: +81-58-293-2984 (or, 2985)
E-mail: renno@gifu-u.ac.jp
Home Page: http://www.ugsas.gifu-u.ac.jp/eng/

Promotion Office of Gifu University Rearing Program
for Basin Water Environmental Leaders, Gifu University
1-1 Yanagido, Gifu 501-1193, Japan
Tel: +81-58-293-2085
E-mail: bwel@green.gifu-u.ac.jp
Home Page: https://www.green.gifu-u.ac.jp/BWEL/eng/index.html

ISBN978-4-909365-05-7

SUPPORTING FOUNDATION:
GIFU CONVENTION AND VISITORS BUREAU, JAPAN

Proceedings of International Symposium on a New Era in Food Science and Technology 2019